

NOTE TO USERS

This reproduction is the best copy available.

UMI[®]

Crystallisation of Inorganic Compounds with Alcohols

by

Georgiana A. Moldoveanu

Department of Mining, Metals and Materials Engineering

McGill University

Montréal, Québec

Canada

March 2005

A Thesis submitted to the Office of Graduate and Postdoctoral Studies
in partial fulfillment of the requirements of the degree of
Doctor of Philosophy

© Georgiana A. Moldoveanu, 2005



Library and
Archives Canada

Bibliothèque et
Archives Canada

Published Heritage
Branch

Direction du
Patrimoine de l'édition

395 Wellington Street
Ottawa ON K1A 0N4
Canada

395, rue Wellington
Ottawa ON K1A 0N4
Canada

Your file *Votre référence*

ISBN: 0-494-12912-3

Our file *Notre référence*

ISBN: 0-494-12912-3

NOTICE:

The author has granted a non-exclusive license allowing Library and Archives Canada to reproduce, publish, archive, preserve, conserve, communicate to the public by telecommunication or on the Internet, loan, distribute and sell theses worldwide, for commercial or non-commercial purposes, in microform, paper, electronic and/or any other formats.

The author retains copyright ownership and moral rights in this thesis. Neither the thesis nor substantial extracts from it may be printed or otherwise reproduced without the author's permission.

AVIS:

L'auteur a accordé une licence non exclusive permettant à la Bibliothèque et Archives Canada de reproduire, publier, archiver, sauvegarder, conserver, transmettre au public par télécommunication ou par l'Internet, prêter, distribuer et vendre des thèses partout dans le monde, à des fins commerciales ou autres, sur support microforme, papier, électronique et/ou autres formats.

L'auteur conserve la propriété du droit d'auteur et des droits moraux qui protègent cette thèse. Ni la thèse ni des extraits substantiels de celle-ci ne doivent être imprimés ou autrement reproduits sans son autorisation.

In compliance with the Canadian Privacy Act some supporting forms may have been removed from this thesis.

Conformément à la loi canadienne sur la protection de la vie privée, quelques formulaires secondaires ont été enlevés de cette thèse.

While these forms may be included in the document page count, their removal does not represent any loss of content from the thesis.

Bien que ces formulaires aient inclus dans la pagination, il n'y aura aucun contenu manquant.


Canada

“Discovery consists in seeing what everyone else has seen and thinking what no one else has thought.”

Albert Szent-Gyorgi

1937 Nobel Prize in Physiology and Medicine

*To my wonderful family
for their love and support*

Abstract

Crystallisation, one of the oldest unit operations, is of major economic importance in the hydrometallurgical industry for the separation and/or production of inorganic metal compounds in the form of good quality crystals, both in terms of purity and size. However, industrial crystallisation techniques usually have high energy requirements (e.g. evaporative crystallisation) and the residual solutions are often extremely corrosive, resulting in elevated operating and maintenance costs. Additionally, the majority of industrial crystallisation methods do not render to the appropriate supersaturation control, therefore the produced salts are agglomerates of fine crystallites with heavy solution entrainment and contamination.

In this work, the **Solvent Displacement Crystallisation (SDC)** technique is investigated as an attractive alternative to the conventional crystallisation methods. SDC involves the addition of low-boiling point, water-miscible organic solvents (MOS) to aqueous solutions to cause salt precipitation based on the **salting out** effect. The crystals are separated by filtration whereas the solvent is subsequently recovered for reuse by low-temperature distillation. The present work was initiated with the main objective to develop a solid scientific understanding of the SDC process and propose specific applications to hydrometallurgical systems of practical interest.

Criteria for the selection of organic solvents with suitable physical and chemical properties have been established and various compounds screened to determine their amenability to SDC; **2-propanol** was selected as an effective salting out agent to cause precipitation of most metallic sulphates of practical interest from acidic solutions and opted for use in further studies. Differences in crystallisation behaviour among the various metal sulphates were attributed to differences in hydration energy (the energy required for a hydrated ion to be separated from its bound water).

None of the tested metal chlorides could be successfully separated from HCl-H₂O system with 2-propanol. This was explained in terms of enhanced metal chlorides solubilities in non-aqueous solvents relative to water by formation of chloro-complexes of larger stability constants. The preferential formation of chloro-complexes in mixed

aqueous and organic solvents is the result of the almost linear drastic increase in the activity of Cl^- with mole fraction organic.

Successful examples of using the SDC method in conjunction with an industrial process involve precipitation of $\text{NiSO}_4 \cdot 6\text{H}_2\text{O}$ from copper electrorefining spent electrolytes, residual sulphate removal as gypsum ($\text{CaSO}_4 \cdot 2\text{H}_2\text{O}$) in chloride leaching processes and ZnO separation /NaOH regeneration in the system $\text{Na}_2\text{ZnO}_2 - \text{NaOH} - \text{H}_2\text{O}$. By maintaining a low supersaturation (i.e. controlled addition of the solvent to the electrolyte) and heterogeneous crystallisation conditions (use of seed/product recycling), crystal growth is favoured while impurity uptake/contamination is minimised.

Abrégé

La cristallisation, l'une des opérations d'unité les plus anciennes, est d'importance économique majeure dans l'industrie hydrometallurgique pour la séparation et/ou production des composés inorganiques en métal sous forme de cristaux de bonne qualité, pureté et taille. Cependant, les techniques industrielles de cristallisation ont habituellement des besoins en énergie élevée (par exemple cristallisation évaporative) et les solutions résiduelles sont souvent extrêmement corrosives, ayant pour résultat des coûts élevés de fonctionnement et d'entretien. De plus, la majorité de méthodes industrielles de cristallisation ne rendent pas à la commande appropriée de sursaturation, en conséquence les sels produits sont des agglomérés des cristallites fines, avec un grand contenu de solution, donc impurs.

Dans cette thèse, la technique de **Cristallisation par Déplacement du Solvant** (SDC) est étudiée comme alternative préférable aux méthodes conventionnelles de cristallisation. Le SDC comporte l'addition des solvants organiques miscibles à l'eau (MOS), à bas point d'ébullition, aux solutés pour causer la précipitation de sel. Les cristaux sont séparés par filtration tandis que le solvant est plus tard récupéré pour la réutilisation par distillation à basse température. Le travail actuel a été lancé avec l'objectif principal pour développer une solide compréhension scientifique du processus de SDC et pour proposer des applications spécifiques aux systèmes hydrometallurgiques d'intérêt pratique.

Des critères pour le choix des solvants organiques avec les propriétés physiques et chimiques appropriées ont été établis et des divers composés ont été examinés afin de déterminer leur applicabilité au SDC; **2-propanole** a été choisi en tant qu'agent efficace pour causer la précipitation de la plupart des sulfates métalliques d'intérêt pratique et opté pour l'usage dans d'autres études. Des différences dans le comportement de cristallisation parmi les divers sulfates métalliques ont été attribuées aux différences dans l'énergie d'hydratation (l'énergie requise pour un ion hydraté pour être séparé d'une molécule d'eau attachée). Aucun des chlorures métalliques examinés n'a pu être séparé avec succès du système de HCl-H₂O avec 2-propanole. Ceci a été expliqué en termes de solubilités augmentées de chlorures métalliques dans l'eau relative au solvant non aqueux, par la

formation des complexes de plus grandes constantes de stabilité. La formation préférentielle des complexes dans les solvants aqueux-organiques mélangés est le résultat de l'augmentation presque linéaire de l'activité du Cl^- avec la fraction du solvant organique.

Des exemples d'application avec succès du SDC à des processus industriels impliquent la cristallisation du $\text{NiSO}_4 \cdot 6\text{H}_2\text{O}$ dans le raffinage électrolytique du cuivre, la précipitation du sulfate résiduel comme gypse ($\text{CaSO}_4 \cdot 2\text{H}_2\text{O}$) dans la lixiviation au chlorures, la séparation du ZnO et régénération du NaOH dans système Na_2ZnO_2 - NaOH - H_2O . Lorsqu'on maintient une basse sursaturation (c.-à-d. addition graduelle du solvant à l'électrolyte) et un médium de cristallisation hétérogène (utilisation de semence cristalline et réutilisant le produit), la croissance des cristaux est favorisée tandis que le degré de contamination est réduit au minimum.

Acknowledgements

First of all I would like to express my deepest appreciation and respect to my supervisor, Professor George P. Demopoulos, who started up this novel work and let me be part of it. He always had time to answer numerous questions but also gave me room to learn on my own. From my teacher, I have learned that time management and careful planning constitute the key of success in any research enterprise; I have learned how to think in a clear and rigorous way, how to make my own decisions. His confidence and optimistic view provided me the courage and will to complete this lengthy journey and helped me realise the extent of my true capabilities.

Extremely thankful I am to Monique Riendeau for her invaluable skills and patient assistance for XRD, to Ed Siliauskas for providing continuous technical expertise during ICP sessions and to Helen Campbell for kindly helping me every time I needed SEM analysis and advice. I would also like to acknowledge the constructive feed-back of George Houlachi and Vicken Aprahamian of the Noranda Technology Centre, regarding parts of this work.

My most grateful thanks also go to the great administrative staff of the Department, Barbara Hanley and Carol Rousseau, who always patiently answered my every question during the years, adding a cordial smile as a bonus.

During the course of this work, I was very fortunate to have many people who were always ready to give me a hand or an advice. Huge thanks to everyone in the Hydromet lab, especially Terry, great colleague and friend for years, who sometimes had to momentarily put aside his work to help me with my own and patiently answered lots of my (not always so clever) questions, to Cinziana and Marie-Claude for their up-beat attitude, to Seref, Vincent and Felipe for being such great colleagues and providing a working environment filled with humour and optimism. It has been a great privilege and learning experience to be one of the members of the McGill Hydrometallurgy Research Group, and I am grateful to everyone for being there and helping me to define my future.

Natural Sciences and Engineering Research Council of Canada (NSERC) is acknowledged for providing financial support for this work.

I am extremely fortunate to have a wonderful family, my parents who always gave me their permanent support and unconditional love. I am particularly indebted to them for their altruistic wisdom in letting me spread my wings and go across the Atlantic to fulfill my destiny.

Last but certainly not least, I am happy to dedicate this work to my husband Corneliu, who has so much confidence in me, continuously encouraged me when I was down and always patiently put up with me through all the hard times. Without his love, optimism and strength, I would have never reached the complete peace of mind and will-power that allowed me to pursue and achieve this journey. Thank you!

Contents

Abstract	i
Abrégé	iii
Acknowledgements	v
List of Figures	xii
List of Tables	xvi
1. Introduction	1
References	5
2. Literature Survey and Theoretical Background	6
2.1 Introduction	6
2.2 Crystallisation from Solution	6
2.2.1 Crystallisation Driving Force	6
2.2.2 Crystal Nucleation	8
2.2.3 Crystal Growth	14
2.2.4 Factors Affecting Crystal Quality	17
2.3 Solvent Displacement Crystallisation	20
2.3.1 Salting Out Effect	20
2.3.2 The Hydrogen Bond	22
2.3.3 Solvent Effects and Solute-Solvent Interactions in Aqueous-Organic Mixtures	24
2.4 Examples of Solvent Displacement Crystallisation Applications	33
2.4.1 SDC Applied to the Sulphate System	33
2.4.2 SDC Applied to the Halide System	37

2.4.3 SDC Applied to Other Systems	39
2.4.4 Extractive Crystallisation	39
References	41
3. Experimental	49
3.1 Introduction	49
3.2 Materials	49
3.3 Equipment and Procedure	51
3.3.1 Experimental Set-up	51
3.3.2 Experimental Procedure	53
3.3.3 Handling of the Solid Products	54
3.4 Analytical Methods	55
3.4.1 Determination of Solution Composition	55
3.4.2 Characterisation of Solid Products	56
References	56
4. Solvent Selection and	
General Behaviour of Sulphate and Chloride Salts	58
4.1 Introduction	58
4.2 Organic Solvent Selection	58
4.2.1 Selection Criteria	58
4.2.2 Solvent Screening	61
4.2.3 Qualitative SDC Tests and Solvent Selection	63
4.3 General Behaviour of Sulphate and Chloride Systems	67
4.3.1 Experimental	68
4.3.2 Sulphate Systems	68
4.3.3 Chloride Systems	78
4.4 Summary and Conclusions	82
References	84
Physical Analysis of Metal Sulphates Crystallised via SDC	88

5. Crystallisation of Nickel Sulphate from H₂SO₄ Media	95
5.1 Introduction	95
5.2 Experimental	96
5.2.1 Research Strategy	96
5.2.2 Experimental Procedure	97
5.3 Systematic Solubility Studies	100
5.3.1 Influence of Temperature and Sulphuric Acid Concentration	100
5.3.2 Influence of Organic Solvent	101
5.4 Analysis of a Typical SDC Experiment	106
5.4.1 Test Progression and Data Analysis	107
5.4.2 Solid Product Properties	110
5.5 Critical Supersaturation Lines	113
5.5.1 Induction Period	114
5.5.2 Metastable Zone Width at 10, 21 and 40°C	117
5.6 Effect of Various Parameters on Solution Composition and Crystal Quality	120
5.6.1 Supersaturation Magnitude and Crystallisation Method	120
5.6.2 Influence of Temperature	126
5.6.3 Seeding (Heterogeneous Crystallisation)	127
5.6.4 Agitation and Ageing	134
5.7 Process Application Considerations	141
5.8 Summary and Conclusions	145
References	146
6. Crystallisation of Gypsum from CaCl₂-HCl Media	152
6.1 Introduction	152
6.2 Experimental	154
6.2.1 Research Strategy	154
6.2.2 Experimental Procedure	155

6.3 Systematic Solubility Studies	157
6.3.1 General Considerations	157
6.3.2 Influence of Temperature, Organic Fraction and Chloride Content	158
6.4 Critical Supersaturation at 21 and 40°C	160
6.5 Solvent Displacement Crystallisation Tests	162
6.5.1 Homogeneous Crystallisation	162
6.5.2 Heterogeneous Crystallisation	165
6.5.3 Data Analysis and Product Quality	168
6.5.4 Integration of Gypsum Production via SDC with HCl Regeneration Process	180
6.6 Summary and Conclusions	181
References	182
7. Precipitation of Zinc Oxide from NaOH Media	187
7.1 Introduction	187
7.2 Experimental	189
7.2.1 Research Strategy	189
7.2.2 Experimental Procedure	190
7.3 Selection of Organic Solvent	192
7.4 Systematic Solubility Studies	193
7.4.1 Influence of Sodium Hydroxide Content	193
7.4.2 Influence of Temperature and Organic Fraction	194
7.4.3 Dissolution Kinetics	195
7.5 Critical Supersaturation at 21°C	196
7.6 Solvent Displacement Crystallisation	197
7.6.1 Crystallisation at 21°C	197
7.6.2 Solid Product Properties	200
7.6.3 Suggested Mechanism for Zincate-Zincite Transformation	204

7.7 Regeneration of NaOH	207
7.8 Summary and Conclusions	208
References	209
8. Dehydration of Metal Sulphate Crystals	213
8.1 Introduction	213
8.2 Experimental	216
8.3 Results and Discussion	218
8.3.1 Calcium Sulphate Dihydrate	218
8.3.2 Copper Sulphate Pentahydrate	222
8.4 Summary and Conclusions	230
References	231
9. Synopsis	236
9.1 Introduction	236
9.2 Global Conclusions	236
9.3 Claims to Originality	239
9.4 Recommendations for Future Work	241
Appendices	242
Appendix A. Modified Free Acid Titration Methodology	242
Appendix B. Liquid-Liquid Separation Techniques	245
Appendix C. Physical and Electrochemical Properties of 2-Propanol	253
Appendix D. Nickel Concentration Profiles during SDC Tests	257
Appendix E. Confirmation of Crystallisation Water Molecules for Copper Sulphate Following Dehydration Tests	260

List of Figures

2.1	Nucleation mechanisms	8
2.2	Free energy diagram for homogeneous nucleation	10
2.3	Interfacial tensions at the boundaries between three phases	12
2.4	Generalised nucleation rate diagram as a function of supersaturation	13
2.5	Growth models	15
2.6	Precipitation regimes as a function of supersaturation magnitude	17
2.7	Solubility of salts in water-methanol mixtures at 20°C	21
2.8	Hydrogen-bonded structures in water	23
2.9	Excess enthalpies of mixing of alcohols and water at 25°C	25
2.10	Structures forming in water-alcohol mixtures	26
2.11	Dependence of dielectric constant on molecular weight of organic	29
2.12	Dielectric constants for water-methanol mixtures	29
2.13	Dielectric constant-related transformations in aqueous solution	30
2.14	Water and organic activities aqueous-organic mixtures at 25°C	32
2.15	Metal solubility in aqueous-organic solutions at 20°C	35
2.16	Fractional crystallisation of metal sulphates with ethanol	36
2.17	NaCl solubility as a function of DMiPA fraction at 5°C	38
2.18	Extractive crystallisation process with water recycle step	40
3.1	Experimental set-up for solubility studies	51
3.2	Experimental set-up for the SDC tests	52
4.1	Water activity coefficient in the system H ₂ O-2-propanol	67
4.2	Solubility of some sulphates in absolute methanol as a function of temperature	69
4.3	SDC behaviour of univalent sulphates	71
4.4	SDC behaviour of divalent sulphates	72
4.5	Detailed view of SDC behaviour of divalent sulphates	72
4.6	SDC behaviour of trivalent sulphates	73
4.7	Orientation of water molecule near a cation and an anion	73

4.8	Fractional crystallisation of mixed metal sulphates with ethanol	77
4.9	SDC behaviour of some metal chlorides	78
4.10	Solubility of metal chlorides in absolute methanol as a function of temperature	79
4.11	Effect of solvent on activity coefficients of anions upon transfer between water and mixed organic-aqueous solvents	82
5.1	Effect of temperature and sulphuric acid on nickel sulphate solubility	100
5.2	Influence of low-molecular alcohols on nickel sulphate solubility	102
5.3	Nickel sulphate solubility in H ₂ O-H ₂ SO ₂ (250 g/L) as a function of 2-propanol at various temperatures	103
5.4	Nickel sulphate solubility in H ₂ O-H ₂ SO ₂ (550 g/L) as a function of 2-propanol at various temperatures	104
5.5	Nickel sulphate dissolution kinetics at different temperatures	105
5.6	Progression of a typical SDC experiment	107
5.7	Water activity in the system H ₂ O-2-propanol	109
5.8	XRD spectrum of SDC product at 21°C	111
5.9	α-NiSO ₄ ·6H ₂ O crystal structure	112
5.10	Solubility–supersaturation diagram and supersaturation–controlled crystallisation process	113
5.11	Induction time and final nickel concentration in solution as a function of organic fraction	116
5.12	log(t _{ind}) as a function of (logS) ⁻²	116
5.13	Critical supersaturation lines and metastable zone width in the system NiSO ₄ -H ₂ O-H ₂ SO ₄ -2-propanol at 10, 21 and 40°C	118
5.14	Influence of temperature on critical supersaturation	119
5.15	Crystallisation strategies with and without supersaturation control	120
5.16	Homogeneous crystallisation kinetics at 10°C	121
5.17	Homogeneous crystallisation kinetics at 21°C	121
5.18	Homogeneous crystallisation kinetics at 40°C	122
5.19	Final nickel concentration in solution at different temperatures as a function of supersaturation	123

5.20	XRD spectra of $\text{NiSO}_4 \cdot 6\text{H}_2\text{O}$ produced via homogeneous SDC (low supersaturation, 10 and 40°C)	124
5.21	Influence of supersaturation magnitude on the quality of $\text{NiSO}_4 \cdot 6\text{H}_2\text{O}$ crystals	125
5.22	Influence of crystallisation method on final nickel concentration	128
5.23	Type of seed material and product of heterogeneous crystallisation tests	130
5.24	Effect of product recycling on crystal quality	131
5.25	Influence of crystallisation strategy on settling velocities	132
5.26	Influence of crystallisation approach on solids density	133
5.27	Influence of agitation speed on induction period for homogeneous nucleation	135
5.28	Influence of agitation on final nickel concentration in solution	136
5.29	Influence of agitation on crystal quality	137
5.30	Influence of ageing (equilibration time) on crystal quality	140
5.31	Conceptual flowsheet of nickel sulphate removal via SDC	142
5.32	Comparative XRD spectra of nickel sulphate produced via SDC and EC	143
5.33	Influence of method of crystallisation on particle size and morphology	144
6.1	Gypsum solubility in hydrochloric acid solutions	157
6.2	Gypsum solubility in the system 2-propanol-HCl (3 M)- H_2O	159
6.3	Influence of MgCl_2 presence on gypsum solubility in the system 2-propanol-HCl (3 M)- H_2O (40°C)	160
6.4	Critical supersaturation lines and metastable zone width in the system CaSO_4 - H_2O -HCl (3 M)-2 propanol at 21 and 40°C	161
6.5	Homogeneous crystallisation kinetics of gypsum at 21 and 40°C (3 M HCl)	163
6.6	Homogeneous crystallisation of gypsum at 21 and 40°C (low S, 3 M HCl)	165
6.7	Heterogeneous crystallisation of gypsum at 21 and 40°C	166
6.8	Influence of crystallisation method on residual sulphate	168
6.9	XRD spectra of $\text{CaSO}_4 \cdot 2\text{H}_2\text{O}$ produced via homogeneous SDC (low supersaturation, 21 and 40°C)	170

6.10	Influence of supersaturation magnitude and temperature on the quality of gypsum crystals produced via homogeneous SDC	171
6.11	Gypsum crystals produced via heterogeneous SDC	173
6.12	Effect of product recycling on crystal quality	174
6.13	Influence of crystallisation strategy on gypsum settling velocity	176
6.14	Influence of recycling on gypsum settling velocity	176
6.15	Influence of crystallisation strategy on gypsum solids density	177
6.16	Influence of recycling on gypsum solids density (40°C)	177
6.17	The CaSO ₄ -H ₂ O-HCl phase diagram	178
6.18	XRD spectra of CaSO ₄ ·xH ₂ O produced via SDC	179
6.19	Integration of gypsum production via SDC with HCl regeneration	181
7.1	Zinc oxide solubility in sodium hydroxide at 21°C	194
7.2	Effect of methanol and temperature on zinc oxide solubility	194
7.3	Dissolution kinetics of ZnO in 6 M NaOH at 21°C	195
7.4	Critical supersaturation line and metastable zone width in the system ZnO-H ₂ O-NaOH-methanol at 21°C	196
7.5	Progression of a typical homogeneous SDC test	198
7.6	Precipitation kinetics of ZnO at 21°C in the absence and presence of seed	200
7.7	XRD spectra of ZnO produced via homogeneous SDC at 21°C	201
7.8	Structure of ZnO	201
7.9	SEM micrographs of ZnO crystals produced via SDC at 21°C	203
7.10	Fraction of ionic species in solution as a function of pH at 25°C	205
8.1	XRD monitoring of gypsum dehydration with 2-propanol at 60°C (3 M HCl)	219
8.2	XRD monitoring of gypsum dehydration with 2-propanol at 60°C (3 M HCl, 1.5 M MgCl ₂)	220
8.3	Calcium sulphate crystals before and after equilibration for 24 hrs at 60°C in aqueous-2-propanol mixtures	221
8.4	The continuous surface growth (or dissolution) model	228
8.5	SEM micrographs of various copper sulphate hydrates	230
B.1	2-propanol-water phase diagram	245

B.2	Fractional distillation set-up	246
D.1	Nickel sulphate homogeneous crystallisation tests at 10 and 21°C	257
D.2	Nickel sulphate homogeneous crystallisation tests at 40°C	258
D.3	Nickel sulphate comparative heterogeneous crystallisation tests at 21°C	258
D.4	Nickel sulphate heterogeneous crystallisation ageing test at 21°C	259
E.1	XRD spectra for various copper sulphate hydrates	260-262
E.2	TGA spectra for various copper sulphate hydrates	263-264

List of Tables

1.1	Industrial crystallisation methods	2
3.1	Inorganic salts and chemical reagents employed in present work	50
4.1	Physical properties of water and selected polar organic solvents	62
4.2	Evolution of preliminary SDC qualitative tests	64
4.3	Summary of the SDC results for most common sulphates with 2-propanol	71
4.4	Ionic radii for most common ions	74
4.5	Heats of hydration of individual ions	75
4.6	Solubility of metal chlorides in various organic solvents (qualitative data)	80
4.7	Chloride stability constants in aqueous, mixed and non-aqueous solvents	81
5.1	Parameters considered in crystallisation of nickel sulphate with 2-propanol	97
5.2	The fitting constants A and B for the solubility of nickel sulphate	101
5.3	Solubility of nickel sulphate as a function of 2-propanol, acidity and temperature	103
5.4	Initial and final parameters of SDC using 2-propanol and azeotrope at 21°C	110
5.5	Precipitation induction periods in the system NiSO ₄ -H ₂ O-2-propanol	115
5.6	Chemical composition of industrial decopperised electrolyte and final nickel sulphate crystalline product	144
6.1	Parameters considered in crystallisation of gypsum with 2-propanol	154

6.2	Gypsum solubility as a function of 2-propanol and temperature	159
6.3	Calcium sulphate concentration as a function of O/A and recycling run	167
7.1	Parameters considered in crystallisation of zinc oxide with methanol	189
7.2	NaOH concentration values	207
8.1	Synopsis of copper sulphate dehydration with 2-propanol	224
A.1	Preparation of H ₂ SO ₄ -NiSO ₄ standard solutions	243
B.1	Theoretical plates required to separate liquid mixtures by distillation	247
B.2	Materials mass balances	250
C.1	Physical properties of 2-propanol	253
D.1	Progression of low S homogeneous SDC tests at 10, 21 and 40°C	257
D.2	Progression of heterogeneous SDC tests at 21°C	259
D.3	Progression of the heterogeneous SDC ageing test	259

Chapter 1. Introduction

Crystallisation, one of the oldest unit operations in chemical processing, is applied extensively in the hydrometallurgical industry for the separation, purification or production of inorganic salts in the form of crystals. Crystallisation may be defined as a phase change in which a crystalline product is obtained from a homogeneous single phase solution formed by mixing two or more species [1]. Typically, the term “solution” has come to describe a mixture consisting of a liquid solvent (usually water) and a solute, which is a dissolved solid. At a given temperature there is a maximum amount of solute that can dissolve in a given amount of solvent. When this maximum is reached the solution is said to be saturated; the amount of solute required to make a saturated solution at a given condition is called “solubility”. Crystallisation from solution occurs when the solute concentration in a solvent exceeds its solubility limit and the solution becomes supersaturated.

The solubility characteristics of a solute in an aqueous solution have a considerable influence on the choice of a method of crystallisation (i.e. the way the supersaturation state is reached). There are several ways to induce supersaturation in a solution. For systems in which the solubility is not a strong function of temperature, solvent evaporation is used. Cooling is employed when the solubility increases with temperature while heating is used when the solubility decreases with temperature. When the product is generated from an irreversible chemical reaction between two reactants present in the system, the process is referred to as “precipitation”. In the case when another miscible component is added to the solution to suppress the solubility of the solute the process is referred as “salting out” or “solvent displacement crystallisation”. Table 1.1 summarizes the main industrial techniques employed for supersaturation generation, hence crystallisation.

As previously explained, when the solubility is minimally dependent on temperature, evaporative crystallisation is used. This method is based on the concept of increasing the solute concentration above its solubility by removing part of the solvent.

Table 1.1 Industrial crystallisation methods [2]

Technique	Applied for salts having...	Supersaturation induced by...
Cooling	Strong solubility-temperature dependence	Temperature reduction
Evaporative	Low solubility-temperature dependence	Solvent removal
Vacuum Cooling	Moderate solubility-temperature dependence	Cooling, flashing and evaporation
Dilution/Solvent Displacement	No or very low solubility in the displacement agent	Displacement agent addition
Reactive	Precipitated subsequent to a chemical reaction	Massive solute generation

Simple boiling is expensive since typically ~1.5 kg of water must be evaporated to recover ~0.5 kg of salt (depending on the specific salt). Since the enthalpy of vaporization of water is high (41.6 kJ/mol, [3]), the method is energy-intensive; moreover, the residual solutions are extremely corrosive, resulting in high operating and maintenance costs. In addition to high costs, evaporative crystallisation does not render to the appropriate supersaturation control, therefore the produced salts are agglomerates of fine crystallites with heavy solution entrainment and contamination.

As an alternative to evaporative crystallisation, the method of Solvent Displacement Crystallisation (SDC) was studied in the present research work. It is well documented that the addition of a water-miscible organic solvent to an aqueous solution can reduce the solubility of some organic or inorganic solutes [4, 5] thus making the solution supersaturated and inducing crystallisation. The method is referred as "Solvent Displacement Crystallisation" and involves the addition of low-boiling point, water-miscible organic solvents (MOS) to aqueous solutions to cause the crystallisation of inorganic salts, based on the concept of "salting out effect". This enables the separation of electrolytes from their aqueous solutions via precipitation and filtration. A general explanation of this effect indicates that there is a competition between the polar organic molecules and inorganic ions for the water molecules. Since the organic solvent exhibits

a higher affinity for water, this will lead to the capture of part of the hydration water molecules, thus causing salt precipitation. The solvent is subsequently recovered for reuse by low-temperature or vacuum distillation.

Research conducted by Cohen in the eighties [6] first suggested that an alternative crystallisation process based on this phenomenon could be developed that would recover nickel sulphate from decopperised electrolytes.

This novel technique appears to offer a number of advantages over the conventional method:

- (a) the potential to reduce energy costs in the recovery of inorganic salts from aqueous process streams;
- (b) a high solute recovery yield may be obtained by selecting the appropriate water-miscible solvent;
- (c) controlled addition of organic maintains a low supersaturation, yielding thus larger crystals with high solids density.

Despite its potential wide range of uses in inorganic processing and hydrometallurgy, there has been no systematic investigation of this technique as it applies to the removal of metal salts from aqueous solutions, neither from a fundamental perspective nor from the standpoint of application to hydrometallurgical processes; only relatively few laboratory applications have been studied and reported in the literature.

It is the overall goal of the present research work to proceed to such a systematic study in order to develop a solid scientific understanding of the solvent displacement crystallisation process and to propose specific applications to hydrometallurgical systems of practical interest. More specifically, the present research work aims to address the following objectives:

- (1) to identify and describe the underlying principles of chemistry and solvation phenomena that govern the salting-out process in aqueous-organic mixtures;
- (2) to establish criteria for the selection of organic solvents with suitable physical and chemical properties for SDC;
- (3) to determine which salts respond to the method by using a screening procedure;

- (4) to select systems with potential of practical application for detailed investigations (solubility studies, critical supersaturation line, heterogeneous vs. homogeneous crystallisation tests, etc.);
- (5) to study the possibility to further dehydrate the produced crystals by using an appropriate organic solvent.

The present work has been organised into a number of chapters as follows: Chapter 2 represents an extensive literature survey of the subject-matter of the thesis which includes the fundamental aspects of crystallisation from solution, with the purpose of highlighting the significance of supersaturation in affecting the nucleation and growth of crystalline particles. After that, the solvent effects and solvent-solute interactions in mixed aqueous-organic solutions are addressed, starting with the description of the salting-out effect and continuing with the description and explanation of the underlying phenomena. In relation to the former, the technical literature is reviewed and various organic solvent-induced salt crystallisation processes are overviewed. Finally, the potential application of the SDC method to an industrial crystallisation process is presented.

Chapter 3 describes the experimental equipment and procedures used to achieve the proposed objectives as well as the analytical methods employed.

Chapter 4 summarises the results of preliminary tests where the criteria for the organic solvent selection were devised and the general behaviour of various sulphate and chloride systems during SDC was investigated.

Following that, Chapter 5 describes in-depth SDC experiments conducted on a sulphate system of practical interest in acidic media (i.e. $\text{NiSO}_4\text{-H}_2\text{SO}_4\text{-H}_2\text{O}$). More specifically, the influence of several factors on solubility and crystal quality was studied (e.g. temperature, volume of organic solvent, agitation rate, crystallisation techniques).

Similarly, Chapter 6 studies the feasibility of residual sulphate removal as gypsum from regenerated hydrochloric acid media by SDC.

Chapter 7 investigates the production of ZnO from alkaline media (i.e. $\text{Na}_2\text{ZnO}_2\text{-NaOH-H}_2\text{O}$) via SDC and the factors affecting it.

The possibility of reducing the number of crystallisation water molecules (i.e. partial crystal dehydration) by the use of organic solvents is investigated in Chapter 8.

Finally, Chapter 9 provides a global summary of the major findings of this work, states the original contributions made to knowledge and gives a brief outline of how the present work can be continued in the future.

The Appendices constitute the last section. They provide information on analysis techniques, properties of 2-propanol and suggested liquid-liquid separation techniques to recover the organic solvent.

References

- [1]. J.W. Mullin, *Crystallisation*, 3rd Ed., Butterworth-Heinemann, Oxford, (1993).
- [2]. N. Tavare, *Industrial Crystallisation: Process Simulation, Analysis and Design*, Plenum Press, N.Y., New York, (1995).
- [3]. R.H. Perry and D.W. Green (editors), *Perry's Chemical Engineer's Handbook*, 7th edition, McGraw-Hill, Montreal, PQ, Canada, (1997).
- [4]. Z.B. Alfassi, "The separation of electrolytes in aqueous solution by miscible organic solvents" *Separation Science and Technology*, **14**(2), pp. 155-161, (1979).
- [5]. Z. B. Alfassi and S. Mosseri, "Solventing out of electrolytes from their aqueous solution" *AIChE Journal*, **30**(5), pp. 874-876, (1984).
- [6]. J.M. Cohen, "Applications of solvent displacement crystallisation in hydrometallurgy" in *Separation Processes in Hydrometallurgy*, (edited by G.A. Davies), pp. 265-273, Ellis Horwood, London, U.K., (1987).

Chapter 2. Literature Survey and Theoretical Background

2.1. Introduction

In this chapter, the fundamentals of crystallisation theory are presented, with the purpose of highlighting the significance of supersaturation in affecting the nucleation and growth of crystalline particles. After that, the solvent effects and solvent-solute interactions in mixed aqueous-organic solutions are addressed, starting with the description of the salting out effect and continuing with the description and explanation of the underlying phenomena. Finally, the technical literature is reviewed and various organic solvent-induced salt crystallisation processes are discussed.

2.2. Crystallisation from Solution

Crystallisation from solution occurs when the solute concentration in a solvent exceeds its solubility limit; such a solution is supersaturated. The process of formation of crystals from a supersaturated solution is a non-equilibrium process and generally is defined by the following steps: (1) Solvated ions and molecules partially desolvate and then associate to form ion pairs, complexes or higher aggregates; (2) The ionic and molecular aggregates gather to form crystal nuclei; (3) Crystal nuclei grow to crystals.

2.2.1 Crystallisation Driving Force

Supersaturation is defined as the concentration of component ions in excess of the saturated concentration. There are several ways to induce supersaturation in a solution. For systems in which the solubility is not a strong function of temperature, solvent evaporation is used. Cooling is employed when the solubility increases with temperature while heating is used when the solubility decreases with temperature. When the product is generated from an irreversible chemical reaction between two reactants present in the system, the process is referred to as “precipitation”. In the case when another miscible

component is added to solution to suppress the solubility of the solute the process is referred as “salting out” or “solvent displacement crystallisation”.

The thermodynamic driving force for crystallisation can be expressed as [1]:

$$\Delta\mu = \mu_1 - \mu_2 = \mu_1^0 + RT\ln(a_1) - \mu_2^0 - RT\ln(a_2) \quad (2.1)$$

μ^0 = standard chemical potential (Jmol^{-1}), R = universal gas constant ($8.3144 \text{ Jmol}^{-1}\text{K}^{-1}$), T = absolute temperature (K), a_1 = activity of the solute, a_2 = activity of the pure solute in equilibrium with a macroscopic crystal.

Furthermore

$$\Delta\mu/RT = \ln(a/a^*) = \ln S \quad (2.2)$$

where a^* is the activity of the saturated solution and S is the fundamental supersaturation, i.e.

$$S = \exp(\Delta\mu/RT) \quad (2.3)$$

Supersaturation acts as crystallisation driving force, any $S > 1$ inducing $\Delta G < 0$ (hence spontaneous process). So, in terms of Gibbs free energy change (Jmol^{-1}) due to crystallisation:

$$\Delta G = -RT\ln(a/a^*) = -RT\ln(S) \quad (2.4)$$

For electrolyte solutions it is more appropriate to use the mean ionic activity, a_{\pm} , defined by

$$a = a_{\pm}^{\nu} \quad (2.5)$$

where $\nu_{\pm} = \nu_+ + \nu_-$ is the number of moles of ions in 1 mole of solute. Therefore,

$$\Delta\mu/RT = \nu \ln S_a \quad (2.6)$$

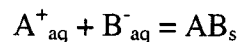
where $S_a = a_{\pm}/a_{\pm}^*$ (2.7)

However, for practical purposes, supersaturations are generally defined in terms of solution concentrations, e.g.

$$S_c = C/C^* = m/m^* \quad (2.8)$$

where c = molarity (mol/L of solution), m = molality (mol/kg of solvent).

For ionic crystals, supersaturation can be expressed with the aid of solubility product:



$$K_{sp} = C_{A+,eq} C_{B-,eq} \quad (2.9)$$

$$S = C_{A+,eq} C_{B-,eq} / K_{sp} \quad (2.10)$$

$C_{A+,eq}$ and $C_{B-,eq}$ are ionic concentrations in supersaturated solutions; for simplicity, concentrations are considered to be equal to activities.

2.2.2. Crystal Nucleation

The condition of supersaturation may not be sufficient to cause crystallisation. Crystals may be formed out of a supersaturated solution either homogeneously or on surfaces that act as centres of crystallisation.

Nucleation processes can be classified according to the following scheme [2]:

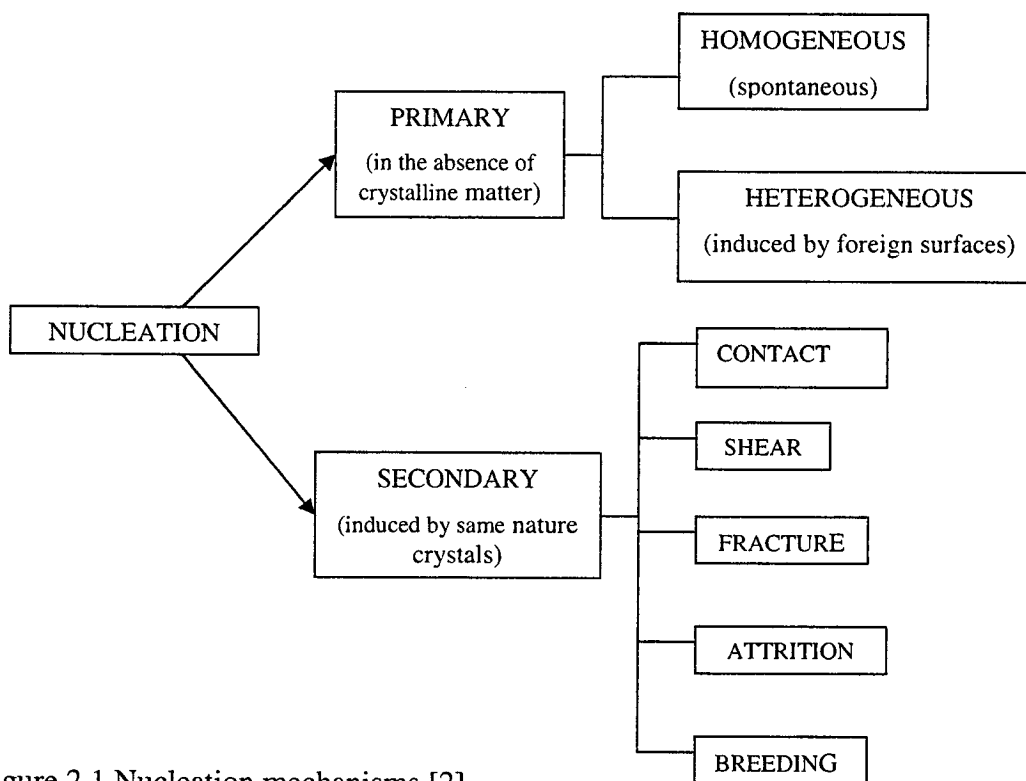
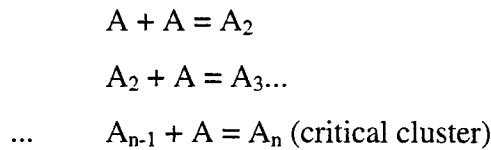


Figure 2.1 Nucleation mechanisms [2]

- **Homogeneous Primary Nucleation**

Homogeneous primary nucleation occurs only in the absence of any solid matter in the supersaturated solution. Generally, most dilute solutions of inorganic salts consist of

ionised species; as concentration gradually increases, ionization decreases and solvated ion pairs (i.e. unionised solute) appear in solution; clusters of solute molecules with the same structure as the crystal form but they are too small to be regarded as a separate phase. This “pre-crystallisation” step proceeds very fast with the rate constant of $10^8 - 10^{10} \text{ s}^{-1}$ [3]. The life span of such clusters is very short and data taken for various species gave cluster sizes of approx. 50-125 Å or $\sim 10^3$ molecules [2]. Mullin [4] proposes a sequence of bimolecular additions to the cluster according to the scheme:



Further additions to the critical cluster would result in nucleation and subsequent growth of the nucleus; the construction process, which occurs very rapidly, can only continue in local regions of very high supersaturation because the nucleus is thermodynamically unstable at low supersaturations [3].

The thermodynamic requirements for crystallisation involve the energy required for nucleus surface formation (ΔG_s) and the energy change required for transition from liquid to solid state (ΔG_v). Thus, the free energy change resulting from a crystal nucleating homogeneously from solution (in J/mol) is given by:

$$\Delta G = \Delta G_s + \Delta G_v \quad (2.11)$$

The former is a positive quantity proportional to the surface area and the latter is a negative quantity, proportional to the nucleus volume and is a function of supersaturation. Assuming a spherical nucleus, Eq. (2.11) can be written as:

$$\Delta G = 4\pi r^2 \gamma + (4/3)\pi r^3 \Delta G_v \quad (2.12)$$

where r is the nucleus radius (Å) and γ is the specific surface energy ($\text{Jm}^{-2}\text{mol}^{-1}$).

Since the two terms of the right-handed side of the Eq. (2.12) are of opposite sign and depend differently on r , the free energy of nucleus formation passes through a maximum (Figure 2.2). This maximum value, ΔG_{crit} , corresponds to activation energy and it is related to the critical nucleus size as follows:

$$r_c = -2\gamma/\Delta G_v \quad (2.13)$$

and
$$\Delta G_{\text{crit}} = 4/3(\pi\gamma r_c^2) \quad (2.14)$$

The critical radius is related to the supersaturation degree of the solution via the Gibbs-Thompson equation:

$$\ln(c/c^*) = \ln S = 2\gamma v/kTr_c \quad (2.15)$$

where c^* is the saturation concentration, k is the Boltzmann constant ($1.3806503 \times 10^{-23}$ JK⁻¹), v is the molecular volume ($\text{m}^3 \text{mol}^{-1}$).

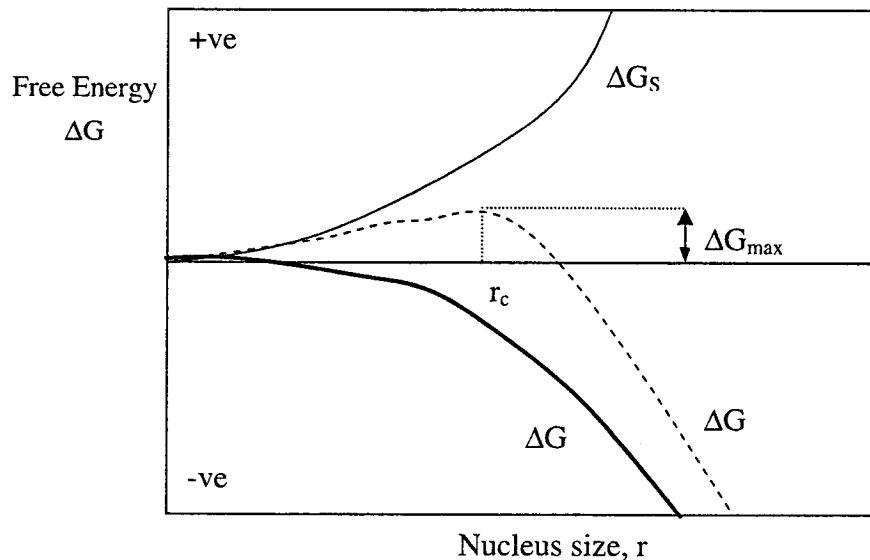


Figure 2.2 Free energy diagram for homogeneous nucleation [4]

It can be observed that as supersaturation increases the critical nucleus size decreases, thus increasing the probability that a viable nucleus will be formed. On the other hand, the size of a critical nucleus increases with temperature [4].

The rate of nucleation represents the number of nuclei formed per unit time per unit volume (more commonly used units are: nuclei·s⁻¹·cm⁻³) and can be expressed as an Arrhenius-type equation:

$$J = A \exp(-\Delta G/kT) \quad (2.16)$$

Combining Eq. (2.16) with Eqs. (2.13), (2.14) and (2.15), the rate of primary homogeneous nucleation at high supersaturations is

$$J = A \exp[-(16\pi\gamma^3 v^2)/3k^3 T^3 (\ln S)] \quad (2.17)$$

The above equation indicates that three main variables govern the rate of nucleation: temperature (T), degree of supersaturation (S) and interfacial tension (γ).

A characteristic feature related to homogeneous nucleation is the “induction period”, which represents the time interval between the achievement of supersaturation and the appearance of crystals (i.e. formation of viable nuclei). The induction period may be considered as the sum of several parts: the “relaxation time” (t_r), required for the system to achieve a quasi-steady-state distribution of molecular clusters; time required for the formation of a stable nucleus (t_n), and time for that nucleus to grow to a detectable size, (t_g) [1]:

$$t_{ind} = t_r + t_n + t_g \quad (2.18)$$

In practice, however, it is impossible to isolate these separate entities. This time lag, inversely proportional to the nucleation rate, is influenced by the level of supersaturation, state of agitation, temperature, presence of impurities and viscosity [4, 5]. The presence of seed crystals reduces the induction period but does not eliminate it.

- ***Heterogeneous Primary Nucleation***

The crystallisation of a solute on suspended dust particles or apparatus surfaces is termed heterogeneous nucleation; its rate depends not only on supersaturation but also on the availability of active sites for nucleation to occur. As the presence of a foreign surface can induce nucleation at degrees of supersaturation lower than those required for spontaneous nucleation, the overall free energy change associated with the formation of a critical nucleus under heterogeneous conditions (ΔG_{hetero}) must be less than the corresponding value associated with the homogeneous conditions (ΔG_{homo}):

$$\Delta G_{hetero} = \phi \Delta G_{homo} \quad (2.19)$$

where $\phi < 1$.

The factor ϕ in equation can be expressed as a function of the contact angle:

$$\phi = [(2 + \cos\theta)(1 - \cos\theta)^2]/4 \quad (2.20)$$

The interfacial tension γ is an important factor in controlling the nucleation process [4, 6]. Figure 2.3 shows an interfacial energy diagram for three phases in contact.

Three cases can be identified, according to θ values:

- (1) $\theta = 180^\circ$, $\phi = 1$ and $\Delta G_{\text{hetero}} = \Delta G_{\text{homo}}$: complete non-affinity between the crystalline solid and the foreign surface. The overall free energy for nucleation is the same as of that required for homogeneous (spontaneous) nucleation.
- (2) $0 < \theta < 180$, $\phi < 1$ and $\Delta G_{\text{hetero}} < \Delta G_{\text{homo}}$: partial affinity between the two solids. Nucleation is easier to achieve on the foreign surface than homogeneously.
- (3) $\theta = 0$, $\phi = 0$ and $\Delta G_{\text{hetero}} = 0$: complete affinity between the two solids. Addition of seed crystals of the same nature as the solute to promote nucleation.

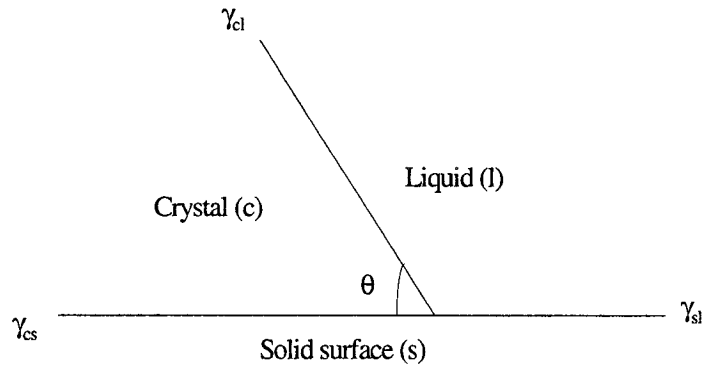


Figure 2.3 Interfacial tensions at the boundaries between three phases [4]

The eq. (2.17) for homogeneous primary nucleation cannot be successfully applied to express the nucleation rate since it is valid only for extreme high supersaturation that are generally not encountered during heterogeneous nucleation. An equation of power-law form that accounts for moderate supersaturations has been proposed [2]:

$$J^0 = k(c - c_s)^i, \text{ (nuclei} \cdot \text{s}^{-1} \text{cm}^{-3}) \quad (2.21)$$

where k is the rate constant ($\text{nuclei} \cdot \text{mol}^{-1} \text{s}^{-1}$), c is the solute concentration and c_s the saturation concentration (both in mol/L).

Since k is a function of temperature, the rate of heterogeneous nucleation can be represented as

$$J^0 = k_0 \exp[-(\Delta E/kT)(c - c_s)^i] \quad (2.22)$$

- **Secondary (Surface) Nucleation**

A supersaturated solution nucleates at lower supersaturation (i.e. easier) when crystals of the solute are already present. Deliberate seeding is often employed in industrial crystallisation to maintain a control over the product size and size distribution.

There are several possible mechanisms of secondary nucleation [2, 4]:

- Initial breeding* results from crystalline dust adhering to larger seeds introduced into the system;
- Fracture processes* occur in the systems that produce soft crystals, especially for dense suspensions and violent agitation, due to impact by the impeller;
- Attrition nucleation* is considered fracture of a lesser degree and results from crystal-crystal or crystal-apparatus interaction at high suspension densities;
- Needle breeding* occurs because of dendritic growth on crystals; it is best avoided by reducing the supersaturation or using additives that change the crystal habit;
- Fluid shear nucleation* results when the fluid velocity relative to the crystal velocity is large and some of the “adsorbed” layer of clusters is removed from the surface and subsequently nucleate, if the supersaturation is high;
- Contact nucleation*, the most important source of secondary nuclei, results when the crystals contact the agitator, pump or reactor.

As described by Figure 2.4, the type of nucleation varies with supersaturation, ($1 < S^*_{\text{surf}} < S^*_{\text{hetero}} < S^*_{\text{homo}}$). S^* is the critical supersaturation level above which nucleation of a certain type occurs.

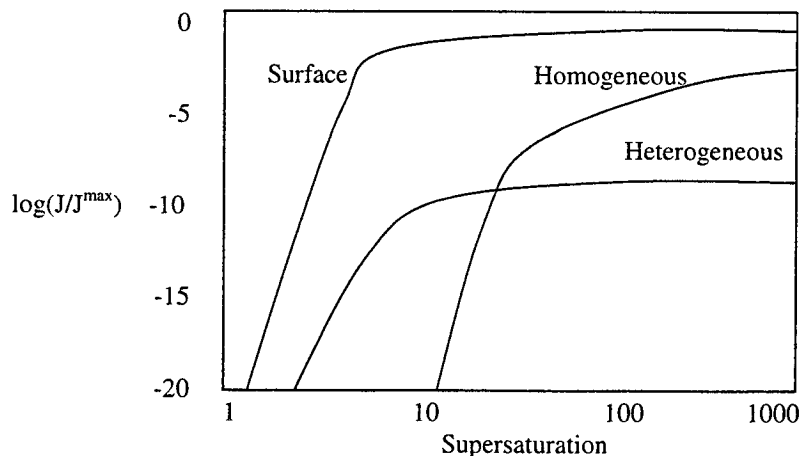


Figure 2.4 Generalised nucleation rate diagram as a function of supersaturation [8]

Both the primary and most of the secondary nucleation processes are activated processes whereas the attrition-induced nucleation process is growth-controlled [7]. It has been estimated that it takes only 10–15 % of the number of nuclei formed in the crystallisation of a highly soluble material via primary nucleation mechanisms to account for 95 % of the mass of the crystalline product (except for the deliberate seeding case) [2].

2.2.3. Crystal Growth

As soon as stable nuclei have been formed in a supersaturated system, they begin to grow into crystals of visible size. Any accurate analysis of the growth process must consider the combined effects of diffusion and surface adsorption.

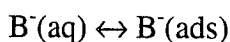
For an electrolyte crystallising from an aqueous solution, the following processes may all be taking place [4]:

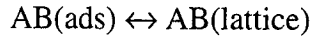
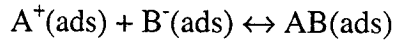
- (1) Bulk diffusion of hydrated ions through the diffusion boundary layer and through the adsorption layer: the process depends linearly on the concentration gradient and inversely on diffusion layer thickness or crystal size [9].
- (2) Surface diffusion of hydrated or dehydrated ions: the distance a particle must diffuse in the adsorbed layer to a kink or growth site depends on crystal size and supersaturation.
- (3) Partial or total dehydration of ions (important for soluble salts only).
- (4) Surface reaction/Integration into the lattice.
- (5) Counter-diffusion of released water through the adsorption and boundary layers.

- ***Growth Mechanisms***

Chiang and Donohue [9] propose two main mechanisms of growth in the case of ionic species. For systems that can grow by both mechanisms, it is the fastest mechanism that determines the growth rate but it is the slowest step in that mechanism that controls the growth rate.

1. Surface Reaction/Molecule Integration





II. Sequential Ionic Integration

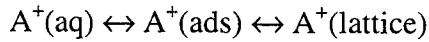


Figure 2.5. describes the main theories for the actual integration step [2, 3]:

- (a) *The Kossel–Frank theory (continuous growth model)*: the stepwise growth of a mononuclear layer is assumed to take place on the rough surface of the crystal; the growth unit will integrate at a site of the lowest binding energy for its orientation (step, kink or vacancy).
- (b) *The birth-and-spread theory (surface nucleation model)*: in the absence of steps and kinks, two-dimensional nucleation occurs on a smooth surface by adsorption of single molecules; thus, a cluster called a two-dimensional island nucleus is formed and subsequently spreads rapidly (due to lower energy requirements). This mechanism is not favoured at low supersaturations.
- (c) *The Burton-Frank-Cabrera (screw dislocation model)*: in crystals containing defects, the angular velocity of step progression near the corner of the defect is faster than at the edge, creating a dislocation that propagates in a spiral form; the addition of a growth unit not only fills a kink site but creates another which is favourable to growth. This mechanism enables a continuous vertical growth without the interruption of the previous two mechanisms and explains also the growth rate at low supersaturations.

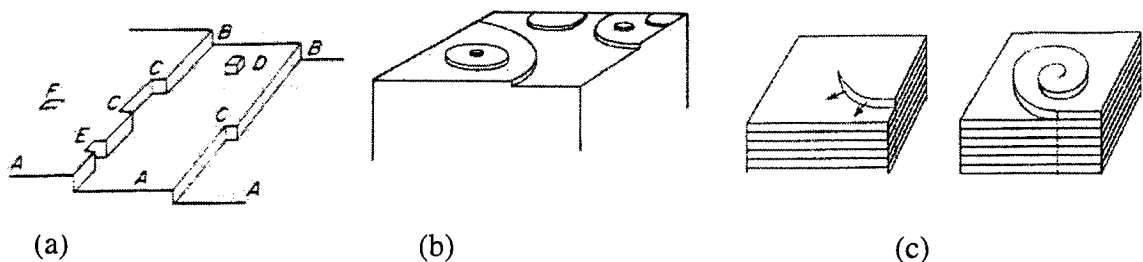


Figure 2.5 Growth models: (a) Kossel – Frank; (b) Birth-and-spread; (c) BFC [3]

- **Growth Rate**

The rate of crystal growth is controlled by a number of physical processes. The rate-limiting step is system-dependent (e.g. temperature, agitation rate, reactor type) and can vary from diffusion-controlled growth to chemical reaction (integration)-controlled growth. These two stages, occurring under the influence of different concentration driving forces, can be represented by the equations:

$$dm/dt = k_d A(c - c_i) \quad (\text{diffusion}) \quad (2.23)$$

and
$$dm/dt = k_r A(c_i - c^*) \quad (\text{reaction}) \quad (2.24)$$

where dm/dt is the growth rate (mol/s); k_d is a mass-transfer coefficient ($\text{mol}\cdot\text{s}\cdot\text{m}^{-1}$); k_r is the rate constant for the integration process ($\text{mol}\cdot\text{s}\cdot\text{m}^{-1}$); A the surface area of the crystal (m^2); c the solute concentration in the supersaturated solution; c_i solute concentration in solution adjacent to the crystal surface and c^* equilibrium saturation concentration (all in mol/m^3).

By considering $(c - c^*)$ an “overall” concentration driving force easier to be measured, a general equation for crystallisation can be written:

$$G = dm/dt = K_G A(c - c^*)^g \quad (2.25)$$

K_G ($\text{mol}\cdot\text{s}\cdot\text{m}^{-1}$) is the crystal growth coefficient and g is the kinetic order of growth.

For most sparingly soluble substances, the growth rate is generally of second order even at high supersaturations, whereas for soluble salts the growth rate follows the first-order dependence [9].

Because crystals are sized based on diameter (or length) rather than mass, the growth rate is usually cast in a form indicating the progression of L , the mean crystal size (m):

$$G = dL/dt = K_G(c - c^*), \quad (\text{m/s}) \quad (2.26)$$

K_G can be expressed as:

$$K_G = (k_d k_r)/(k_d + k_r) \quad (2.27)$$

Obviously, when k_r is very large, $K_G \sim k_d$ and the growth process is diffusion-controlled. Similarly, if k_d is large, $K_G \sim k_r$ and the process is reaction-controlled.

2.2.4 Factors Affecting Crystal Quality

- **Supersaturation**

The degrees of dependency of growth rate G and nucleation rate J on supersaturation are different. The critical parameters ΔG_{crit} and r_{crit} decrease when supersaturation is increased, translating to faster nucleation rates [10]. Similarly, higher concentration driving force (i.e. supersaturation) enables faster growth rates. In general, G is proportional to S^{1-2} whereas J is proportional to S^{6-12} . Based on this, two distinctly different precipitation regimes can be defined (Figure 2.6) [11]. For $S < S^*_{\text{hom}}$, growth dominates and well-grown crystals are expected to be produced, provided that seed is used. On the other hand, for $S > S^*_{\text{hom}}$, homogeneous nucleation prevails and colloidal (or very fine) particles are produced.

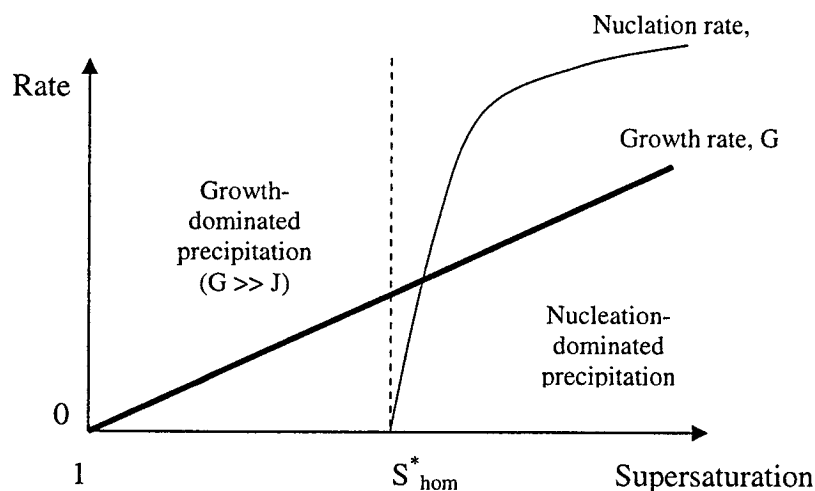


Figure 2.6 Precipitation regimes as a function of supersaturation magnitude [11]

- **Impurities**

The presence of impurities in a system can considerably affect nucleation behaviour [5]. The higher the charge on the impurity cation, the more powerful the inhibiting effect, e.g. $\text{Cr}^{3+} > \text{Fe}^{3+} > \text{Al}^{3+} > \text{Ni}^{2+} > \text{Na}^+$. The heteronuclei are rendered inactive by impurity adsorption on their surfaces. Mullin [3] suggested that if the impurity suppresses primary nucleation, secondary nucleation could occur if the uptake of impurity by the growing crystals is significant. The seed crystal creates an impurity concentration gradient about itself; the concentration of impurity near the crystal surface becomes lower than that in

the bulk solution and if it is reduced enough, nucleation can occur. Another possibility is that certain impurities induce secondary nucleation by adsorbing at defects on existent crystal surfaces and initiating crack propagation and subsequent fragmentation.

Impurities can influence crystal growth rates in a variety of ways. They can change the structural properties of solutions or the equilibrium saturation concentration and hence the supersaturation; as explained in the previous section, any change in supersaturation will affect both the nucleation and growth rate. Impurities are often adsorbed selectively on to different crystal faces and retard their growth rates, modifying thus the crystal habit. The effect of impurities results from two effects of adsorption on the surface of the growing crystal: the adsorption of additives generally decreases the interfacial tension, providing thus greater surface nucleation in the birth and spread mode of growth; the same effect narrows the step packing in the BCF model. In each case growth rate is increased. On the other hand, impurity adsorption would block active sites, thus reducing growth rate [2]. It is generally accepted that the impurity uptake increases at high supersaturations, but it was also reported [12] that the retarding effect of an impurity (generally a surface reaction) becomes weaker at high supersaturations due to a change of the rate-determining step of growth from surface integration to volume diffusion control.

- ***Organic additives***

Of particular interest for this work are the organic compounds present in solution. Large molecules of tailor-made additives and polyelectrolyte impurities adsorbed on the surface are considered to be practically immobile; the coverage of potential growth sites is fast even at low concentrations of organic and growth is retarded [13, 14]; possible modification of the crystal habit results [15]. Some organic additives act as “stabilisers”, affecting nuclei surface free energy by adsorption and also changing the microscopic structure of growth solutions (via functional groups). For instance, the addition of 5% (vol/vol) ethanol to a saturated solution of KH_2PO_4 (potassium dihydrogen phosphate, KDP) retarded the homogeneous nucleation by prolonging the induction period (since $J \sim 1/t_{\text{ind}}$), as compared to that of a pure KDP solution [16, 17].

Barata and Serrano [18] also conducted SDC tests by crystallizing KDP with various alcohols (ethanol, propanol, 2-propanol). They reported that the organic does not affect the kinetic order of growth process (i.e. $g = 1$ in Eq. 2.25) but increased alcohol content and higher surface entropy factors induced smoother surfaces and consequently lower mass deposition rates for all three cases. When the effect of the type of alcohol on the growth process was analysed, the size of alcohol molecules, the dielectric constant of the solution and the adsorption of alcohol molecules on the crystal surface were considered. The influence of ethanol and propanol on the mass deposition rate was similar, whereas lower values were obtained for 2-propanol. This was explained in terms of preferential adsorption of 2-propanol molecules on the active growth sites of the KDP crystal.

Similarly, Oosterhof *et al.* [19] observed that the growth rate of sodium nitrate from water-isopropoxyethanol mixtures decreased with increasing IPE fraction but the kinetic order of growth and the crystal habit were not modified.

- **Agitation**

Hydrodynamics have a significant impact on the resultant product from a crystallisation system. During agitation, two forms of mixing predominate: macromixing and micromixing. Solids suspension and overall circulation are governed by macromixing; micromixing involves contacting and mixing at a molecular level. Micromixing can greatly influence nucleation and growth processes by decreasing the thickness (i.e. resistance) of the diffusion layer and improving the mass transfer process. The effect of stirring is more pronounced the more concentrated are the solutions being mixed. Studies on precipitation of aluminum-potassium sulphate by various alcohols have indicated that the product crystal size is largely affected by the physical properties of alcohols, particularly by the viscosity, which influences the micromixing process [20]. As the precipitating agent is added to solution, a good micromixing is required in order to avoid formation of “pockets” of high supersaturation at the interface between the aqueous solution and the organic.

At low agitation rates (usually < 400 rpm for bench-scale reactors), a barrier to the process at the molecular level exists; this results in an increase of the induction periods and fewer nuclei formed at any supersaturation value (i.e. lower nucleation rate).

Moreover, mother liquor solution is incorporated in the crystals during growth [20, 21]. The increase of the agitation intensity promotes a reduction of the induction periods, thus increasing the nucleation rate and favouring the mass deposition rate (i.e. growth). However, for very high agitation intensities (> 500 rpm) the large degree of entropy transmitted to the growing crystals hinders additional mass deposition; moreover, fracture and attrition processes become predominant, resulting in a broad crystal size distribution.

2.3. Solvent Displacement Crystallisation

The process of crystallisation from a supersaturated solution requires that solvated ions partially desolvate and then associate to form ion pairs that eventually will precipitate. Addition of low-boiling point, water miscible organic solvents to aqueous solution favours this desolvation-ion association process through effects described below.

The activity of water in multi-component aqueous and aqueous-organic solutions is an important parameter in understanding the salting out mechanism and subsequent crystallisation of salts; it describes the behaviour of “free water”. Since the ions are soluble in “free water” only, any change in solution composition that results in decreasing the water activity will influence the solubility of the dissolved solute. For example, the addition of inorganic acids, their salts [22] and/or organic compounds [23] in aqueous solutions result in a marked decrease in water activity.

2.3.1. Salting Out Effect

One of the ways by which a solution can be made supersaturated, with respect to a given solute, is by the addition of another miscible liquid phase (organic solvent) that reduces the solubility of the solute in the initial solvent and causes precipitation/crystallisation. The process is commonly referred to as “salting out”, although it applies to inorganic and organic salts alike. Figure 2.7 exemplifies the relationship between salt solubility and organic content for some common salts in methanol-water mixtures at 20°C.

The separation technique based on this phenomenon is designated as “*Solvent Displacement Crystallisation*” (SDC) and enables the separation of salts from their

aqueous solutions by precipitation and filtration. The organic is recovered for reuse by low-temperature distillation or other techniques. The characterisation of an experiment by salting out means an increase in the activity coefficient of the electrolyte with increasing organic solvent concentration or, inversely, a decrease in water activity.

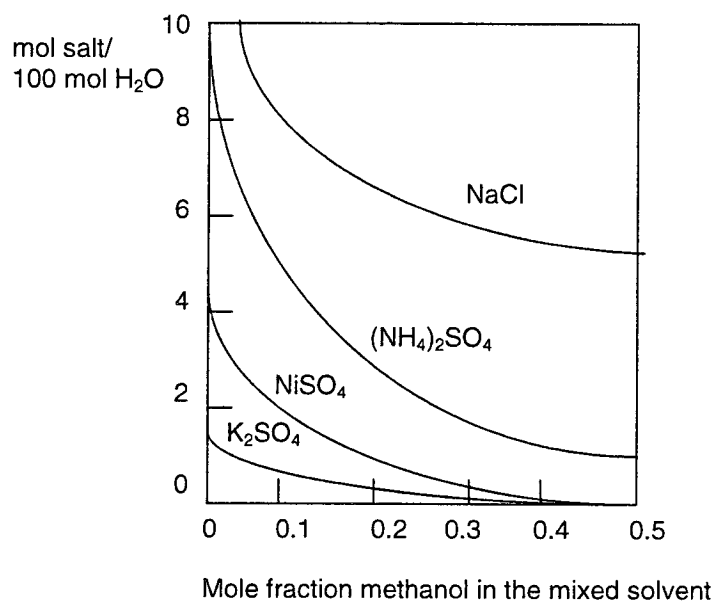


Figure 2.7 Solubility of salts in water-methanol mixtures at 20°C [4]

Schneider [24] reviews the main theories developed over the time to explain salting out phenomena.

- A. Hydration theories treated the solute as a substance soluble only in “free water”, i.e. the water that is not bound to the hydration shell of the ions or to other substances. It was also suggested that the specific effects of water-miscible organic solvents (MOS) on the salt solubility might be explained by the dipole orientation of the water molecules in the hydration shell and by the dipole orientation toward the organic solvent.
- B. Electrostatic theories (involving also van der Waals forces) consider the size of solvated ion and the charge distribution within the hydration sphere when calculating its mutual electrostatic energy with the surrounding ions and water molecules. It was predicted that salting out occurs when the dielectric constant of solution is decreased below a certain limit by the organic.

- C. Thermodynamic theories explain the salting out as a modification of thermodynamic properties of pure water (such as compressibility and thermal expansion coefficient) upon addition of a miscible organic.

Alfassi and Mosseri [25] described this process as a competition between the inorganic salt and the polar organic solvent on the water molecules on one hand and of preferential bonding between MOS and water on another hand. Alfassi [26] has found that the solubility of a solute in a homogeneous mixture of water and MOS can be empirically represented as a function of the MOS concentration by:

$$S = S^w \exp(-\lambda f), \text{ (g/L)} \quad (2.28)$$

where S^w is the solubility in pure water (g/L), f is the volume fraction of MOS and λ is a constant characteristic of the salt and the solvent termed “the precipitating constant”.

Neglecting the change of volume with mixing, the fraction of salt precipitated by the addition of V mL of MOS to 1 mL of saturated aqueous solution is given by:

$$P = S^w \{1 - (V + 1) \exp[-\lambda V / (V + 1)]\}, \text{ (g)} \quad (2.29)$$

This is a maximum type function; increasing V always leads to a smaller solubility per unit volume but a larger volume of solution. The maximum fraction of salt that can be precipitated is obtained for $V = \lambda - 1$:

$$P_{\max} = 1 - \lambda \exp(1 - \lambda) \quad (2.30)$$

One important conclusion of these equations is that if $\lambda \leq 1$ for a salt–MOS system, no precipitation occurs when the MOS is added to the aqueous solution ($P_{\max} = 0$). On the other hand, for a $\lambda = 10$, $P_{\max} = 0.999$, meaning that all the salt was precipitated.

2.3.2. The Hydrogen Bond

The hydrogen bond is a type of intermolecular force between strongly charged dipoles located on different molecules or different parts of one large molecule; one part of the bond involves a hydrogen atom. The hydrogen must be attached to a strongly electronegative heteroatom, such as oxygen or nitrogen, the hydrogen-bond **donor**. This

electronegative element has the effect of removing the electron cloud surrounding the hydrogen nucleus, leaving it with a very strong positive charge density. A hydrogen bond involves the positive proton (hydrogen nucleus) becoming attracted to the lone pair of electrons on another heteroatom, the hydrogen bond **acceptor**. These two elements each have strong, opposite charges, which is why the hydrogen bond is so stable (e.g. in water the intermolecular hydrogen bond is of 23 kJ/mol) [27, 28]; hydrogen bonds are one order of magnitude weaker than the ionic bond.

The simplest example of a hydrogen bond is found in the interaction among water molecules, which contain two hydrogen atoms and one oxygen atom (H – O – H). The oxygen of one water molecule has two lone pairs of electrons, each of which can form a hydrogen bond with hydrogen on two other water molecules. This can repeat so that every water molecule is H-bonded with four other molecules, forming tridimensional clusters (Figure 2.8).

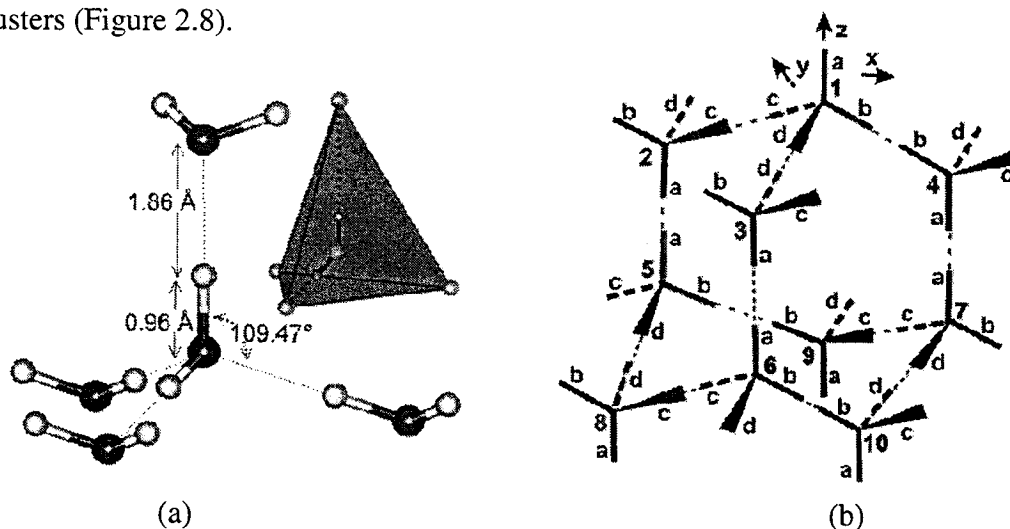


Figure 2.8 Hydrogen-bonded structures in water: a) tetrahedral structure; b) cluster [27]

Liquid water's unusual properties (e.g. values for boiling point, thermal conductivity, dielectric constant and surface tension) are explained by the presence of the hydrogen bonds that form a short-range ordered “glass-like” structure. The strength of the hydrogen bond rapidly decreases with temperature [29]; the energy required for breaking the bond is 9.80 kJ/mol at 25°C [30].

Polar protic organic solvents (e.g. alcohols, aldehydes and ketones, carboxylic acids and amines) contain electronegative heteroatoms and in consequence these interact

with water forming strong hydrogen bonds; this accounts for the solubility (miscibility) of these compounds in water. The solubility depends on the balance between the size of the alkyl chain (hydrophobic) and the electronegative - OH or - NH₂ part (hydrophilic). If the alkyl chain is small, as in C1 – C4 series, the organic is freely soluble in water; inversely, the larger the alkyl chain, the lower the solubility.

This ability of low-molecular polar organic solvents to break the water structure and establish preferential hydrogen bonds with water molecules when added to electrolyte solutions accounts for the salting out effect and crystallisation of salts.

2.3.3. Solvent Effects and Solute-Solvent Interactions in Aqueous-Organic Mixtures

Water is almost exclusively used as the solvent of choice for the industrial crystallisation of inorganic substances from solution. As explained above, the existence of hydrogen bonds and establishment of a short-range structural order explain its unusual properties; the presence of a solute in water alters its properties profoundly.

In aqueous solutions of electrolytes the electrostatic forces exerted by the ions lead to a local disruption of the hydrogen-bond structure. In the primary hydration sphere, containing dipole oriented water molecules, the four hydrogen bonds orientate themselves in such a manner as to one hydrogen bond points toward the bulk solution and three bonds straddle the surface of the solute [31]. For monovalent ions, the hydration number N (i.e. number of water dipoles in the first hydration sphere) is most probably 4, $N \sim 6$ for divalent ions and $N \sim 8-9$ for trivalent [4, 32]. There is also a much larger region around the ion that contains loosely bound, non-orientated water, known as “secondary hydration sphere”.

When water-miscible organic solvents are added to the electrolyte solution, they modify the structure, properties and behaviour of water, leading to changes in the mobility and solvation of inorganic ions. In order to be miscible, the organic must break the water bonds and replace them with bonds of similar strength, i.e. hydrogen bonds. Franks [33] studied the excess enthalpies of mixing of alcohols and water at 25°C (Figure 2.9). The negative enthalpies are generally explained in terms of preferential hydrogen bonding between alcohol and water at the expense of the bonds among water molecules

(i.e. there is decrease in the number of “free water” molecules that would be available to hydrate a potential electrolyte dissolved in the mixture).

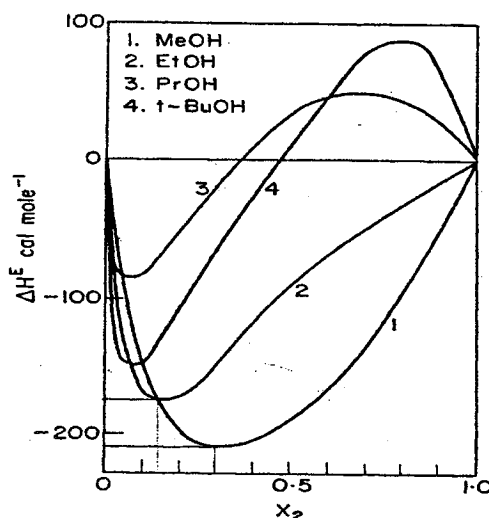
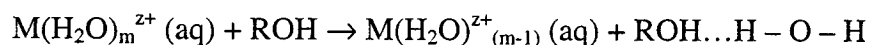


Figure 2.9 Excess enthalpies of mixing of alcohols and water at 25°C [33]

The positive trend for propanol and tert-butanol in the organic-rich regions denote a molecular aggregation process characteristic for longer-chain alcohols, where clusters of organic are formed due to hydrophobic interactions between the alkyl groups [34].

The proposed general mechanism is that the molecules of organic solvent will gradually remove the water from the solvation sheaths:



It can be thus inferred that the addition of polar organic molecules to aqueous solutions of electrolytes will lead to capturing part of water molecules and subsequently reducing the solubility of salt. This complex process can be deconstructed and studied by investigating separately: (1) water-alcohol interactions [35, 36] and (2) alcohol-hydrated ions interactions [37].

• *Water-Alcohol Interactions*

When alcohols are added to a solution, their molecules disrupt the water structure by breaking the water-water hydrogen bonds and replacing them with alcohol-water hydrogen bonds. At very low alcohol concentrations, the overall water structure is

conserved, but alcohol molecules begin to insert themselves into the clusters (Figure 2.10-a). They are monomolecularly dispersed and surrounded by water molecules. With an increase in alcohol mole fraction, the inherent water cluster structure is disintegrated; the number of alcohol molecules in the cluster is increased and it is considered that molecules of organic and water form a kind of layer structure (Figure 2.10-b). With further increase in alcohol content, almost all of the water is involved in the hydrogen bonds with the organic; consequently, the organic molecules start to form clusters due to the hydrophobic attraction of the alkyl tails. These clusters trap water molecules and are surrounded by additional hydrogen-bond water molecules (Figure 2.10-c).

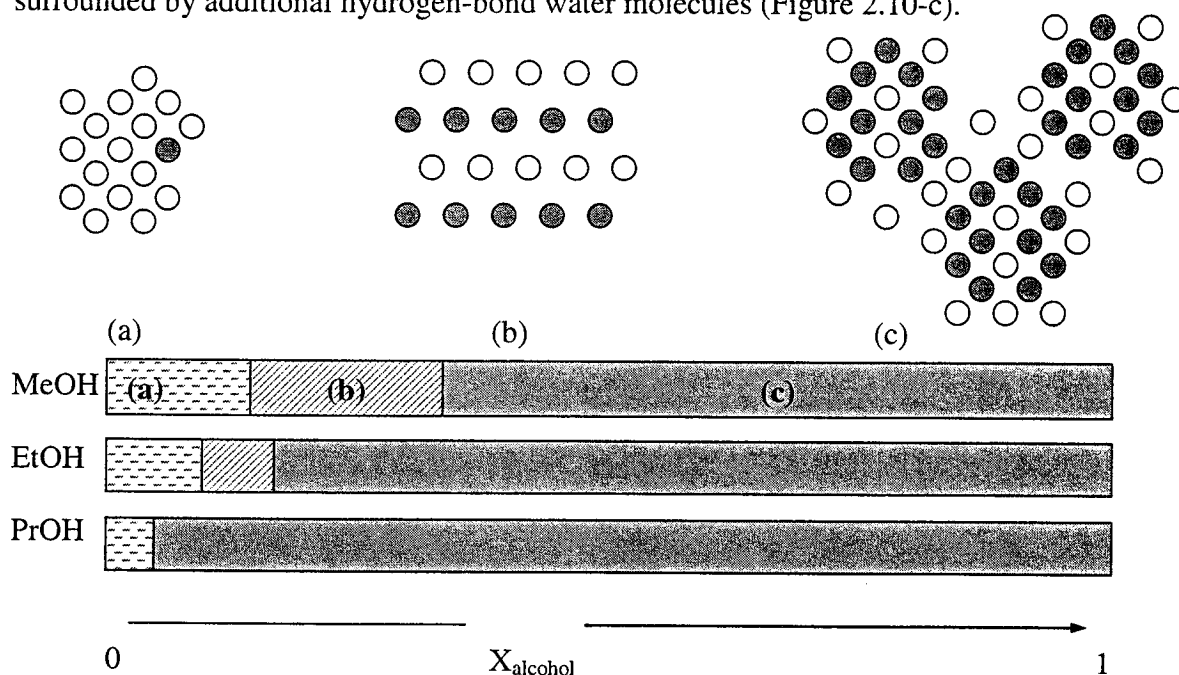


Figure 2.10 Structures forming in water-alcohol mixtures [36]

(a) Water cluster structure; (b) Layer mixed structure; (c) Alcohol self-aggregation.

The longer the alkyl chain, the higher the hydrophobicity; consequently, the disruption of water clusters and alcohol self-aggregation are promoted at lower organic concentrations, as suggested by mass-spectra analysis of alcohols-water mixtures, where regions (a) and (b) decrease in width with increasing alcohol content for the series propanol > ethanol > methanol [36]. A first-hand inference of the above finding is that propanol should be more effective as salting out agent than methanol and ethanol for it binds more water molecules at a lower alcohol level.

- ***Alcohol-Ion Interactions***

As described earlier, solid ionic crystals dissociate completely in solution via a reversible physical interaction when coming into contact with the water molecules. Water dipoles are electrostatically attracted by the solute ions of opposite sign and form a primary solvation sheath around them; there is also a much larger region around the ion that contains loosely bound, non-orientated water, known as “secondary hydration sphere”.

The addition of water-miscible organic solvents such as alcohols to an electrolyte solution triggers considerable changes in the solution structure and chemistry. The effect of these solvents has been studied by measuring the amount of solvent transported into the cathode region of a transference cell relative to the amount transported to the anode region using ethanol-water-electrolyte solutions [37]. The relative amount of organic increased with increasing weight percent of the alcohol. For low organic concentrations (10-20% weight of alcohol, depending on the alcohol structure), the secondary hydration layer of the cation is in the process of being displaced by the organic solvent. As the alcohol content increases, a maximum is reached and the quantity of solvent transported to the cathode decreases in the region 20-40% wt. organic; this decrease is explained in terms of the smaller outer hydration shell of the anion being disrupted (i.e. no more alcohol is associated with the cathode for the moment). The process continues by removing the remaining water molecules from the primary hydration sphere of the anion and finally, for organic contents > 50% wt., the inner hydration shell of the cation is attacked. The rather rapid displacement of water from the cation's first hydration shell is evidenced by a marked increase in the relative amount of organic transferred; at high organic concentrations, the water is completely removed from the hydration shells of the ions.

- ***Dielectric Constant of Solution***

Lee [38] defines three possible types of ion pairs existent in solution: contact ion pairs (CIP), solvent-shared ion pairs (SShIP) and solvent-separated ion pairs (SSIP). As the organic is added and removes water molecules, first from the bulk and then from the hydration spheres, the number of SSIP decreases and more SShIP and CIP appear as precursors to completely un-solvated ion pairs that will crystallise out.

The solubility of substances and chemical reactions which take place in various solvents depend to a great extent of the dielectric constant of the medium. This can be seen from the expression of the coulomb force that exists between two charged ions in solution:

$$F = (e_1 e_2) / (\epsilon r^2) \quad (2.31)$$

where e_1 and e_2 are electrical charges (C), r the distance between them (cm) and ϵ the dielectric constant.

When e_1 and e_2 are of opposite charge, the attraction between them decreases as ϵ increases, so the larger the dielectric constant of a certain solvent, the higher its ability to dissolve ionic solids will be. Hence, small, highly charged ions and solvents having high ϵ will exhibit the strongest attraction for one another and form strong, stable solvates. The opposite relationship is responsible for the precipitation of salts, since solvents with low ϵ cannot overcome coulomb forces [39]. The dielectric constant of a solvent reflects its polarity (orientation of the dipoles along an externally applied electric field, resulting in polarisation of the molecule) and it correlates to its molecular weight. The longer the alkyl chain of the organic (i.e. the more hydrophobic the character and the higher the molecular weight) the lower the dielectric constant will be [40] (Figure 2.11, for 25°C). On the other hand, to insure that the organic is miscible with water (i.e. able to form hydrogen bonds) the hydrophobic character must not surpass the hydrophilic one.

Hence the means by which organic solvents affect the solvation of ions is the decrease of the dielectric constant of solution (ϵ) by breaking the water-water hydrogen bonds [29]. For example, for pure water $\epsilon_w = 78$ while for methanol it is 32.6. Wang and Anderko [41] explain this process in terms of solvation effects. As the organic is added, it breaks the hydrogen bonds between water molecules and replaces them with stronger bonds, thus immobilizing the water molecules, which become unable to be oriented in the external electrical field. These water molecules do not contribute anymore to creating the effective dipole moment of the system, causing a decrease of the dielectric constant.

The behaviour of water dielectric constant in the presence of organic solvent has been reported for a large variety of mixtures [41, 42]. The influence of temperature for H₂O-CH₃OH mixtures is shown in Figure 2.12.

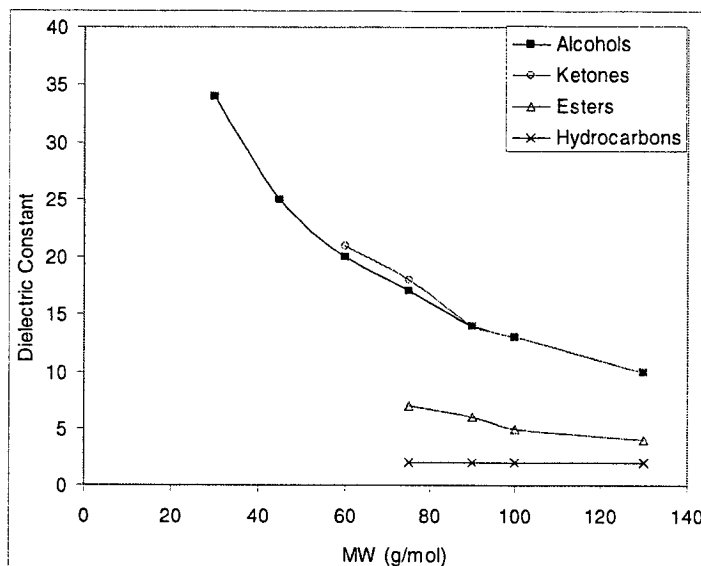


Figure 2.11 Dependence of dielectric constant on molecular weight of organic [40]

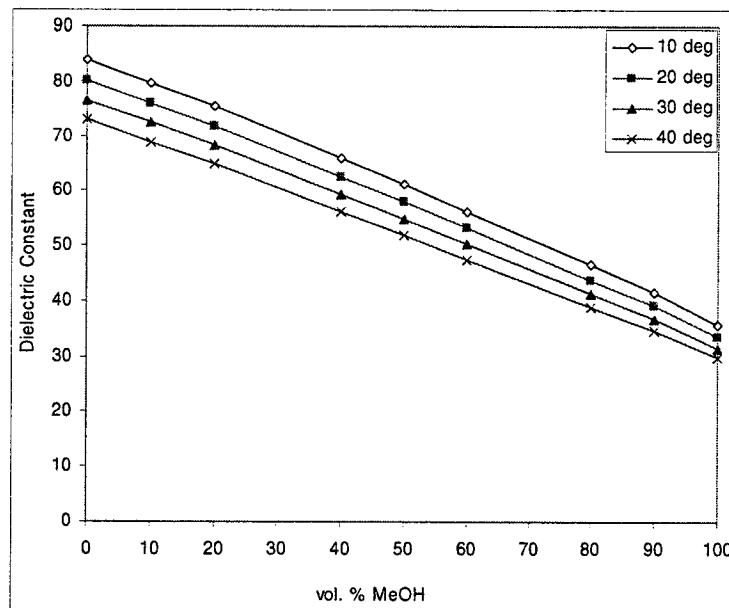


Figure 2.12 Dielectric constants for water-methanol mixtures [41]

Elevated temperatures cause a decrease in dielectric constant by diminishing the strength of the hydrogen bonds and ultimately breaking them via increased Brownian motion and higher energy, as explained by Nezbeda [31].

As previously explained, the decrease of ϵ in solution upon addition of organic correlates to the increase of the electrostatic interaction between ions of opposite

charges; this favours ionic association (the formation of SShIP and CIP). For each ϵ value, there is a critical distance d_{cr} for which the electrostatic interaction energy to separate ions equals the mean kinetic energy of the charged ions. Below d_{cr} ions cannot be separated and start forming CIP; when $\epsilon < 40$, the formation of CIP generally predominates throughout of solution [43]. This finding is confirmed by the work of Das and Rath [44], who calculated the free energy of formation of ion pairs of $Sr(NO_3)_2$ and $Cd(NO_3)_2$ in aqueous-organic solvents from conductance data. It was determined that the ion pairs are in a lower free energy state in the aqueous-organic mixture than water, suggesting that the ion pair formation is favoured by decreasing the dielectric constant of the medium (i.e. when the organic content is increased). The more efficient an organic is in breaking the water structure, the lower the dielectric constant of the mixture will be. Similar conclusions have been drawn by studying the thermodynamics of $CdCl_2$ and $CdBr_2$ in aqueous-organic mixtures [45].

Lyashchenko and coworkers propose a very clear model that correlates the behaviour of ions in solution to the gradual change in the dielectric constant when an organic solvent is added [46, 47]. In aqueous solutions of electrolytes, part of the water molecules are immobilized in the ions' hydration shells but the bulk of solution retains the tetrahedral water structure; the dielectric constant of solution is high ($\epsilon \sim 70$) and the predominant species are individual ions and possible SSIP uniformly distributed throughout the solution (Figure 2.13 a).

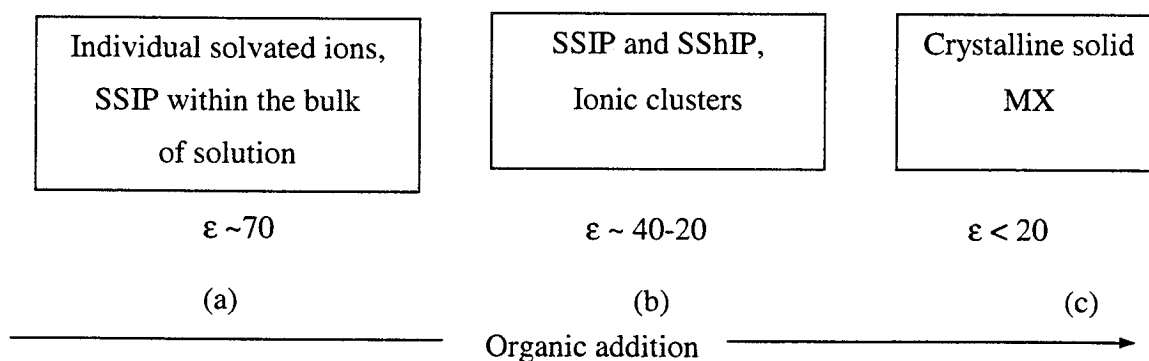


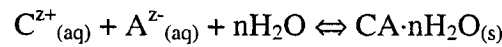
Figure 2.13 Dielectric constant-related transformations in aqueous solution [46]

As the organic solvent is added, it breaks the hydrogen bonds between water molecules; consequently, the bulk tetrahedral water structure starts disappearing and the dielectric

constant decreases even more ($\epsilon \sim 40-20$). SSIP and SShIP become predominant species and more complex ionic clusters are stable (Figure 2.13 b). When the water molecules are displaced from the primary hydration shells, the dielectric constant becomes extremely low ($\epsilon < 20$), CIP form and crystallise out from solution (Figure 2.13 c).

- **Water Activity in Aqueous-Organic Mixtures**

The activity of water in multi-component aqueous and aqueous-organic solutions is an important parameter in understanding the salting out mechanism and subsequent crystallisation of salts; it describes the behaviour of “free water”. Since the ions are soluble in “free water” only, any change in solution composition that results in decreasing the water activity will influence the solubility of the solute. The crystallisation of an ionic salt from aqueous solution may be represented by the following equilibrium:



The equilibrium constant expressed in terms of activities will be:

$$K = 1/(a_{C^+} \cdot a_{A^-}) \cdot a_w^n \quad (2.32)$$

where K is the equilibrium constant and a_{C^+} , a_{A^-} and a_w are the thermodynamic activities of the cation, anion and water, respectively (activity for the pure solid salt is considered to be equal to 1).

The activity of water in aqueous solutions is defined as [48]:

$$a_w = \gamma_w X_w = f_w/f_w^0 \quad (2.33)$$

where a_w is the water activity, X_w is the mole fraction of water, γ_w is the activity coefficient for water and f_w , f_w^0 are the fugacities (kPa) of water in the system and at reference conditions, respectively.

Under normal conditions it is assumed that gas phases behave ideally, so the ratio of fugacities can be taken as ratio of partial pressures, so that:

$$a_w = f_w/f_w^0 = p_w/p_w^0 = RH/100 \quad (2.34)$$

where p_w and p_w^0 are the vapour pressures (kPa) of water in the system and of pure water at the same temperature, respectively, and RH is the percent relative humidity of the air layer in equilibrium with the sample.

From the previous formulae can be concluded that water activity in a crystallisation medium can be modified by changing the composition of solution via addition of organic solvents, which influence both the mole fraction and partial pressure of water. The decrease in water activity upon addition of various organic compounds (solid or liquid state) is a well-known process that has been studied by numerous authors. Thus, Na et al. [22] measured the water activity in supersaturated aqueous solutions of some amino-acids of importance in biochemistry whereas Sereno et al. [49] observed water activity decrease in aqueous solutions of glucose and sucrose.

More relevant to our research topic, the influence of low molecular weight alcohols on water activity has been reported by Hansen and Miller for ethanol and 1-propanol [50], Udoenko and Mazanko for 2-propanol [51], Zhu et al. for methanol and 2-propanol [52] and Degn and Frigaard for various solvents [53]. Because of its comprehensive character, the latter reference has been selected to provide a graphic demonstration of the influence of organic fraction on water activity in binary mixtures at 25°C (Figure 2.14); it can be observed that water activity decreases and organic activity increases with organic mole percent.

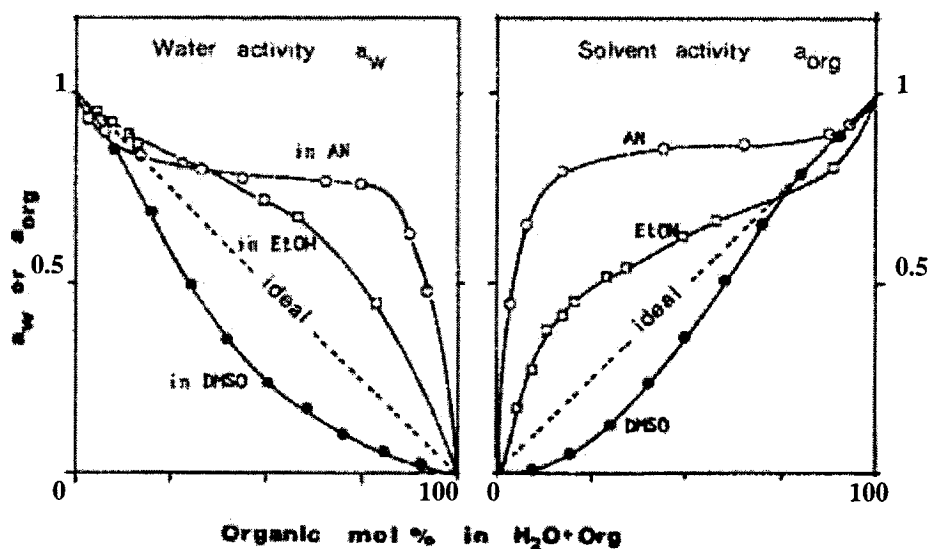


Figure 2.14 Water and organic activities in aqueous-organic mixtures at 25°C [53]

The broken line represents Raoult's law reference line describing ideal behaviour. The increasingly positive deviations with larger molecular weight may be attributed to higher hydrophobic interaction in the solution resulting from the greater volume and surface area of the cavity created in water by more voluminous alkyl groups.

2.4. Examples of Solvent Displacement Crystallisation Applications

The SDC technique is common practice in organic and analytical chemistry for the recovery of dissolved solids from solution and is frequently used for commercial purification in the biochemical and pharmaceutical industries. The relationship between the decrease of inorganic salt solubility and addition of organic solvents is well documented by Seidell and Linke in their exhaustive compilation of solubility data [54].

Despite its potential wide range of uses in inorganic processing and hydrometallurgy, there has been no systematic investigation of this technique as it applies to the removal of metal salts from aqueous solutions, neither from a fundamental perspective nor from the standpoint of application to hydrometallurgical processes. Only relatively few laboratory applications have been studied and reported in the literature; the overwhelming majority of the research work involves the sulphate system, most probably due to the importance of this system in the inorganic and metallurgical fields and also to the fact that the sulphate salts are more amenable to the SDC technique.

2.4.1. SDC Applied to the Sulphate System

In 1979, Alfassi reported methanol, acetone, tetrahydrofuran and dioxane as the most efficient MOS to induce salt precipitation in the system MSO_4-H_2O ($M=Na, K, Mg$). He developed the empirical equation that correlates the fraction of precipitated salt to the volume of organic [26] (see eq. 2.29 in Section 2.3.1 of this Chapter).

In 1984 Alfassi and Mosseri compared the effectiveness of acetone and isopropyl amine in precipitating potassium sulphate, underlined some of the main criteria in selecting an organic solvent and explained the process in terms of competition between the salt and organic for the water molecules [25]. They observed that the precipitated

fraction of K_2SO_4 increased steeply with the organic addition up to a certain point, after which it reached a plateau. For example, an organic-to-aqueous volumetric ratio (O/A) of 0.7 removed ~ 90% of the salt; to reach 99% removal, an O/A of 5 was required.

Various sulphate systems have been investigated during the last decade in conjunction to SDC, but not as much as from a practical point of view but for the purpose of fundamental crystallisation studies in the aqueous-organic mixed systems.

Pina et al. derived [39] equations for evaluating the supersaturation and nucleation rate for isothermal batch salting out crystallisation by studying the solubility and metastability of M_2SO_4 ($M = Na, Li, Rb$ and double salts) in water-methanol systems.

Mullin, Teodossiev and Söhnel [55] studied the nucleation and early growth characteristics of K_2SO_4 under metastable zone conditions relevant to salting out from aqueous solutions by the addition of aqueous acetone. They determined that diluting the organic with water has beneficial effects on crystal quality since it avoids excessive supersaturation (hence homogeneous nucleation) in the regions of primary contact and offers a better process control.

Barata and Serrano studied extensively the salting out precipitation of potassium dihydrogen phosphate (KDP) with different organic solvents (e.g. ethanol, 1-propanol, 2-propanol) by investigating the precipitation mechanism [56], the influence of agitation intensity on induction periods and crystal quality [57], the growth kinetics and factors that affect it [17]. They also related the precipitation yield and characteristics of the final product to the operational variables (i.e. supersaturation, agitation intensity and type of organic) [58].

Similarly, Jianzhong et al. [15] studied the effect of different alcoholic additives on the nucleation of KDP from aqueous solutions. Induction periods as a function of supersaturation were measured, the surface free energy, Gibbs free energy and the radius of critical nuclei were calculated and the effect of the additives on crystal growth was discussed.

Potential applications of SDC to hydrometallurgical systems have been reported only relatively recently but the studies were not expanded beyond the laboratory scale. Research conducted by Cohen [59] in mid-eighties suggested for the first time that a SDC process could be developed that would recover copper sulphate from ore leaching streams

and nickel sulphate from bleed-off electrolyte in copper electrorefining with less energy consumption.

- *System $\text{CuSO}_4\text{-H}_2\text{O-H}_2\text{SO}_4$*

The solutions studied simulated aqueous streams in copper leaching processing containing 5 g/L Cu, 1g/L Fe^{3+} and ~1.8 g/L H_2SO_4 . Copper sulphate was precipitated by the addition of different organic solvents (acetone, 2-propanol, tetrahydrofuran) to the leach liquor. Of the solvents investigated, acetone was the most effective in depressing Cu solubility; by adding 60% (vol/vol) acetone to the aqueous solution, 92% of the copper was recovered as $\text{CuSO}_4\cdot 5\text{H}_2\text{O}$ of 99.3% purity (Figure 2.15 a).

- *System $\text{NiSO}_4\text{-H}_2\text{O-H}_2\text{SO}_4$*

SDC can be successfully employed to remove Ni from Cu ER spent electrolytes, becoming thus an attractive alternative to the conventional method of evaporative crystallisation. Cohen worked on synthetic solutions that reproduced the actual composition of decopperised electrolytes (16 g/L Ni, 10 g/L As, 0.5 g/L Cu, 200 g/L H_2SO_4). From the solvents tested (i.e. tetrahydrofuran, 2-propanol, methyl acetate), 2-propanol was selected as being the most effective at depressing Ni solubility; by adding 75% (vol/vol) 2-propanol to the aqueous solution, 67% of the nickel was recovered as $\text{NiSO}_4\cdot 6\text{H}_2\text{O}$ of 99% purity (Figure 2.15 b).

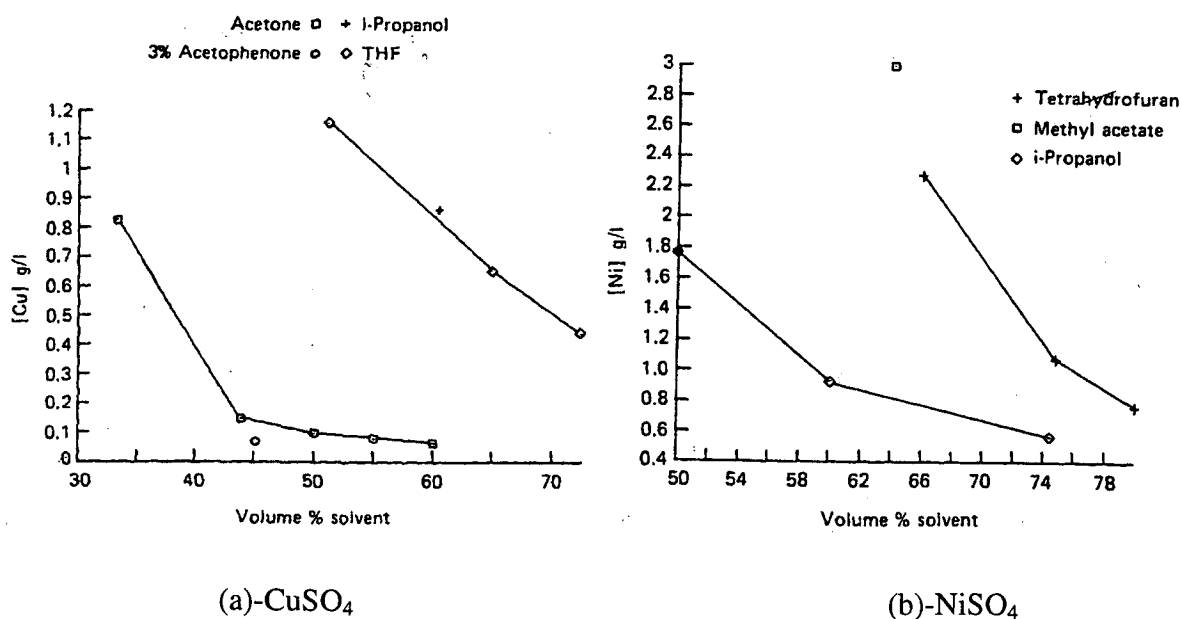


Figure 2.15 Metal solubility in aqueous-organic solutions at 20°C [49]

Both solvents had good recovery yields via fractional distillation (94% for acetone and 98% for 2-propanol). Cohen also addressed process considerations in terms of energy savings and cost-efficiency in employing low-boiling point organic solvents to crystallise copper and nickel sulphates from acidic solutions as compared to the industrial methods (i.e. water removal by evaporative crystallisation).

To investigate the use of alcohols in hydrometallurgical processes, Okada, Zhang and Yazawa [60] conducted an extensive research work in late eighties that studied the solubility isotherms and phase diagrams for the following systems: $\text{CuSO}_4\text{-NiSO}_4\text{-H}_2\text{O-C}_2\text{H}_5\text{OH}$, $\text{CuSO}_4\text{-CoSO}_4\text{-H}_2\text{O-C}_2\text{H}_5\text{OH}$, $\text{Na}_2\text{SO}_4\text{-NiSO}_4\text{-H}_2\text{O-CH}_3\text{OH}$ and $\text{Na}_2\text{SO}_4\text{-CoSO}_4\text{-H}_2\text{O-CH}_3\text{OH}$. Windows that allow a selective fractional crystallisation in these systems were determined and possible applications of the results to practical processes were proposed; more specifically, a treatment technique of spent copper electrolyte was tested. Regarding the latter, it was found that it is possible to produce almost pure crystals of $\text{CuSO}_4\cdot 5\text{H}_2\text{O}$ with the yield ranging 70 to 98%. For a mole ratio of $\text{CuSO}_4/\text{NiSO}_4$ of 0.36 in the mother liquor, between 0.23 and 0.43 kg ethanol/kg water were required to achieve the above-mentioned recovery yields at 35°C. Beyond that organic content, $\text{NiSO}_4\cdot 6\text{H}_2\text{O}$ started to co-precipitate.

In 1998 Sato *et al.* [61] employed ethanol to selectively recover neodymium from rare earth magnet scraps (Figure 2.16).

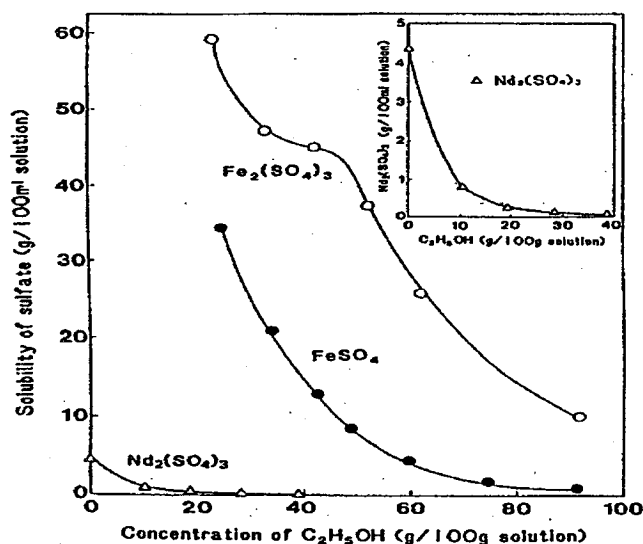


Figure 2.16 Fractional crystallisation of metal sulphates with ethanol [61]

Powders of Nd-Fe sintered magnet scraps were dissolved at 100-120°C in 2.5 M H₂SO₄ and HNO₃ (to promote Fe²⁺ → Fe³⁺ oxidation). The solution, containing 22.8 g/L Nd and 47.3 g/L Fe, was mixed with different amounts of ethanol at 50°C for 24 hr. Neodymium of 93-97% purity was obtained (as Nd₂(SO₄)₃·8H₂O), with yields ranging between 88 and 97% (depending on the ethanol fraction) while Fe³⁺ largely remained in solution. As observed, the product purity decreased with increasing alcohol content due to co-precipitation; the optimum ratio that achieved maximum recovery and purity was ~ 40% (wt.) ethanol.

2.4.2. SDC Applied to the Halide System

The literature data report very few applications of the salting out process to such systems. Generally, most halide salts are more soluble than sulphates in the organic solvents usually employed for crystallisation (e.g. low-molecular alcohols, acetone), making the SDC process economically inefficient or even impossible. This is believed to be due to the smaller halide molecule (as compared to sulphate) and also because of the low or zero hydration numbers of halide ions in concentrated aqueous solutions (hence the water displacement mechanism does not apply). New solvents such as amines have been studied in recent years; they show good promise in salting out halide salts from their aqueous solutions. Since the nitrogen contained in the amine molecule is not as electronegative as the oxygen would be in alcohols, hydrogen bonds formed between N and O from water will be stronger than those between two N atoms; this means that more amine molecules will be available to hydrogen-bond for water displacement.

In 1997 Zijlema *et al.* [62] investigated the suitability of diisopropyl amine (DiPA) and dimethyl-isopropyl amine (DMiPA) as salting out agents for the crystallisation of sodium chloride from aqueous solution. Both amines proved efficient antisolvents for NaCl and reduced its solubility substantially (see Figure 2.17); at amine fractions above 0.7 the salt solubility approached zero but for high organic content the contamination of the crystals increased (solution entrapment) and the size decreased.

Subsequent work evaluated the use of DMiPA to recrystallize pure NaCl from impure NaCl.2H₂O that has been earlier produced by salting out with the same amine [63]. The amine contamination of the crystals decreased from ~1000 ppm to 6 ppm.

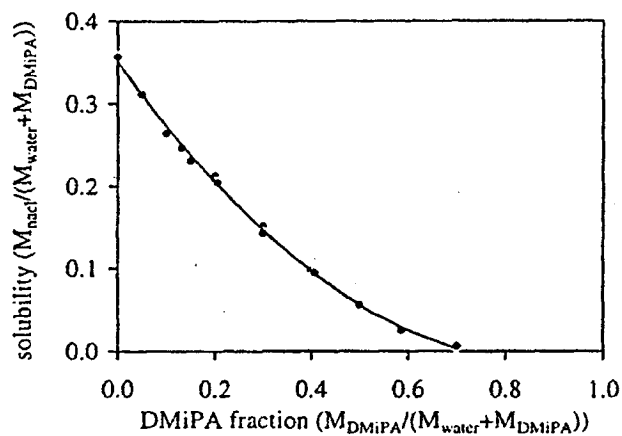


Figure 2.17 NaCl solubility as a function of DMiPA fraction at 5°C [62]

More recently, Bader [64] studied the precipitation of chloride and sulphate salts from aqueous streams by using isopropylamine (IPA) and ethylamine (EA). The measurements targeted the following systems: (1) chloride salts (Ca, Ba, Ca-Na, Ca-K, Ca-Mg, Ca-Sr and Ca-Ba) at 5 g/L total concentration using EA; (2) chloride salts (Sr and Ba) at 5 and 10 g/L total concentration using IPA; (3) combination of calcium sulphate (1 g/L) and calcium chloride (5 g/L) using IPA. Both amines were added in increments of 0.2 organic-to-aqueous (O/A) ratios (vol.), from 0.2 to 2.0. In all systems, the salt precipitation fractions increased with the organic content. The precipitated fractions of different chlorides over the studied range of O/A were nearly identical, for the same O/A. It was found that, for the first two chloride systems, precipitation fractions to be only ~16% to ~60% by both EA and IPA. No selectivity was achieved in the mixed chloride-sulphate system. A ratio of 0.2 O/A precipitated 79% CaSO₄ and 28% CaCl₂, whereas a ratio of 2 removed 99% of sulphate and 62% of chloride.

2.4.3. SDC Applied to Other Systems

Except for sulphate and chloride, other inorganic salt systems have limited applications and use in both chemistry and metallurgy. Consequently, data on salting out of these systems are very limited.

Hull and Owens [65] demonstrated in 1975 that KIO_3 could be selectively separated from a solution containing KI and KIO_3 by the addition of dioxane. Similarly, Alfassi and Feldman [66] used acetone to separate KBrO_3 from a KBr-KBrO_3 mixture. Mosseri and Alfassi [67] studied the separation of the systems $\text{KX-KXO}_3\text{-KXO}_4$ ($\text{X}=\text{Cl, Br, I}$) by employing acetone or acetonitrile. In 1986, Ata and Alfassi [68] investigated the selective separation of nitrates and nitrites of various elements by salting out from aqueous solutions by three miscible organic solvents: acetone, acetonitrile and tetrahydrofuran. All applications are of relevance in radiochemistry.

2.4.4. Extractive Crystallisation

This technique can be regarded as a variation of SDC, in which the crystallisation of salt is induced by the addition of a completely or partly miscible organic solvent capable of extracting water hence causing the solute concentration in the aqueous phase to exceed its solubility and precipitate out of solution. The salt could be readily separated from the remaining solution by filtration and the organic regenerated by simply shifting the temperature, causing thus a phase-splitting into a relatively dry organic phase and salt-depleted aqueous phase. The basic criterion of this process is that the organic must be more hydrophilic at the crystallisation temperature (T_C), thus able to form a homogeneous mixture with the aqueous phase, and more hydrophobic at the regeneration temperature (T_R), inducing phase splitting. T_C could be higher or lower than T_R , and this fundamental choice is dependent on the nature of both the salt and the organic solvent. The most usual organic solvents to be employed when $T_C > T_R$ are oxygenated molecules such alcohols (e.g. 1-propanol, butanol and its isomers), diols, glycols and carbonylic compounds. When $T_C < T_R$ is sought, amines, ketones or ethers can be employed.

Weingaertner *et al.* [69] have assessed the recovery of inorganic salts from concentrated aqueous solution via extractive crystallisation and proposed a process in

which the salts are separated and filtered, the mother liquor is regenerated into two phases by change of temperature and addition of more feedstock, then both liquid phases are recycled (Figure 2.18). Enhanced recovery of salt and economical use of organic were achieved. Thus, NaCl was precipitated from an aqueous solution by adding 2-propanol or diisopropyl amine and Na_2CO_3 was separated by the use of 1-propanol or 1-butanol.

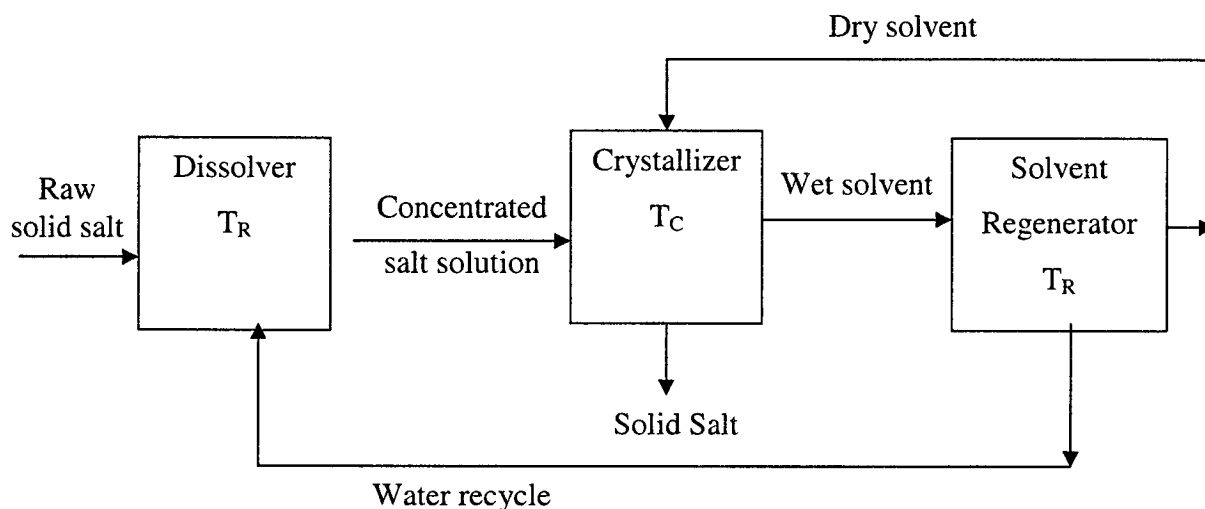


Figure 2.18 Extractive crystallisation process with water recycle step [69]

In 1996, Lynn *et al.* [70] applied the same principle to the recovery of anhydrous Na_2SO_4 from SO_2 -scrubbing liquors that contained a mixture of Na_2SO_4 and Na_2SO_3 . All three organic solvents tested (acetone, 2-propanol and tert-butanol) exhibited similar lower consolute (i.e. complete miscibility) temperatures between 20 and 30°C and water-extraction capabilities in the order acetone > 2-propanol > tert-butanol (due to decreasing hydrophilicity). However, since no selectivity was achieved, it was proposed that the sulphite to be converted to sulphate prior to the extractive crystallisation step.

More recently, Osterhof *et al.* [71] investigated the solubility of sodium carbonate between 40 and 90°C in mixtures with different alkane-diol to water ratios. They chose diols that feature temperature-dependent phase behaviour: the organic and aqueous are completely or partly miscible at a certain temperature and undergo phase separation when the temperature changes, facilitating thus the liquid-liquid separation process. It was found that an organic-to-aqueous ratio of 0.8 of di-ethylene-glycol achieves 99% recovery of sodium carbonate at 80°C.

The same research team proved that sodium nitrate could be successfully separated from solution by the addition of isopropoxyethanol (IPE). The NaNO_3 solubility decreases with increasing amount of IPE and decreasing temperature and [18].

References

- [1]. A.E. Nielsen, "Electrolyte crystal growth mechanisms" *Journal of Crystal Growth*, **67**, pp. 289-310, (1984).
- [2]. A.E. Randolph and M.A. Larson (editors), *Theory of Particulate Processes; Analysis and Techniques of Continuous Crystallisation*, 2nd Ed., Academic Press, Toronto, (1988).
- [3]. K. Sawada, "Mechanism of crystal growth of ionic crystals in solution" in *Crystallisation Processes*, (edited by H. Ohtaki), pp. 39-47, John Wiley & Sons Ltd., Toronto, (1998).
- [4]. J.W. Mullin, *Crystallisation*, 3rd Ed., Butterworth-Heinemann, Oxford, (1993).
- [5]. C.Y. Tai and W.C. Chien, "Effects of operating variables on the induction period of $\text{CaCl}_2\text{-Na}_2\text{CO}_3$ system" *Journal of Crystal Growth*, **237-239**, pp. 2142-2147, (2002).
- [6]. W. Wu and G.H. Nancollas, "Determination of interfacial tension from crystallisation and dissolution data: a comparison with other methods" *Advances in Colloid and Interface Science*, **79**, pp. 229-279, (1999).
- [7]. A. Mersmann and K. Bartosch, "How to predict metastable zone width" *Journal of Crystal Growth*, **183**, pp. 240-250, (1998).
- [8]. J.A. Dirksen and T.A. Ring, "Fundamentals of crystallisation: kinetic effects on particle size distribution and morphology" *Chem. Eng. Sci.*, **46**(10), pp. 2389 – 2427, (1991)

- [9]. P.P. Chiang and M.D. Donohue, "Crystallisation from ionic solution" in *Fundamental Aspects of Crystallisation and Precipitation Processes* (edited by D.M. Briedis and K.A. Ramanarayanan), pp. 8-14, AIChE, New York, N.Y., (1987).
- [10]. C. Mahadevan, D.I. Latha, and V. Umayorubhagan, "Nucleation studies in supersaturated aqueous solutions of magnesium- and zinc-doped nickel sulphate heptahydrate", *J. Indian Chem. Soc.*, **76**, pp. 335-338, (1999).
- [11]. G.P. Demopoulos, "Precipitation in aqueous processing of inorganic materials: a unified colloid-crystallisation approach to the production of powders with controlled properties" in *1st International Conference on Processing Materials for Properties* (edited by H. Henein and T. Oki), pp. 537-540, TMS, Warrendale, PA, (1993).
- [12]. N. Kubota, M. Yokota and J.W. Mullin, "Supersaturation dependence of crystal growth in solutions in the presence of impurities" *Journal of Crystal Growth*, **182**, pp. 86-94, (1997).
- [13]. K. Sangwal, "Effect of impurities on the process of crystal growth" *Journal of Crystal Growth*, **128**, pp. 1236-1244, (1993).
- [14]. G.M. van Rosmalen and P. Bennema, "Characterization of additive performance on crystallisation: habit modification" *Journal of Crystal Growth*, **99**, pp. 1053-1060, (1990).
- [15]. M. Giulietti, M.M. Seckler, S. Derenzo, L.H. Schiavon, J.V. Valarelli and J. Nyvlt, "Effect of selected parameters on crystallisation of copper sulphate pentahydrate" *Cryst. Res. Technol.*, **34**(8), pp. 959-967, (1999).
- [16]. C. Jianzhong, L. Sukun, Y. Fengtu, W. Jiahe and L. Jianming, "Effect of alcoholic additives on the nucleation of KDP and DKDP crystals" *Journal of Crystal Growth*, **179**, pp. 226-230, (1997).
- [17]. V.A. Kuznetzov, T.M. Okhrimenko and M. Rak, "Growth-promoting effect of organic impurities on growth kinetics of KAP and KDP crystals" *Journal of Crystal Growth*, **193**, pp. 164-173, (1998).

- [18]. P.A. Barata and M.L. Serrano, "Salting out precipitation of KDP; III. Growth process" *Journal of Crystal Growth*, **194**, pp. 101-108, (1998).
- [19]. H. Oosterhof, R.M. Geertman, G.J. Witkamp and G.M. van Rosmalen, "The growth of sodium nitrate from mixtures of water and isopropoxyethanol" *Journal of Crystal Growth*, **198/199**, pp. 754-759, (1999).
- [20]. J. Nyvlt and S. Zacek, "Effect of the rate of stirring on crystal size in precipitating or salting out systems" *Collection of Czechoslovak Chem. Commun.*, **51**, pp. 1609-1617, (1986).
- [21]. J.C. Givand, A.S. Teja and R.W. Rousseau, "Manipulating crystallisation variables to enhance crystal purity" *Journal of Crystal Growth*, **198-199**, pp. 1340-1344, (1999).
- [22]. H. Majima and Y. Awakura, "Water and solute activities in the solution systems $\text{H}_2\text{SO}_4\text{-CuSO}_4\text{-H}_2\text{O}$ and $\text{HCl-CuCl}_2\text{-H}_2\text{O}$ " *Metallurgical Transactions B*, **19B**, pp. 347-354, (1998).
- [23]. H.S. Na, S. Arnold and A.B. Myerson, "Water activity in supersaturated aqueous solutions of organic solutes" *Journal of Crystal Growth* **149**, pp. 229-235, (1995).
- [24]. H. Schneider, "The selective solvation of ions in mixed solvents" in *Solute-Solvent Interactions* (edited by J.F. Coetzee and C.D. Ritchie), pp. 329-342, Marcel Dekker, New York, N.Y., (1969).
- [25]. Z.B. Alfassi and S. Mosseri, "Solventing out of electrolytes from their aqueous solution" *AIChE Journal*, **30(5)**, pp. 874-876, (1984).
- [26]. Z.B. Alfassi, "The separation of electrolytes in aqueous solution by miscible organic solvents" *Separation Science and Technology*, **14(2)**, pp. 155-161, (1979).
- [27]. C. N. R. Rao, "Theory of hydrogen bonding in water", in *Water: A comprehensive treatise*, (edited by F. Franks), Vol. 1, pp. 93-114, Plenum Press, New York, N.Y., (1972).

- [28]. S. J. Suresh and V. M. Naik, "Hydrogen bond thermodynamic properties of water from dielectric constant data" *J. Chem. Phys.* **113** pp. 9727-9732, (2000).
- [29]. D. Peeters, "Hydrogen bonds in small water clusters: a theoretical point of view" *Journal of Molecular Liquids*, **67**, pp. 49-61, (1995).
- [30]. K. A. T. Silverstein, A. D. J. Haymet and K. A. Dill, "The strength of hydrogen bonds in liquid water and around nonpolar solutes" *J. Am. Chem. Soc.* **122** pp. 8037-8041 (2000).
- [31]. I. Nezbeda, "On the role of short- and long-range forces in aqueous systems" *Journal of Molecular Liquids*, **85**, pp. 249-255, (2000).
- [32]. F. David, V. Vokhmin and G. Ionova, "Water characteristics depend on the ionic environment. Thermodynamics and modelisation of the aquo ions" *Journal of Molecular Liquids*, **90**, pp. 45-62, (2001).
- [33]. F. Franks, "The properties of aqueous solutions of non-electrolytes" in *Physico-Chemical Processes in Mixed Aqueous Solvents*, (edited by F. Franks), pp. 50-69, Elsevier, New York, N.Y., (1967).
- [34]. M.I. Davis, J.B. Rubio and G. Douhèret, "Excess molar enthalpies of 2-propanol and water at 25°C" *Thermochimica Acta*, **259**, pp. 177-185, (1995).
- [35]. G. Onori and A. Santucci, "Dynamical and structural properties of water/alcohol mixtures" *Journal of Molecular Liquids*, **69**, pp. 161-181, (1996).
- [36]. A. Wakisaka, S. Komatsu and Y. Usui, "Solute-solvent and solvent-solvent interactions evaluated through clusters isolated from solutions; Preferential solvation in water-alcohols mixtures" *Journal of Molecular Liquids*, **90**, pp. 175-184, (2001).
- [37]. E.S. Amis and J.F. Hinton (editors), *Solvent Effects on Chemical Phenomena*, vol. 1, pp. 182-205, Academic Press, New York, N.Y., (1973).

- [38]. L.L. Lee, "A molecular theory of Setchenov's salting out principle and applications in mixed solvent electrolyte solutions" *Fluid Phase Equilibria*, **131**, pp. 67-82, (1997).
- [39]. R.A. Zingaro, *Non-Aqueous Solvents*, D.C. Heath & Co., Lexington, MA., (1968).
- [40]. G. Wypych (Editor), *Handbook of Solvents*, ChemTec Publishing, Toronto, Canada, pp. 54, (2001).
- [41]. R.G. Bates and R.A. Robinson, "Acid-Base Behaviour in Methanol-Water Solvents" in *Chemical Physics of Ionic Solutions*, edited by B.E. Conway and R.G. Barradas, John Wiley and Sons Inc., New York, N.Y., pp. 211-235, (1966).
- [42]. P. Wang and A. Anderko, "Computation of dielectric constants of solvent mixtures and electrolyte solutions" *Fluid Phase Equilibria*, **186**, pp. 103-122, (2001).
- [43]. C.M. Pina, L. Fernandez-Diaz, M. Prieto and S. Veintemillas-Verdaguer, "Metastability in drowning-out crystallisation: precipitation of highly soluble sulphates" *Journal of Crystal Growth*, **222**, pp. 317-327, (2001).
- [44]. D.K. Das and P.B. Das, "Thermodynamics of $\text{Sr}(\text{NO}_3)_2$ and $\text{Cd}(\text{NO}_3)_2$ in aquo-organic solvents from conductance data" *Thermochimica Acta*, **55**, pp. 35-42, (1982).
- [45]. S.C. Rath and P.B. Das, "Thermodynamics of CdCl_2 and CdBr_2 in aquo-organic solvents from conductance data" *Thermochimica Acta*, **60**, pp. 77-86, (1983).
- [46]. A.K. Lyashchenko, "Concentration transition from water-electrolyte to electrolyte-water solvents and ionic clusters in solutions" *Journal of Molecular Liquids*, **91**, pp. 21-31, (2001).
- [47]. A.K. Lyashchenko, A.S. Lileev, T.A. Novskova and V.S. Kharkin, "Dielectric relaxation of aqueous nonelectrolyte solutions (experimental, structural and molecular-kinetic aspects)" *Journal of Molecular Liquids*, **93**, pp. 29-33, (2001).

- [48]. J.M. Prausnitz, R.N. Lichtenthaler and E.G. Azevedo, *Molecular Thermodynamics of Fluid-Phase Equilibria*, 2nd Edition, Prentice-Hall, Englewood Cliffs, N.Y., (1986).
- [49]. A.M. Sereno, M.D. Hubinger, J.F. Comesaña and A. Correa, "Prediction of water activity of osmotic solutions" *Journal of Food Engineering*, **49**, pp. 103-114, (2001).
- [50]. R.S. Hansen and F.A. Miller, "A new method for determination of activities of binary solutions of volatile liquids" *The Journal of Physical Chemistry*, **58(3)**, pp. 193-196, (1954).
- [51]. V.V. Udovenko and T.F. Mazanko, "Liquid-vapour equilibrium in the propan-2-ol-water and propan-2-ol-benzene system" *Russian Journal of Physical Chemistry*, **41(7)**, pp. 863-866, (1967).
- [52]. H. Zhu, C. Yuen and D.J.W. Grant, "Influence of water activity in organic solvent + water mixtures on the nature of the crystallizing drug phase. I. Theophylline." *International Journal of Pharmaceutics*, **135**, pp. 151-160, (1996).
- [53]. H. Degn and N.-U. Frigaard, "Membrane inlet manometry for the measurement of water activity in aqueous and organic solutions" *Analytica Chimica Acta*, **274**, pp. 355-359, (1993).
- [54]. W.F. Linke and A. Seidell (editors), *Solubilities of Inorganic and Metal-Organic Compounds (a compilation)* 4th edition, Van Nostrand, Princeton, N.J., (1958).
- [55]. J.W. Mullin, N. Teodossiev and O. Söhnel, "Potassium sulphate precipitation from aqueous solution by salting out with acetone" *Chem. Eng. Process.*, **26**, pp. 93-99, (1989).
- [56]. P.A. Barata and M.L. Serrano, "Salting out precipitation of potassium dihydrogen phosphate (KDP). I. Precipitation mechanism" *Journal of Crystal Growth*, **160**, pp. 361-369, (1996).

- [57]. P.A. Barata and M.L. Serrano, "Salting out precipitation of potassium dihydrogen phosphate (KDP). II. Influence of agitation intensity" *Journal of Crystal Growth*, **163**, pp. 426-433, (1996).
- [58]. P.A. Barata and M.L. Serrano, "Salting out precipitation of potassium dihydrogen phosphate (KDP). IV. Characterisation of the final product" *Journal of Crystal Growth*, **194**, pp. 109-118, (1998).
- [59]. J.M. Cohen, "Applications of solvent displacement crystallisation in hydrometallurgy" in *Separation Processes in Hydrometallurgy*, (edited by G.A. Davies), pp. 265-273, Ellis Horwood, London, U.K., (1987).
- [60]. S. Okada, D. Zhang and A. Yazawa, "Selective crystallisation from mixed aqueous sulfate-alcohol solutions" *Metallurgical Review of MMIJ*, **5(2)**, pp. 38-50, (1988).
- [61]. N. Sato, Y. Wei, M. Nanjo and M. Tokuda, "Recovery of samarium and neodymium from rare magnet scraps by fractional distillation method" *Metallurgical Review of MMIJ*, **15(1)**, pp. 1-13, (1998).
- [62]. T.G. Zijlema, H. Oosterhof, G.J. Witkamp and G.M. van Rosmalen, "Crystallisation of Sodium Chloride with amines as antisolvents" in *Separation and Purification by Crystallisation*, (edited by G.D. Botsaris and K. Toyokura), pp. 230-241, ACS, Washington, DC, (1997).
- [63]. T.G. Zijlema, R.J.A.J. Hollman, G.J. Witkamp and G.M. van Rosmalen, "The production of pure NaCl by the antisolvent crystallisation of NaCl.2H₂O and a consecutive recrystallisation step" *Journal of Crystal Growth*, **198/199**, 789-795. (1999).
- [64]. M.S.H. Bader, "Separation of chloride and sulphate ions in univalent and divalent cation forms from aqueous streams" *Journal of Hazardous Materials*, **B73**, 269-283, (2000).
- [65]. D.R. Hull and C.W. Owens, "Separation of KI and KIO₃ using 1,4-dioxane" *Radiochem. Radioanal. Lett.*, **21**, pp. 39-45, (1975).

- [66]. Z.B. Alfassi and L. Feldman, "The preparation of carrier-free radiobromine: the separation of KBr and KBrO_3 using an organic solvent" *Int. J. App. Radiation Isot.*, **27**, pp.125-131, (1976).
- [67]. S. Mosseri and Z.B. Alfassi, "Separation of $\text{KX-KXO}_3\text{-KXO}_4$ ($\text{X}=\text{Cl, Br, I}$) system by solventing-out process" *Sep. Sci. and Technol.*, **18**, pp. 165-175, (1983).
- [68]. L. Ata and Z.B. Alfassi, "Precipitation of nitrates and nitrites by solventing-out from aqueous solutions" *Sep. Sci. and Technol.*, **21**(6&7), pp. 655-664, (1986).
- [69]. D.A. Weingaertner, S. Lynn and D.H. Hanson, "Extractive Crystallisation of salts from concentrated aqueous solutions" *Ind. Chem. Eng. Res.*, **30**, pp. 490-501, (1991).
- [70]. S. Lynn, A.L. Schiozer, W.L. Jaecksch, R. Cos and J.M. Prausnitz, "Recovery of anhydrous Na_2SO_4 from SO_2 -scrubbing liquor by extractive crystallisation: liquid-liquid equilibria for aqueous solutions of sodium carbonate, sulphate and/or sulfite plus acetone, 2-propanol, or tert-butyl alcohol" *Ind. Eng. Chem. Res.*, **35**, pp. 4236-4245, (1996).
- [71]. H. Oosterhof, G.J. Witkamp and G.M. van Rosmalen, "Some antisolvents for crystallisation of sodium carbonate" *Fluid Phase Equilibria*, **155**, pp. 219-227, (1999).

Chapter 3. Experimental

3.1. Introduction

The experimental work reported in this thesis consists of five parts: (1) Organic solvent selection and general behaviour of sulphate and chloride salts during SDC; (2) Crystallisation of nickel sulphate from H_2SO_4 media; (3) Sulphate removal as gypsum from HCl media; (4) Precipitation of zinc oxide from NaOH media; and (5) Dehydration of copper and calcium sulphate crystals.

In each of these chapters, a separate experimental section is given according to its specific nature; however, to a great extent, there exist certain common features such as the experimental set-up and analytical characterization methods used that are encountered throughout this work. In this chapter, these common features are presented starting with the identification of the materials used, followed by description of the experimental apparatus along with the applied operating procedure, and concluding with the analytical and characterization methods. In conjunction to this Chapter, two appendices are provided at the end of the thesis, where the procedures followed for determination of free sulphuric acid concentration (Appendix A) are described and possible liquid-liquid separation methods for the recovery of the solvent are reviewed (Appendix B).

3.2. Materials

For the preparation of all solutions used in this study, A.C.S. reagent grade chemicals were used (extensive list in Table 3.1). All solutions were prepared with deionized water which contained less than 0.01 ppm sodium [1].

Table 3.1 Inorganic salts and chemical reagents employed in present work

Compound Name	Formula	Provider	Purity/Concentration %
Sulphuric Acid	H ₂ SO ₄	Fisher Scientific	95-98 (d=1.84 g/cm ³)
Hydrochloric Acid	HCl	ACRÖS Organics	37.5 (d=1.18 g/cm ³)
Sodium Hydroxide	NaOH	Fisher Scientific	98 %
2-Propanol (isopropanol)	(CH ₃) ₂ CHOH	Fisher Scientific	99.9 (d=0.7855 g/cm ³)
Methanol	CH ₃ OH	Fisher Scientific	99.9 (d=0.7914 g/cm ³)
Nickel Sulphate	NiSO ₄ ·6H ₂ O	Fisher Scientific	99.24
Copper Sulphate	CuSO ₄ ·5H ₂ O	Fisher Scientific	100
Calcium Sulphate	CaSO ₄ ·2H ₂ O	ACRÖS Organics	98.5
Ferrous Sulphate	FeSO ₄ ·7H ₂ O	Sigma Aldrich	99
Ferric Sulphate	Fe ₂ (SO ₄) ₃ ·5H ₂ O	Sigma Aldrich	97
Zinc Sulphate	ZnSO ₄ ·7H ₂ O	Sigma Aldrich	98
Magnesium Sulphate	MgSO ₄ ·7H ₂ O	Sigma Aldrich	98
Cobalt Sulphate	CoSO ₄ ·7H ₂ O	Fisher Scientific	99.5
Sodium Sulphate	Na ₂ SO ₄	Fisher Scientific	99
Potassium Sulphate	K ₂ SO ₄	Fisher Scientific	99
Aluminum Sulphate	Al ₂ (SO ₄) ₃ ·18H ₂ O	Fisher Scientific	100
Zinc Oxide	ZnO	Fisher Scientific	99.3
Magnesium Chloride	MgCl ₂ ·6H ₂ O	A&C American Chemicals Ltd.	99-100
Zinc Chloride	ZnCl ₂	Fisher Scientific	97
Ferrous Chloride	FeCl ₂ ·4H ₂ O	Fisher Scientific	100
Ferric Chloride	FeCl ₃ ·6H ₂ O	Sigma Aldrich	98
Aluminum Chloride	AlCl ₃ ·6H ₂ O	Fisher Scientific	98

3.3. Equipment and Procedure

3.3.1. Experimental Set-up

Generally, almost all the experiments conducted for the present research work consisted of two parts: solubility/critical supersaturation measurements and crystallisation tests.

- *Solubility/Critical Supersaturation Measurements*

Measured amounts of aqueous solutions and organic solvents were added to 250 mL Erlenmeyer flasks plugged with rubber stoppers (A). The flasks were equipped with Teflon-coated stirring bars and placed on a stirring magnetic plate to ensure agitation (B). For the tests conducted at higher temperatures, the flasks were immersed in a clear vinyl water bath fitted with a Cole-Parmer heating circulator (C); the water was mixed, heated and maintained at the desired temperature with an accuracy of $\pm 1^\circ\text{C}$ (Figure 3.1).

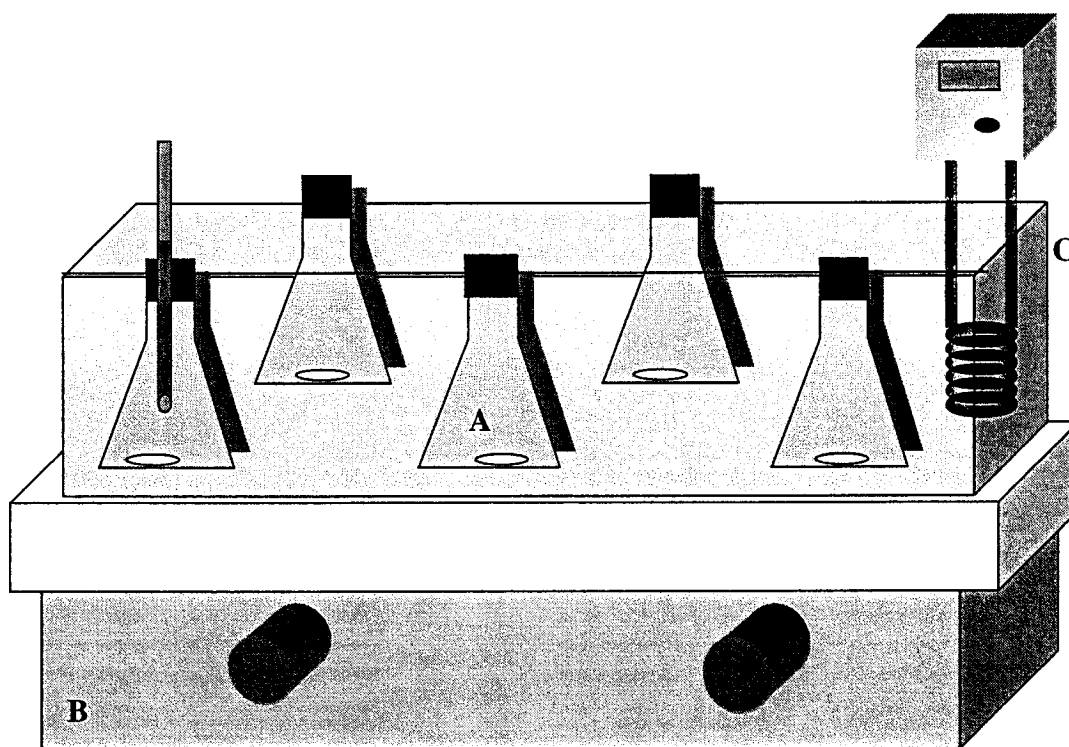


Figure 3.1 Experimental set-up for solubility studies: A-Erlenmeyer flask with rubber stopper and stirring bar; B-magnetic stirring plate; C-water bath with heating circulator.

- **Crystallisation Tests**

Solvent displacement crystallisation tests were performed at ambient temperature (21°C), in a cylindrical 1 litre Pyrex reactor (A) with a separate glass lid containing 4 holes (B). Each hole was plugged with rubber stoppers to prevent solution loss or to allow insertion of a stirrer, manual burette, sampling pipette or thermometer (C) (when required). An axial-mixing type plastic-coated metal impeller (D) (diameter of 4.5 cm, with 3 blades inclined at 45°) agitated the solution; a Dayton stirrer was used with variable speed control (E). The organic solvent was added to the aqueous solution via a 100 mL manual burette (F). A schematic diagram of the experimental set-up used in this work is presented in Figure 3.2. For the experiments conducted at higher temperatures, the reactor was immersed in a Cole-Parmer circulating water bath (G); the water was mixed, heated and maintained at the desired temperature with an accuracy of $\pm 1^\circ\text{C}$.

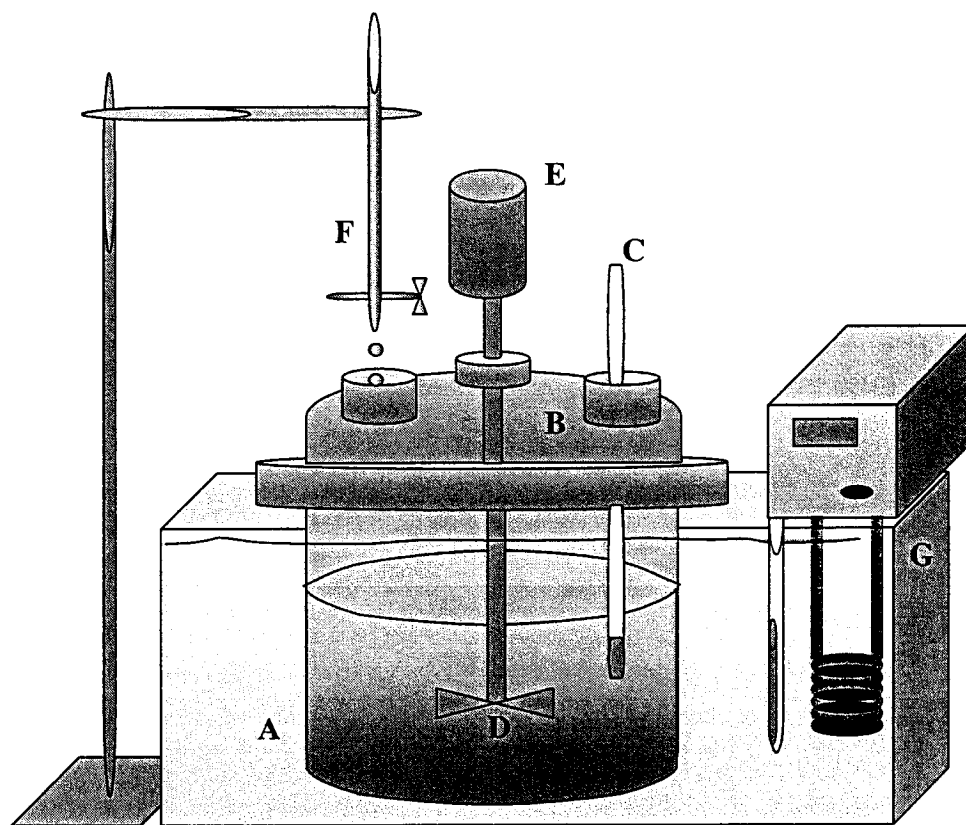


Figure 3.2 Experimental set-up for the SDC tests: A-reactor; B-lid; C-sampling pipette or thermometer; D-impeller; E-motor; F-manual burette; G- water bath with circulator.

3.3.2. Experimental Procedure

- ***Solubility Measurements in Aqueous-Organic Mixtures***

One hundred mL of pre-made mixtures containing aqueous solution (either acidified or containing NaOH) and different amounts of organic were agitated in 250 mL Erlenmeyer flasks while solid compounds whose solubility was to be determined were added to the system. When crystals in equilibrium with solution were detected (i.e. no more dissolution), the addition of salt stopped and the system was allowed to equilibrate for 24 to 48 hours. Subsequently, the crystals were separated by filtration, washed with organic, dried in the oven at 50°C and further analyzed. The mother liquor was diluted with 5% HCl and analysed for metal content.

- ***Determination of Critical Supersaturation***

Pure 100 mL solutions of 10, 20, 30, 40, 50 and 60 g/L cation were agitated with a magnetic stirrer in Pyrex flasks. Small volumes of organic were slowly added to the aqueous solutions by the means of a manual burette; after each addition, a 15-minute equilibration period was allowed. At the moment a “cloud” was seen (initiation of the homogeneous crystallisation process), the volume of organic solvent that induced crystallisation was recorded and the solutions were stirred for 24 hours, to reach complete equilibrium. Subsequently, the crystals were separated by filtration, washed with organic, dried at ambient temperature or in the oven at 50°C for ~20 hr and further analyzed. The mother liquor was diluted with 5% HCl and analysed for metal content.

- ***Solvent Displacement Crystallisation Tests***

In a typical SDC test, 200 mL aqueous solution were agitated at ambient temperature (21°C) while the organic was added from a 100 mL manual burette at various organic-to-aqueous (O/A) ratios. The duration of standard SDC tests was 60-90 minutes, unless otherwise mentioned.

Homogeneous Crystallisation: To homogeneously precipitate the inorganic salt, the organic solvent was added at once to the aqueous phase. The mixture was agitated for 120-180 minutes and samples were taken every 2, 5, 10, 15 minutes, then every 15

minutes, in order to monitor metal content and hence the kinetics of the process. Samples taken by pipette were diluted 10 times immediately with 5% HCl solution to prevent further precipitation within the sample.

Heterogeneous Crystallisation: Low supersaturation was maintained via a slow organic delivery; for a certain volume of solvent corresponding to a supersaturation below the critical value, organic addition was stopped and crystalline seed was provided to the system, in order to favour the secondary nucleation process and hence crystal growth. After a 15-minute equilibration period, organic addition was resumed in a controlled, step-wise manner, small volumes at a time, followed by 15-minute equilibration periods, as to maintain $S < S_{cr,homo}$ throughout the whole experiment. After each addition/stirring period the agitation was stopped and 2-mL samples were taken, diluted and analysed for metal content.

When the precipitation test was over, the crystals were separated by filtration, washed with organic to displace the mother liquor from the cake, air-dried at room temperature or in the oven at 50°C for ~20 hr, weighted and collected for further analysis.

- *Liquid-liquid separation*

No liquid-liquid separation for the recovery of the organic solvent was performed during this research project. Previous work [2] demonstrated it is possible to successfully recover the organic by moderate temperature fractional distillation following the procedure described by Pavia et al. [3]. Appendix B explains the principles of fractional distillation process and outlines the experimental procedure. Pervaporation is also reviewed as possible alternative liquid-liquid separation method.

3.3.3. Handling of the Solid Products

At the end of each crystallisation test, the final slurry was filtered by using a vacuum filtration unit (i.e. a Buchner-type funnel plugged to a filtering flask connected to a vacuum pump). “Fisherbrand” qualitative filter was employed to separate the solids; for the coarse precipitates a P8-type of paper was used (0.45 μm pore size), whereas a P2-

type was employed for the fine products (0.2 μm pore size). In all cases, the filtrate was clear of any solid suspensions.

To ensure the quality of the solid products was not affected by other components of the mother liquor (e.g. sulphuric acid, sodium hydroxide), a standard washing and drying procedure was followed. After the solid product was filtered, it was washed first with a mixture of deionised water and organic solvent (in a ratio that ensures that no salt will dissolve) with volume equal to half of the filtrate collected. After that, the crystals were washed with pure organic, of volume equal to half of the filtrate, added in small portions. Subsequent to washing, the solids were dried until next day (~20 hours). For the experiments conducted at room temperature, the crystals were dried at ambient temperature in the fume-hood; when crystallisation was realised at higher temperatures, the solids were dried in the oven at 50°C, conditions under which phase transformations for most salts studied in this work were avoided.

3.4. Analytical Methods

3.4.1. Determination of Solution Composition

Solution samples collected at regular intervals and after filtration were diluted with 5% HCl solution and subjected to analysis for their metal content by Inductively Coupled Plasma Spectroscopy (ICP). ICP offers several advantages over measurements via Atomic Absorption Spectroscopy:

- lower detection limit;
- lower inter-element interference due to higher flame temperature;
- lower sample dilution required (up to 100 ppm element concentration allowed [4]);
- determination of several elements simultaneously (e.g. cation and sulphate as sulphur).

ICP analyses were performed on a Thermo Jarrell Ash ICP-AES which was calibrated for each element using 50 and 100 ppm standards prepared from 1000 mg/L certified ICP standard solutions (Fisher Scientific).

Since direct pH measurements in highly concentrated sulphuric acid solutions cannot be made, sulphuric acid values at different stages of the experiments were

monitored by titration with standard NaOH 1N solution using the EDTA-assisted method developed by Principe [5] (detailed description provided in Appendix A). An automatic titrator was used (Radiometer Copenhagen Titrab™90), equipped with a high precision ABU 900 Autoburette System and glass pH electrode (Fisher Accu-pHast).

Where experiments required the measurement of NaOH concentration, this was done by direct simple acid-base titration using standard 1 N HCl solution.

3.4.2. Characterisation of Solid Products

The crystalline materials produced were characterised with a variety of methods.

The confirmation of crystalline phases and the determination of the number of crystallisation water molecules were achieved by X-ray Powder Diffraction analysis (XRD), using a Phillips PW1710 machine. The spectrum obtained for a certain sample was matched to different standard spectra contained in the computer's database.

The general morphology and approximate size of the particles were established by performing Scanning Electron Microscopy (SEM) using a JEOL 840A scanning microscope at 15kV on a gold-coated sample.

The solids composition in terms of metal species and/or sulphate content (as sulphur) was determined by digesting a known amount of solid in 5% HCl solution and performing ICP analysis. For the ZnO samples, the composition was additionally verified by using a Philips PW2400 X-ray Fluorescence Spectrometer (XRF).

The number of crystallisation water molecules was estimated by the Thermo-Gravimetric Analysis method (TGA) as the percent weight loss upon gradual heating, using a Perkin-Elmer TGA7 Thermogravimetric Analyzer.

References

- [1]. M. Riendeau, Dept. of Mining, Metals and Materials Eng., McGill University, Montreal, Canada, Personal communication, October 15, 1999.

- [2]. G.A. Moldoveanu, *Precipitation of Nickel Sulphate from Decopperised Acid Solution by Solvent Displacement Crystallisation*, M.Eng. Thesis, McGill University, Montreal, PQ, Canada, (1999).
- [3]. D.L. Pavia, G.M. Lampman and G.S. Kriz, jr., *Introduction to Organic Laboratory Techniques (a contemporary approach)*, Saunders College Publishing, Philadelphia, Pa., pp. 514-635, (1982).
- [4]. E. Siliauskas, Dept. of Chemical Engineering, McGill University, Montreal, Canada, Personal communications, January 10, 2000.
- [5]. F.T. Principe, *Separation of Iron (III) from Zinc Sulphate-Sulphuric Acid Using Organophosphoric Acid Extractants*, M.Eng. Thesis, McGill University, Montreal, PQ, Canada, (1999).

Chapter 4. Solvent Selection and General Behaviour of Sulphate and Chloride Salts

4.1. Introduction

As already discussed in Chapter 2, despite the wide range of potential applications that SDC might find in inorganic processing and hydrometallurgy, there has been no systematic investigation of this technique as it applies to the removal of metal salts from aqueous solutions, neither from a fundamental perspective nor from the standpoint of application to hydrometallurgical processes. Although the relationship between the decrease of inorganic salt solubility and addition of organic solvents is well documented by Seidell and Linke in their exhaustive compilation of solubility data [1], only relatively few laboratory applications have been studied and reported in the literature.

This Chapter represents the first step towards achieving the overall goal of the present research work (i.e. to proceed to a systematic study in order to develop a scientific understanding of the solvent displacement crystallisation process and to propose applications to hydrometallurgical systems of practical interest), by establishing criteria for the selection of organic solvents with suitable physical and chemical properties and by screening various salt systems to determine their amenability to SDC.

4.2. Organic Solvent Selection

4.2.1. Selection Criteria

The selection of “the best” water-miscible organic solvent for the SDC process is not always an easy matter. There are countless organic liquids that are potentially capable of acting as a crystallising agent, but many factors must be considered in order to achieve optimum performance, shortening thus the list to a few industrial solvents. Of course, it is impossible to isolate one single organic solvent that would act as universal precipitant for all salt systems investigated.

Some of the main aspects to be considered when selecting an appropriate organic solvent for SDC include the following:

- (1) It is necessary for the added organic solvent to be miscible with water partly or in all proportions, in other words to have a polar protic nature (i.e. to contain an electronegative heteroatom such as O or N), being thus able break the water structure and establish same nature bonds (i.e. hydrogen) with water molecules.
- (2) Low dielectric constant, i.e. to have a non-polar alkyl chain, in order to decrease the solution dielectric constant and thus favour ion-pairing.
- (3) Normal boiling point and specific heat of vaporisation lower than those of water, in order to decrease the energy consumption during liquid-liquid separation (via distillation). However, the volatility must not be too high, in order to avoid solvent losses and flammability hazards. Moreover, the boiling point should not be too low when applications at higher than ambient temperatures are sought.
- (4) Low/moderate viscosity, in order to facilitate product washing and filtration.
- (5) Not reactive with aqueous phase elements, to avoid valuable metal loss through new compounds/complexes formation.
- (6) Low/nil toxicity, inexpensive, easily available, if the SDC method is to be implemented at industrial scale.
- (7) Electrochemically inert (e_h -pH operating window equal or wider than that of water).
- (8) High crystallisation yield: small volumes of organic to precipitate large fractions of salt. The organic of choice should possess the optimum balance between the polar (hydrophilic) and non-polar (hydrophobic) groups, i.e. to have a long enough alkyl chain to displace the maximum number of water molecules at low organic content but still remain miscible.

There are many exceptions to the rule that "like dissolves like", but this rough empiricism can still serve as a useful guide; in order to be miscible with water, the organic solvent must break the intermolecular bonds of water and replace them with similar bonds. The closer the chemical similarity between two substances, the higher their mutual solubility will be. On the other hand, an advanced degree of chemical similarity should be avoided since their mutual solubility will be so high that subsequent liquid-liquid separation will be extremely difficult and energy-intensive.

Based on the nature of their intermolecular bonding interactions, organic solvents may be divided into three main classes [2, 3]:

- (a) polar protic;
- (b) dipolar aprotic;
- (c) non-polar aprotic.

(a) Polar protic solvents (high and medium-high dielectric constants) such as water, alcohols, amines, carbonyl and carboxylic compounds contain electronegative heteroatoms and hydrogen, sometimes in the same functional group, and in consequence these interact with water forming multiple strong hydrogen bonds (i.e. the heteroatom with the hydrogen from water and the hydrogen from solvent with the oxygen from water). This process accounts for the solubility (miscibility) of these compounds in water; the solubility depends on the balance between the size of the alkyl chain (hydrophobic) and the electronegative - OH or - NH₂ functional group (hydrophilic). If the alkyl chain is small, as in C1 – C4 series, the organic is freely soluble in water; inversely, the larger the alkyl chain, the lower the solubility.

(b) Dipolar aprotic solvents of medium dielectric constants such as ketones, dimethylsulphoxide, dimethylformamide, nitriles (e.g. aceto- and benzonitrile), nitromethane or nitrobenzene, etc. are highly polar (i.e. contain a heteroatom) but the molecules of this class of solvents are characterized by dipole-dipole interactions; they are weak hydrogen donors, meaning they have less ability to break the water structure and establish similar stable hydrogen bonds with water molecules (i.e. moderate miscibility with water).

(c) Non-polar aprotic solvents of very low dielectric constants such as benzene, toluene, hexane, etc. do not contain heteroatoms at all and their molecules interact by very weak van der Waals forces only. According to the above classification, it would appear that non-polar aprotic solvents are the best candidates for SDC; however, this intrinsic non-polar nature accounts for the impossibility to establish hydrogen bonds with water molecules and hence their highly hydrophobic character (i.e. total immiscibility in water). As a comparison, the strength of hydrogen bonds is ~10 kJ/mol whereas van der Waals bonds are one order of magnitude lower [4].

4.2.2. Solvent Screening

As explained in Section 2.3.3., a high dielectric constant (ϵ) favours ion dissociation whereas the decrease in ϵ leads to the increase of the electrostatic attraction between ions of opposite charge, ionic association and subsequent crystallisation [5]. When $40 < \epsilon < 20$, the formation of contact ion-pairs generally predominates throughout of solution and further decrease in ϵ leads to salt separation [6]. Other researchers have also related the decrease in ϵ upon addition of polar organic solvents to lower free energy of formation of ion-pairs in the mixed solutions. [7].

The means by which organic solvents affect the solvation of ions is the decrease of the dielectric constant of solution (ϵ) by breaking the water-water hydrogen bonds [8] and immobilizing the water molecules. Since the ions are soluble in “free water” only, any change in solution composition upon addition of organic will result in decreasing the water activity and consequently influences the solubility of the dissolved salt. The more efficient an organic in breaking the water structure, the lower the dielectric constant of the mixture will be and the more effective the latter in precipitating out the salt. Therefore, it can be inferred that any organic solvent with $\epsilon_{\text{org}} < \epsilon_{\text{w}}$ to be tested for SDC must have a polar character; the longer the alkyl chain of the organic is (i.e. the more hydrophobic the character) the lower the dielectric constant. On the other hand, the polar nature is very important since it accounts for the total or partial miscibility of the organic with water; to insure that the organic is miscible with water (i.e. able to form hydrogen bonds) the hydrophobic character must not surpass the hydrophilic one.

Revisiting the selection criteria outlined at the beginning of Section 4.2. and considering also the importance of the organic in lowering the aqueous solution dielectric constant [9], some widely-employed industrial solvents from the following groups: alcohols, esters, carbonyl compounds and amines were selected for preliminary SDC studies (Table 4.1); water properties are indicated for better comparison purposes. After reviewing these physical properties, it was decided to eliminate organic solvents with boiling point higher than 90°C (to minimize energy consumption during recovery by distillation), excessive volatility (to avoid losses) and toxic nature and susceptibility to reaction with complex cations (such as amines). On the basis of this review, the following

organic solvents believed to provide the best salting out performances were selected for further practical testing: methanol, ethanol, 2-propanol, tert-butanol, acetone, methyl-ethyl-ketone (MEK), ethyl-acetate and isopropyl-acetate.

Table 4.1 Physical properties of water and selected polar organic solvents [10]

Compound	Molecular Weight (g/mol)	Boiling Point (°C)	Vapour Pressure (mmHg) @ 20°C	Dielectric Constant @ 20°C	Solubility in Water @ 20°C (wt %)
Water	18	100	17.54	78	∞
Methanol	32	64.6	17.5	32.7	∞
Ethanol	46	78	44	24.55	∞
1- Propanol	60	97	15	20.7	∞
2- Propanol	60	82.4	33	18.62	∞
1- Butanol	74	118	4.4	17.8	7.8
2- Butanol	74	99.5	12	16.5	22.5
iso-Butanol	74	108	8.8	17.9	7.04
tert-Butanol	74	77 (m.p. 25°C)	57.3	12.5	∞
Acetone	58	56	108	20.7	∞
Methyl-Ethyl Ketone	72	79.8	77.5	18.5	27
Methyl-Propyl Ketone	86	101	27.8	17	3
Butyr-Aldehyde	72	75	88	13.4	7
Propion-Aldehyde	58	48	258	18.5	22
iso-Butyr-Aldehyde	72	64	138	N/A	6.5
Isopropyl-Ether	102	68.5	119.4	3.88	1.1

Butylene-Oxide	72	63	141	N/A	6
Dioxane	88	101	29	2.2	∞
Tetrahydrofuran	72	66	150	7.6	∞
Compound	Molecular Weight (g/mol)	Boiling Point (°C)	Vapour Pressure (mmHg) @ 20°C	Dielectric Constant @ 20°C	Solubility in water @ 20°C (wt %)
Methyl Acetate	74	57	173	6.68	24
Ethyl Acetate	88	77	73	6	8
Propyl Acetate	102	90	23	3.1	3
Isopropyl Acetate	102	88.8	45.7	8.1	2.3
Diethyl Amine	73	56	200	3.58	∞
Triethyl Amine	101	89.5	50	2.42	∞
Propyl Amine	59	48	240	5.31	∞
Butyl Amine	73	77.8	75	4.88	∞
Isobutyl Amine	73	69	N/A	4.43	∞
sec-Butyl Amine	73	66	N/A	N/A	∞

4.2.3. Qualitative SDC Tests and Solvent Selection

In order to test the applicability of the selected organic solvents to SDC, an acidic solution of nickel sulphate was prepared following Cohen's information, containing 25 g/L Ni²⁺ and 200 g/L H₂SO₄ [11]. Ten mL of aqueous solution were added to 100 mL Erlenmeyer flasks plugged with rubber stoppers, at 21°C; the flasks were equipped with Teflon-coated stirring bars and placed on a stirring magnetic plate to ensure agitation (refer to Figure 3.1). Doses of 5 mL organic (i.e. O/A = 0.5) were added to the aqueous solutions by means of a manual burette; after each addition, a 10-minute equilibration period was allowed. Because of the preliminary and qualitative nature of these screening

tests, it was not considered important to refine the dosage towards smaller increments. At the moment a “cloud” was seen (initiation of the homogeneous crystallisation process), the volume of organic solvent that induced crystallisation was recorded and the addition stopped. A synopsis of these preliminary qualitative tests is given in Table 4.2.

Table 4.2 Evolution of preliminary SDC qualitative tests

(Initial solution composition: 25 g/L Ni²⁺, 200 g/L H₂SO₄, 21 °C)

TOTAL WATER-MISCIBLE POLAR ORGANIC SOLVENTS				
Methanol (MeOH)	Ethanol (EtOH)	2-propanol (2PrOH)	Tert-Butanol (t-BuOH)	Acetone (Ac₂O)
+ 5 mL: no ppt. + 5 mL: no ppt. + 5 mL: no ppt. + 5 mL: no ppt. + 5 mL: rapid crystallisation (< 5 min)	+ 5 mL: no ppt. + 5 mL: no ppt. + 5 mL: rapid crystallisation (< 5 min)	+ 5 mL: no ppt. + 5 mL: rapid crystallisation (< 5 min)	+ 5 mL: no ppt. + 5 mL: no ppt. + 5 mL: slow crystallisation (> 15 min)	+ 5 mL: no ppt. + 5 mL: rapid crystallisation (< 5 min)
Required for crystallisation: O/A = 2.5	Required for crystallisation: O/A = 1.5	Required for crystallisation: O/A = 1.0	Required for crystallisation: O/A = 1.5	Required for crystallisation: O/A = 1.5
PARTLY WATER-MISCIBLE POLAR ORGANIC SOLVENTS				
Methyl-ethyl-ketone (MEK) + 2PrOH	Ethyl-acetate (AcOEt) + 2PrOH	Isopropyl-acetate (AcOiPr) + 2PrOH		
+ 5 mL: 2 liq. phases, no ppt. + 5 mL: 2 liq. phases, no ppt. + 5 mL: liq. phases, no ppt. + 5 mL: 2 liq. phases, no ppt. + 5 mL 2PrOH: water extracted to the upper organic layer, small portion of aqueous concentrate at the bottom;	+ 5 mL: 2 liq. phases, no ppt. + 5 mL: 2 liq. phases, no ppt. + 5 mL: liq. phases, no ppt. + 5 mL: 2 liq. phases, no ppt. + 5 mL 2PrOH: 2 liq. phases no ppt. + 5 mL 2PrOH: water extracted to the upper organic layer, small	+ 5 mL: 2 liq. phases, no ppt. + 5 mL: 2 liq. phases, no ppt. + 5 mL: liq. phases, no ppt. + 5 mL: 2 liq. phases, no ppt. + 5 mL 2PrOH: 2 phases, no ppt. + 5 mL 2PrOH: water extracted to the upper organic layer, small portion of aqueous concentrate at		

after 10 minutes of stirring, crystallisation and 1 phase (2PrOH acts as mutual solvent)	portion of aqueous concentrate at the bottom; + 5 mL 2PrOH: rapid crystallisation (< 5 min), 1 phase	the bottom; + 5 mL 2PrOH: water extracted to the upper organic phase, smaller volume of concentrated aqueous solution at the bottom; + 5 mL 2PrOH: rapid crystallisation (< 5 min), 1 phase
Required for crystallisation: O/A = 2.5 (20 mL MEK + 5 mL 2PrOH)	Required for crystallisation: O/A = 3.5 (20 mL AcOEt + 15 mL 2PrOH)	Required for crystallisation: O/A = 4 (20 mL AcOEt + 20 mL 2PrOH)

It can be observed that all completely miscible solvents exhibit good crystallisation performances with reasonable volume requirements. The only notable exception is methanol ($\epsilon=32.7$), which requires the highest volume addition in order to initiate crystallisation. This is expected and explained in terms of: (1) higher dielectric constant as compared to the other alcohols [12] making it less favourable to ion-association phenomena (since the attraction force between two ions in solution is inversely proportional to dielectric constant); (2) very small molecule, meaning that more alcohol is required to “immobilize” free water via hydrogen bonds. Ethanol ($\epsilon=24.5$) has a larger molecule than methanol and provides good crystallisation performance, but it is not considered a solvent of choice because of its high cost. Tert-butanol ($\epsilon=12.5$) appears to exhibit somewhat slower crystallisation kinetics, most probably due to its bulky structure that may induce a steric hindrance when hydrogen bonds between alcohol and water molecules are to be established. Moreover, its melting point of 25°C restricts the application at lower temperatures. Acetone ($\epsilon=20.7$) has good crystallisation capabilities, but its rather low boiling point (56°C) and high volatility prevents it to be employed for applications at higher temperatures (above 50°C).

The partly-miscible organic solvents did not induce salt separation by themselves, but produced extraction of water in the organic layer, leaving a more concentrated aqueous solution at the bottom; when additional 2PrOH was added, it readily induced salt crystallisation in the supersaturated aqueous solution. This technique, known as

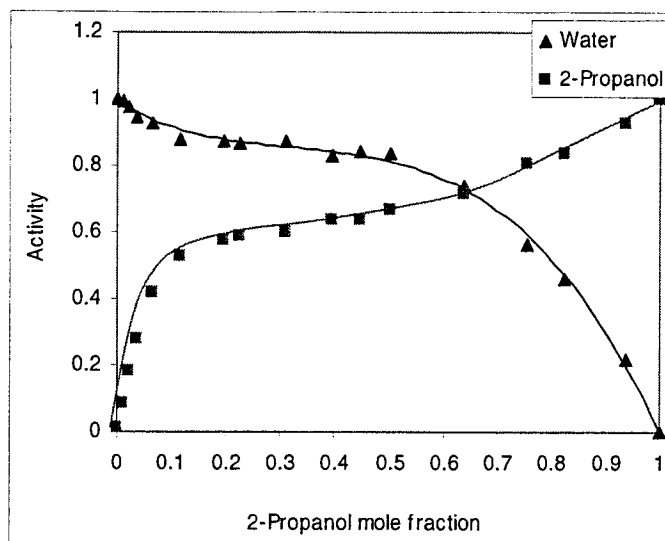
“extractive crystallisation”, can be regarded as a variation of SDC, in which the crystallisation of salt is induced by the addition of a partly miscible organic solvent capable of extracting water into a separate phase, hence causing the solute concentration in the aqueous phase to exceed its solubility and precipitate out of solution (refer to Section 2.4.4).

Although partly miscible organic solvents have good physical properties and acceptable crystallisation results, they were not actually selected for further application due to the large volume involved and the fact that the use of an additional solvent would be required, complicating thus the final liquid-liquid separation and organic recovery step.

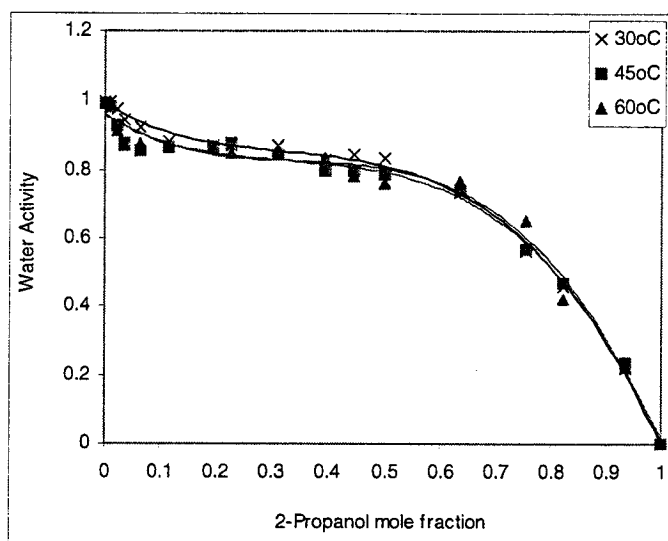
Finally, **2-propanol** ($\epsilon=18.6$) was considered to meet most of the selection criteria outlined in Section 4.2.1 for the organic solvent of choice in SDC and opted for use in further systematic in-depth studies. Physical and chemical properties of 2-propanol are presented in Appendix C.

As explained, the means by which the organic solvents affect the solvation of ions is the decrease of the dielectric constant of solution by breaking the water-water hydrogen bonds and immobilizing the water molecules. Since the ions are soluble in “free water” only, any change in solution composition upon addition of organic will result in decreasing water activity and consequently influences the solubility of the solute.

Udovenko and Mazanko [13] studied the changes in water activity upon organic addition for the H₂O-2-propanol system at different temperatures. As observed, water activity decreases from 1 in the absence of 2-propanol to 0.2 for an organic mole fraction of 0.9 whereas the opposite trend is observed for the alcohol (Figure 4.1 a). Zhu *et al.* [14] reported similar trends for water activity in methanol and 2-propanol-aqueous systems. Temperature had no effect on water activity, similar values being reported at each temperature for the same organic mole fraction (Figure 4.1 b).



(a)



(b)

Figure 4.1 Water activity coefficient in the system H₂O-2-propanol [adapted from 13]:

(a) influence of organic fraction; (b) influence of temperature

4.3. General Behaviour of Sulphate and Chloride Systems

Once 2-propanol was selected as the preferred organic solvent for further SDC tests, the applicability of this crystallisation technique to various salt systems of practical interest in hydrometallurgy (i.e. sulphate and chloride compounds) was studied. Literature data regarding electrolyte solubility in alcohols were consulted (where available) and a

screening procedure was developed in order to determine the amenability of most common salts to SDC and to evaluate their response to the method.

4.3.1. Experimental

Measured amounts of reagent-grade salts (either sulphate or chloride compounds) were dissolved into acidified aqueous solution. The initial metal concentration in solution was arbitrarily selected to be 1 mol/L while the initial free acid concentration was set with concentrated mineral acids (H_2SO_4 or HCl) to desired levels, depending on the system.

One hundred mL of the prepared solution were transferred into 1-litre glass reactor (see Figure 3.2) and agitation was applied at 400 rpm under ambient conditions (i.e. 21°C , atmospheric pressure) while 2-propanol was added from a manual burette in doses of 20 mL (i.e. $\text{O/A}=0.2$); after each organic addition a 10-minute equilibration period was allowed. A total O/A ratio of 4 was selected, meaning 400 mL of 2-propanol were added. The solution was sampled at every 0.4 O/A increments, filtered and diluted with 5% HCl in order to determine the metal content via ICP. The standard retention time of each experiment was set at 200 min with additional agitation up to 48 hrs to monitor the evolution of solution towards the equilibrium concentration. After that, agitation was stopped and the slurry was processed (i.e. filtered, washed and dried) according to the procedure outlined in Section 3.3.3. The confirmation of crystalline phases and the determination of the number of crystallisation water molecules were achieved by XRD while the general morphology and estimative size of the particles were established by performing SEM examination of the solid product.

4.3.2. Sulphate Systems

Extensive experimental data compiled by Linke and Seidell [1] indicate that most inorganic sulphates are sparingly soluble or insoluble in low molecular organic alcohols even at elevated temperatures (Figure 4.2). Consequently, sulphate solubility in H_2SO_4 - H_2O solutions decreases with increasing miscible polar organic fraction, at constant temperature.

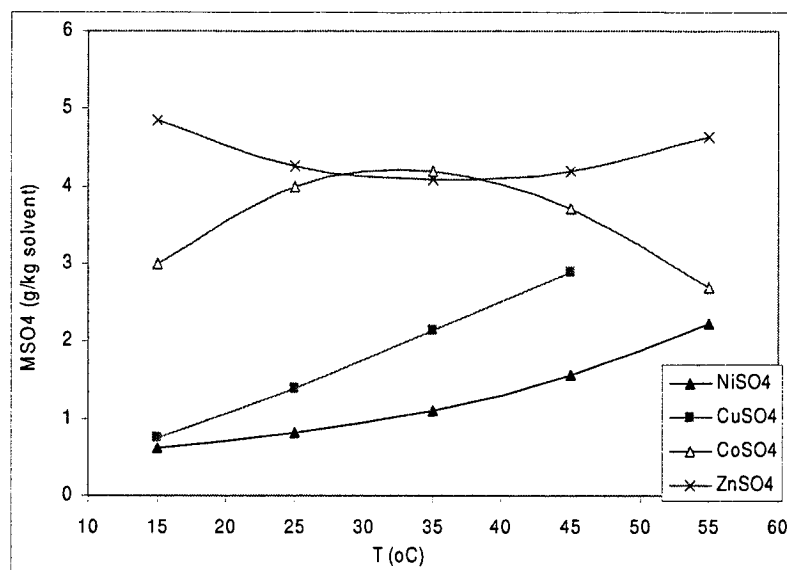


Figure 4.2 Solubility of some sulphates in absolute methanol as a function of temperature (data from [1])

Most of the reported values are for methanol and ethanol addition, but the theoretical and practical knowledge gained throughout the present research work led us to infer that the same behaviour is to be expected in the presence of 2-propanol. Moreover, the larger the organic molecule, the lower the fraction required to initiate crystallisation and the sharper the drop in solubility.

Based on these considerations, preliminary SDC testes were conducted with the following objectives:

- to study the crystallisation of some metal sulphates of interest from synthetic solutions using 2-propanol as precipitant;
- to evaluate the percent salt recovery as a function of organic content.

• **Results**

The actual crystallisation tests were conducted as described in Section 4.3.1.; initial solutions containing 1 M metal and 100 g/L H_2SO_4 were prepared for the following sulphate compounds (selected as most representative for hydrometallurgical processes):

- univalent: K^+ and Na^+ ;
- divalent: Mg^{2+} , Fe^{2+} , Cu^{2+} , Ni^{2+} , Co^{2+} and Zn^{2+} ;
- trivalent: Fe^{3+} and Al^{3+} .

A summary of the results is given in Table 4.3. To facilitate the assessment of the sulphates' behaviour during SDC with 2-propanol, the experimental data are presented in graphical form as metal molarity vs. organic-to-aqueous volumetric ratio (Figures 4.3 to 4.6) for each set of cations.

The final solid products were analysed for crystallinity via XRD and the morphology of particles was studied by SEM. All these diffraction spectra and micrographs are given as Appendix at the end of this Chapter.

It can be observed that:

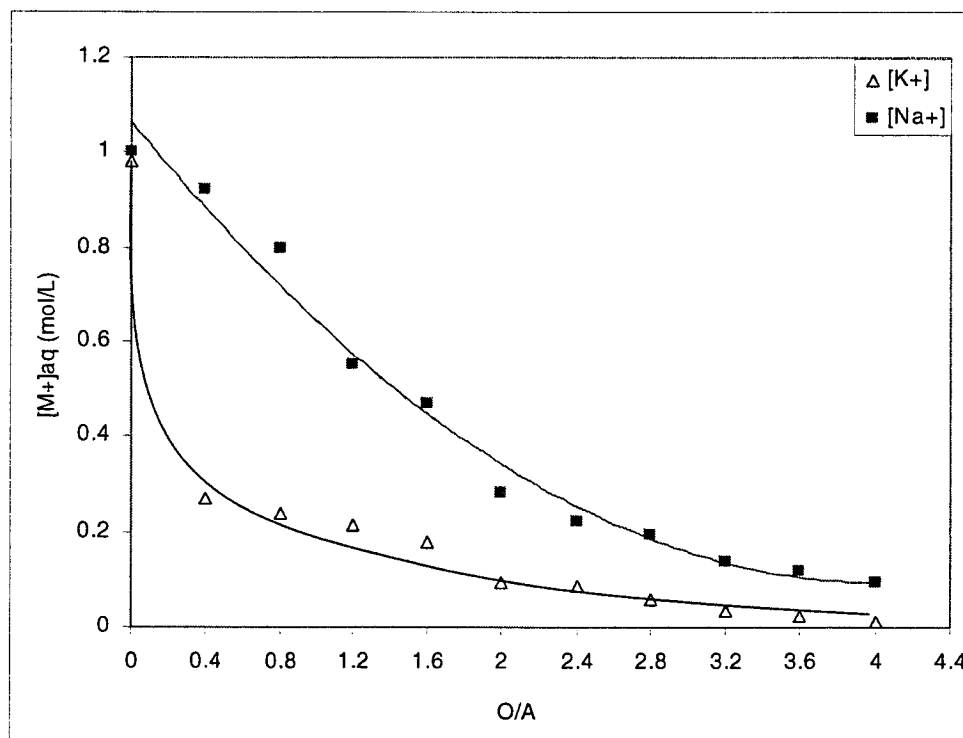
- 2-propanol acted as an efficient salting out agent for the metal sulphates tested, with the exception of $\text{Fe}_2(\text{SO}_4)_3$, which did not precipitate; the system underwent phase splitting, exhibiting a thin layer of very concentrated salt solution at the bottom of the reactor and a large amount of aqueous-alcohol mixture. For the rest of the metal sulphates, as the organic fraction increases, the dielectric constant of the medium decreases thus favouring the ion pair formation process. Consequently, the supersaturation of the salt slowly increases until exceeds the critical value and homogeneous crystallisation is initiated, leading to a gradual decrease in metal concentration.
- An organic-to-aqueous (O/A) ratio of 4 removed more than 90% of metal from solution (with the exception of magnesium) in the form of crystalline sulphates with various number of crystallisation water molecules associated to them (Table 4.3), but the choice of an optimum O/A depends on the specific requirements (in terms of final tolerated metal concentration) of a given industrial process.
- Final metal concentration values for constant O/A over time indicate fast precipitation, no significant change being detected after the first hour of equilibration or during the subsequent 48 hours.

By monitoring the evolution of the metal concentration profiles in solution during SDC, clear differences are noticed for sulphates of same valence. This behaviour could be explained empirically in terms of difference in salt solubility, as indeed extensive solubility data compiled by Linke and Seidell [1] indicate. Nevertheless, this approach is not satisfactory in describing the process from a more fundamental perspective.

Table 4.3 Summary of the SDC results for most common sulphates with 2-propanol

([M]_{in} = 1 mol/L, 21°C, 100 g/L H₂SO₄, O/A=4)

Metal	Final Crystalline Form	% Removal	[M] _{1 hr} (mol/L)	[M] _{final} (mol/L)
Al(3+)	Al ₂ (SO ₄) ₃ ·17H ₂ O	98	0.017	0.010
Fe(3+)	-	-	0.152	0.148
Na(+)	Na ₂ SO ₄ ·H ₂ O	90	0.097	0.089
K(+)	K ₂ SO ₄ ·H ₂ O	99	0.009	0.009
Mg(2+)	MgSO ₄ ·6H ₂ O	75	0.263	0.245
Zn(2+)	ZnSO ₄ ·H ₂ O	98	0.02	0.019
Ni(2+)	NiSO ₄ ·6H ₂ O	98	0.017	0.017
Co(2+)	CoSO ₄ ·6H ₂ O	99	0.008	0.008
Fe(2+)	FeSO ₄ ·6H ₂ O	99	0.010	0.010
Cu(2+)	CuSO ₄ ·5H ₂ O	99.7	0.003	0.003

Figure 4.3 SDC behaviour of univalent sulphates (21°C, 2-propanol, 100 g/L H₂SO₄)

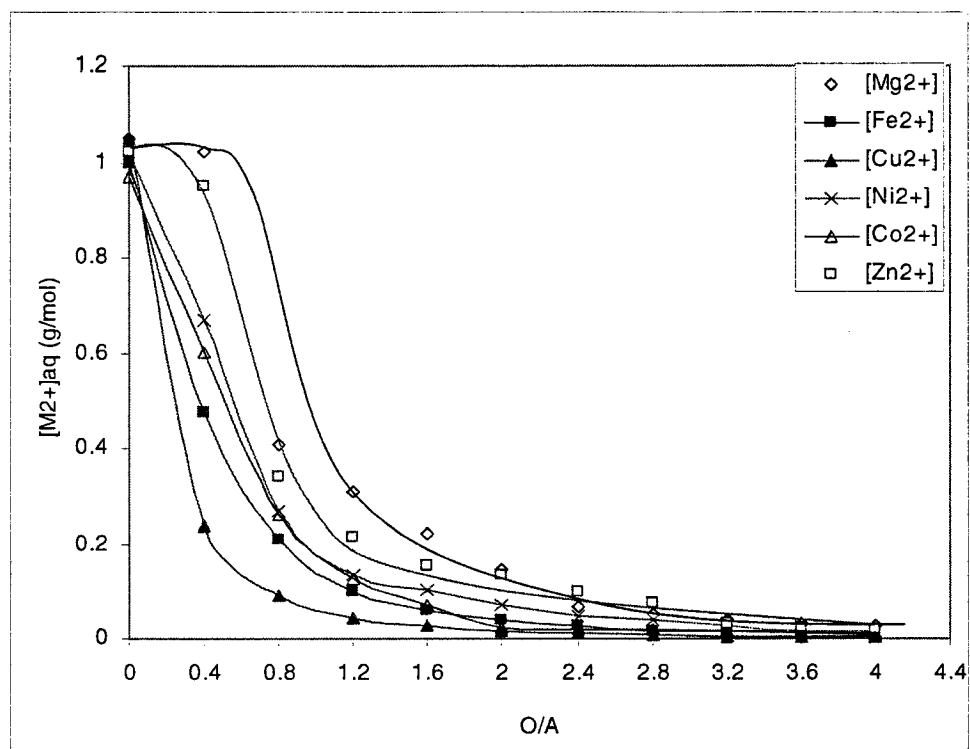


Figure 4.4 SDC behaviour of divalent sulphates (21°C, 2-propanol, 100 g/L H₂SO₄)

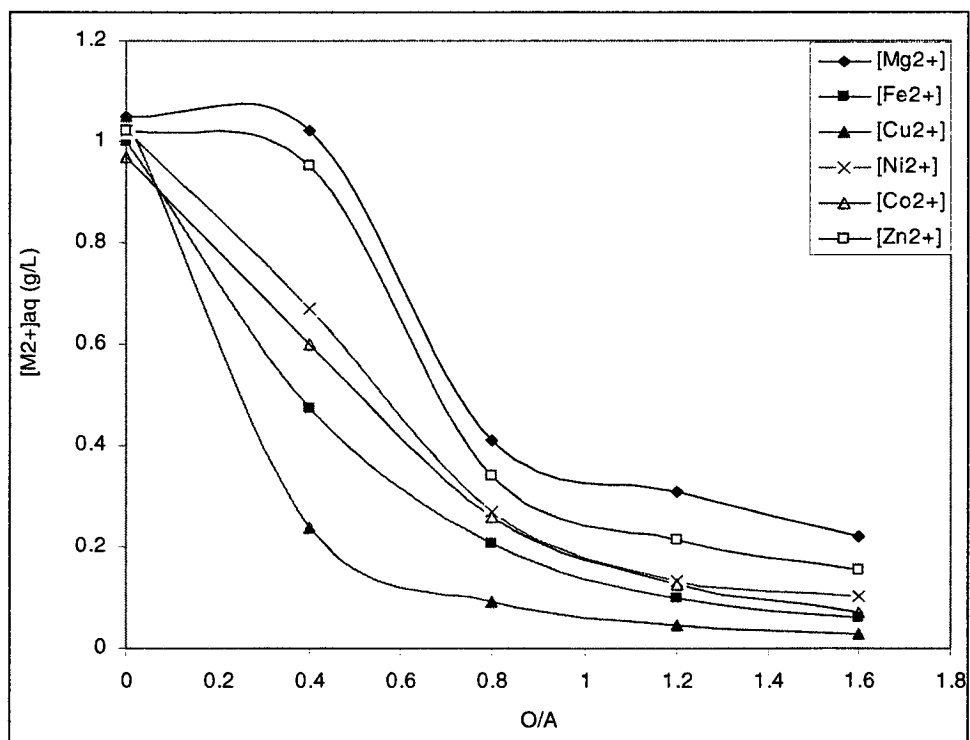


Figure 4.5 Detailed view of SDC behaviour of divalent sulphates in region $0 < O/A < 1.6$

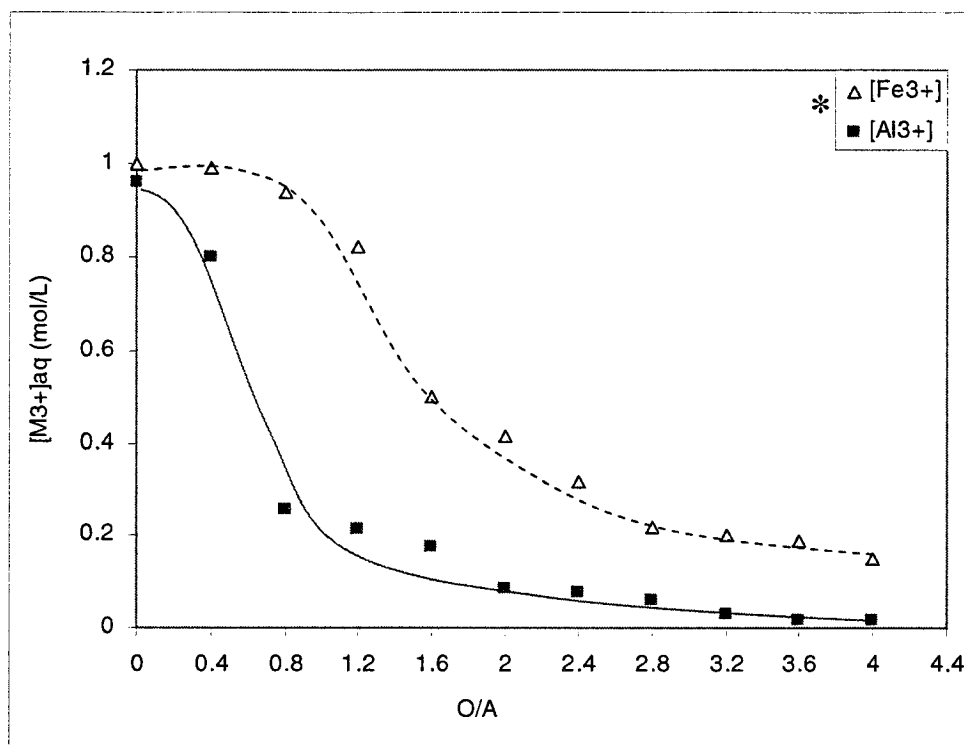


Figure 4.6 SDC behaviour of trivalent sulphates (21°C, 2-propanol, 100 g/L H₂SO₄)

(* Note: iron concentration refers to the upper aqueous-alcohol mixture, the remaining iron reported in a highly concentrated aqueous bottom layer).

• Discussion

When an ion is dissolved in water, it interacts electrostatically with the water dipoles to form hydrated ionic species. Cations interact with the first hydration layer of water molecules by bonding preferentially through the negatively charged oxygen atoms of water that point inwards, with the lone-pair orbitals overlapping the acceptor orbitals of the cations, i.e. via coordinate covalent bonds (Figure 4.7 a). On the other hand, anions bond primarily through the hydrogen atoms of the water molecules [15, 16, 17].

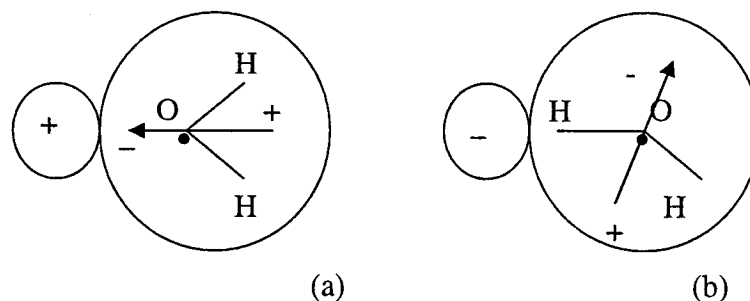


Figure 4.7 Orientation of water molecule near a cation (a) and an anion (b) [15]

It is generally accepted that the strength of interactions between ions and water dipoles depends on the charge density of the ions which in turn is related to the ionic radius; the strongest bond is established with the element of smallest radius and highest charge density. Inversely, water molecules are more loosely bound by large radius ions with low charge density [18]. Table 4.4 presents ionic radii for cations employed in the general SDC tests with metal sulphates.

Table 4.4 Ionic radii for most common ions [18]

Ion	r (Å)	Ion	r (Å)
Al(+3)	0.54	Cu(2+)	0.73
Fe(3+)	0.55	Fe(2+)	0.61
K(+)	1.38	Co(2+)	0.65
Na(+)	0.98	Mg(2+)	0.72
Cl(-)	1.81	Ni(2+)	0.69
OH(-)	1.36	Zn(2+)	0.74

This basic approach suffices to explain the different behaviour of Na_2SO_4 and K_2SO_4 during SDC. The smaller Na^+ ($r_i = 0.98 \text{ \AA}$) ion has a higher charge density and bonds stronger the water molecules than the larger K^+ ($r_i = 1.38 \text{ \AA}$). This translates in higher solubility of Na_2SO_4 as opposed to K_2SO_4 in water-organic mixtures as it is more difficult for the alcohol to break the water-sodium bond and displace water from the hydration sphere. This behaviour, also in accordance with classical solubility data reported for water [1], has been reported for all group 1 univalent cations, where the ionic radii increase from Li to Cs [15]. However, the ionic radius theory is not adequate to explain the difference in crystallisation trends of divalent and trivalent sulphate systems studied, since all the cations involved have very close ionic sizes within the same valence class.

The most distinctive discussion on solvation in water has been given by Desnoyers and Jolicoeur [19] in which they define Δw as the energy required to separate water molecules at a distance Δr where they cannot form hydrogen bonds. Δw is the energy reference by which hydration is characterized. Likewise, an energy ΔH is required for a hydrated ion to similarly be separated from its bound water; this is the measure of

the hydration of the ion relative to the bulk solvent. If $\Delta H > \Delta w$, adjacent water molecules are more firmly bound to the ion than to the bulk and the ion is said to be **positively hydrated**. If $\Delta H < \Delta w$, adjacent water molecules are more loosely bound to the ion and can be easily removed from the hydration sphere; this is described as **negative hydration**. As a general rule when comparing ΔH for different ions, the smaller the ΔH the easier it will be for the water molecules to be removed from the hydration sphere.

Values for heats of hydration of various ions, as reported by Conway and Bockris [15] and Muirhead-Gould and Laidler [20] are given in Table 4.5. A similar trend is observed in free energy of hydration (ΔG) values for group I and II ions and for lanthanides, calculated by David et al. [21].

Table 4.5 Heats of hydration of individual ions [15, 20]

I. Z=1		II. Z=2		III. Z=3	
Ion	ΔH (Kcal/g ion)	Ion	ΔH (Kcal/g ion)	Ion	ΔH (Kcal/g ion)
H(+)	276	Be(2+)	608	Fe(3+)	1200
Li(+)	120	Mg(2+)	536	Al(3+)	1149
Na(+)	95	Zn(2+)	528	In(3+)	980
K(+)	75	Ni(2+)	516	La(3+)	768
Rb(+)	70	Co(2+)	504	-	-
Cs(+)	61	Fe(2+)	500	-	-
F(-)	122	Cu(2+)	490	-	-
Cl(-)	89	Mn(2+)	479	-	-
Br(-)	81	Ca(2+)	410	-	-
I(-)	73	Sr(2+)	376	-	-
-	-	Ba(2+)	346	-	-

On entering into a crystal structure the ions must release the hydration water attached; Pina et al. [22], working on crystallisation of alkali sulphates with methanol,

suggested that the higher the energy required for the dissociation of the water molecule from the ion, the more stable the hydrate is and the slower the nucleation kinetics. They found the order of increasing stability to be $\text{Rb}_2\text{SO}_4 < \text{Na}_2\text{SO}_4 < \text{Li}_2\text{SO}_4$. Similarly, from Table 4.5 it can be observed that $\Delta H_{\text{K}} < \Delta H_{\text{Na}}$, enforcing thus the experimental observation regarding crystallisation behaviour of K_2SO_4 and Na_2SO_4 during crystallisation with 2-propanol, and explained so far by the simple ionic radii theory.

Moreover, Prue [23] states that it would be easier for two oppositely charged large ions to associate than if there is a marked difference in the atomic radii; with two large ions the electrostatic attraction is reinforced by ion-induced dipole and dispersion forces. As the cation size increases the anion competes more successfully with water molecules for access to the coordination sphere of the cation. Experimental results demonstrate that oxyanions with a well distributed charge (such as SO_4^{2-} or NO_3^-) show a tendency to associate with alkali metal and alkaline earth cations which increases with the size of cation. This is the reason for which the order of solubilities of alkali metal salts with large anions of strong acids fall almost invariably into the sequence $\text{Li} > \text{Na} > \text{K} > \text{Rb} > \text{Cs}$.

For trivalent cations, the relationship $\Delta H_{\text{Al}} < \Delta H_{\text{Fe}}$ could explain the difference in SDC behaviour of the two sulphates. Since water molecules are more loosely bound in the primary hydration sphere of Al^{3+} as compared to Fe^{3+} , they are more easily displaced by alcohol, hence the more accentuated decrease in $\text{Al}_2(\text{SO}_4)_3$ solubility. Actually, it was impossible to crystallise ferric sulphate even with elevated organic fractions. The system underwent phase splitting, exhibiting a thin layer of very concentrated salt solution at the bottom of the reactor and a large amount of aqueous-alcohol mixture. Most probably extreme high volumes of organic would have eventually been initiated the crystallisation process, but it was not considered an economically attractive option. Sato et al. [24] reported similar results regarding the unusual high solubility of $\text{Fe}_2(\text{SO}_4)_3$ during fractional crystallisation with ethanol from acidified aqueous solutions containing mixtures of ferrous, ferric and rare earth metals (Nd and Sm) sulphates, although they did not provide an explanation for their observation (Figure 4.8).

Heats of hydration for divalent ions are in accordance with literature solubility data in aqueous-only solutions and experimental trends observed during SDC for the respective sulphates, presented in Figure 4.4. Mg^{2+} and Zn^{2+} exhibit the largest ΔH ,

which translates to higher stability of the hydrated forms upon organic addition, hence higher solubility, whereas for Fe^{2+} and Cu^{2+} the opposite is true.

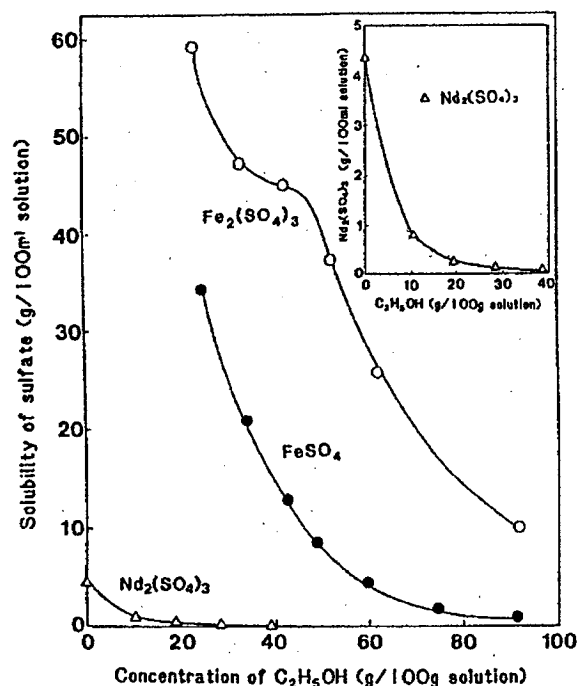


Figure 4.8 Fractional crystallisation of mixed metal sulphates with ethanol [24]

The 2-step behaviour shown by K_2SO_4 , $\text{Al}_2(\text{SO}_4)_3$ and to some extent MgSO_4 could be explained in terms of somewhat slower kinetics as compared to other sulphate systems that exhibit a steeper decrease in concentration or by applying the theory of Amis and Hinton, who measured the amount of solvent transported into the cathode region of a transference cell relative to the amount transported to the anode region using ethanol-water-electrolyte solutions [25]. The periodic variation of the relative amount of organic was related to the gradual replacement of water molecules from the secondary hydration sheath of the cation first, then of the anion (in this case SO_4^{2-}), and finally the attack of the inner hydration spheres of cation and anion.

4.3.3. Chloride Systems

In order to evaluate the separation of some metal chlorides from $\text{HCl-H}_2\text{O}$ system, preliminary SDC tests were designed at 21°C using 2-propanol as precipitant.

Crystallisation tests were conducted according to the procedure described in Section 4.3.1.; initial solutions of pH 0.5 (HCl) containing 1 mol/L metal were prepared for the following chloride salts (selected as representative for hydrometallurgical processes): Mg^{2+} , Fe^{2+} , Zn^{2+} and Al^{3+} .

• Results

None of the tested metal chlorides could be successfully separated from HCl- H_2O system with 2-propanol. As the alcohol was added to the aqueous solution, it formed a homogeneous mixture without separating the salt, even for high organic contents. Consequently, metal concentration in solution did not decrease during experiment progression (Figure 4.9). The slight variations in metal concentration in aqueous phase are most probably due to non-perfect reproducibility in sampling and ICP analysis.

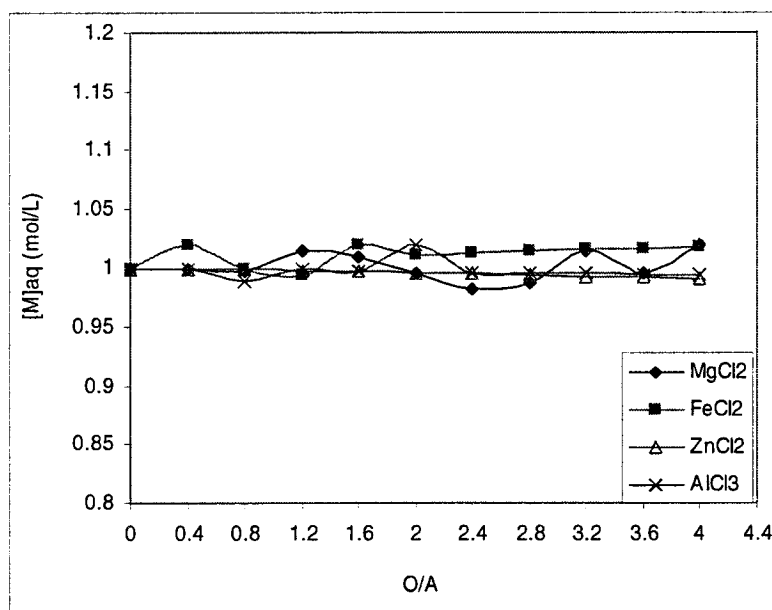


Figure 4.9 SDC behaviour of some metal chlorides (21°C, 2-propanol, HCl, pH 0.5)

• Discussion

Extensive experimental data compiled by Linke and Seidell [1] indicate that most polar organic solvents (e.g. low-molecular alcohols, acetone) are in general able to dissolve

(completely or partly) most metal chlorides of practical interest even in the absence of water, making the SDC process economically inefficient or even impossible. For example, Figure 4.10 indicates the solubility of some chlorides (expressed as kg salt/100 kg alcohol) in absolute methanol as a function of temperature.

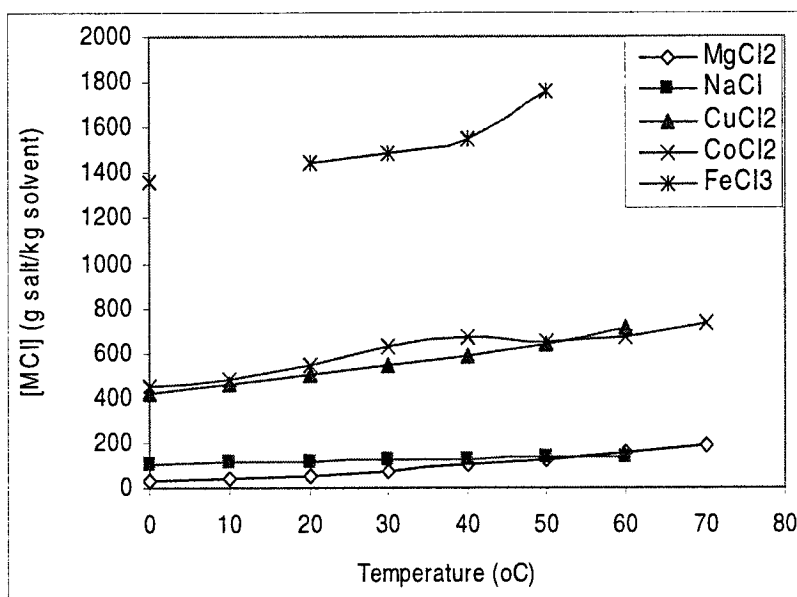


Figure 4.10 Solubility of metal chlorides in absolute methanol as a function of temperature (data from [1])

It can be observed that appreciable amounts of salt dissolve even at low temperatures and the values increase for more elevated temperatures.

There are organic solvents in which metal chlorides are insoluble but these are not suitable for SDC because of their complete immiscibility with water and/or extreme toxicity (e.g. ethers, superior ketones, pyridine, aromatic derivatives, furfural, etc.). Table 4.6, based on data compiled by Linke and Seidell [1], offers a qualitative overview on the solubility of metal chlorides studied in various organic solvents.

New solvents such as amines have been studied in recent years. Since the nitrogen contained in the amine molecule is not as electronegative as the oxygen would be in alcohols, hydrogen bonds formed between N and O from water will be stronger than those between two N atoms; this means that more amine molecules will be available to hydrogen-bond for water displacement. Amines show good promise in salting out

chloride salts from their aqueous solutions but these applications are restricted to alkali and alkaline earth metals. The literature data indicate very few applications of the salting out process to MCl-HCl-H₂O systems where M=Na and Ca [26, 27, 28] but virtually no crystallisation with organic solvents of metal chlorides of interest in hydrometallurgy (such as Al, Cu, Ni, Fe, Zn) has been attempted or reported.

Table 4.6 Solubility of metal chlorides in various organic solvents (qualitative data) [1]

(++ very soluble; + soluble (or partly); - insoluble)

Organic Solvent	MgCl ₂	FeCl ₂	ZnCl ₂	AlCl ₃
Aliphatic Alcohols	++	++	++	++
Acetone	++	++	++	++
MEK, MPK	+	+	+	+
Pyridine	+	N/A	++	N/A
Methyl Acetate	+	++	+	++
Aromatic Nitriles	+	+	+	N/A
Methyl & Ethyl Sulphide	N/A	-	+	-
Ethyl Ether & higher	-	-	-	-
CS ₂	-	-	-	-
Nitrobenzene	-	-	-	-

Stronger solvation of halide anions (as opposed to SO₄²⁻) by polar protic solvents such alcohols via formation of hydrogen bonds cannot explain the unusual high solubility of metal chlorides in such media, since Price [18], after calculating solvation numbers of ions in several solvents using Stokes' law, concluded that similar to water, halide ions appear to be unsolvated in polar protic solvents (i.e. solvation numbers are 0).

Ahrland [29] suggested that a combination of weak or non-existent solvation and low dielectric constant of the medium can promote the formation of complexes between ions; the anions enter the inner coordination sphere of the cation as ligands, displacing water molecules in the process. The equilibria between metal ion species in aqueous-organic solvents containing Cl⁻ is more complicated due to the fact that the complexing ligand could be either Cl⁻ or the organic solvent. Senanayake and Muir [30] demonstrated

that, in contrast with dimethylsulfoxide or acetonitrile, ethanol does not participate in the formation of any complexes in aqueous solution, but favours the formation of chloro-complexes alone.

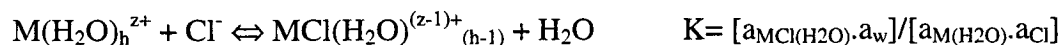
It appears thus that the solubilities of metal chlorides in non-aqueous solvents relative to water are actually enhanced by formation of chloro-complexes of larger stability constants. It is clear from the scattered information in the literature [29, 30], summarised in Table 4.7, that $\log K_1$ or β_n increases in mixed aqueous-organic or pure organic solvents for a wide range of metal complexes.

Table 4.7 Chloride stability constants in aqueous, mixed and non-aqueous solvents at 25°C [29, 30]

Cation	Water		Mixed or Protic	
	Medium	$\log K$ or $\log \beta$	Medium	$\log K$ or $\log \beta$
Na ⁺	0	N.D.	80% Acetone	$K_1=1.5$
Cr ³⁺	4.4 M HCl	$K_1=-0.98$	70% MeOH	$K_1=1.22$
Co ²⁺	0	$K_1=0.83$	50% EtOH	$K_1=1.63$
Ni ²⁺	0	$K_1=0.37$	MeOH	$K_1=3.2$
Cu ²⁺	5 M NaClO ₄	$\beta_2=-0.22$	MeOH	$\beta_2=6.3$
Zn ²⁺	3 M NaClO ₄	$K_2=-0.4$	MeOH	$K_2=4.3$
Pb ²⁺	0	$\beta_2=1.78$	MeOH	$\beta_2=3.66$
Cd ²⁺	3 M NaClO ₄	$K_1=1.59$	MeOH	$K_1=5.95$

In water, metal chloride complexes are extremely weak (small $\log K$ or $\log \beta$ values) but a marked increase is observed in mixed or pure organic solvents. The complexes are more stable due to stronger electrostatic interaction between ions and weaker solvation.

The chloro-complexation of the metal ion M^{z+} in aqueous chloride solutions is described as follows:



The formation of complexes depends mainly on the activity of cation and chloride ion. Since polar protic solvents are moderate cation solvators but very good anion solvators, cation activities are only slightly modified in the presence of organic whereas anion activities undergo more dramatic changes [30]. Parker [31] explains the preferential formation of chloro-complexes in mixed aqueous or organic solvents as a result of the

almost linear drastic increase in the activity of Cl^- with mole fraction organic (Figure 4.11), since the formation of complexes is very sensitive to a_{Cl^-} and solvent composition. It can be observed that the increase of Cl^- activity in ethanol is more drastic than that for SO_4^{2-} . Similarly, Jana et al. [32] attributed better recovery of metals in a diluted hydrochloric leaching system containing alcohols (methanol, ethanol, propanol and butanol) to the increased Cl^- activity that favours complex formation.

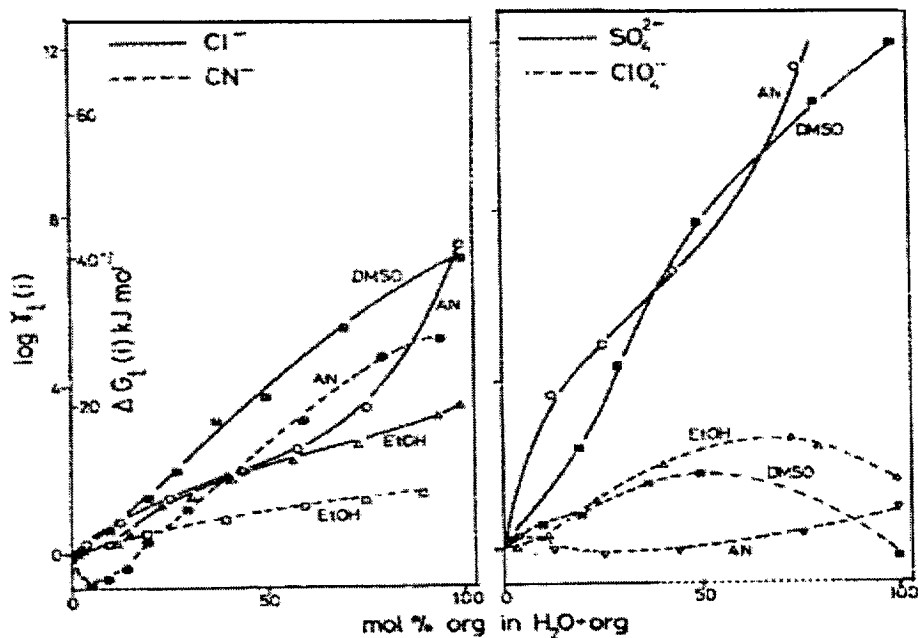


Figure 4.11 Effect of solvent on activity coefficients of anions upon transfer between water and mixed aqueous-organic solvents (molar scale, 25°C) [31]

4.4. Summary and Conclusions

1. Selection criteria for the organic solvent were established and screening procedures based on most important physical properties were developed. It was decided to eliminate organic solvents with: limited solubility in water (which would require larger volumes), boiling point higher than 90°C (to minimise energy consumption during recovery by distillation), excessive volatility (to avoid losses) and toxic nature. Finally, **2-propanol** was considered to meet most of the selection criteria outlined in

Section 4.2.1. for the organic solvent of choice in SDC and opted for use in further systematic in-depth studies.

2. Regarding the crystallisation of sulphate salts from the system $\text{MSO}_4\text{-H}_2\text{SO}_4\text{-H}_2\text{O}$, 2-propanol acted as an efficient salting out agent for the metal sulphates tested (with the exception of Fe (III) salt, which did not precipitate but instead caused the splitting of the aqueous phase). An organic-to aqueous (O/A) ratio of 4 removed more than 90% of metal from solution (with the exception of magnesium) in the form of crystalline sulphates with various number of crystallisation water molecules, but the choice of an optimum O/A depends on the specific requirements (in terms of final tolerated metal) of a given industrial process. The differences in crystallisation behaviour were attributed to differences in hydration energy; this was defined as the energy required for a hydrated ion to be separated from its bound water; this is the measure of the hydration of the ion relative to the bulk solvent. As a general rule when comparing ΔH for different ions, the smaller the ΔH the easier it will be for the water molecules to be removed from the hydration sphere.
3. None of the tested metal chlorides could be successfully separated from $\text{HCl-H}_2\text{O}$ system with 2-propanol. As the alcohol was added to the aqueous solution, it formed a homogeneous mixture without separating the salt, even for high organic contents. This was explained in terms of enhanced metal chlorides solubilities in non-aqueous solvents relative to water by formation of chloro-complexes of larger stability constants. The preferential formation of chloro-complexes in mixed aqueous or organic solvents is the result of the almost linear drastic increase in the activity of Cl^- with mole fraction organic.

References

- [1]. W.F. Linke and A. Seidell (editors), *Solubilities of Inorganic and Metal-Organic Compounds (a compilation)* 4th edition, Van Nostrand, Princeton, N.J., (1958).
- [2]. J.W. Mullin, *Crystallisation*, 3rd Ed., Butterworth-Heinemann, Oxford, (1993).

- [3]. J.I. Padova, "Ionic Solvation in Non-Aqueous and Mixed Solvents" in *Modern Aspects of Electrochemistry*, vol. 7, edited by B.E. Conway and J.O'M. Bockris, Plenum Press, New York, N.Y., pp. 1-82, (1972).
- [4]. J.M. Widon and S.J. Edelstein, *General Chemistry*, W.H. Freeman and Co., San Francisco, CA, pp. 202-203, (1981).
- [5]. C.M. Pina, L. Fernandez-Diaz, M. Prieto and S. Veintemillas-Verdaguer, "Metastability in drowning-out crystallisation: precipitation of highly soluble sulphates" *Journal of Crystal Growth*, **222**, pp. 317-327, (2001).
- [6]. A.K. Lyashchenko, "Concentration transition from water-electrolyte to electrolyte-water solvents and ionic clusters in solutions" *Journal of Molecular Liquids*, **91**, pp. 21-31, (2001).
- [7]. S.C. Rath and P.B. Das, "Thermodynamics of CdCl₂ and CdBr₂ in aquo-organic solvents from conductance data" *Thermochimica Acta*, **60**, pp. 77-86, (1983).
- [8]. D. Peeters, "Hydrogen bonds in small water clusters: a theoretical point of view" *Journal of Molecular Liquids*, **67**, pp. 49-61, (1995).
- [9]. P. Wang and A. Anderko, "Computation of dielectric constants of solvent mixtures and electrolyte solutions" *Fluid Phase Equilibria*, **186**, pp. 103-122, (2001).
- [10]. E.W. Flick (Editor), *Industrial Solvents Handbook*, 3rd edition, Publications Noyes, Parkridge, N.J, p. 223, 1985
- [11]. J.M. Cohen, "Applications of solvent displacement crystallisation in hydrometallurgy" in *Separation Processes in Hydrometallurgy*, (edited by G.A. Davies), pp. 265-273, Ellis Horwood, London, U.K., (1987).
- [12]. G. Wypych (Editor), *Handbook of Solvents*, ChemTec Publishing, Toronto, Canada, pp. 54, (2001).

- [13]. V.V. Udovenko and T.F. Mazanko, "Liquid-vapour equilibrium in the propan-2-ol-water and propan-2-ol-benzene system" *Russian Journal of Physical Chemistry*, **41**(7), pp. 863-866, (1967).
- [14]. H. Zhu, C. Yuen and D.J.W. Grant, "Influence of water activity in organic solvent + water mixtures on the nature of the crystallizing drug phase. I. Theophylline." *International Journal of Pharmaceutics*, **135**, pp. 151-160, (1996).
- [15]. B.E. Conway and J. O'M. Bockris, "Ionic Solvation" in *Modern Aspects of Electrochemistry*, vol. 1, edited by B.E. Conway and J.O'M. Bockris, Butterworth Scientific Publications, London, pp. 47-102, (1954).
- [16]. E.R. Nightingale, JR., "On the Specificity of Electrolyte Solvation. Viscosity and Infrared Characterization of Ionic Hydration" in *Chemical Physics of Ionic Solutions*, edited by B.E. Conway and R.G. Barradas, John Wiley & Sons Inc., New York, N.Y., pp. 87-100, (1966).
- [17]. D. Feakins, "Ionic Solvation in Mixed Aqueous Solvents" in *Physico-Chemical Processes in Mixed Aqueous Solvents*, edited by F. Franks, Elsevier, New York, N.Y., pp. 71-90, (1967).
- [18]. E. Price, "Solvation of Electrolytes and Solution Equilibria" in *The Chemistry of Non-Aqueous Solvents. Volume 1: Principles and Techniques*, edited J.J. Lagowski, Academic Press, New York, N.Y., pp. 67-96, (1966).
- [19]. J.E. Desnoyers and C. Jolicoeur, "Hydration Effects and Thermodynamic Properties of Ions" in *Modern Aspects of Electrochemistry*, vol. 5, edited by B.E. Conway and J.O'M. Bockris, Plenum Press, New York, N.Y., pp. 1-89, (1969).
- [20]. J.S. Muirhead-Gould and K.J. Laidler, "The Thermodynamic Properties of Charge-Bearing Systems in Aqueous Solutions: A Discontinuous Model for Octahedral Hydration" in *Chemical Physics of Ionic Solutions*, edited by B.E. Conway and R.G. Barradas, John Wiley & Sons Inc., New York, N.Y., pp. 75-86, (1966).

- [21]. F. David, V. Vokhmin and G. Ionova, "Water characteristics depend on the ionic environment. Thermodynamics and modelisation of aquo ions", *Journal of Molecular Liquids*, **90**, pp. 45-62, (2001).
- [22]. N. Sato, Y. Wei, M. Nanjo and M. Tokuda, "Recovery of samarium and neodymium from rare magnet scraps by fractional distillation method" *Metallurgical Review of MMIJ*, **15**(1), pp. 1-13, (1998).
- [23]. J.E. Prue, "Ion Association and Solvation" in *Chemical Physics of Ionic Solutions*, edited by B.E. Conway and R.G. Barradas, John Wiley & Sons Inc., New York, N.Y., pp. 163-173, (1966).
- [24]. C.M. Pina, L. Fernandez-Diaz, M. Prieto and S. Veintemillas-Verdaguer, "Metastability in drowning-out crystallisation: precipitation of highly soluble sulphates" *Journal of Crystal Growth*, **222**, pp. 317-327, (2001).
- [25]. E.S. Amis and J.F. Hinton (editors), *Solvent Effects on Chemical Phenomena*, vol. 1, pp. 182-205, Academic Press, New York, N.Y., (1973).
- [26]. T.G. Zijlema, H. Oosterhof, G.J. Witkamp and G.M. van Rosmalen, "Crystallisation of Sodium Chloride with amines as antisolvents" in *Separation and Purification by Crystallisation*, (edited by G.D. Botsaris and K. Toyokura), pp. 230-241, ACS, Washington, DC, (1997).
- [27]. T.G. Zijlema, R.J.A.J. Hollman, G.J. Witkamp and G.M. van Rosmalen, "The production of pure NaCl by the antisolvent crystallisation of NaCl.2H₂O and a consecutive recrystallisation step" *Journal of Crystal Growth*, **198/199**, 789-795. (1999).
- [28]. M.S.H. Bader, "Separation of chloride and sulphate ions in univalent and divalent cation forms from aqueous streams" *Journal of Hazardous Materials*, **B73**, 269-283, (2000).
- [29]. S. Ahrland, "Solvation and Complex Formation in Protic and Aprotic Solvents" in *The Chemistry of Non-Aqueous Solutions. Volume 5A: Principles and Basic*

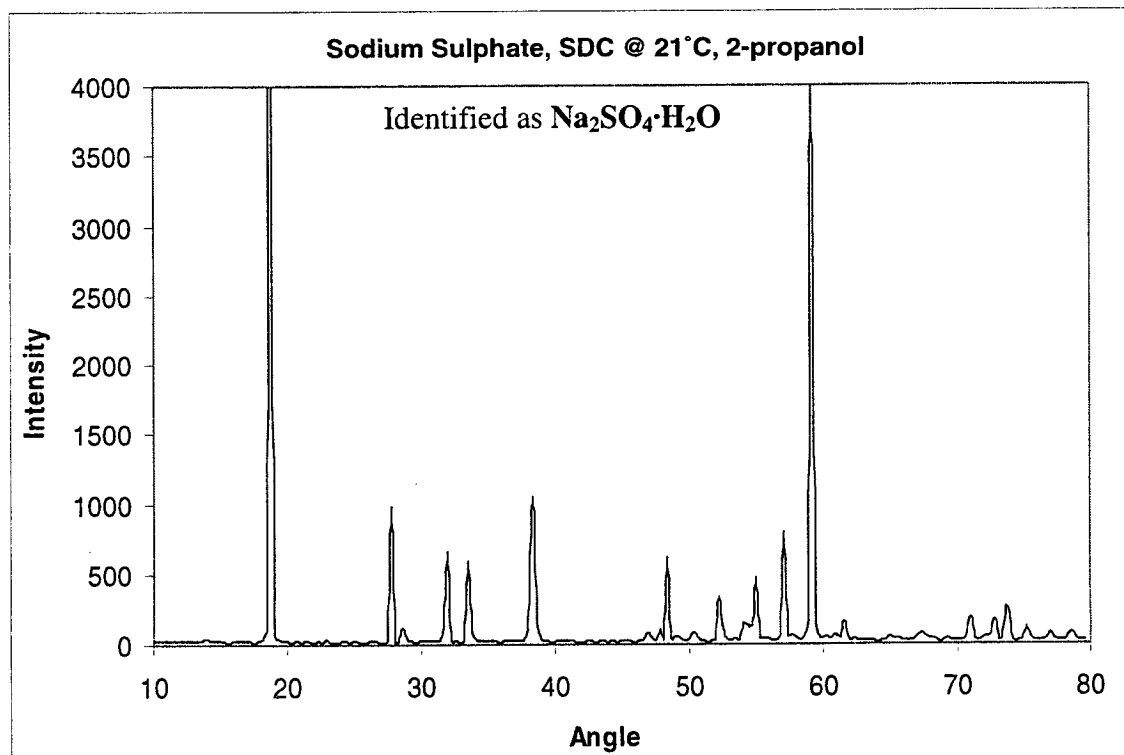
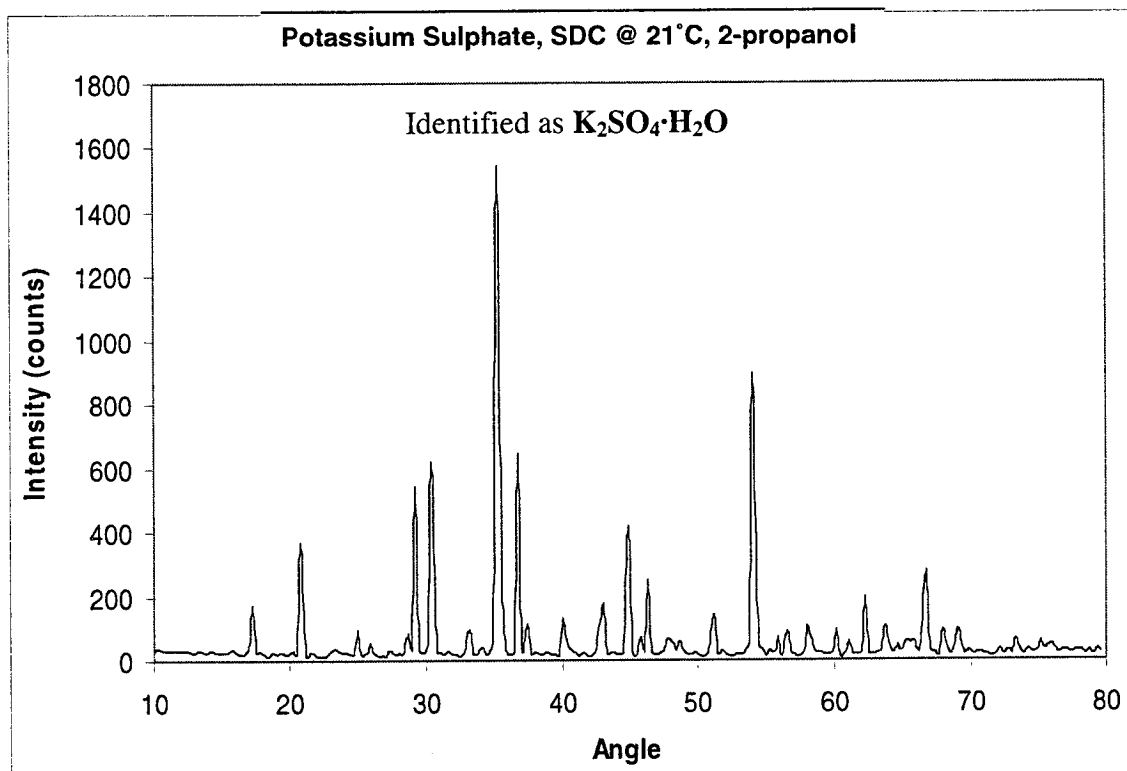
Solvents, edited by J.J. Lagowski, Academic Press, New York, N.Y., pp. 1-62, (1978).

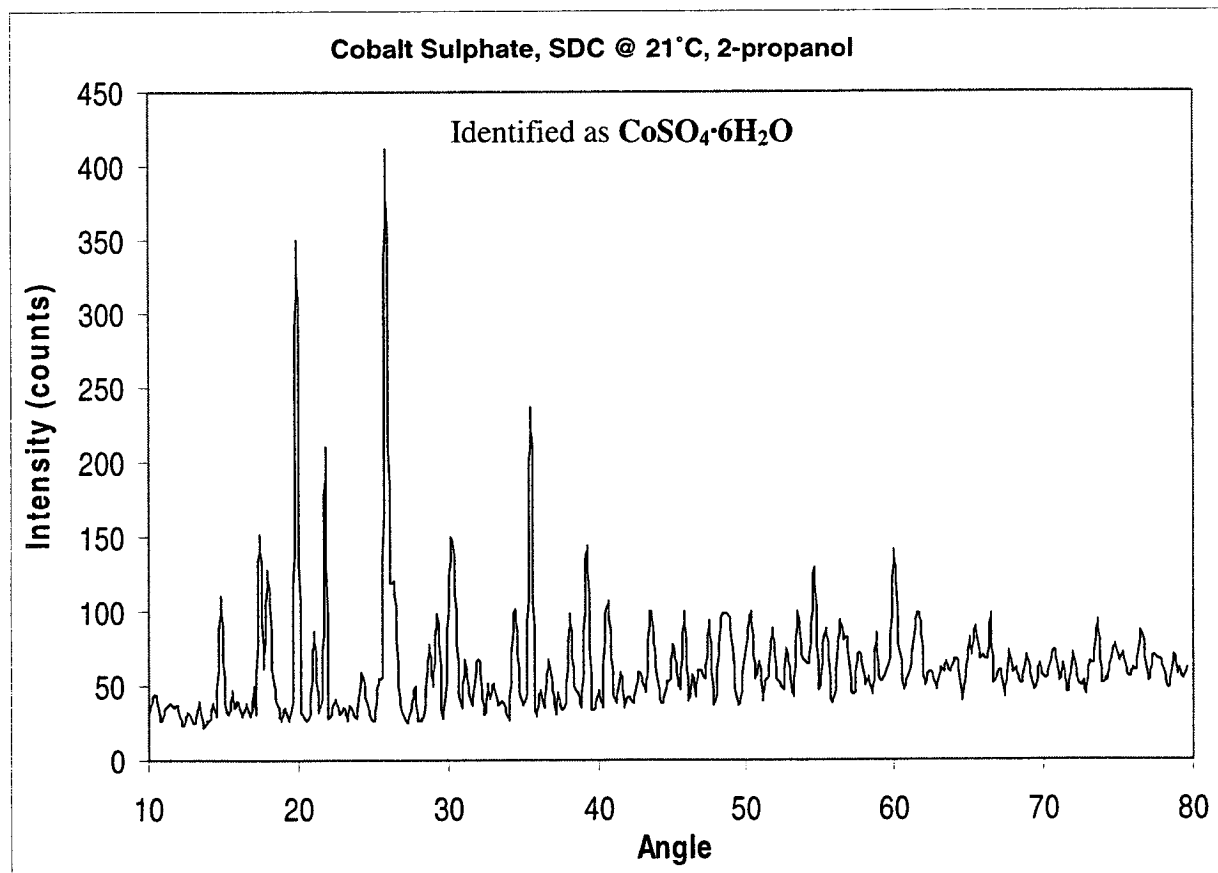
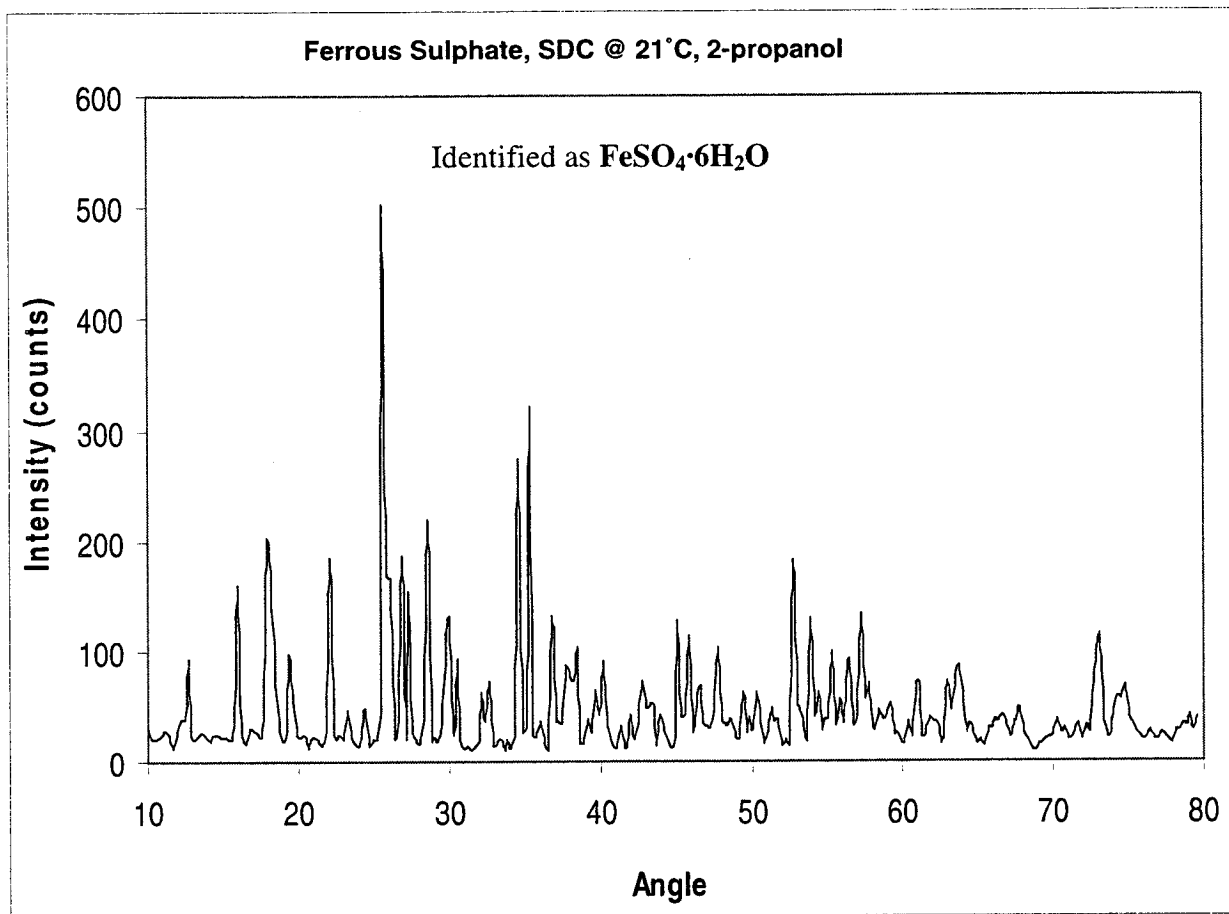
- [30]. G. Senanayake and D.M. Muir, "Competitive Solvation and Complexation of Cu(I), Cu(II), Pb(II), Zn(II) and Ag(I) in Aqueous Ethanol, Acetonitrile and Dimethylsulfoxide Solutions Containing Chloride Ion with Applications to Hydrometallurgy" *Metallurgical Transactions B*, **21B**, pp. 439-448, (1990).
- [31]. A.J. Parker, "Solvation of ions – enthalpies, entropies and free energy of transfer" *Electrochimica Acta*, **21**, pp. 671-679, (1976).
- [32]. R.K. Jana, D.D.N. Singh and S.K Roy, "Alcohol-modified hydrochloric acid leaching of sea nodules" *Hydrometallurgy*, **38**, pp. 289-298, (1995).

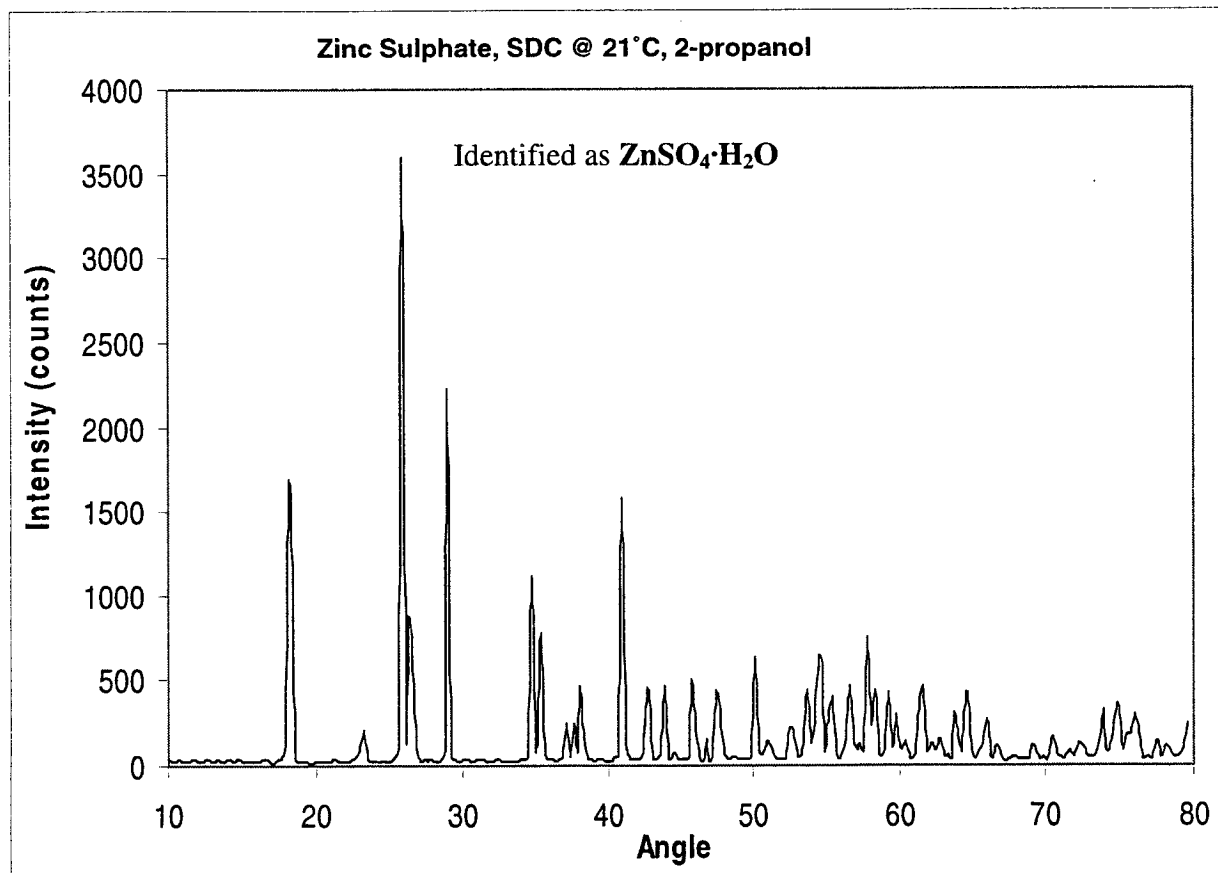
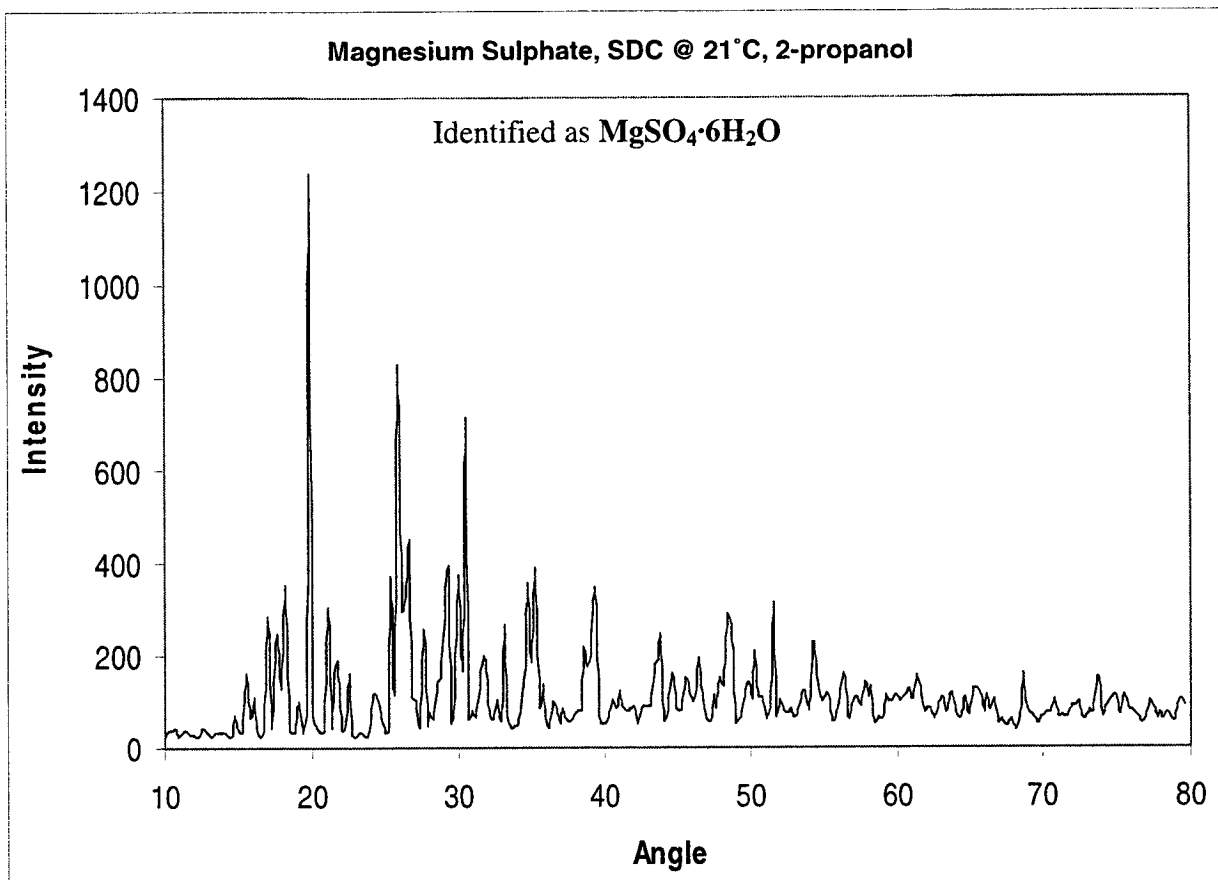
Physical Analysis of Metal Sulphates Crystallised via SDC

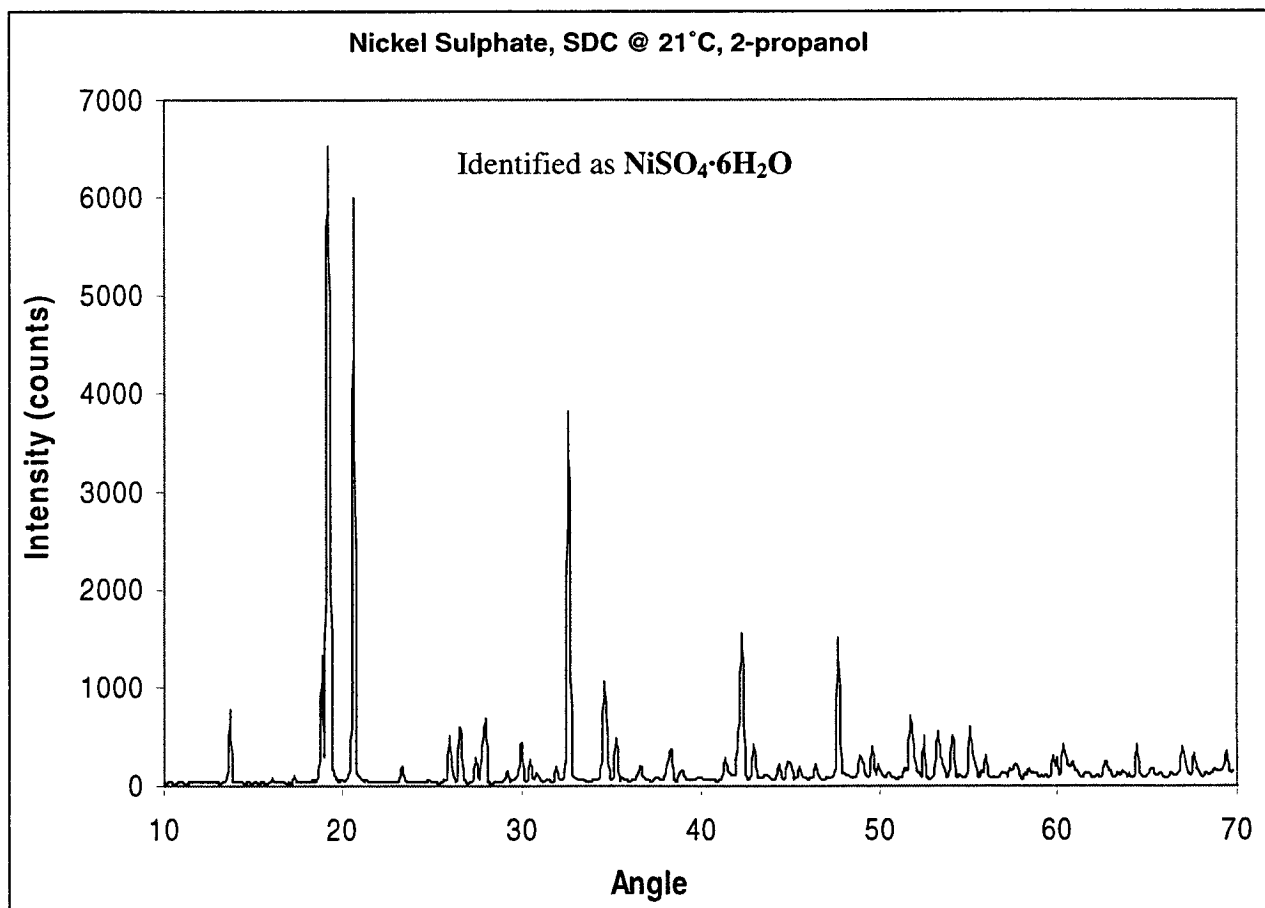
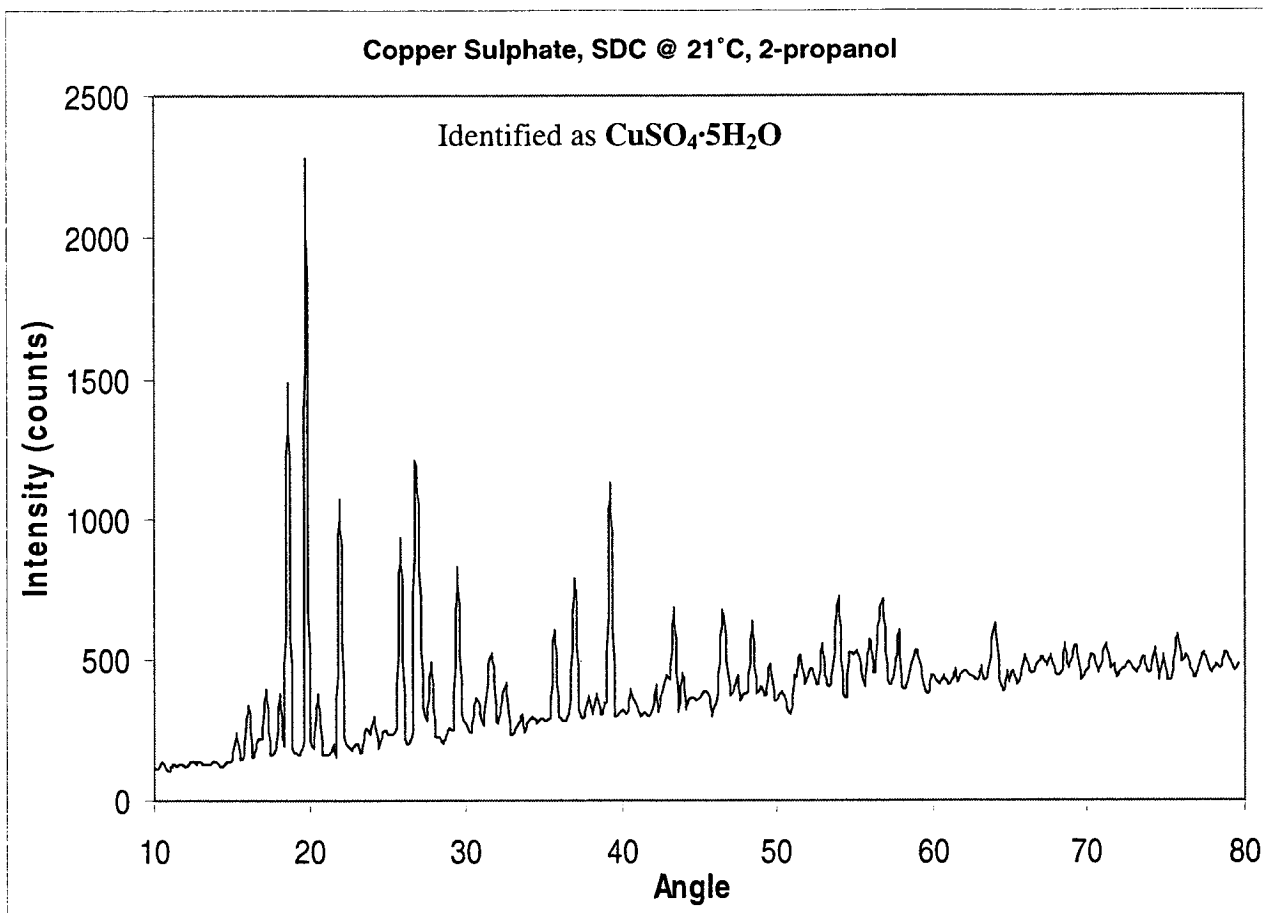
1. XRD Spectra

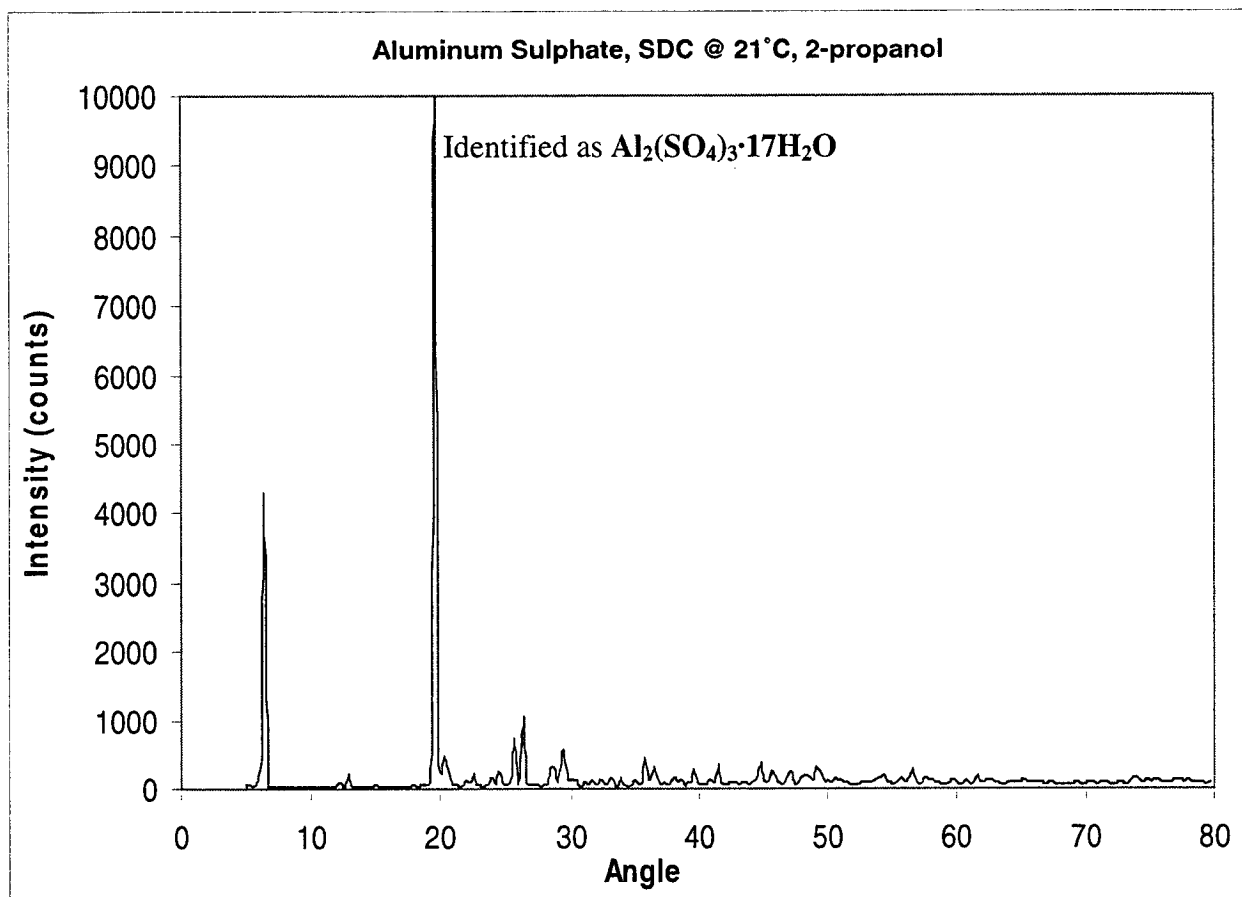
The confirmation of crystalline phases and the determination of the number of crystallisation water molecules were achieved by XRD analysis; the spectra obtained were matched to different standard spectra contained in the computer's database.





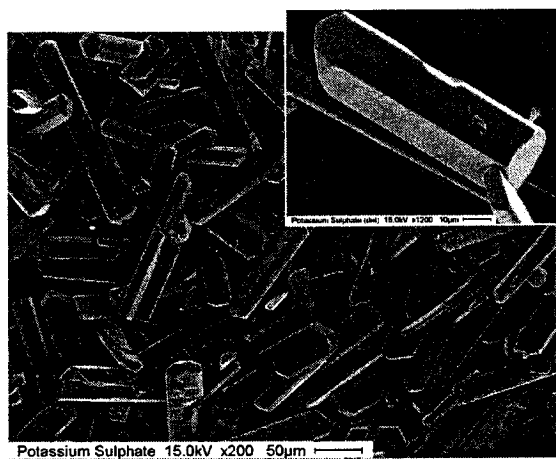




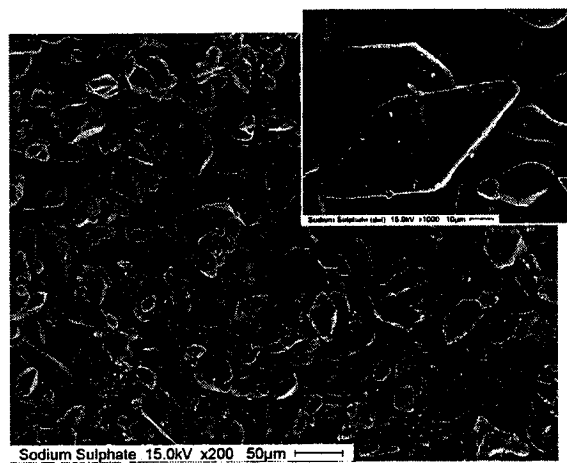


2. SEM Micrographs

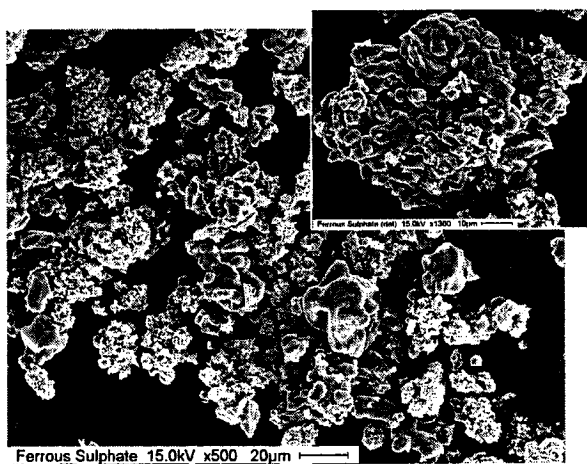
The morphology (general and detailed) and approximate size of the crystals were established by performing Scanning Electron Microscopy (SEM) using a JEOL 840A scanning microscope at 15kV on a gold-coated sample. The data on typical crystallisation system characteristic to each sulphate analysed was provided by “Web Minerals” (<http://webmineral.com>), an extensive mineral database containing information on crystallography, chemical composition, physical and optical properties, etc.



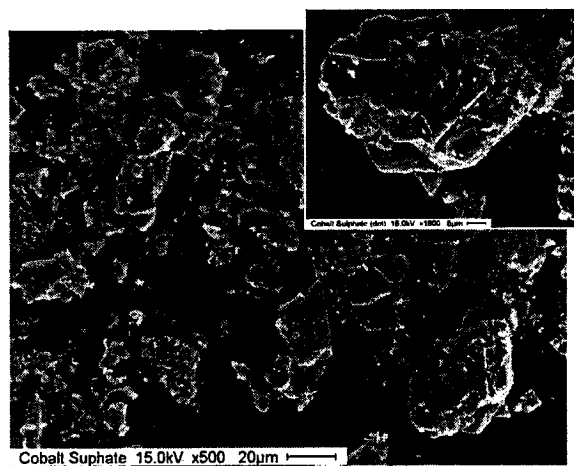
(a) $\text{K}_2\text{SO}_4 \cdot \text{H}_2\text{O}$: Orthorhombic-Dipyramidal
Smooth white crystals, $\sim 100 \mu\text{m}$.



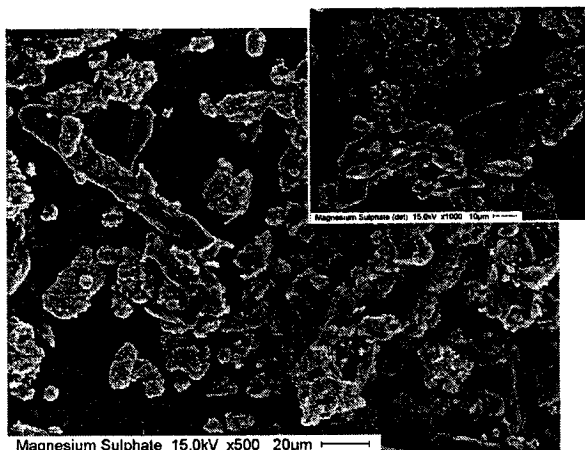
(b) $\text{Na}_2\text{SO}_4 \cdot \text{H}_2\text{O}$: Orthorhombic-Dipyramidal
Smooth white crystals, $< 50 \mu\text{m}$.



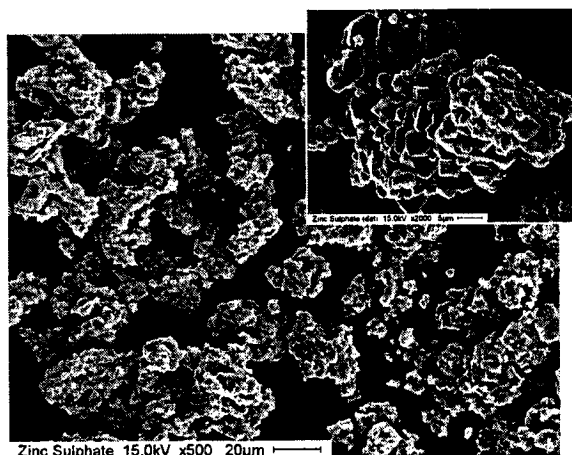
(c) $\text{FeSO}_4 \cdot 6\text{H}_2\text{O}$: Monoclinic Prismatic
Irregular light-green crystals, $< 5 \mu\text{m}$.



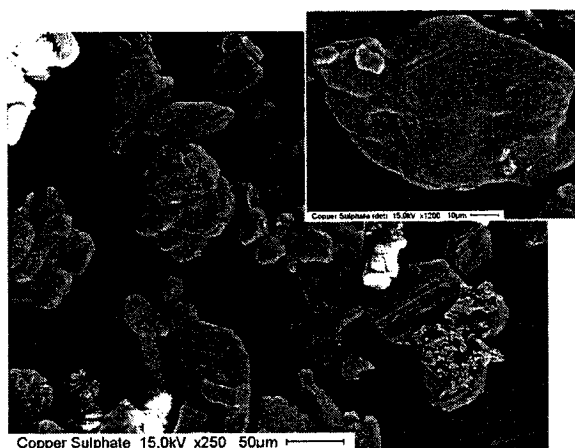
(d) $\text{CoSO}_4 \cdot 6\text{H}_2\text{O}$: Monoclinic prismatic
Irregular pink crystals, $\sim 20 \mu\text{m}$.



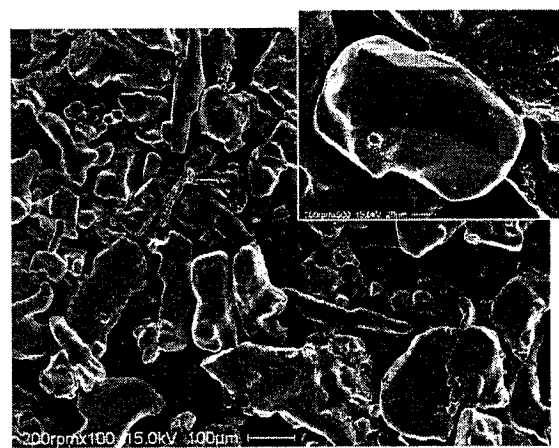
(e) $\text{MgSO}_4 \cdot 6\text{H}_2\text{O}$: Orthorhombic
Irregular white crystals, ~ 20 μm .



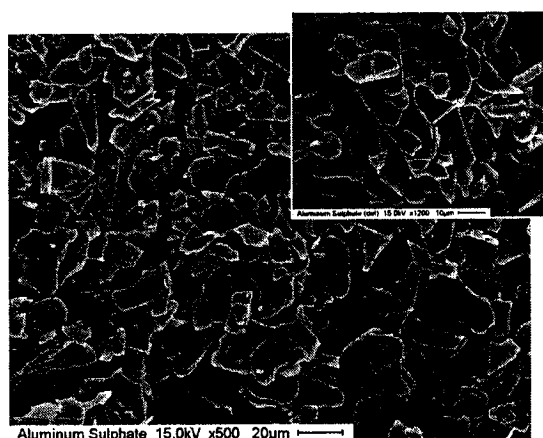
(f) $\text{ZnSO}_4 \cdot \text{H}_2\text{O}$: Orthorhombic
Irregular white crystals, < 5 μm .



(g) $\text{CuSO}_4 \cdot 5\text{H}_2\text{O}$: Triclinic-Pinacoidal
Smooth light-blue crystals, ~ 50 μm .



(h) $\text{NiSO}_4 \cdot 6\text{H}_2\text{O}$: Tetragonal-Trapezohedral
Smooth light green crystals, ~ 100 μm .



(i) $\text{Al}_2(\text{SO}_4)_3 \cdot 17\text{H}_2\text{O}$: Triclinic-Pinacoidal
Lamellar white crystals, ~20 μm .

Chapter 5. Crystallisation of Nickel Sulphate from H₂SO₄ Media

5.1 Introduction

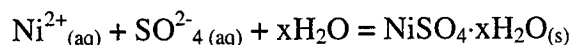
Many inorganic salts are produced industrially via a hydrometallurgical process, involving at a certain point the crystallisation of the salt from solution. When the solubility is minimally dependent on temperature, evaporative crystallisation (EC) is used, which entails the removal of water to increase the solute concentration above its solubility, achieve supersaturation and subsequent salt separation.

A practical illustration of this problem is the recovery of nickel as crystalline nickel sulphate from copper electrorefining spent electrolytes [1, 2]. During electrolytic refining of copper the amount of soluble impurities from the anodes accumulate in the electrolyte to a level that can affect the quality of the copper cathodes [3, 4]. Nickel is one of the worst impurities in contributing to decreased copper electrical conductivity because it forms a solid solution with copper; the maximum permissible level of nickel in copper cathodes must be < 7 ppm, hence nickel build-up in solution must not surpass 10 g/L [5].

The conventional practice of impurity control consists of continuously withdrawing electrolyte from the circulation system (the “bleed-off”) to recover its copper content and isolate/remove the soluble impurities via the following steps:

- (1) Cu recovery by electrowinning;
- (2) Removal of As, Sb, Bi by electrowinning or , more recently, by IX/SX [6, 7];
- (3) Ni recovery as nickel sulphate via evaporative crystallisation.

Nickel is separated as crude (impure) nickel sulphate (NiSO₄·2H₂O) from decopperised electrolytes. The crystallisation occurs according to the reaction [8]:



(x = number of crystallisation water molecules, depends on temperature and possible presence of dehydrating agents in the medium).

Although effective, this technique presents some major disadvantages:

- (1) The residual solutions are extremely corrosive, resulting in high operation and maintenance costs;
- (2) The evaporation step required to remove water is energy-intensive, increasing operating costs;
- (3) Due to violent boiling, supersaturation control is difficult, resulting in a final product of poor chemical (purity) and physical (crystal size) quality.

Solvent Displacement Crystallisation, by offering better process control, has the potential of providing an alternative to the traditional technique. Because of the interest in integrating the novel process to nickel sulphate recovery in copper electrorefining, the system 2-propanol-NiSO₄-H₂O-H₂SO₄ – first explored by Cohen [9] - was selected for in-depth SDC studies and the findings are reported in this Chapter. The main objective of this investigation is to examine closely the changes in solution composition and solids properties under the influence of various experimental conditions such as 2-propanol fraction, temperature, supersaturation magnitude, crystallisation regime (homogeneous vs. heterogeneous). Based on these observations, a process flow-sheet for industrial applications is developed.

5.2 Experimental

5.2.1 Research Strategy

The experiments conducted for the present research work consisted of two parts: (i) in order to establish a “reference” behaviour of the crystallisation of nickel sulphate from acidic media with 2-propanol, solubility measurements were conducted as a function of various factors; (ii) based on these results, critical supersaturation determinations and crystallisation tests were developed to further study and control the crystallisation process. In all these experiments, both changes in solution composition (Ni²⁺ and H₂SO₄ concentrations) on one hand and product quality on the other were monitored. The key parameters studied and the research goals are enumerated in Table 5.1.

All solubility and critical supersaturation tests were performed in 250 mL conical flasks, using magnetic stirring, as described in Chapter 3 (Section 3.3.1., Figure 3.1).

Crystallisation tests were conducted using the 1 L batch reactor, mechanical stirring and set-up presented in Section 3.3.1., Figure 3.2.

Table 5.1 Parameters considered in crystallisation of nickel sulphate with 2-propanol

Parameter	Evaluated Aspect
Organic Fraction (expressed as O/A)	<ul style="list-style-type: none"> • Equilibrium metal concentration in aqueous as a function of organic (O/A=0, 0.25, 0.43, 0.66, 1, 1.5, 2.33). • The optimum compromise between organic fraction and the final metal concentration tolerable in the aqueous phase.
Sulphuric Acid	<ul style="list-style-type: none"> • Equilibrium metal concentration in aqueous as a function of acid (0; 100, 250, 400, 550 g/L H_2SO_4).
Temperature	<ul style="list-style-type: none"> • Equilibrium metal concentration in aqueous as a function of temperature (10, 21, 40, 60°C). • Influence on SDC process and crystal quality (10, 21, 40°C).
Supersaturation (S)	<ul style="list-style-type: none"> • Critical supersaturation lines at 10, 21 and 40°C. • No S control vs. controlled S during SDC: Influence on metal content in solution and crystal quality.
Crystallisation Regime	<ul style="list-style-type: none"> • Homogeneous vs. Heterogeneous: Influence on metal content in solution and crystal quality. • Influence of seed quality on crystal properties (reagent-grade vs. "home-made").
Agitation and Ageing	<ul style="list-style-type: none"> • Influence of agitation magnitude on nucleation kinetics and crystal quality (0, 100, 200, 400 and 800 rpm). • Influence of equilibration time (ageing, ripening) following SDC on crystal quality (1, 2, 3, 4 hrs).

5.2.2 Experimental Procedure

De-ionised water, reagent-grade nickel sulphate ($NiSO_4 \cdot 6H_2O$, 99.24% purity, Fisher Scientific) and concentrated sulphuric acid (H_2SO_4 , 95-98% concentration) were used to prepare the aqueous solutions; 2-propanol Optima-grade (99.9% purity) was employed.

- ***Solubility Measurements***

- *Influence of temperature and sulphuric acid:*

100 mL aqueous solution containing 0, 100, 250, 400 and 550 g/L H_2SO_4 were agitated at 21°C in 250 mL Erlenmeyer flasks; small amounts of $NiSO_4 \cdot 6H_2O$ were added, allowing an equilibration period of 15 minutes. When crystals in equilibrium with solution were detected (i.e. no more dissolution), no more salt was added and the system was allowed to equilibrate for 24 to 48 hours. Subsequently, the crystals were separated by filtration, washed as described in Section 3.3.3., dried at ambient temperature for ~20 hrs in the fume-hood and further analysed. The mother liquor was diluted with 5% HCl and analysed for metal ion content. Same procedure was repeated for 10, 40 and 60°C.

- *Influence of organic content:*

100 mL of aqueous-organic mixtures were prepared starting from solutions containing 250 and 550 g/L H_2SO_4 , respectively, and 2-propanol, with the following organic-to-aqueous ratio (O/A): 0, 0.25, 0.43, 0.66, 1.00, 1.50 and 2.33. Small amounts of $NiSO_4 \cdot 6H_2O$ crystals were added under stirring at 21°C, allowing an equilibration period of 15 minutes. When crystals in equilibrium with solution were detected (i.e. no more dissolution), no more salt was added and the system was allowed to equilibrate for 24 to 48 hours. Subsequently, the crystals were separated by filtration, washed, air-dried in the fume-hood at ~21°C and further analysed. The mother liquor was diluted with 5% HCl and analysed for nickel. Same procedure was repeated for 10 and 40°C.

- ***Determination of Critical Supersaturation***

100 mL solutions containing different amounts of Ni^{2+} and 250 g/L H_2SO_4 were agitated at 21°C with a magnetic stirrer in Erlenmeyer flasks. Small volumes of organic were slowly added to the aqueous solutions by the means of a manual burette; after each addition, a 15-minutes equilibration period was allowed. At the moment a “cloud” was seen (initiation of the homogeneous crystallisation process), the volume of organic solvent that induced crystallisation was recorded and the solutions were stirred for 24 hours, to reach complete equilibrium. Subsequently, the crystals were separated by filtration, washed, dried at ambient temperature for ~20 hr and further analysed. The

mother liquor was diluted with 5% HCl and analysed for metal content. Same procedure was repeated for 10 and 40°C.

- ***Solvent Displacement Crystallisation Tests***

In a typical SDC test, 100 mL aqueous solution containing ~ 20 g/L Ni^{2+} and 250 g/L H_2SO_4 was agitated (200 rpm) in 1 L glass reactor maintained in a water bath at various temperatures (10, 21 and 40°C, respectively) while the organic was added from a 100 mL manual burette at various organic-to-aqueous (O/A) ratios. Subsequently, the crystals were separated by filtration, washed as described in Section 3.3.3., dried at ambient temperature in the fume-hood and further analysed. The mother liquor was diluted with 5% HCl and analysed for nickel content. Similar tests were performed at different agitation speeds (0, 100, 200, 400, 800 rpm).

Homogeneous Crystallisation: To homogeneously precipitate the inorganic salt, the organic solvent (various volumes) was added at once to the aqueous phase. At each temperature, three experiments were conducted, with a O/A ratio corresponding to: (i) $S = S_{cr,homo}$, (ii) $S \sim 2$, and (iii) $S \sim 10$. The mixture was agitated for 120 minutes and samples were taken every 2, 5, 10, 15 minutes, then every 15 minutes, in order to monitor cation content and hence the kinetics of the process. Samples taken by pipette were diluted 10 times immediately with 5% HCl solution to prevent further precipitation within the sample.

Heterogeneous Crystallisation: low supersaturation was maintained via a slow organic delivery at 21°C; for a certain volume of solvent corresponding to a supersaturation below the critical value ($O/A < 1.08$), organic addition was stopped and crystalline $NiSO_4 \cdot 6H_2O$ seed (~80 g/L) was provided to the system, in order to favour the secondary nucleation process and hence crystal growth. After a 30-minutes equilibration period, organic addition was resumed in a controlled, step-wise manner, small volumes at a time, followed by 30-minutes equilibration periods, as to maintain $S < S_{cr,homo}$ throughout the whole experiment (total $O/A = 1.5$). After each addition/stirring period the agitation was stopped and 2-mL samples were taken, diluted and analysed for nickel content.

- **Liquid-liquid separation**

No liquid-liquid separation was performed during this research project in order to recover the organic. Previous work [10] demonstrated it is possible to successfully recover the organic by moderate temperature fractional distillation following the procedure described by Pavia *et al.* [11]. Appendix B explains the principles of fractional distillation process and outlines the experimental procedure. Other possible liquid-liquid separation methods are also reviewed.

5.3 Systematic Solubility Studies

5.3.1 Influence of Temperature and Sulphuric Acid Concentration

The solubility of nickel sulphate in solutions of various free sulphuric acid concentrations (0, 100, 250, 400 and 550 g/L) was determined at temperatures ranging from 10 to 60°C (Figure 5.1). The plotted data-points are the average of three separate solubility measurements. The reproducibility is better at higher temperatures (due to improved dissolution kinetics), with errors ranging between 12-15 % at 10°C, 7-10 % at 21°C, ~5 % at 40°C and 2-3% at 60°C.

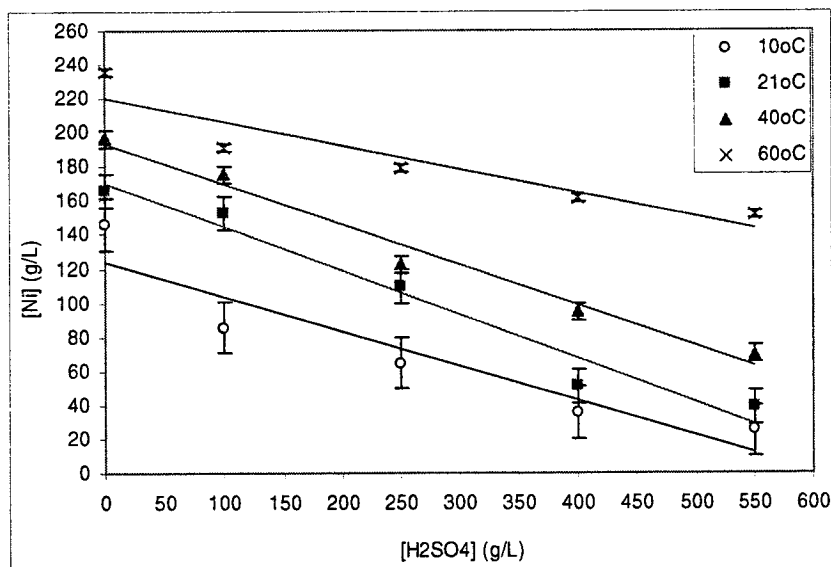


Figure 5.1 Effect of temperature and sulphuric acid concentration on nickel sulphate solubility

The solubility values were found to be linearly dependent on free acid concentration in the temperature range of interest, as per relationship in Eqn. 5.1:

$$C_{\text{Ni(II),eq}} \text{ (g/L)} = A \cdot C_{\text{H}_2\text{SO}_4} + B \quad (5.1)$$

Where A and B are the slope and y-intercept of a fitted straight line. These numbers summarised in Table 5.1. below are compared to the solubility values reported by Rohmer [12] at different temperatures for 0 g/L H₂SO₄.

Table 5.2 The fitting constants A and B for the solubility of nickel sulphate as a function of sulphuric acid concentration and temperature

T (°C)	A (slope)	B (y-intercept)	
		Experimental (0 < C _{H₂SO₄} (g/L) < 550)	Rohmer [12] (0 g/L H ₂ SO ₄)
10	- 0.20	124	125
21	- 0.25	170	145
40	- 0.23	194	182
60	- 0.13	220	215

Under tested conditions, negative slopes were found in all cases, i.e. the solubility of nickel sulphate decreased as the free acid concentration increased; furthermore, the solubility values were consistently higher at elevated temperatures for all the acid concentration range. These results are consistent to similar findings reported by Nyirenda and Phiri [8], Seidell and Linke [13], and Havlik *et al.* [14].

5.3.2 Influence of Organic Solvent

No literature data is known to exist on the solubility of nickel sulphate in the system H₂O-H₂SO₄ as a function of 2-propanol content. For trend evaluation and comparison purposes, literature values compiled by Linke and Seidell [13] as a function of pure alcohol type and of methanol fraction at 15°C were reviewed prior to actual solubility tests employing 2-propanol. These values are reproduced in Figure 5.2.

It can be observed that nickel sulphate is sparingly soluble in absolute alcohols, even at elevated temperatures (Figure 5.2 a); while temperature has a certain positive effect on salt solubility in pure methanol, there is virtually no temperature influence on the solubility in pure ethanol, which is considerably lower. This is explained in terms of structure and properties similarities to water, which are higher for methanol than for ethanol.

When alcohol is added to an aqueous solution of nickel sulphate (Figure 5.2 b), salt solubility decreases continuously with increasing amount of organic.

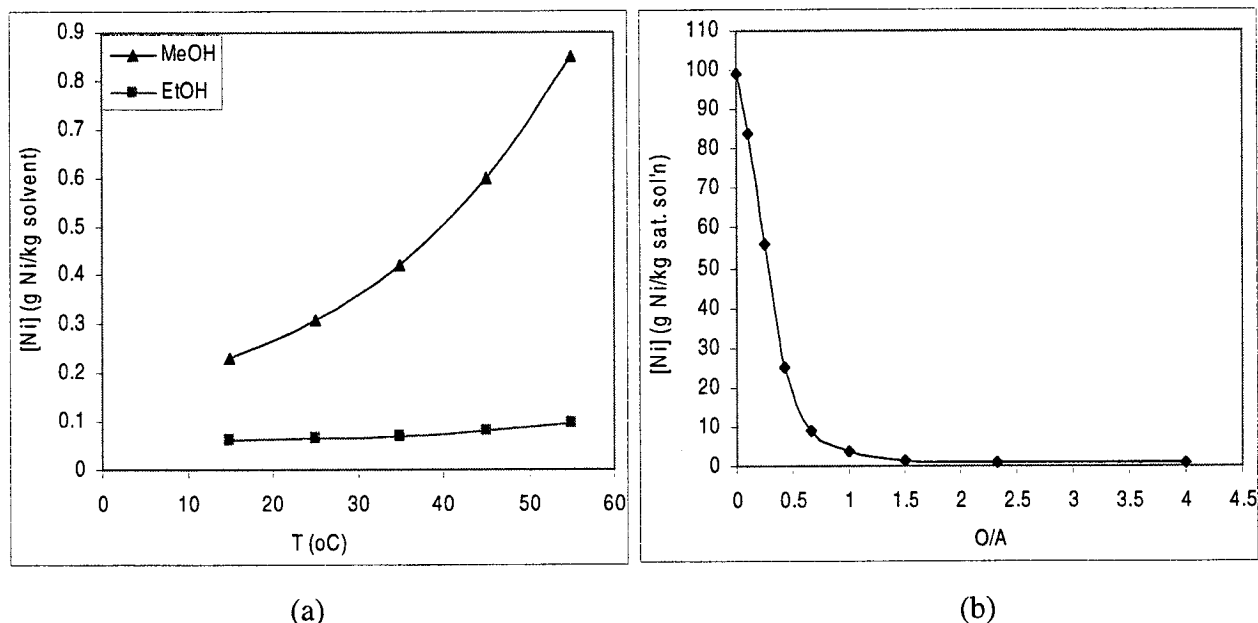


Figure 5.2 Influence of low-molecular alcohols on nickel sulphate solubility:

(a) pure alcohol type and temperature; (b) fraction of methanol at 15°C (from [13])

Based on these trends, it can be thus inferred that nickel sulphate solubility in 2-propanol should be even lower than in methanol and ethanol (explained in terms of capability of higher molecular chain compounds to decrease the dielectric constant of the medium and thus promote ion-pairing and crystallisation).

Next, the solubility of nickel sulphate in aqueous-acidic media (250 and 550 g/L H_2SO_4) was experimentally determined as a function of 2-propanol at various temperatures (10, 21 and 40°C) (according to set-up and procedures extensively described in Sections 3.3.1, 3.3.2 and 5.2.2). The results are given in Table 5.3 and

Figures 5.3 and 5.4, respectively. The plotted data-points are the average of three separate solubility measurements. The reproducibility is better at higher temperatures (due to improved dissolution kinetics), with errors ranging between 10-13 % at 10°C, 5-7 % at 21°C and 3-4 % at 40°C.

Table 5.3 Solubility of nickel sulphate as a function of 2-propanol, acidity and temperature

Organic Fraction (O/A)	[Ni] (g/L)					
	250g/L acid			550g/L acid		
	10°C	21°C	40°C	10°C	21°C	40°C
0	64.50	109.13	122.78	24.90	38.41	69.84
0.25	25.12	52.67	78.81	6.72	26.57	58.74
0.42	13.74	38.34	62.10	3.51	20.24	42.03
0.66	9.16	26.45	48.59	2.05	14.36	34.36
1.00	6.60	14.56	37.04	1.68	8.58	20.22
1.50	3.80	6.68	25.61	1.37	5.33	13.46
2.33	2.19	4.43	9.22	0.66	3.67	6.28

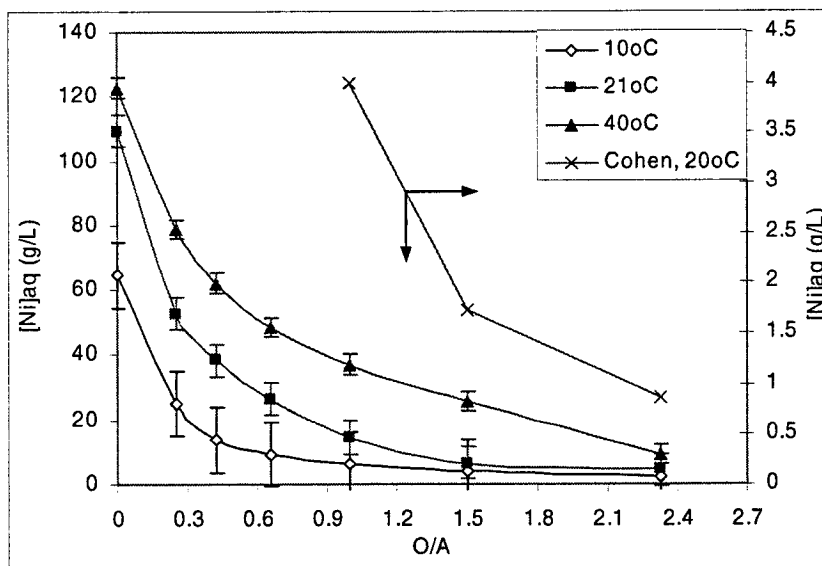


Figure 5.3 Nickel sulphate solubility in H₂O-H₂SO₄ (250 g/L) media as a function of 2-propanol fraction at various temperatures

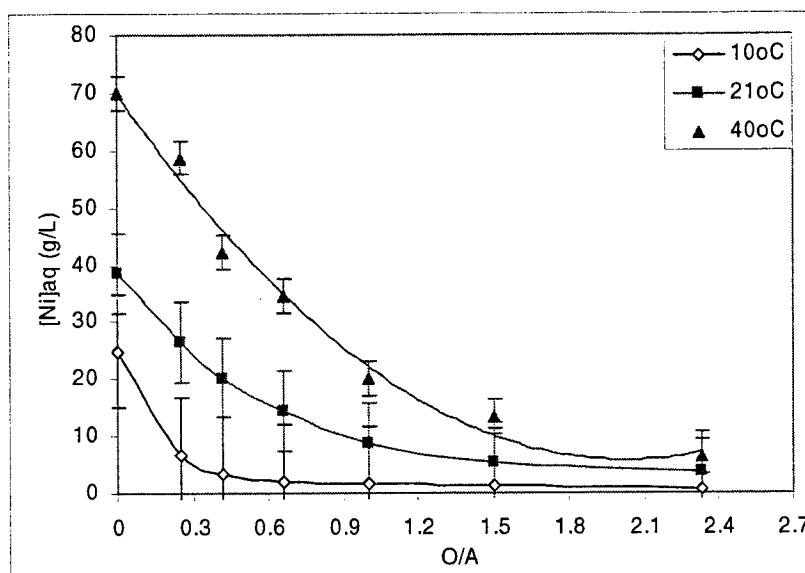


Figure 5.4 Nickel sulphate solubility in H₂O-H₂SO₄ (550 g/L) media as a function of 2-propanol fraction at various temperatures

As expected, the solubility (measured as g/L Ni²⁺ in the aqueous phase – not in the mixed aqueous - organic solutions) decreases with increasing organic fraction and sulphuric acid concentration and decreasing temperature. At low O/A ratios, increased acidity or decreased temperature bring an additional effect in suppressing nickel sulphate solubility, but as organic fraction increases (O/A>1), the solubility tends to be influenced solely by the organic content (due most likely to removal of water molecules from the ions' hydration spheres on one hand and on the other hand to drastic decrease of water dielectric constant upon organic addition, which in turn favours ion pairing).

For a typical solution containing 250 g/L H₂SO₄, it can be seen (Figure 5.3) that a volumetric ratio of 2-propanol to aqueous phase (expressed as O/A) of 2.3 is required to lower the solubility of nickel down to 9.22 g/L at 40°C, 4.43 g/L at 21°C and only 2.19 g/L at 10°C. It should be noted that the values found here are higher than solubility data reported by Cohen [9], e.g. Cohen reported at O/A = 1.5 the concentration of Ni to be 1.73 g/L as opposed to 6.68 g/L determined in the present work. However, as no details on to the exact procedure and conditions employed in Cohen's work were reported, the present work's solubility values are considered reliable due to their consistency.

- **Dissolution Kinetics**

Solubility data presented in Table 5.2 above represent equilibrium values at specific O/A. For an arbitrary selected O/A ratio ($O/A = 0.66$), the kinetics of dissolution process as a function of temperature were also studied and the information gathered is presented in Figure 5.5. This information is important to validate the equilibrium solubility values determined experimentally, when equilibration periods of 24 or 48 hours were selected.

As expected, dissolution kinetics of nickel sulphate hexahydrate are faster as temperature increases: 2 hrs are considered enough to reach equilibrium values at 40°C as opposed to ~ 4 hrs at 21° and ~ 6 hrs at 10°C , respectively.

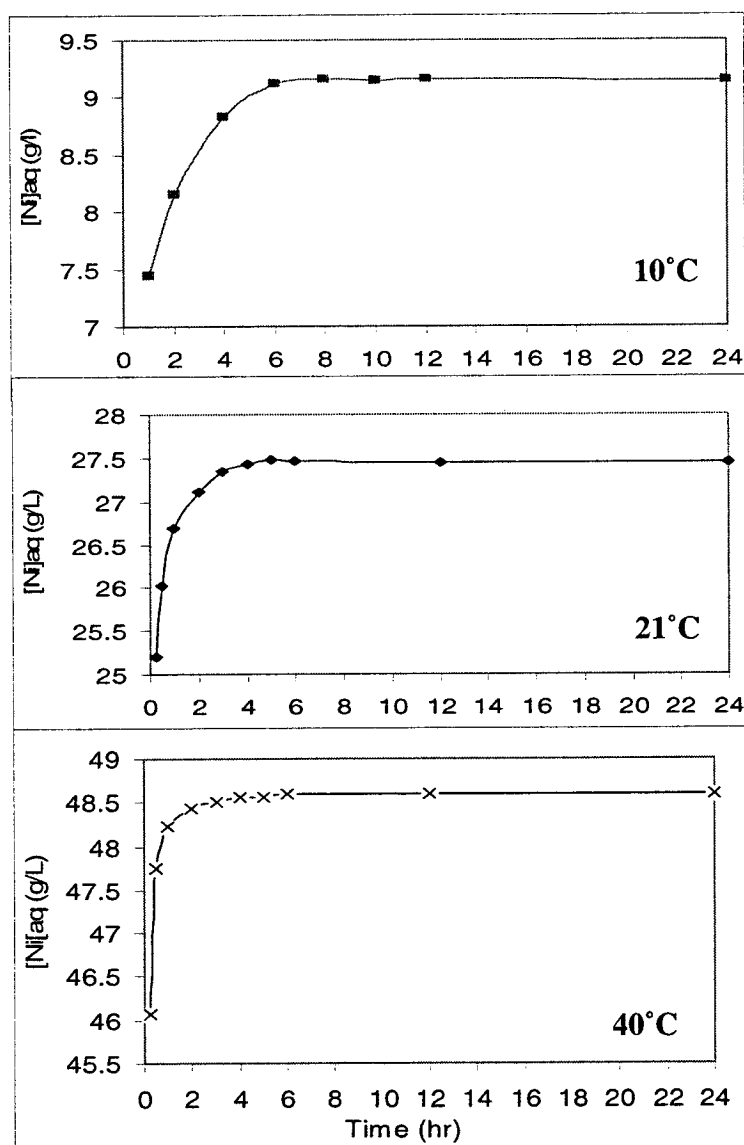


Figure 5.5 Nickel sulphate dissolution kinetics at different temperatures ($O/A=0.66$)

5.4 Analysis of a Typical SDC Experiment

Once the solubility lines are established, the next step was to conduct preliminary SDC tests in order to validate the effectiveness of 2-propanol as salting-out agent for nickel sulphate and to determine the optimum procedure for further experiments.

- ***Crystallisation***

Due to the lack of information in Cohen's article [9] concerning the experimental procedure, preliminary tests were performed following a gradual organic addition to the aqueous phase, employing the set-up described in Section 3.3.1.

In a typical SDC test 100 mL aqueous solution containing ~25 g/l Ni^{2+} and ~250 g/l H_2SO_4 (as in Cohen's work, these values simulate industrial conditions) were agitated at ambient temperature (21°C). 2-propanol was added from a 100 mL manual burette, in increments of 10 mL; an organic/aqueous total ratio $(O/A)_{total}$ of 1.5 was selected, meaning 150 mL of alcohol were used. After each addition, an equilibration period of 15 minutes was allowed then the solution was sampled to monitor nickel concentration. In the end, the solid product was filtered, washed and dried according to procedures described in Section 3.3.3.

- ***Distillation and Material balances***

No liquid-liquid separation was performed during this research project to recover the organic. Previous work [10] demonstrated it is possible to successfully recover the organic by moderate temperature fractional distillation following the procedure described by Pavia et al. [11]. Based on the data derived from the typical crystallisation test and distillation trial, a general material balance for nickel, 2-propanol and water was also undertaken. Appendix B explains the principles of fractional distillation process; other possible liquid-liquid separation methods are also reviewed.

5.4.1 Test Progression and Data Analysis

- *Solvent Displacement Crystallisation*

Figure 5.6 presents the progression of a SDC experiment, indicating the influence of the organic fraction on the concentration of nickel in the aqueous phase; the total duration of the experiment was 225 min; as observed, the significant drop in nickel concentration occurred when reached an O/A of ~ 0.9 .

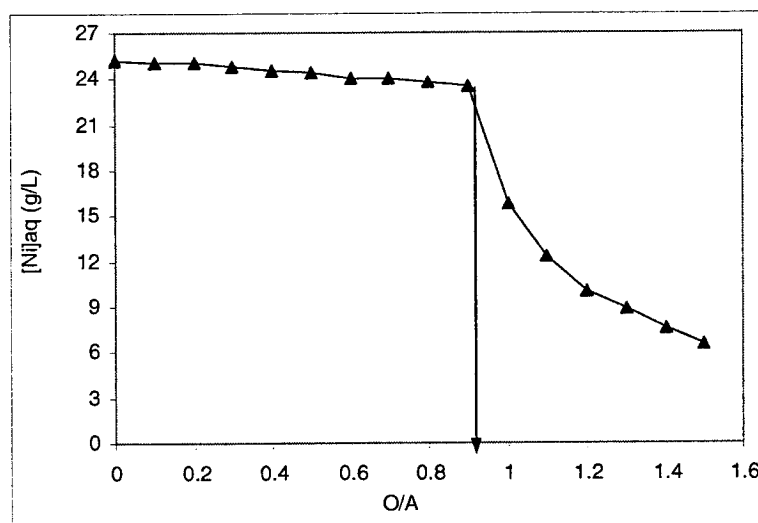


Figure 5.6 Progression of a typical SDC experiment (250 g/L H_2SO_4 , 21°C)

Nevertheless, this process does not occur instantaneously: as the organic corresponding to $O/A=0.9$ fraction was added under mild stirring, a certain “induction period” elapsed (approx. 10 minutes) before signs of crystallisation were observed. The turbidity increased as the clear solution became opaque (denoting the initiation of the nucleation process) then fine light-green crystals started to separate. The crystallisation process continued through the rest of the experiment as more organic was added. The final $[Ni]_{aq}$ corresponding to $(O/A)_{total}=1.5$ was 6.55 g/L meaning that $\sim 74\%$ of nickel had precipitated. The selected O/A_{total} ratio was considered effective enough to lower nickel concentration to values comparable to those obtained in industry via evaporative crystallisation ([1] and [2]). Addition of more solvent (i.e. $O/A>1.5$) can further reduce the final nickel concentration.

The precipitation process requires a certain O/A ratio, depending on the initial nickel concentration. In the initial stages, 2-propanol addition to the aqueous solution had no visible effect on nickel solubility: The appearance of the solution remained unchanged (clear, deep green) and nickel concentration practically constant, meaning that the first hydration sphere of Ni^{2+} is occupied by water molecules only.

Neutron diffraction studies conducted by Howell and Neilson [15] demonstrated that Ni^{2+} hydration is relatively unaffected by the nature of the bulky SO_4^{2-} counterion, i.e. Ni^{2+} maintains an octahedral hydration structure (i.e. $n=6$). Furthermore, thermodynamic studies performed by Plyasunova, Zhang and Muhammed [16] showed that Ni^{2+} in octahedral coordination is the main species of nickel in aqueous solution and forms weak complexes $NiSO_4^0$ and $Ni(SO_4)_2^{2-}$ in sulphate/acidic solutions only.

As extensively described in Section 2.3.3 [17], when alcohols are added to an aqueous solution, their molecules disrupt the water structure by breaking the water-water hydrogen bonds and replacing them with alcohol-water hydrogen bonds. With an increase in alcohol mole fraction, the inherent water cluster structure is disintegrated and, after a certain point, the water molecules from the ions' hydration spheres start to be displaced. In the end, almost all of the water is involved in the hydrogen bonds with the organic, thus provoking an increase in nickel sulphate saturation (decrease in solubility) and initiation of nucleation process. The disruption of hydrogen bonds between water molecules upon addition of organic leads to the decrease of the dielectric constant of solution, which in turn correlates to the increase of the electrostatic interaction between ions of opposite charge; this favours ionic association, formation of nuclei and subsequent homogeneous crystallisation [18, 19].

The activity of water in multi-component aqueous and aqueous-organic solutions is an important parameter in understanding the salting-out mechanism and subsequent crystallisation of salts; it describes the behaviour of "free water". By adding organic solvents (i.e. 2-propanol) and changing the composition of solution, water activity in a crystallisation medium can be modified, which influence both the mole fraction and partial pressure of water. With relevance to our research, Udovenko and Mazanko [20] studied the changes in water activity upon organic addition for the H_2O -2-propanol system at different temperatures (Figure 5.7). Water activity decreases from 1 in the

absence of 2-propanol to 0.2 for an organic mole fraction of 0.9 whereas the opposite trend is observed for the alcohol. Since the ions are soluble in “free water” only, any change in solution composition that results in decreasing the water activity will influence the solubility of the dissolved solute. In the present study, the combined effect of inorganic acids (H_2SO_4) and organic compounds (2-propanol) in the aqueous solution results in a marked decrease in water activity, as predicted by numerous authors [21, 22].

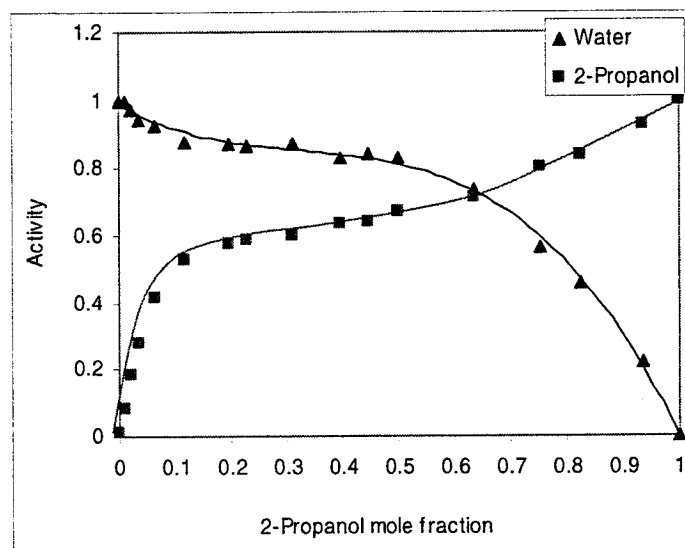


Figure 5.7 Water activity in the system H_2O -2-propanol [adapted from 20]

- *Use of Azeotrope*

Since in a potential industrial implementation of the SDC technique it will be preferable to recover the alcohol by distillation of the 2-propanol-water azeotropic mixture as opposed to the pure solvent, a test was performed to determine the effectiveness of the former in causing salt crystallisation. The azeotrope composition is 88% (wt.) 2-propanol and 12% (wt.) water, with a fixed boiling point of 80.4°C.

Table 5.3 gives comparative data from SDC tests performed with pure 2-propanol and azeotrope, respectively. It must be mentioned that "O" in the case of the azeotrope does not represent the organic component only, but the whole azeotrope addition.

Since the azeotrope contains only 88% (wt) alcohol, it is clear that more azeotrope had to be added to start crystallisation ($(O/A)_{cr} = 1.9$ vs. 1.1 for pure 2-propanol). Nevertheless, if $(O/A)_{cr}$ for the azeotrope was recalculated on the basis of 2-propanol content only, the converted value became 1.16, close to $(O/A)_{cr}$ when using pure solvent (Table 5.3).

Table 5.4 Initial and final parameters of SDC using 2-propanol and azeotrope (T = 21°C)

CONDITIONS	INITIAL		FINAL	
	2-propanol	Azeotrope	2-propanol	Azeotrope
[Ni ²⁺] _{aq} , g/L	18.91	18.91	6.15	8.03
(O/A) _{cr}	-	-	1.10	1.90
(O/A) _{total}	-	-	1.50	2.50
[H ₂ SO ₄], g/L	200.70	200.70	~ 270.00 (*)	~ 206.78

(*) after distillation, when part of water is removed with the azeotrope

Finally, another important consequence of using the azeotrope mixture as opposed to pure 2-propanol is that the supersaturation level is easier to control due to the dilution of the precipitating agent. Consequently, the crystals produced are expected have better physical properties. Moreover, the acid concentration of the electrolyte remains practically unaltered (i.e. 201 g/L initial vs. ~ 207 g/L final sulphuric acid).

5.4.2 Solid Product Properties

- **Crystalline Form**

The confirmation of crystalline phases and the determination of the number of crystallisation water molecules were achieved by X-ray Powder Diffraction analysis (XRD), using a Phillips PW1710 machine. The XRD pattern obtained for this sample (Figure 5.8) was matched to different standard spectra (NiSO₄·xH₂O x=2, 4, 6 and 7) contained in the computer database. The sharp peaks indicate that good degree of crystallinity was attained; moreover, it was found that **NiSO₄·6H₂O** offered the best match to the crystals produced.

Various solubility and crystal stability studies compiled by Linke and Seidell [23] indicate the heptahydrate (i.e. orthorhombic NiSO₄·7H₂O) as the predicted stable hydrate form in the temperature range between 0 and ~30°C while the hexahydrate (NiSO₄·6H₂O) constitutes the predicted stable phase from ~30 to 100°C (which exists under two polymorphism phases: tetragonal α-NiSO₄·6H₂O, stable from 30 to ~53°C, and

monoclinic β - $NiSO_4 \cdot 6H_2O$, stable from 53 to 100°C, [24]). It was determined that the hexahydrate produced in this work to be of the α -polymorphism.

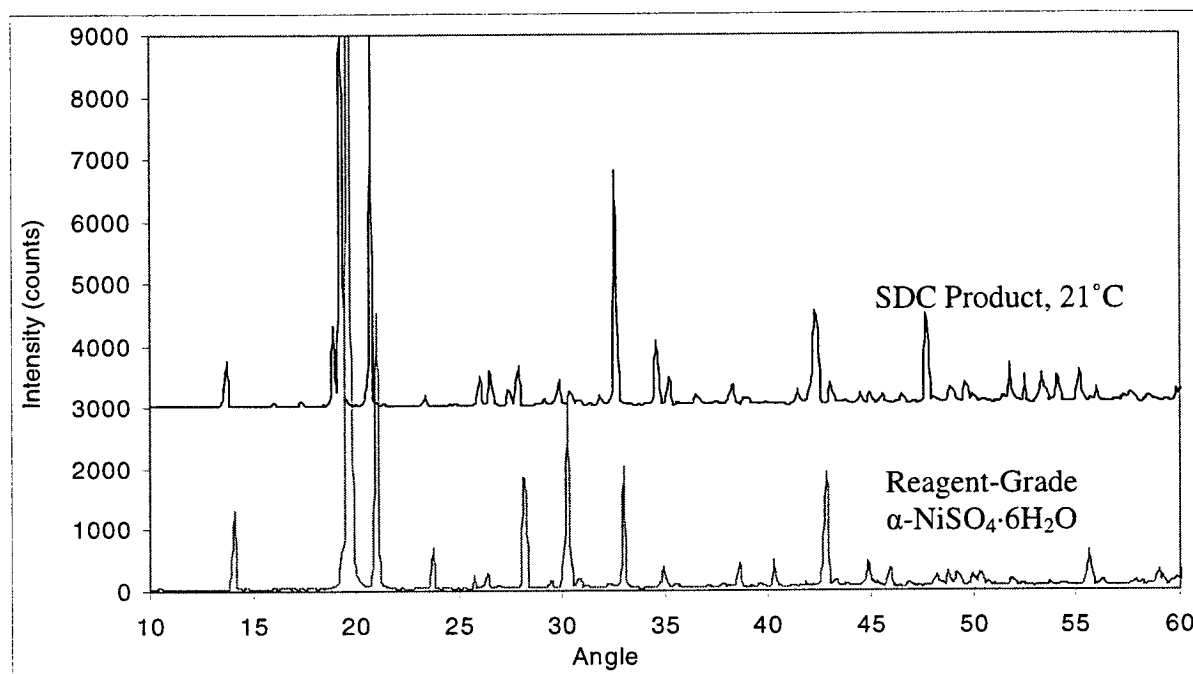


Figure 5.8 XRD spectrum of SDC product at 21°C

The systematic production of α -hexahydrate via the present and all subsequent crystallisation experiments is perfectly explained according to Stranski's Rule (or "Ostwald Rule of Stages"), which states that "the least stable phase (metastable) nucleates first as long as homogeneous nucleation determines the rate" [25].

In his comprehensive study of nickel sulphate solubility and stability, Rohmer [12] proves experimentally that the hexahydrate form can exist in metastable equilibrium even under 30°C. Moreover, at ambient temperature the transition kinetics between the metastable $NiSO_4 \cdot 6H_2O$ and the stable $NiSO_4 \cdot 7H_2O$ are extremely slow even in the presence of crystalline heptahydrate seed (6-7 weeks, according to Soboleva *et al*, [26]).

- **Morphology**

The green crystals produced at 21°C via SDC with 2-propanol were identified (see above) as α - $NiSO_4 \cdot 6H_2O$, which belongs to the tetragonal system with the unit cell parameters $a=b=6.780 \text{ \AA}$, $c=18.285 \text{ \AA}$, $Z=4$, and space group $P4_12_12$ [24, 26].

The general morphology and approximate size of the particles were established by performing Scanning Electron Microscopy (SEM) using a JEOL 840A electron scanning microscope at 15kV on a gold-coated sample.

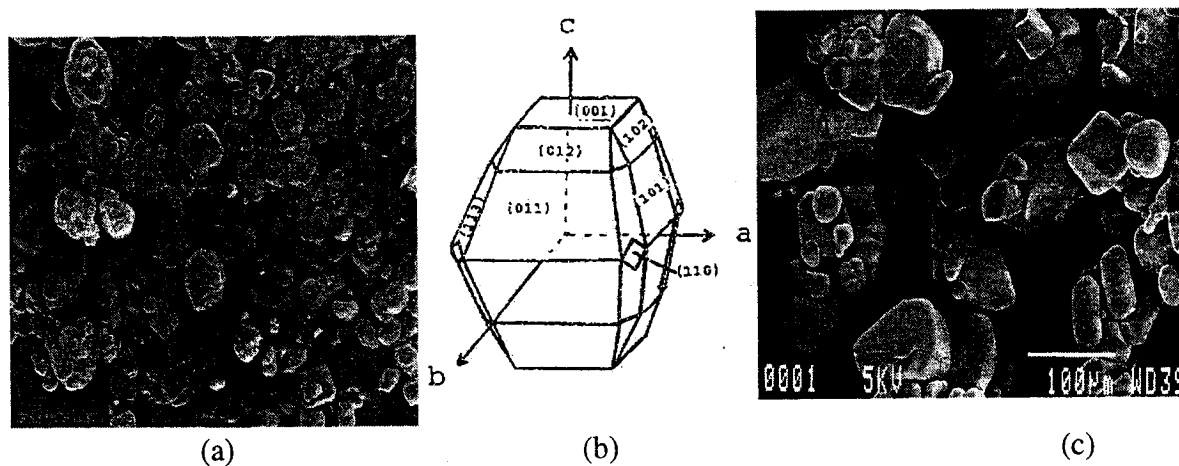


Figure 5.9 α -NiSO₄·6H₂O crystal structure: (a) synthetic α -NiSO₄·6H₂O (Fisher Scientific) employed to prepare initial aqueous solution; (b) tetragonal structure characteristic for α -NiSO₄·6H₂O; (c) α -NiSO₄·6H₂O produced via SDC at 21°C.

As can be observed from Figure 5.9 c, the crystals produced via SDC, averaging in size ~50-100 μ m, do not exhibit in their entirety the “perfect” tetragonal structure characteristic for α -NiSO₄·6H₂O (Figure 5.9 a and b). This irregular shape is due to homogeneous crystallisation conditions and insufficient equilibration time to allow for crystal maturation (ripening). However, even in the absence of rigorous optimisation of crystallisation conditions (i.e. controlled supersaturation, use of seed, sufficient equilibration time, etc.) the crystal size is appreciable, the compact surface does not exhibit major defects (i.e. no pores or cracks) and some of the crystals show a tendency of uniform growth towards the tetragonal characteristic structure. These encouraging preliminary results indicate that 2-propanol constitutes an efficient precipitating agent capable of producing good quality nickel sulphate crystals from acidic aqueous solutions.

5.5 Critical Supersaturation Lines

One of the objectives of the present research work is to optimise the crystallisation conditions by conducting the process inside the metastable zone as to form large particles with good settling properties and filterability. In order to achieve this goal, the critical supersaturation lines for the system $NiSO_4-H_2O-H_2SO_4-2$ -propanol are to be determined at 10, 21 and 40°C and compared to the equilibrium solubility curves. The critical supersaturation represents the concentration limit beyond which uncontrolled, spontaneous homogeneous crystallisation takes place.

Supersaturated solutions can be described using solubility-supersaturation diagrams as the one in Figure 5.10, applying to SDC process. In such a diagram, three zones can be defined [27]:

- (I) The stable (unsaturated) zone, where crystallisation is impossible;
- (II) The metastable (supersaturated) zone, where homogeneous crystallisation is improbable; however, if a crystal seed were placed in such a solution, growth would occur on it (“heterogeneous crystallisation”); well-grown particles obtained.
- (III) The labile (unstable) zone where spontaneous (homogeneous) crystallisation is probable; poor quality fine particles obtained.

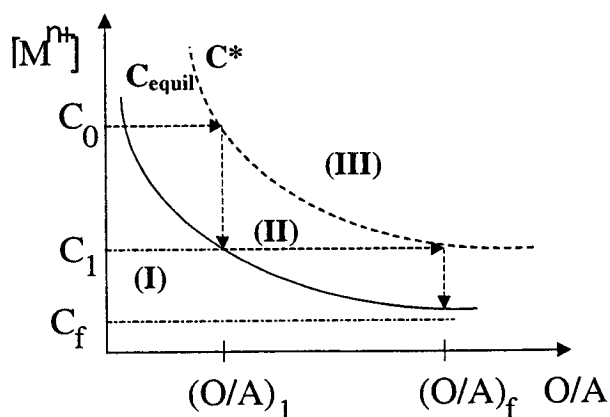


Figure 5.10 Solubility-supersaturation diagram and supersaturation-controlled SDC process concept (C_0 , C_1 : initial and intermediate salt concentration; C_f , C^* : final and critical salt concentration; $(O/A)_1$, $(O/A)_f$: organic-to-aqueous ratios used to reach C_1 and C_f , respectively)

As Demopoulos discussed [28], crystalline products can be obtained by controlling supersaturation below the critical value ($S_{cr,homo}$), in the metastable (growth-dominated) zone, via a staged addition of the precipitating agent. During the first step seed material is added to the solution to induce growth and to avoid homogeneous nucleation.

5.5.1 Induction Period

In a precipitation process, the appearance of a new solid phase from solution is only possible if supersaturation conditions are established; once this is attained, a period of time elapses until the new solid phase is detected.

Nielsen [29] defines the induction time as “the time interval between mixing two reacting solutions and the appearance of the first crystals that can be visually observed”. More specifically, Mullin [28] defines induction time as “the time needed for the assembly of a critical nucleus”, period which depends on supersaturation, temperature, impurities and agitation.

Although the induction time is a subjective value, the phenomena involved in a precipitation process could be established based on experimental determinations of the induction period against the solution’s initial supersaturation. The induction period is considered to be inversely proportional to the rate of nucleation [30]:

$$\log(t_{ind}) \propto [\gamma^3/T^3(\log S)^2] \quad (5.2)$$

where γ is the interfacial tension (mN/m or dyne/cm), T the temperature (K) and S the saturation ratio.

Barata and Serrano [31] determined that if the plot $\log(t_{ind})$ versus $(\log S)^{-2}$ is linear, then the crystallisation mechanism is primary nucleation (either homogeneous or heterogeneous) followed by growth (either diffusional limited, spiral or normal).

Nyvlt *et al* [32] and Mullin *et al.* [33] relate the metastable zone width to the induction period by the definition they give to the critical supersaturation line, which is considered “the supersaturation limit at which crystals of the new solid phase become visible”. In order to gain a better understanding of the initiation of the crystallisation process of nickel sulphate in the presence of 2-propanol and determine critical

supersaturation, induction periods were determined at 20°C and the dependence on the supersaturation assessed.

- **Experimental Procedure**

100 mL of aqueous solutions containing ~ 20 g/L Ni^{2+} and 250 g/L H_2SO_4 were agitated with a magnetic stirrer in Pyrex flasks at 21°C. 2-propanol was instantaneously added by means of a funnel to the aqueous solutions, in the following O/A ratios: 0.5, 0.75, 1, 1.5 and 2. Induction periods were determined visually by recording the time elapsed between the addition of the alcohol and the appearance of turbidity in solution (i.e. formation of first crystals); the solutions were stirred for 24 hours, to reach complete equilibrium. The mother liquor was diluted with 5% HCl and analysed for cationic content. When the precipitating agent was added to the aqueous phase, small air bubbles were also dispersed in the bulk solution; since the bubbles left the liquid mixture after ~10 seconds, in order to avoid any ambiguity in the observation of nucleation-related turbidity, this technique required induction periods larger than 15 seconds.

- **Discussion**

The experimental induction periods for the system $NiSO_4$ - H_2O - H_2SO_4 -2-propanol are recorded in Table 5.4 and their dependence on organic fraction (O/A) and supersaturation are plotted in Figures 5.11 and 5.12, respectively.

Table 5.5 Precipitation induction periods in the system $NiSO_4$ - H_2O - H_2SO_4 -2-propanol at different saturation ratios (21°C)

O/A	t_{ind} (sec)	[Ni] _{eq} (g/L)	S
0	no crystals	20.66	1
0.50	no crystals	20.66	1
0.75	no crystals	20.66	1
1.00	1680	14.56	1.42
1.50	107	5.68	3.63
2.00	15	4.33	4.77

Figure 5.11 indicates that for small O/A fractions the crystallisation process is not initiated. Consequently, nickel concentration in solution is constant and induction period

approaches infinity. The fact that visible crystals do not develop until some minimum supersaturation is established relates to the existence of a supersaturation limit below which either primary nucleation practically ceases (i.e. the system lays in the “metastable zone” depicted in Figure 5.10). Similar behaviour is reported by Mullin *et al.* for the system potassium sulphate-acetone [33].

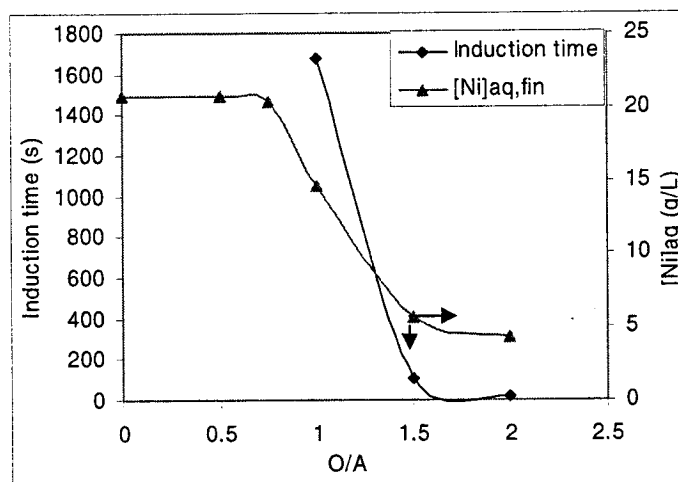


Figure 5.11 Induction time and final nickel concentration in solution as a function of organic fraction

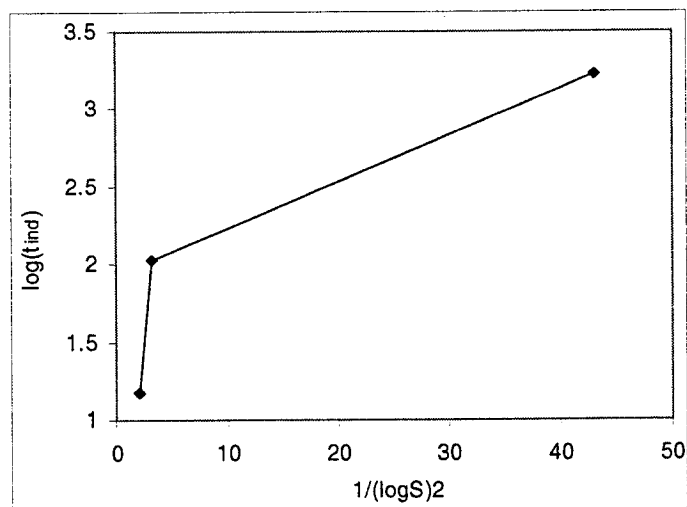


Figure 5.12 $\log(t_{ind})$ as a function of $(\log S)^{-2}$

Once the organic fraction increases, water molecules start to be displaced from ions' hydration spheres, the ion pairing process is accelerated and stable nuclei start to form, followed by apparition of crystals; consequently, nickel concentration in solution

decreases. Similarly, induction time decreases rapidly with increasing organic fraction, from ~28 minutes for O/A=1 to only 15 seconds when O/A=2.

The plot of $\log(t_{ind})$ versus $(\log S)^{-2}$ in Figure 5.12 indicates that the limiting step on the formation of the new solid phase is primary nucleation followed by growth, as explained by Barata and Serrano, who obtained similar plots for potassium dihydrogen phosphate salted-out with different alcohols (e.g. ethanol, 1-propanol and 2-propanol) [31].

Two regions with different slopes are evident: in the higher supersaturation range, $\log(t_{ind})$ has a strong dependence on $(\log S)^{-2}$ and in the lower supersaturation range the dependence is less pronounced. These two different regions are respectively related to the existence of homogeneous and “heterogeneous” nucleation. The homogeneous nucleation mechanism occurs in a short supersaturation range, while the “heterogeneous” mechanism prevails in almost all the supersaturation range since there are always some heteronuclei in solution, either impurities or crystallites already formed via homogeneous nucleation. Similar reasons were provided by Mahadevan *et al.* [34] to explain the two slopes of the plot $\log(t_{ind})$ versus $(\log S)^{-2}$ obtained for cooling crystallisation of $NiSO_4 \cdot 7H_2O$.

5.5.2 Metastable Zone Width at 10, 21 and 40°C

Critical supersaturation lines of nickel sulphate at various temperatures in aqueous-acidic media (250 g/L H_2SO_4 for 10° and 21°C and 550 g/L H_2SO_4 for 40°C) were experimentally determined as a function of 2-propanol (according to set-up and procedures extensively described in Sections 3.3.1, 3.3.2 and 5.2.2). The results are shown in Figure 5.13.

Nyvt *et al.* explained [32] that the width of the metastable zone depends firstly on the probability of ion-pairing and viable nuclei formation in solution; the degree of probability depends on the inter-molecular distances and therefore on the solution concentration. Accordingly, nucleation in concentrated solutions of highly soluble salts (such as $NiSO_4 \cdot 6H_2O$) should occur at relatively low supersaturation levels, which is indeed the case for the system under study: the average critical supersaturation level is ~ 2 at 10°C, ~1.4 at 21°C and ~1.2 at 40°C, respectively.

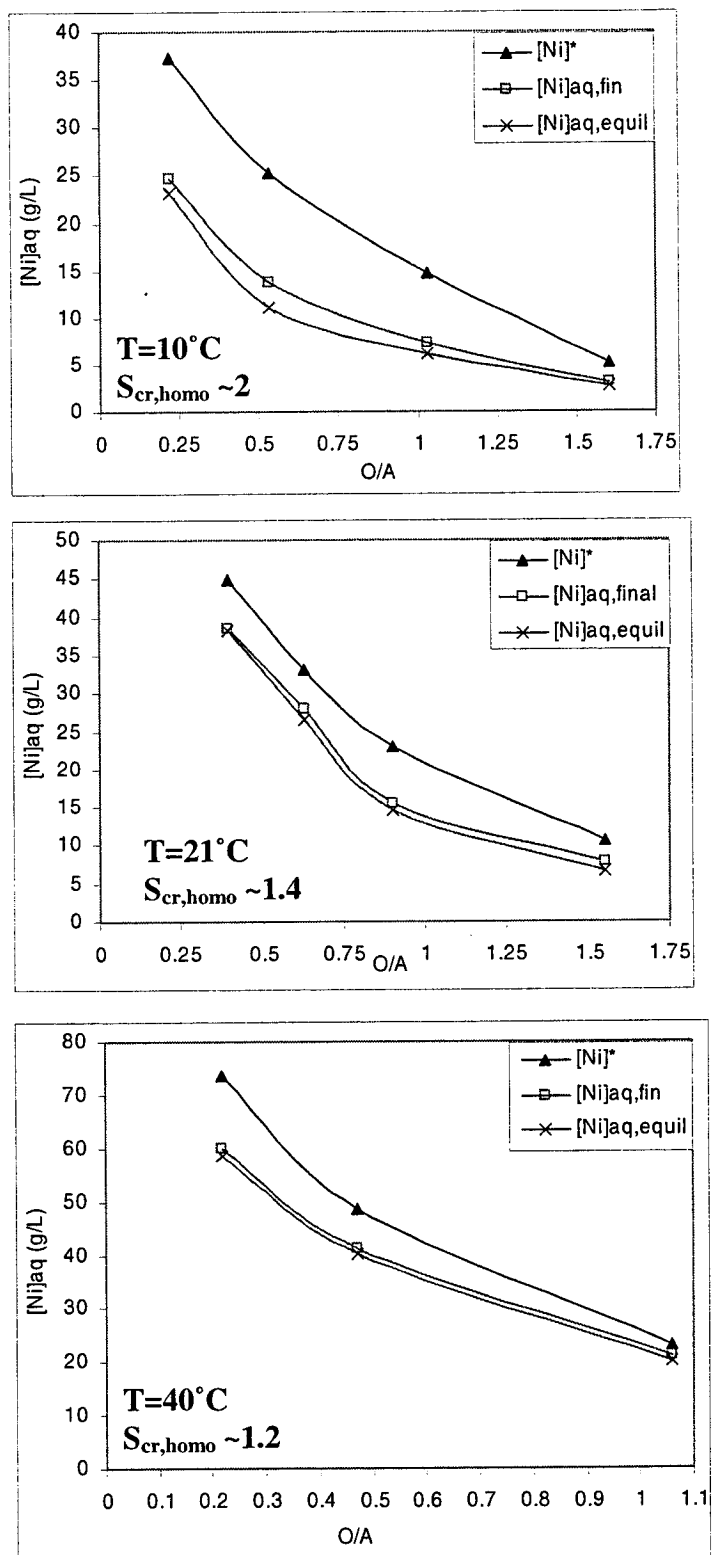


Figure 5.13 Critical supersaturation lines ($[Ni]^*$ vs. O/A) and metastable zone width in the system $NiSO_4-H_2O-H_2SO_4-2$ Propanol at 10, 21 and 40°C

The experimental results show that the metastable zone boundary decreases with increasing temperature (Figure 5.14).

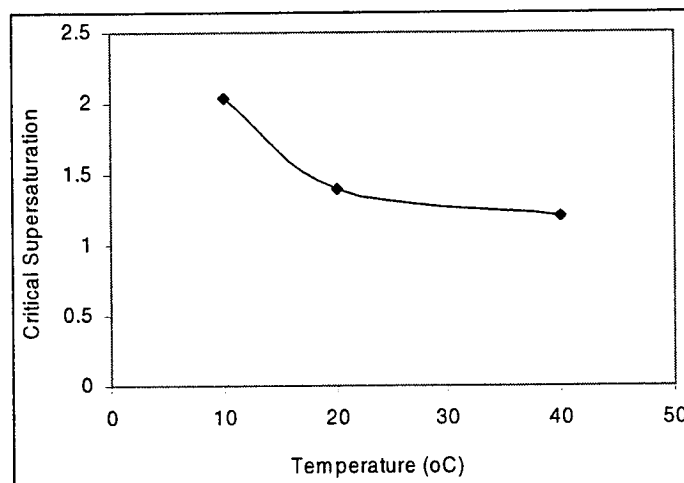


Figure 5.14 Influence of temperature on critical supersaturation

The results are similar to observations reported by Tai and Chien [30], Nyvlt *et al.* [32] and Franke and Mersmann [35]. According to the classical nucleation theory, the decrease in induction period at higher temperatures is not only caused by the effect of temperature as shown in Eqn. (5.2), but also by the smaller interfacial energy of crystal. They also present strong evidence that in the presence of solid phase (i.e. seed) the metastable zone becomes narrower, due to higher interfacial supersaturation near the surface of seeds as compared to the bulk of solution.

As described in the previous section, the induction period, which defines the time-lapse before the first crystals are detected, is intrinsically related to the metastable zone width and it is directly proportional to the interfacial energy and inversely proportional to the temperature and supersaturation (Eqn.5.2).

The metastable zone boundary and the early crystal growth mechanism for salting-out precipitation are considered by Mullin *et al.* [33] to be similar to those relevant to cooling crystallisation of unseeded solutions. Namely, nucleation appears to proceed predominantly via primary mechanism, when a certain overall supersaturation is reached, followed by surface-reaction growth mechanism, similar to what Barata and Serrano found [31].

5.6 Effect of Various Parameters on Solution Composition and Crystal Quality

In this section the influence of various crystallisation conditions such as supersaturation, temperature, seeding and agitation will be assessed in relation to final nickel sulphate concentration and the quality of the solid product.

5.6.1 Supersaturation Magnitude and Crystallisation Method

Based on the critical supersaturation lines determined in Section 5.5.2, there are different possible crystallisation paths to follow starting from an initial metal concentration in order to reach the targeted final concentration in solution (Figure 5.15):

(I) High supersaturation case: The required quantity of precipitating agent (2-propanol) can be added all at once to the aqueous solution.

(II), (III) Controlled low supersaturation case: The required quantity of alcohol is added in small increments; in one case (II) critical supersaturation C^* (corresponding to $S_{cr,homo}$) is exceeded order to initiate homogeneous nucleation, then S is kept always inside the metastable zone to promote growth; alternatively (III) same-nature seed may be added prior to reaching $S_{cr,homo}$ to promote surface nucleation hence growth without generation of fines.

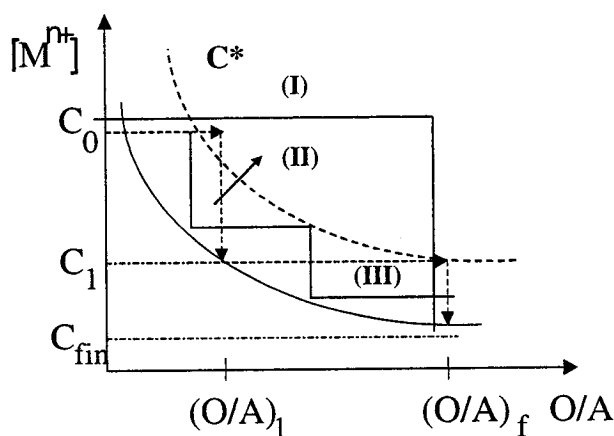


Figure 5.15 Crystallisation strategies with and without supersaturation control

- **High Supersaturation Homogeneous Crystallisation**

In this series of tests, 2-propanol was added all at once to the aqueous solutions and the kinetics of homogeneous crystallisation were assessed by monitoring the aqueous nickel concentration at 10, 21 and 40°C, following the experimental procedure described in Section 5.2.2. At each temperature, three tests were conducted, with O/A ratio corresponding to the critical supersaturation value, 1.5 and 3, respectively.

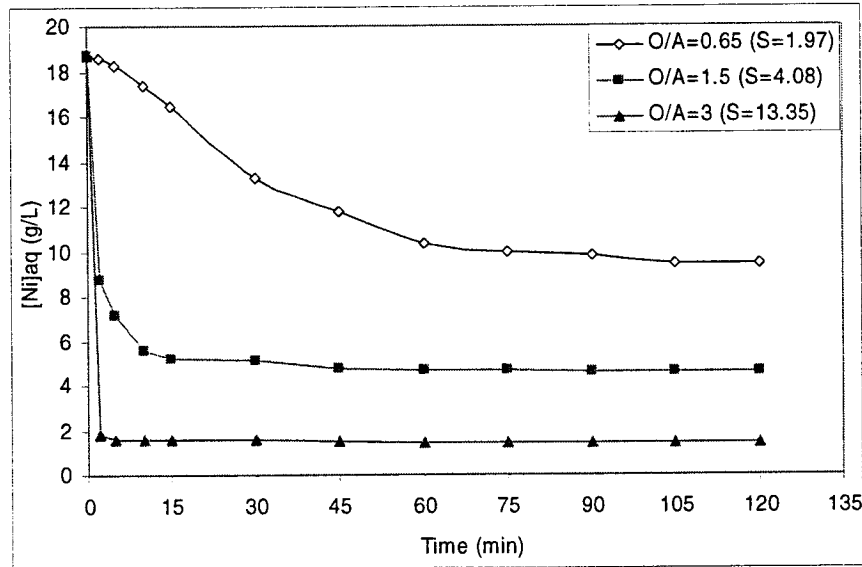


Figure 5.16 Homogeneous crystallisation kinetics at 10°C (250 g/L H_2SO_4 , $S_{cr,homo}=1.97$))

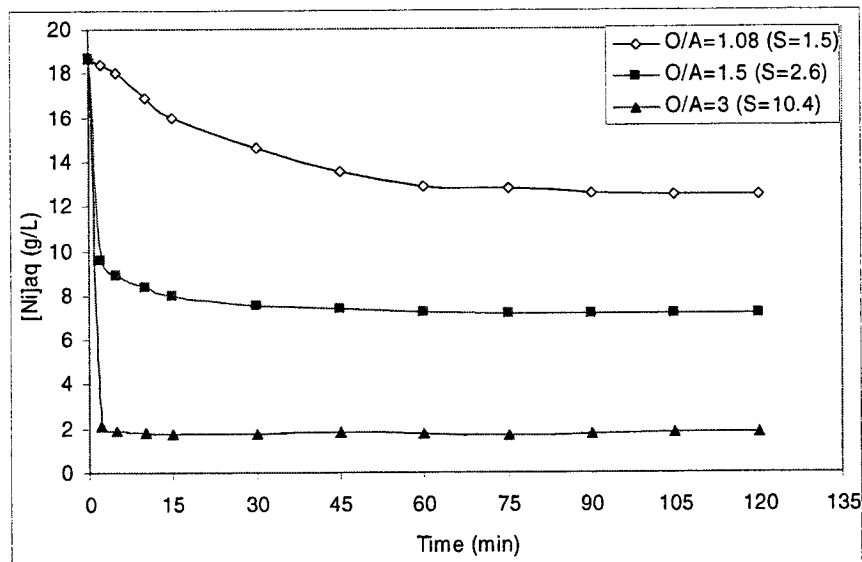


Figure 5.17 Homogeneous crystallisation kinetics at 21°C (250 g/L H_2SO_4 , $S_{cr,homo}=1.5$)

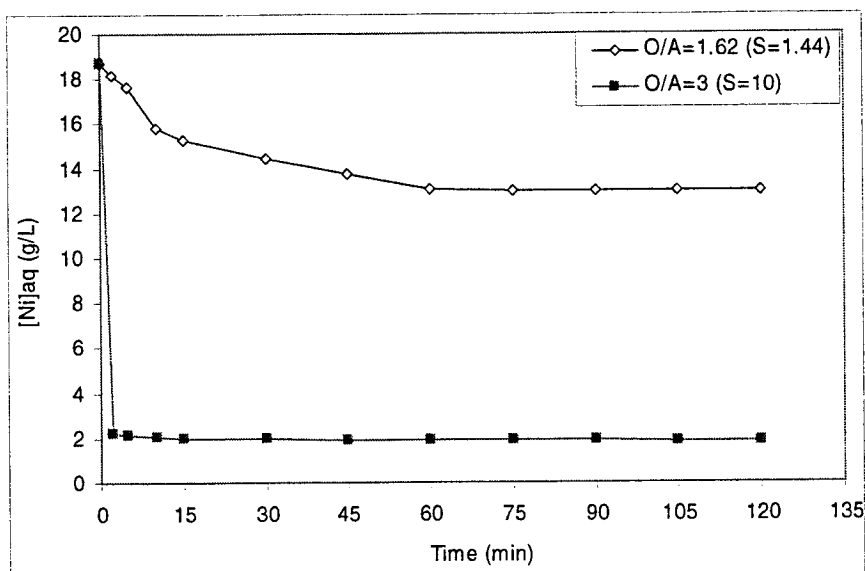


Figure 5.18 Homogeneous crystallisation kinetics at 40°C (550 g/L H_2SO_4 , $S_{cr,homo}=1.44$)

As described in section 5.5, the induction period (i.e. the time-lapse before crystals become visible) is considered to be inversely proportional to the supersaturation and temperature. For each temperature studied, at low supersaturation (i.e. critical value) the induction period is lengthy and nucleation rate is slow; consequently, the crystallisation kinetics are slower and the concentration profile requires a longer period of time to reach a plateau, as shown in Figures 5.16 to 5.18. Due to the positive effect of high supersaturation on induction time and nucleation, crystallisation kinetics of $NiSO_4 \cdot 6H_2O$ are generally fast at medium and high supersaturation values, less than 30 minutes being sufficient to reach a plateau in aqueous metal concentration even at 10°C.

The effect of temperature on crystal quality and final metal concentration in solution is addressed in Section 5.6.2.

- **Low Supersaturation Homogeneous Crystallisation**

SDC tests at low supersaturation were performed at 10, 21 and 40°C on solutions containing initially ~20 g/L Ni^{2+} in order to study and compare the influence of supersaturation magnitude on nickel concentration in solution and crystal quality, following the procedure described in section 5.2.2. The acid concentration was 250 g/L H_2SO_4 at 10 and 21°C, and 550 g/L H_2SO_4 at 40°C, respectively.

A typical test was conducted by adding the organic in small doses, according to the step-wise crystallisation path described in Figure 5.15 (path II) applied within the metastable zone previously determined for each temperature in Section 5.5.2, Figure 5.13 (nickel concentration profiles as a function of O/A ratio shown in Appendix D).

As depicted in Figure 5.19, for all temperature ranges studied, SDC performed at low supersaturation ($S \leq S_{cr,homo}$) resulted in lower nickel concentrations in solution than SDC done at high supersaturation. Moreover, the final Ni concentrations in the case of low supersaturation SDC were very close to the equilibrium values, especially at the higher temperature test.

At low S , following a short duration homogeneous nucleation event that gave birth to a relatively small number of nuclei crystals, most crystallisation takes place within the growth zone (“secondary nucleation”), avoiding the formation of colloidal particles. In conditions of high supersaturation, Franke and Mersmann [36] demonstrated that nucleation already starts during the feeding period and an initial amorphous or poorly crystalline precursor is built first. This explains slightly higher concentration values since amorphous or poorly crystalline products have usually higher solubility compared to the crystalline phases.

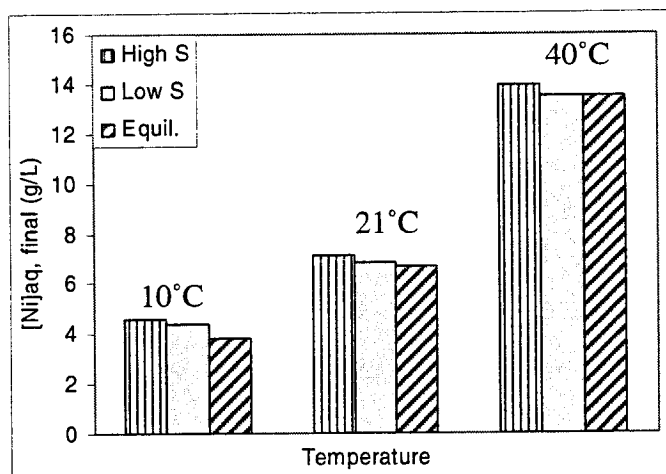


Figure 5.19 Final nickel concentration in solution at different temperatures as a function of supersaturation, compared to equilibrium values (O/A=1.5)

- **Solid Product Properties**

Figure 5.8, Section 5.4.2 gives the XRD pattern for the product obtained at 21°C whereas spectra for products at 10 and 40°C are depicted in Figure 5.20 below (all samples produced via homogeneous crystallisation, low supersaturation, $(O/A)_{total}=1.5$). The sharp peaks indicated higher degree of crystallinity; moreover, it was found that $NiSO_4 \cdot 6H_2O$ offered the best match to the crystals produced.

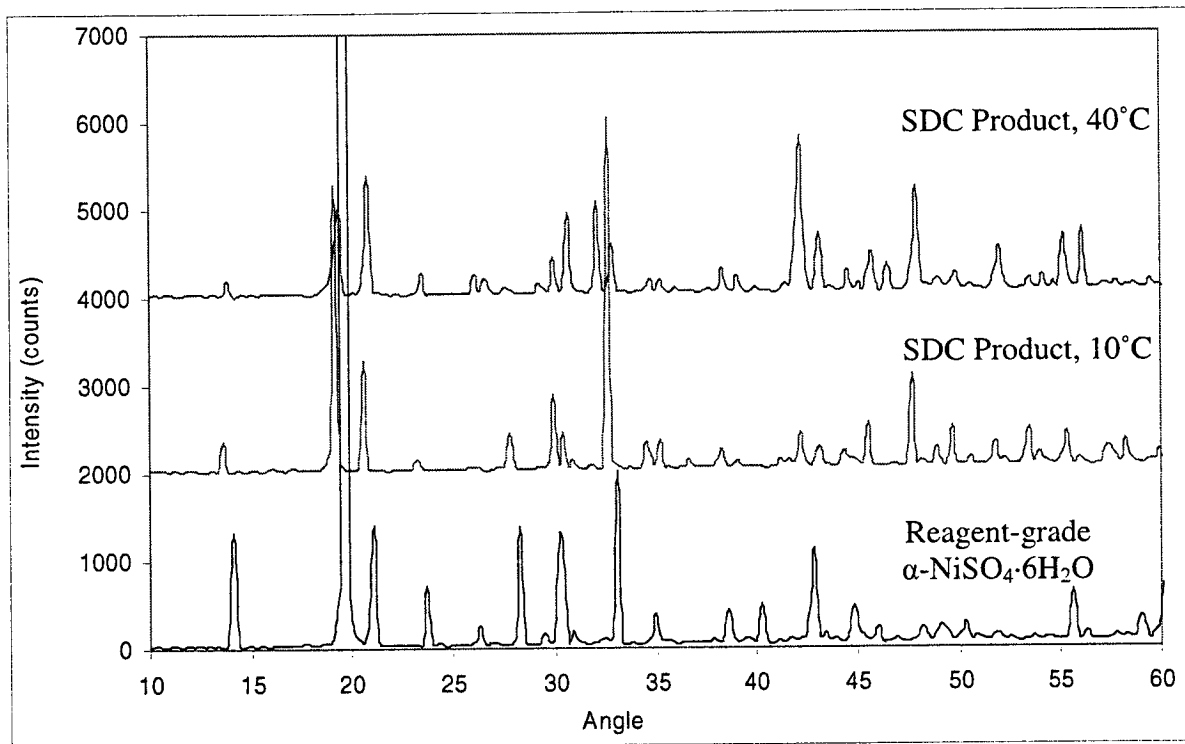
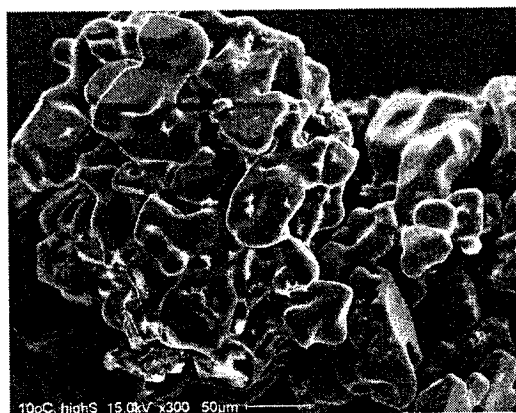


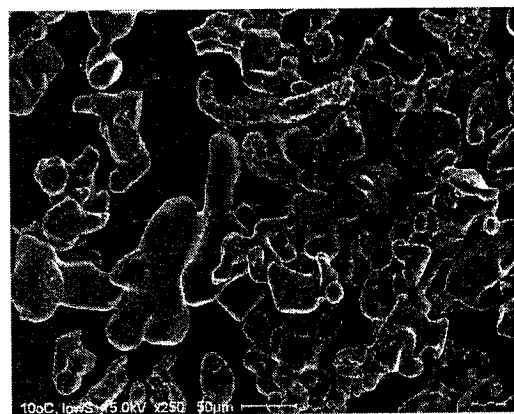
Figure 5.20 XRD spectra of $NiSO_4 \cdot 6H_2O$ produced via homogeneous SDC under low supersaturation conditions at 10 and 40°C, compared to reagent-grade crystals

As mentioned earlier (Section 5.4.2), the produced hexahydrate (of the α -tetragonal morphology) is metastable below 30°C, as the result of Stranski's Rule. On the other hand, the hexahydrate produced at 40°C is in agreement with the thermodynamic predictions.

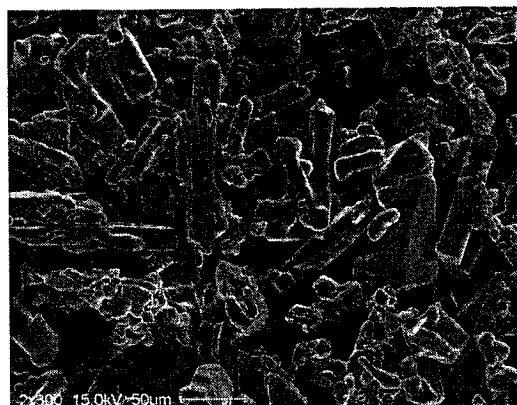
The homogeneously produced crystals were examined by SEM (Figure 5.21).



(a) 10°C, high S



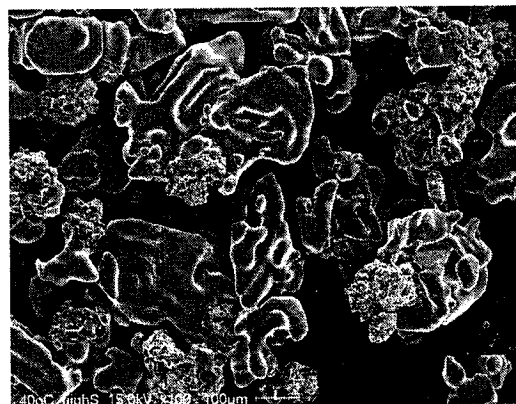
(b) 10°C, low S



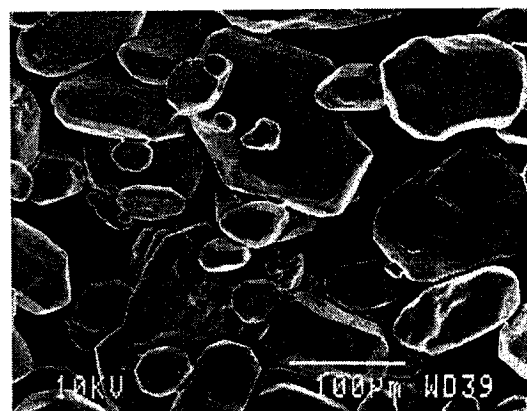
(c) 21°C, high S



(d) 21°C, low S



(e) 40°C, high S



(f) 40°C, low S

Figure 5.21 Influence of supersaturation magnitude on the quality of $NiSO_4 \cdot 6H_2O$ crystals produced via SDC at 10, 21 and 40°C (2-propanol, $O/A_{total}=1.5$)

The SEM micrographs show distinct crystal morphology and size dependence on supersaturation magnitude. Tests conducted at high supersaturation yielded fine, irregular crystals of $\sim 50\mu\text{m}$ average size for all temperatures, with tendency towards agglomeration (Figure 5.21 a, c, e). Tests conducted at low supersaturation, where the initial homogeneous generation of a smaller number of nuclei is followed by growth, show a certain increase in average particle size $\sim 50\text{-}100\mu\text{m}$ (Figure 5.21 b, d, f). The crystals exhibit a smoother appearance, as the shape tends to become closer to the specific tetragonal morphology of $\text{NiSO}_4 \cdot 6\text{H}_2\text{O}$ [24, 26].

As Barata and Serrano explain for salting-out of potassium dihydrogen phosphate with various alcohols [36, 37], at high supersaturations the number of active nuclei increases, which progressively induces the generation of a product with numerous small particles that easily agglomerate. Prior to that, Nielsen and Söhnel [38] indicated that at low values of S , the number of particles (nuclei) per volume is almost constant and of the order $10^6\text{-}10^8$ particles/ cm^3 . This number increases rapidly with S and, for high S values, the number of nuclei levels off and approaches a constant value of $10^{11}\text{-}10^{12}$ particles/ cm^3 . The logarithmic plot of number of nuclei per volume versus S indicates that at low supersaturation the nucleation is heterogeneous while at higher supersaturation it becomes homogeneous.

To conclude, crystallisation under low supersaturation conditions ensures that amorphous precursors and extensive aggregation are avoided [35], the external mass transport process is decelerated and the solid/liquid interface becomes less crowded, thus allowing the surface integration step to proceed uninhibited. Consequently, the particles produced under these conditions have improved physical (size) characteristics.

5.6.2 Influence of Temperature

- *Solution Composition*

As indicated by solubility data determined in Section 5.3.2, final nickel concentration in solution increases with temperature at constant organic content (Figure 5.19, for $O/A=1.5$). Also, according to critical supersaturation values (Section 5.5.2, Figure 5.13),

SDC tests performed at more elevated temperatures require higher O/A ratios to initiate crystallisation; consequently, more 2-propanol is to be employed in order to reach a similar final nickel concentrations in solution at 21 and 40°C as compared to 10°C.

- ***Solid Product Properties***

SEM images presented in Figure 5.21 indicate a net beneficial effect of temperature on crystal morphology. Even for high supersaturations, agglomerated particles obtained at low temperatures (10°) tend to grow slightly and become better defined individually at 21 and especially 40°C, even if irregular (Figure 5.21 a, c, e), whereas the combined effect of low supersaturation and more elevated temperatures greatly favours both the growth process and the morphology, which tends more towards the specific tetragonal shape (Figure 5.21 b, d, f).

Huitema and van der Eerden [39] observed that during crystal growth, the interface is the most defect-rich region since defects form at the surface first. They studied the competition between the generation of defects at the growing surface and partial “healing” in a wider interface region and assumed that the driving force for healing is the reduction of the excess free energy of the defect and the essential kinetic parameter was the defect mobility, both factors favoured by elevated temperatures. Hence, crystals produced at higher temperatures tend to have a smoother surface and a more regular morphology.

5.6.3 Seeding (Heterogeneous Crystallisation)

The previous section demonstrated that homogeneous crystallisation under controlled (low) supersaturation conditions has beneficial effects on crystals' quality and final nickel concentration in solution. If same-nature crystalline seed is provided during the first stages of a precipitation process at low supersaturation ($S < S_{cr,homo}$), growth should be favoured via secondary nucleation on the seed's surface. This concept is investigated in this section via a series of seeding-recycling tests.

In particular, in this series of tests the effect of seeding and product recycling on crystal growth under low supersaturation (as per step-wise path of Figure 5.13) was

studied. All heterogeneous recycling tests were performed at 21°C , for $O/A_{\text{total}}=1.5$, following the procedure described in Section 5.2.2.

Two comparative seeding experiments were conducted, in order to study the influence of seed quality on the final product morphology and size: (i) using reagent-grade tetragonal $\alpha\text{-NiSO}_4\cdot 6\text{H}_2\text{O}$ from Fisher Scientific; and (ii) employing $\text{NiSO}_4\cdot 6\text{H}_2\text{O}$ obtained in the laboratory via homogeneous SDC tests under low supersaturation. The seed was added in the range $0.8 < O/A < 1.1$ (refer to Figure 5.10) as if were added at lower O/A it would have dissolved. The profiles of the tests are shown in Appendix D. A 30-minute equilibration time was allowed after seeding; the remaining solvent was added in doses as per Figure 5.13.

- **Solution Composition**

From Figure 5.22 it can be observed that the type of seed material (i.e. reagent-grade or “home-made” $\text{NiSO}_4\cdot 6\text{H}_2\text{O}$) and crystallisation strategy (heterogeneous vs. homogeneous under low S) do influence modestly the final value of nickel achieved in the aqueous phase. Indeed, a better quality seed (i.e. no surface defects, regular shape) allows a better incorporation of the incoming “building blocks” and a faster, more isotropic growth process, hence it permits closer to equilibrium values (it is reminded that solubility is influenced by crystal size).

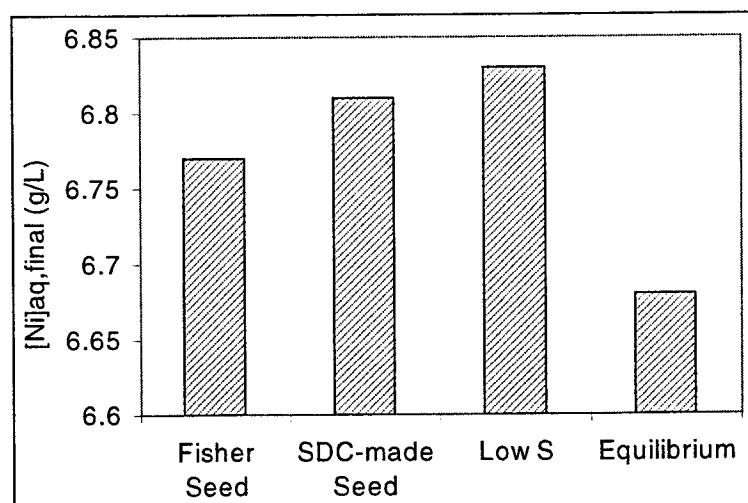


Figure 5.22 Influence of crystallisation method (homogeneous vs. heterogeneous) on final nickel concentration, compared to equilibrium values (21°C , $O/A_{\text{total}}=1.5$)

More importantly, the final nickel concentration in the aqueous phase is strongly dependent on O/A and temperature and only marginally on recycling (if it is performed under similar conditions); hence, the effect of product recycling was monitored only by those properties whose values are most influenced by the growth process, i.e. crystal size and morphology, percent solids density and settling velocity.

- ***Solid Product Properties***

- I. Influence of Seed Quality

In terms of crystal size and properties, the quality of seed had a dramatic effect on solid product properties. Figure 5.23 presents comparatively the two types of $NiSO_4 \cdot 6H_2O$ crystals used as seed and the products of the respective seeding experiments ($21^\circ C$, 80 g/L seed, $O/A_{total}=1.5$). It can be observed that the reagent-grade seed (Fisher Scientific) has a superior quality in terms of size and morphology (i.e. large, tetragonal particles of ~ 300-400 μm with smooth surfaces) whereas the “home-made” seed appears to be of lesser quality (irregular, elongated particles of ~100 μm).

When using reagent-grade $NiSO_4 \cdot 6H_2O$ as seed during SDC, SEM micrographs of the final product (Figure 5.23 c) show large tetragonal crystals (the characteristic morphology for α - $NiSO_4 \cdot 6H_2O$, [24, 26]), with defect-free, smooth surfaces and a rather uniform particle size distribution, similar to the seed material (Figure 5.23 a), indicating a uniform growth process; this leads to a more compact filter cake, meaning less solution retention. Also, the smooth, defect-free surfaces decrease the chances for impurity uptake. Smaller particles that appear on the larger crystals’ surfaces may constitute either fragments produced due to attrition or crystallites issued by a secondary nucleation and growth process.

When the particles crystallised on “home-made” seed are compared to those of the original seed material (Figure 5.23 b) it can be observed that some radial growth was indeed taking place; the crystals retain the elongated form but tend to become more tetragonal, the surfaces are smoother and the average length exceeds 100 μm . The crystals do not exhibit in their entirety the “perfect” tetragonal structure characteristic for α - $NiSO_4 \cdot 6H_2O$; this irregular shape is due to homogeneous crystallisation conditions and insufficient equilibration time to allow for crystal maturation (ripening); should the

crystallisation process be continued by recycling part of material as seed in further experiments, significant growth will be achieved. On the other hand, even with some growth involved, the crystals deposited on the homogeneously prepared seed retain a more irregular form prone to retain solution in the filter cake. Moreover, the surface defects (cracks) can induce further fragmentation and more impurity uptake.

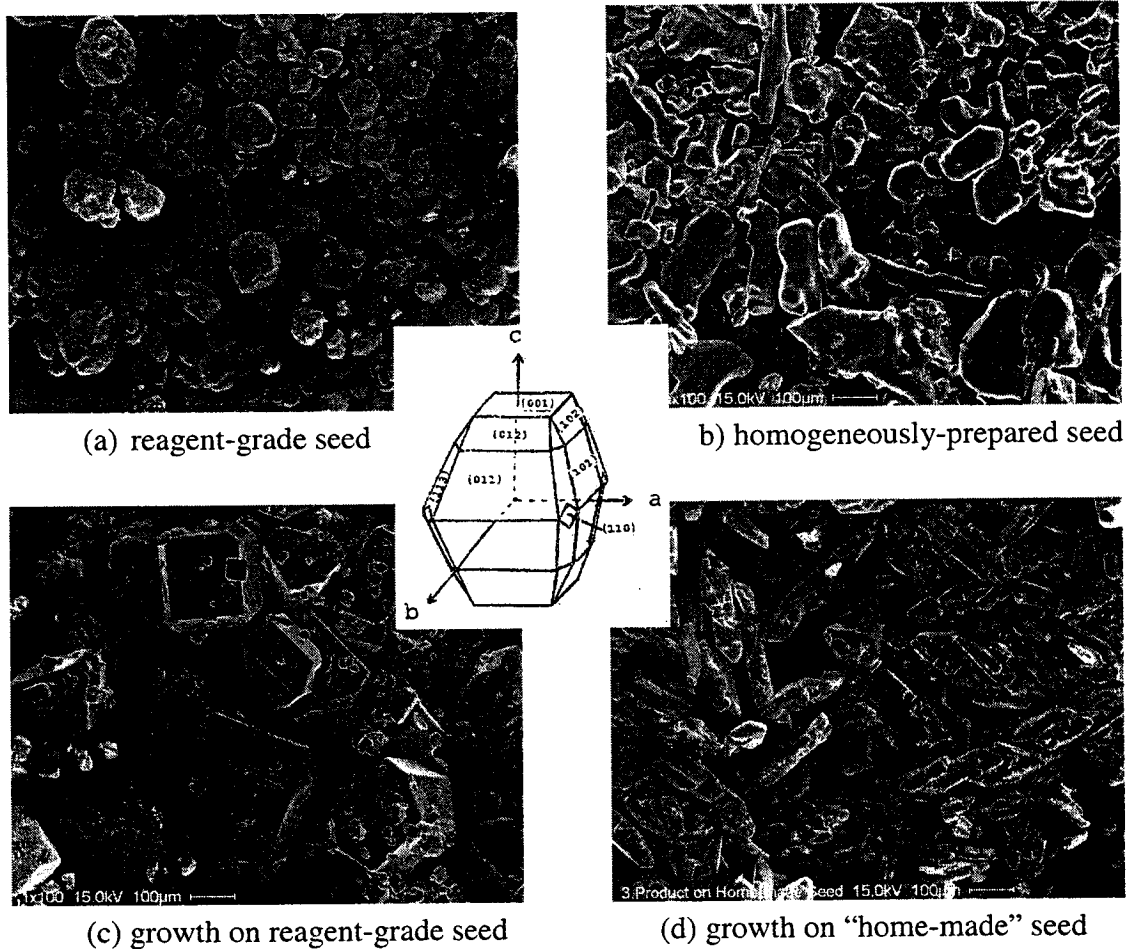


Figure 5.23 Type of seed material and product of heterogeneous crystallisation tests and characteristic tetragonal habit for α - $NiSO_4 \cdot 6H_2O$ ($21^\circ C$, 80 g/L seed, $O/A_{total}=1.5$)

II. Influence of Recycling

Since the use of reagent-grade seed material showed dramatic improvement of solid product properties after just one heterogeneous test, product recycle experiments have been performed starting with "home-made" seed only, to investigate the possibility of

further upgrading the morphology and size of homogeneously-prepared $NiSO_4 \cdot 6H_2O$ without resorting to “outside” material (seed material presented in Figure 5.23 b).

Following the initial seeding test, part of the product was used as seed for the following (corresponding to ~ 80 g/L seed); the number of product-recycling tests was arbitrarily chosen to be 5. All heterogeneous recycling tests were performed at $21^\circ C$, for $O/A_{total}=1.5$, following the procedure described in Section 5.2.2.

As expected, increased extent of recycling leads indeed to significant growth, producing polygonal particles (closer to the characteristic shape for $\alpha-NiSO_4 \cdot 6H_2O$), with smooth, defect-free surfaces (Figure 5.24).

It can also be observed that most probably significant crystal fragmentation took place after the 3rd recycle most certain due to increased slurry density (the generation of fines via homogeneous nucleation cannot be ruled out but it is considered to be minimal because of the good S control exercised); as the particles grow, they become more susceptible to breakage by crystal-crystal, crystal-reactor or crystal-impeller collisions (even under mild stirring, 200 rpm).

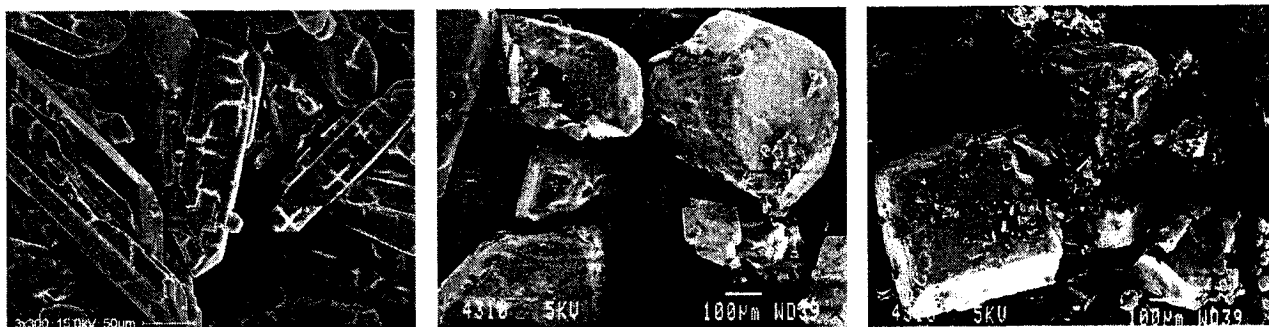
(a) 1st recycle(b) 3rd recycle(c) 5th recycle

Figure 5.24 Effect of product recycling on crystal quality (80 g/L seed, $21^\circ C$, low S, $O/A_{total}=1.5$)

Settling velocity and percent solids density are important industrial properties in the handling of slurries/solids separation. The respective measurements for the crystals obtained by different crystallisation methods are shown in Figures 5.25 (settling velocity) and 5.26 (solids density).

As the settling velocity is a function of solids content and not a definitive indication of increased particle size, the results were not used to evaluate the precipitation for each run. However, for equivalent solids loading, the settling velocities are considered as a semi-quantitative means to evaluate crystal growth (i.e. high settling velocity = large particle).

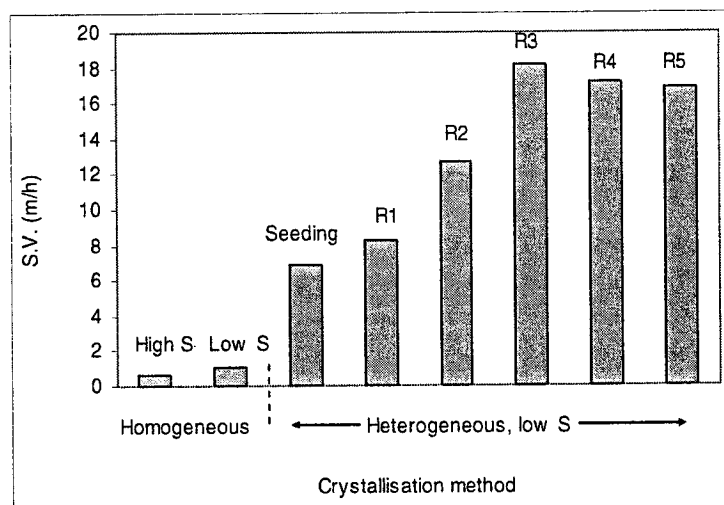


Figure 5.25 Influence of crystallisation strategy on settling velocities (250 g/L H_2SO_4 , 21°C)

As expected, low supersaturation and use of seed/product recycling (heterogeneous crystallisation) favour growth, fact assessed by the increasing trend in settling velocities when compared to the values issued by the homogeneous SDC tests. The small drop in settling velocities for both systems after the 3rd recycle is related to the fragmentation process revealed by the SEM pictures; as the particles reach a critical size, they break due to cracks and collisions, the amount of fines increases resulting thus in lower settling velocities.

The solids density represents another semi-quantitative measure of the growth process. Large crystals have a smaller specific surface area hence retain less water form solution. Therefore, higher solids density indicates larger particles. After the slurry was allowed to settle by gravity, three aliquots of the solids were sampled from the settled mass and weighted. They were dried under ambient conditions and re-weighted. The following calculation was performed to check the solids density:

$$\text{S.D. (\%)} = (\text{dry sample mass})/(\text{wet sample mass}) \times 100 \quad (5.3)$$

The increasing trend in S.D. values (Figure 5.26) proves the growth process was enhanced by the use of seed and product recycling under low supersaturation.

The information offered by Fig. 5.26 is again consistent to the information given by the SEM images: Heterogeneous crystallisation and product recycling strategies generate crystals that have superior solids content (i.e. larger size). The same results show that product recycling beyond a certain limit (in this case, the third recycle) results in lower values of these properties due to the apparent fragmentation of crystals as noticed with the SEM micrographs.

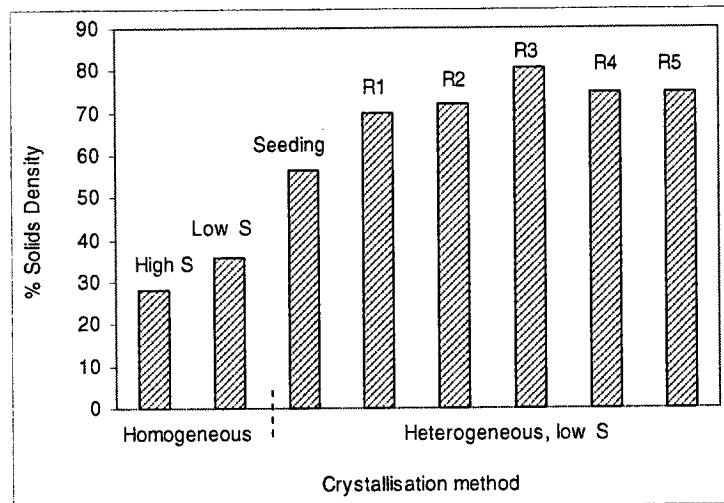


Figure 5.26 Influence of crystallisation approach on solids density (250 g/L H_2SO_4 , 21°C)

To summarise:

- The type of seed material or heterogeneous crystallisation strategy do not influence significantly the final value of nickel achieved in the aqueous phase but have dramatic effect on the quality of the solid product (in terms of morphology and size).
- SEM pictures confirm the growth process upon product recycling under low S; Settling velocities and solids density have also been employed as semi-quantitative methods to evaluate the growth process (as they are related to particle size). These properties also show an increasing tendency.
- There is a limit on the recycling extent, after which a decrease in particle size occurs due to apparent crystal fragmentation following collisions.

5.6.4 Agitation and Ageing

Mixing is an important event in the initiation of the precipitation reaction, and therefore the mixing conditions can strongly affect the crystallisation process: Nucleation, growth, habit and particle size. These in turn have a significant impact on the quality of the resultant product such as crystal size distribution, purity, morphology, filtration and drying properties.

Two forms of mixing predominate in reactor: macromixing and micromixing. Solids suspension and overall circulation are governed by macromixing, which determines the residence time distribution, overall bending and desupersaturation in the reactor and can be expressed via speed of the impeller, tip speed, volumetric flow or velocity. Micromixing involves contacting and mixing at the molecular level and can greatly influence nucleation and growth within the crystalliser [40].

Nyvtl [41, 42] describes in detail the several stages of mixing in salting-out crystallisation (stages I and II are collectively called macromixing, while III and IV form the micromixing):

- I. Distributive mixing: the salting-out agent is distributed into large eddies, so that a macroscopically non-uniform mixture is obtained and circulated in the crystalliser. The interface boundary area is so small that the mass transfer process can be neglected (no reaction occurs at the phase boundary).
- II. Dispersive mixing: large regions of alcohol split into smaller ones as a result of turbulence, but on the molecular scale the segregation is still high. The reaction begins to occur at the boundary of the regions.
- III. Diffusive mixing: the size of the elementary eddies decreases and diffusion starts to mix the components at the molecular scale, resulting in an extensive reaction at the interface. This stage is considered to be most important for salting-out and precipitation.
- IV. Lamellar model: the size of the eddies is further reduced due to shearing forces.

In order to evaluate the influence of agitation on solution and solid product properties, 100 mL of aqueous solution containing ~ 19.5 g/L Ni^{2+} and 250 g/L H_2SO_4 were placed at $21^\circ C$ in 1-Liter Pyrex reactor. 105 mL of 2-propanol (corresponding to the

critical amount required to initiate spontaneous homogeneous crystallisation) were added through a manual burette. The mixture was agitated at different rotation in each experiment (0, 100, 200, 400 and 800 rpm) and solution samples were taken at regular time intervals for a period of 4 hours. At the end of the experiment, the solid product was handled according to guidelines described in Section 3.3.3.

- **Induction Time and Solution Composition**

From Figure 5.27 it can be seen that agitation speed has an important effect on the induction time: The faster the agitation, the shorter the induction time required for the initiation of the homogeneous crystallisation process. For example, for similar initial nickel concentration and O/A ratio, first crystals become visible after 120 minutes when no agitation was employed, 30 minutes at 200 rpm and only 7 minutes at 800 rpm!

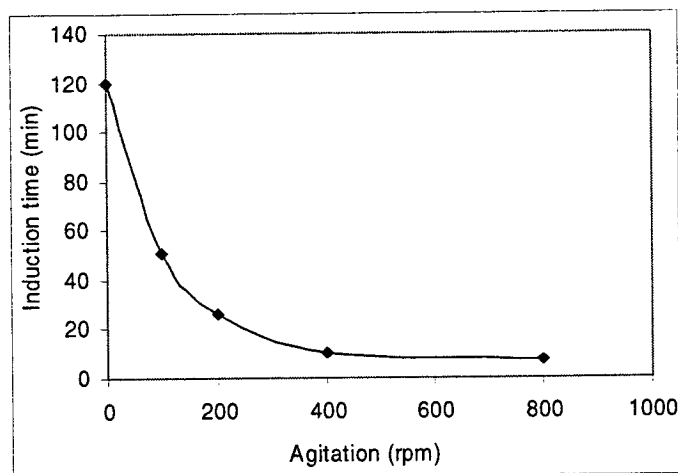


Figure 5.27 Influence of agitation speed on induction period for homogeneous nucleation

According to Nyvlt and Zacek [41], as the rate of stirring is increased, the number of crystal nuclei generated increases and induction time decreases.

This direct effect of micromixing, which impacts on the nucleation process, was also reported by Barata and Serrano [43] during salting-out of potassium dihydrogen phosphate with various alcohols. They observed that the induction period decreases with agitation intensity, this effect being more accentuated at low supersaturation (closer to the critical value). At very high supersaturations, the agitation intensity does not influence

significantly the induction time for nucleation, which now depends mainly on the alcohol concentration.

In terms of final nickel concentration achieved (Figure 5.28), this was lower when agitation was employed as opposed to no agitation (e.g. $[Ni]_{aq,final} \sim 12.4$ g/L with agitation vs. ~ 16.5 g/L in the absence of agitation). The agitation magnitude did not seem to influence drastically the final value of metal concentration, since it affects mostly the nucleation parameters and not the crystallisation yield/equilibrium state, as noted by Barata and Serrano [37].

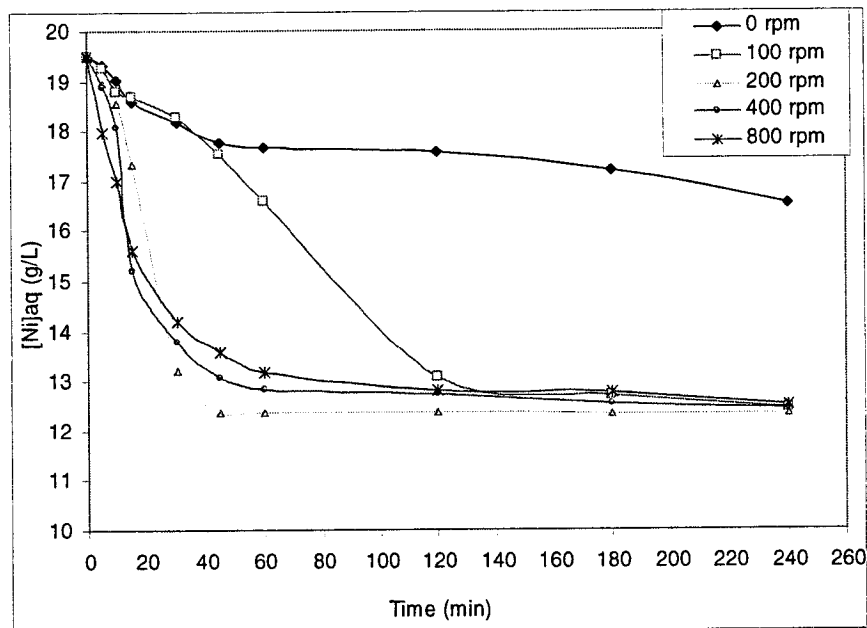


Figure 5.28 Influence of agitation on final nickel concentration in solution (21°C, $O/A_{total}=1.05$)

- **Solid Product Properties**

Figure 5.29 comparatively presents the crystalline material homogeneously produced at 21°C at different agitation conditions (i.e. 0, 100, 200, 400 and 800 rpm).

Crystals obtained in the absence of agitation (Figure 5.29 a) have two main configurations: numerous acicular crystals of $> 500 \mu\text{m}$ in length and few polygonal ones of $\sim 400 \mu\text{m}$. This is to be expected since in the absence of mixing to disperse the salting-out agent (as previously explained) pockets of both undersaturated and supersaturated solution will exist in the reactor. The high supersaturation regions (predominant) will

generate the elongated, irregular particles via a fast mass deposition process, whereas the zones of low supersaturation (created by slow, continuous diffusion of alcohol into undersaturated regions of solution) will yield almost-perfect tetragonal crystals under constant conditions.



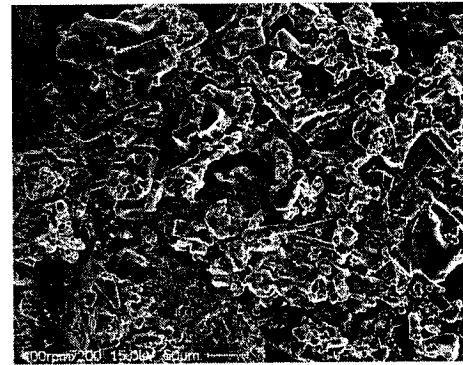
(a) 0 rpm



(b) 100 rpm



(c) 200 rpm



(d) 400 rpm



(e) 800 rpm

Figure 5.29 Influence of agitation on crystal quality (21°C, 250 g/L H_2SO_4 , $O/A_{cr} = 1.05$)

When 100 rpm agitation is used, crystals become smaller (200-300 μm) and more irregular (Figure 5.29 b). At 200 rpm, the particle size distribution is narrower ($\sim 200 \mu\text{m}$) and the shape tends to become round (as opposed to elongated), more similar to the “perfect” tetragonal morphology (Figure 5.29 c). This may be explained by the fact that at moderate agitation intensities, the induction period for nucleation is shortened and the thickness of the boundary layer is reduced, favouring the mass transfer from the bulk of solution to the crystal interface and contributing thus to a more uniform growth (this translates also to a smoother crystal texture, without defects such as cracks or pores).

As the agitation speed increases to 400 and 800 rpm, (Figure 5.29 d and e, respectively), the number of crystal nuclei generated increases and therefore the particle size decreases, the crystals appear to have irregular or elongated shapes again, presenting cracks and fragmentation due to attrition, with a wide particle size distribution (on average under 100 μm). Franke and Mersmann [35] relate the decrease of the median crystal size at higher stirring rates to the increasing power input, which shortens the time the particles stay together (aggregate) and do not allow enough time for the construction of stabilizing bridges between them and subsequent growth.

However, in their exhaustive 4-part study concerning salting-out of potassium dihydrogen phosphate with various alcohols, Barata and Serrano stated that the agitation intensity does not influence the precipitation mechanism during salting-out, which is essentially primary nucleation followed by normal first order growth process [36, 43]. Moreover, the agitation intensity has a more pronounced effect on median crystal size at low and moderate supersaturations.

To conclude, agitation intensity affects the nucleation process, especially at low supersaturations, but does not influence the crystallisation yield (i.e. solution composition). On the other hand, mixing has a dramatic effect on crystal quality: with increasing agitation speed, the morphology becomes irregular and median crystal size decreases due to inferior growth rates and fragmentation.

- **Ageing**

As previously explained, industrial requirements often call for solid crystalline products with enhanced size and morphology, which in turn ensure good filtration and drying

properties. Ageing tests were performed to investigate the influence of equilibration time on $NiSO_4 \cdot 6H_2O$ crystal ripening at moderate agitation intensity, following SDC tests.

In order to evaluate the influence of ageing on solid product properties, 100 mL of aqueous solution containing ~ 50 g/L Ni^{2+} and 250 g/L H_2SO_4 were placed at $21^\circ C$ in 1-Liter Pyrex reactor and 31 mL of 2-propanol (corresponding to the critical amount required to initiate spontaneous homogeneous crystallisation, i.e. $O/A=0.31$) were added through a manual burette, at 200 rpm. After that, 50 g/L crystal seed (reagent-grade α - $NiSO_4 \cdot 6H_2O$) was introduced to the system, followed by a 30-minutes equilibration period. The rest of the alcohol was added in a step-wise manner, as to maintain a low supersaturation, up to $O/A_{total}=1$; after each addition, the mixture was equilibrated for 30 minutes (the profile of the SDC test presented in Appendix E). At the end of the experiment, the system was further equilibrated under constant conditions ($21^\circ C$, 200 rpm) and the slurry was sampled every hour for four hours; the solid product was handled according to guidelines described in Section 3.3.3.

Figure 5.30 shows SEM micrographs of crystals obtained at different equilibration times. A discernible growth can be observed during the first two or three hours of slurry equilibration, accompanied by improved crystal morphology: SEM images of the final product (Figure 5.30 b, c and d) show large tetragonal crystals (the characteristic morphology for α - $NiSO_4 \cdot 6H_2O$, [24, 26]), with defect-free, smooth surfaces and a rather uniform particle size distribution, indicating a uniform growth process.

However, when equilibrating beyond a certain period, it seems that crystals of same initial size, subjected to identical conditions (such as temperature, hydrodynamics and supersaturation), can grow at different rates. This phenomenon, defined as “growth rate dispersion” (GRD) by Zacher and Mersmann [44], has as consequence an enlargement of small slow growing crystals at the expense of larger crystals, resulting thus in overall reduction of the mean particle size and narrowing of particle size distribution. They related the origin of GRD to the surface integration step: smaller crystals exhibit increased roughness, dislocation and lattice strain, which favour the addition of the growth building blocks (especially with increasing supersaturation).

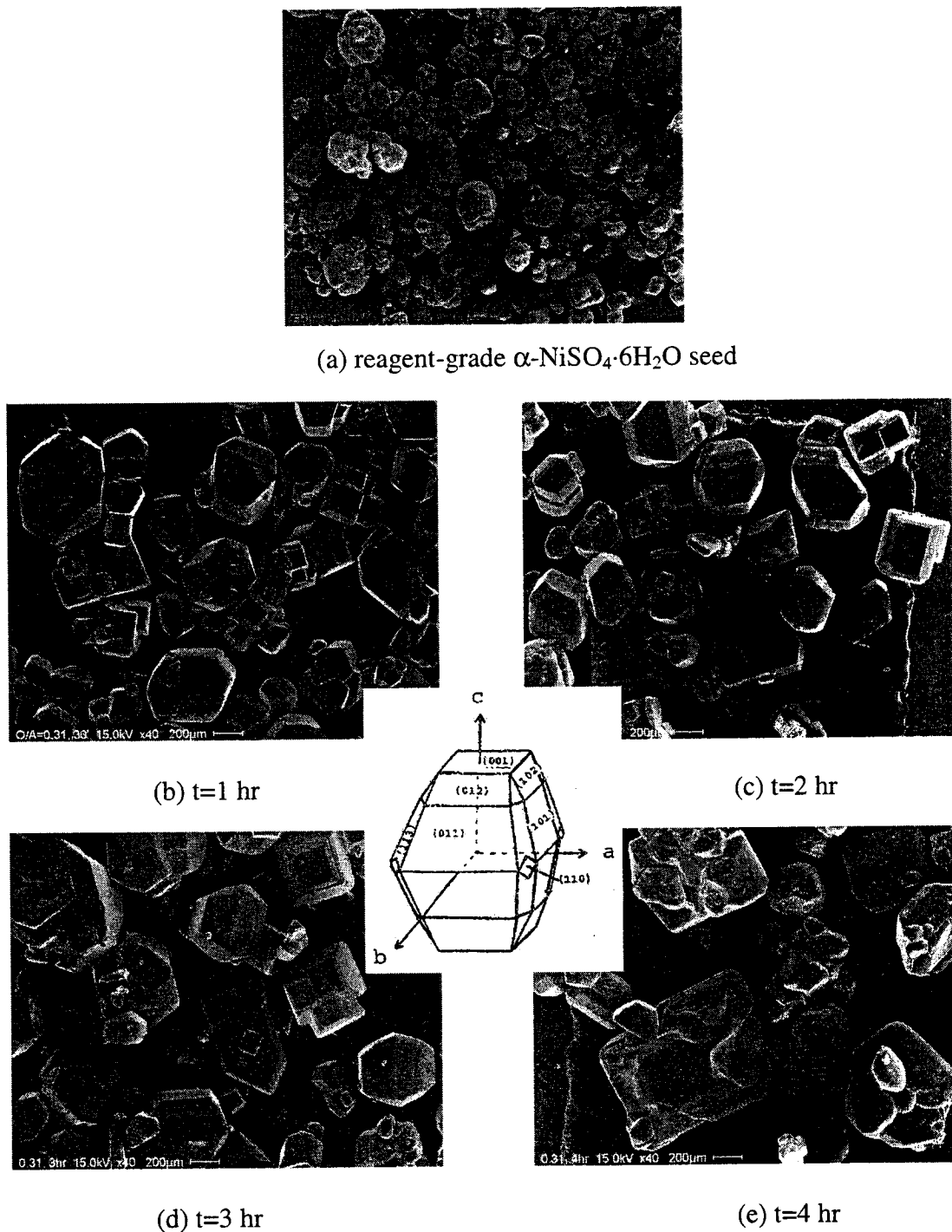


Figure 5.30 Influence of ageing (equilibration time) on crystal quality and characteristic tetragonal habit for $NiSO_4 \cdot 6H_2O$ (50 g/L Ni, 250 g/L H_2SO_4 , O/A=1, 21°C)

Following prolonged equilibration periods, the population of small particles seems to increase (Figure 5.30 d and e), most probably due to secondary nucleation,

which occurs when the impact energy in collision of a crystal with impeller, reactor or other crystals is above a critical value [45]. Because of that, small fragments are born and the dimensions of the original crystals are reduced. This phenomenon is mostly visible after 4 hours (Figure 5.30 e), when large crystals show not only fragmentation due to secondary nucleation via breeding, but also rough surfaces and rounded edges due to impact velocity and friction.

Consequently, it can be concluded that slurry equilibration time has a beneficial effect on $NiSO_4 \cdot 6H_2O$ crystal morphology and size, provided that an optimum period is determined, beyond which the soft sulphate crystals would exhibit deterioration of morphology and increase in particle size distribution due to friction, secondary nucleation and fragmentation.

5.7 Process Application Considerations

Research work conducted by the author of this thesis and reproduced elsewhere [10, 46] demonstrated the feasibility of producing high purity nickel sulphate by adding 2-propanol to industrial decopperised electrolyte solutions supplied by Canadian Copper Refineries, a Division of Noranda Inc. The process was controlled by maintaining low supersaturation (i.e. step-wise addition of the organic) and creating heterogeneous crystallisation conditions (i.e. use of seed and product recycling), which led to a final product with superior qualities. Both the crystal size (Figure 5.33) and chemical purity (Table 5.6) were at least one order of magnitude higher than those of the product obtained via the conventional evaporative crystallisation (EC) method. It was also calculated that the energy cost is equal or lower than that of the EC process.

A simplified flowsheet of the solvent displacement crystallisation process as applied to nickel recovery from decopperised electrolyte is shown in Figure 5.31. As an option, if this is desired from the water balance point of view, the decopperised feed electrolyte may be pre-evaporated (it has been determined that at least 50% of the water can be removed by evaporation before reaching the crystallisation point) to reduce the volume of solution treated by SDC and consequently lowering the required solvent

inventory. Alternatively, evaporation of excess water may be practised on the denickelised acid prior to recirculation to the tank-house.

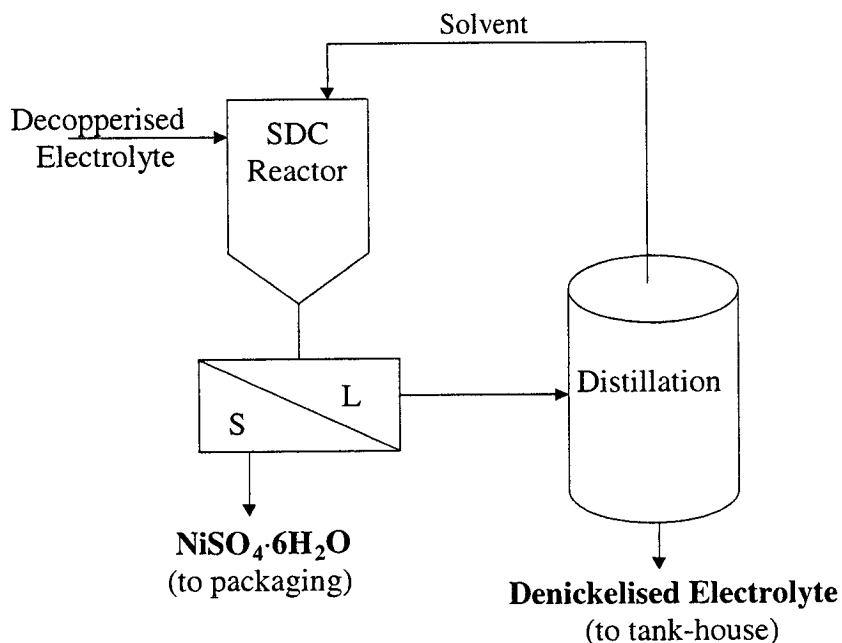


Figure 5.31 Conceptual flowsheet of nickel removal via SDC

Simple laboratory distillation tests at 80.4°C yielded 98% 2-propanol recovery as azeotropic mixture (87.2% 2-propanol, 12.2% H_2O wt/wt). Based on vapour-liquid equilibrium data presented by Cohen [9], 99.5% 2-propanol recovery can be achieved in an eight theoretical plate distillation column. Cathodic polarisation tests performed with copper sulphate electrolyte containing up to 5 g/L 2-propanol (representing the worst-case scenario) simulating the transfer of 2-propanol from the nickel sulphate recovery section to the tank-house showed no adverse effects on copper deposition as long as additives were used [47]; therefore, the integration of SDC in a CuER plant should not cause metallurgical quality problems. Another feature not shown in the simplified flowsheet is the cooling of the feed electrolyte down to $\sim 10^{\circ}\text{C}$ so to reduce the solvent inventory requirements (according to solubility studies, Section 5.3.2).

In terms of maintenance cost, it is expected that SDC (with or without pre-evaporation) will be significantly less costly than evaporative crystallisation (due handling of less corrosive aqueous solutions). Typically, in the case of the latter, the

maintenance costs cause operating costs to double. Taking into account further the credit from the sales of the high-grade nickel sulphate product of the SDC process, the latter clearly becomes a very attractive alternative to the current technology.

XRD analysis of the product obtained from the industrial electrolyte via SDC with 2-propanol revealed the crystals to be $NiSO_4 \cdot 6H_2O$.

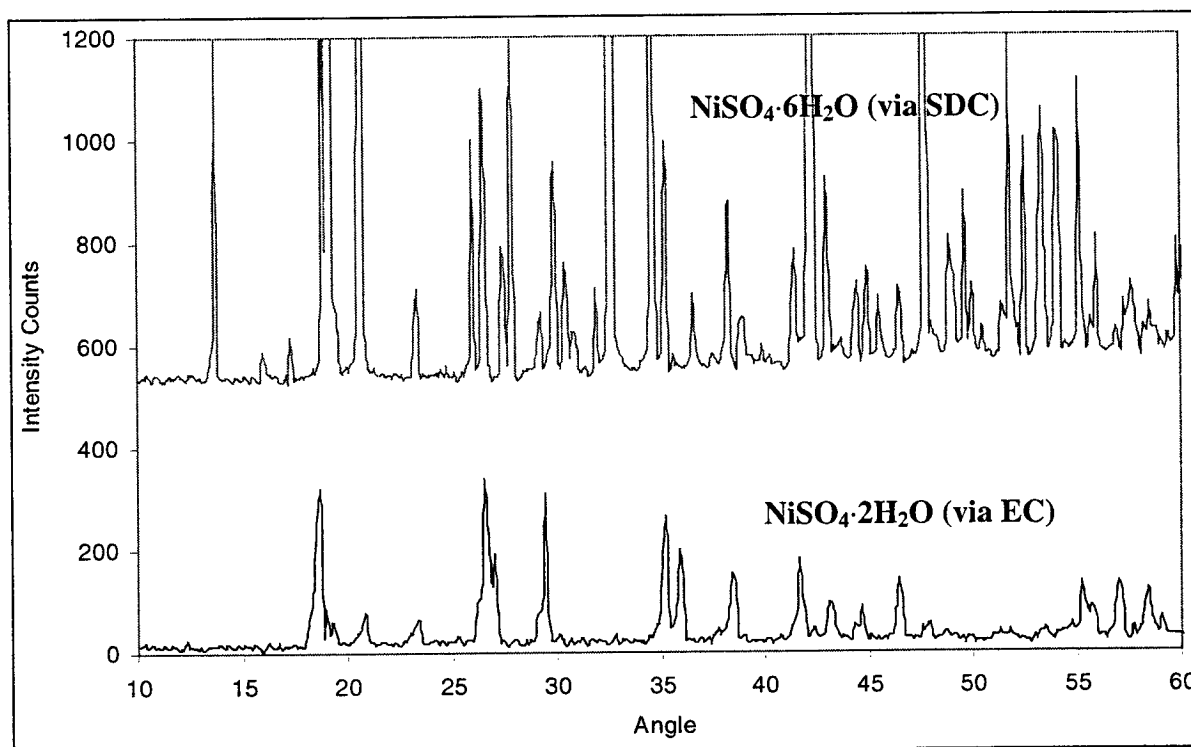


Figure 5.32 Comparative XRD spectra of nickel sulphate produced via SDC and EC

The large number of crystallisation water for SDC product, due to the low temperature of crystallisation, is in agreement with literature data [12, 13]. The product obtained via EC (temperature range 100-130°C) has instead only 2 crystallisation waters; their greenish-yellow colour is characteristic to low hydration nickel sulphate that forms at high temperature in the presence of dehydrating agents (e.g. sulphuric acid) [12].

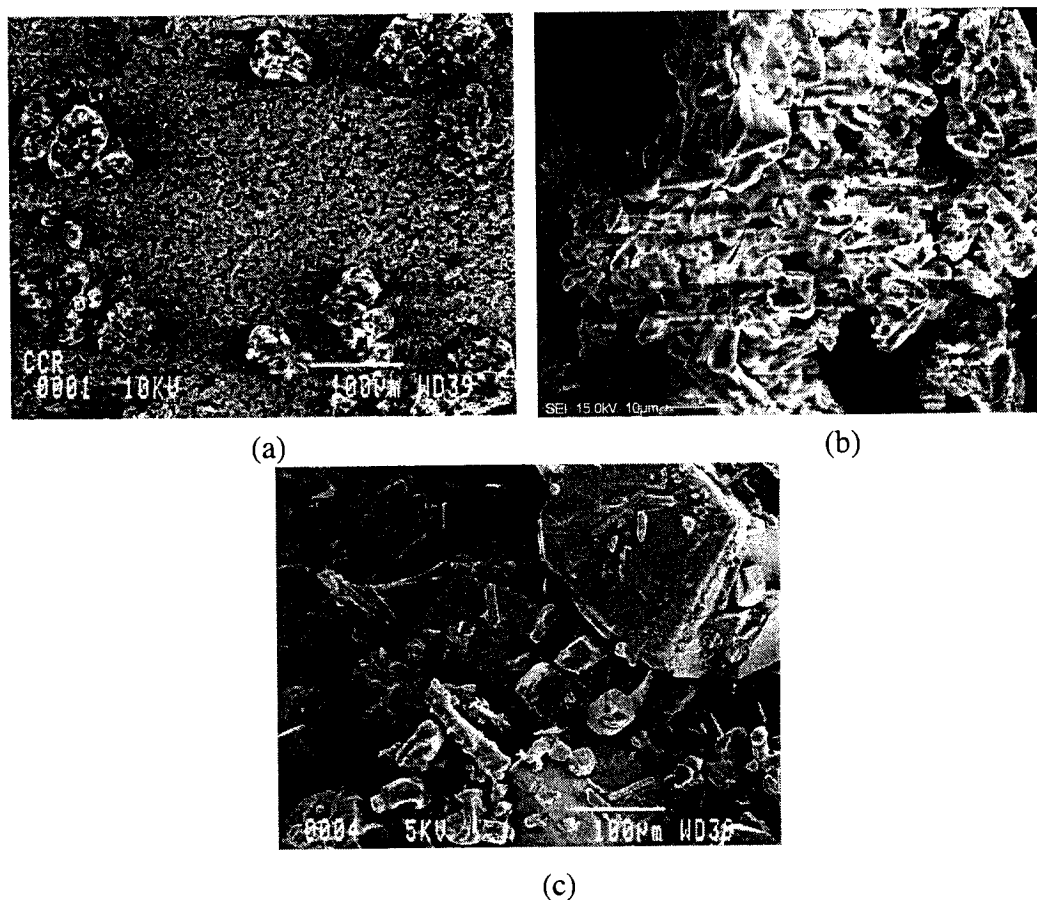


Figure 5.33 Influence of method of crystallisation on particle size and morphology:

(a) EC, 130°C, >1000 g/L H_2SO_4 ; (b) detail of (a); (c) SDC, heterogeneous crystallisation (low S, 1st recycle), 21°C, 250 g/L H_2SO_4 (from refs. [10] and [46]).

Table 5.6 Chemical composition of industrial decopperised electrolyte and final nickel sulphate crystalline product

Element (%)	Industrial Electrolyte Composition (g/L)	Purity of $NiSO_4 \cdot 6H_2O$ (SDC)	Purity of $NiSO_4 \cdot 2H_2O$ (EC-Industrial)	Electroplating-Quality $NiSO_4 \cdot 6H_2O$
Ni	18.70	21.90	31.40	22
Cu	1.14	0.11	1.25	0.02
Fe	0.29	0.01	0.59	0.005
As	0.99	< 0.02	0.05	0.001
Sb	0.11	0.01	0.10	
Bi	0.02	0.02	0.02	
Al	0.11	0.02	0.26	0.002
Ca+Mg	0.47	0.10	0.72	0.025
H_2SO_4	250	0.44	5.00	

5.8 Summary and Conclusions

1. The present work confirmed 2-propanol to be an effective salting-out agent to cause precipitation of $NiSO_4 \cdot 6H_2O$ from acidified aqueous solutions. The solubility of $NiSO_4 \cdot 6H_2O$ as a function of 2-propanol content, sulphuric acid concentration and temperature was established. The final nickel concentration decreased with increasing organic fraction and sulphuric acid concentration and with decreasing temperature.
2. The metastable zone boundary, an important parameter in designing controlled-crystallisation tests, has been determined at 10, 21 and 40°C. It was found that the metastable zone width decreases with increasing alcohol concentration and temperature.
3. The precipitation kinetics of $NiSO_4 \cdot 6H_2O$ were determined at 10, 21 and 40°C. At constant temperature, near critical supersaturation the crystallisation kinetics are slower, but due to the positive effect of high supersaturation on induction time and nucleation, crystallisation kinetics of $NiSO_4 \cdot 6H_2O$ are generally fast at medium and high supersaturation values. On the other hand, crystallisation kinetics are faster at higher temperatures, even at low supersaturation values.
4. The crystal size, settling velocity and percent solids density of the product were found to depend on the method of crystallisation. High supersaturation (homogeneous crystallisation) leads to fine crystal product while low supersaturation and seeding/product recycling were found to promote growth, producing particles with improved physical (size) and chemical (purity) properties.
5. The type of seed material or heterogeneous crystallisation strategy do not influence significantly the final value of nickel achieved in the aqueous phase but have dramatic effect on the quality of the solid product (in terms of morphology and size), promoting growth by secondary nucleation on crystal's surface.
6. There is a limit on the recycling extent, after which a decrease in particle size occurs due to crystal fragmentation.
7. Temperature had a net beneficial effect on crystal morphology. Even for high supersaturations, agglomerated particles obtained at low temperatures, 10°C, tend to grow slightly and become better defined individually at 21 and especially 40°C, whereas the combined effect of low supersaturation and more elevated temperatures

greatly favours both the growth process and the morphology, which tends more towards the specific tetragonal shape.

8. Agitation affects the nucleation process, especially at low supersaturations, but does not influence significantly the crystallisation yield (i.e. solution composition). On the other hand, mixing has a dramatic effect on crystal quality: with increasing agitation speed, the morphology becomes irregular and median crystal size decreases due to inferior growth rates and fragmentation.
9. Crystal equilibration (ageing) time has a beneficial effect on $NiSO_4 \cdot 6H_2O$ crystal morphology and size, provided that an optimum period is determined, beyond which the soft sulphate crystals exhibit deterioration of morphology and increase in particle size distribution due to friction, secondary nucleation and fragmentation.

References

- [1]. J.E. Hoffmann, "Process Options in the Treatment of Copper Refinery Electrolyte Bleed" in *EPD Congress 1997*, (edited by B. Mishra), TMS, Warrendale, Pa., pp. 435-451, (1997).
- [2]. R.F. Dobner, "Bleed-off Treatment at Hutterwerke's Secondary Copper Electrorefinery" in *EPD Congress 1997*, (edited by B. Mishra), TMS, Warrendale, Pa., pp. 413-424, (1997).
- [3]. A.K. Biswas, W.G. Davenport (editors), *Extractive Metallurgy of Copper*, 3rd edition, Pergamon, London, U.K., pp. 324-335, (1994).
- [4]. T.B. Braun, J.R. Rawling, K.J. Richards, "Factors Affecting the Quality of Electrorefined Cathode Copper" in *Extractive Metallurgy of Copper*, vol. I: + "Pyrometallurgy and Electrolytic Refining", (edited by J.C. Yannopoulos and J.C. Agarwal), The Metallurgical Society of AIME, New York, N.Y., pp. 511-524, (1976).

- [5]. T.T. Chen and J.E. Dutrizac, "A mineralogical overview of the behaviour of nickel during copper electrorefining" *Metallurgical Transactions B*, **21B**, pp. 229-238, (1990).
- [6]. K. Ando and N. Tsuchida, "Recovering Bi and Sb from Electrolyte in Copper Electrorefining" *JOM*, **49**(12), pp. 49-51, (1997).
- [7]. J.R.L. Bravo, "Aspects of Impurity Control at Caraiba Metais Electrorefinery" in "EPD Congress 1997", (edited by B. Mishra), TMS, Warrendale, Pa., pp. 403-412, (1997).
- [8]. R.L. Nyirenda and W.S. Phiri, "The Removal of Nickel from Copper Electrorefining Bleed-off Electrolyte" *Minerals Engineering*, **11**(1), pp. 23-37, (1998).
- [9]. J.M. Cohen, "Applications of solvent displacement crystallisation in hydrometallurgy" in *Separation Processes in Hydrometallurgy*, (edited by G.A. Davies), pp. 265-273, Ellis Horwood, London, U.K., (1987).
- [10]. G.A. Moldoveanu, *Precipitation of Nickel Sulphate from Decopperized Acid Solution by Solvent Displacement Crystallisation*, M.Eng. Thesis, McGill University, Montreal, PQ, Canada, (1999).
- [11]. D.L. Pavia, G.M. Lampman and G.S. Kriz, jr., *Introduction to Organic Laboratory Techniques (a contemporary approach)*, Saunders College Publishing, Philadelphia, Pa., pp. 514-635, (1982).
- [12]. E. Rohmer, "Contribution a l'Étude du Sulfate de Nickel et du Sulfate de Cobalt" *Annales de Chimie*, **11**, pp. 611-721, (1939).
- [13]. W.F. Linke and A. Seidell (editors), *Solubilities of Inorganic and Metal-Organic Compounds (a compilation)* 4th edition, Van Nostrand, Princeton, N.J., (1958).

- [14]. T. Havlik, M. Skrobjan, R. Kammel and J. Curilla, "Refining of Crude Nickel Sulfate Obtained from Copper Electrolyte" *Hydrometallurgy*, **41**, pp. 79-88, (1996).
- [15]. I. Howell and G.W. Neilson, " Ni^{2+} coordination in concentrated aqueous solutions" *Journal of Molecular Liquids*, **73/74**, pp. 337-348, (1997).
- [16]. N.V. Plyasunova, Y. Zhang and M. Muhammed, "Critical evaluation of thermodynamics of complex formation of metal ions in aqueous solutions" *Hydrometallurgy*, **48**, pp. 43-63, (1998).
- [17]. A. Wakisaka, S. Komatsu and Y. Usui, "Solute-solvent and solvent-solvent interactions evaluated through clusters isolated from solutions; Preferential solvation in water-alcohols mixtures" *Journal of Molecular Liquids*, **90**, pp. 175-184, (2001).
- [18]. S. J. Suresh and V. M. Naik, "Hydrogen bond thermodynamic properties of water from dielectric constant data" *J. Chem. Phys.* **113** pp. 9727-9732, (2000).
- [19]. R.A. Zingaro, *Non-Aqueous Solvents*, D.C. Heath & Co., Lexington, MA., pp.1-20, (1968).
- [20]. V.V. Udovenko and T.F. Mazanko, "Liquid-vapour equilibrium in the propan-2-ol-water and propan-2-ol-benzene system" *Russian Journal of Physical Chemistry*, **41(7)**, pp. 863-866, (1967).
- [21]. H. Majima and Y. Awakura, "Water and solute activities in the solution systems $H_2SO_4-CuSO_4-H_2O$ and $HCl-CuCl_2-H_2O$ " *Metallurgical Transactions B*, **19B**, pp. 347-354, (1998).
- [22]. H.S. Na, S. Arnold and A.B. Myerson, "Water activity in supersaturated aqueous solutions of organic solutes" *Journal of Crystal Growth* **149**, pp. 229-235, (1995).
- [23]. W.F. Linke and A. Seidell (editors), *Solubilities of Inorganic and Metal-Organic Compounds (a compilation)* 4th edition, Van Nostrand, Princeton, N.J., (1958).

- [24]. H. Youping, S. Genbo, Y. Xianchun, L. Zhengdong, H. Bingrong, J. Rihong and Z. Qingran, "Growth of α -nickel sulphate hexahydrate for ultraviolet filters" *Journal of Crystal Growth*, **169**, pp. 193-195, (1996).
- [25]. M.E. Blesa and E. Matijevic, "Phase transformation in aqueous media" *Adv. Coll. Interf. Sci.*, **29**, pp. 173-231, (1989).
- [26]. L.V. Soboleva, E.B. Rudneva and I.L. Smolsky, "Growth of single crystals of α -nickel sulphate hexahydrate, α - $NiSO_4 \cdot 6H_2O$ " *Crystallography Reports*, **43(4)**, pp. 706-710, (1998).
- [27]. J.W. Mullin, *Crystallisation*, 3rd Ed., Butterworth-Heinemann, Oxford, pp.172, (1993).
- [28]. G.P. Demopoulos, "Aqueous Precipitation and Crystallisation-Production of Particulate Solids with Designed Properties" *Hydrometallurgy*, (2004), in press.
- [29]. A.E. Nielsen, "Electrolyte Crystal Growth Mechanisms" *Journal of Crystal Growth*, **67**, pp. 289-310, (1984).
- [30]. C.Y. Tai and W-C. Chien, "Effects of operating variables on the induction period of $CaCl_2$ - Na_2CO_3 system" *Journal of Crystal Growth*, **237-239**, pp. 2142-2147, (2002).
- [31]. P.A. Barata and M.L. Serrano, "Salting-out precipitation of potassium dihydrogen phosphate (KDP): I. Precipitation mechanism" *Journal of Crystal Growth*, **160**, pp. 361-369, (1996).
- [32]. J. Nyvlt, R. Rychly, J. Gottfried and J. Wurzelova, "Metastable Zone Width of Some Aqueous Solutions" *Journal of Crystal Growth*, **6**, pp. 151-162, (1970).
- [33]. J.W. Mullin, N. Teodossiev and O. Söhnle, "Potassium Sulphate Precipitation from Aqueous Solution by Salting-out with Acetone" *Chem. Eng. Process.*, **26**, pp. 93-99, (1989).

- [34]. C. Mahadevan, D.I. Latha and V. Umayorubhagan, "Nucleation studies in supersaturated aqueous solutions of magnesium- and zinc-doped nickel sulphate heptahydrate" *J. Indian Chem. Soc.*, **76**, pp.335-338, (1999).
- [35]. J. Franke and A. Mersmann, "The influence of the operational conditions on the precipitation process" *Chemical Engineering Science*, **50(11)**, pp. 1737-1753, (1995).
- [36]. P.A. Barata and M.L. Serrano, "Salting-out precipitation of potassium dihydrogen phosphate (KDP): III. Growth process" *Journal of Crystal Growth*, **194**, pp. 101-108, (1998).
- [37]. P.A. Barata and M.L. Serrano, "Salting-out precipitation of potassium dihydrogen phosphate (KDP): IV. Characterisation of the final product" *Journal of Crystal Growth*, **194**, pp. 109-118, (1998).
- [38]. A.E. Nielsen and O. Söhnel, "Interfacial tensions in electrolyte-aqueous solution, from nucleation data" *Journal of Crystal Growth*, **11**, pp. 233-242, (1971).
- [39]. E. Huitema and J.P. van der Eerden, "Defect formation during crystal growth" *Journal of Crystal Growth*, **166**, pp. 141-145, (1996).
- [40]. W.J. Genck, "Understanding mixing in crystallisation" *Chemical Processing*, **57(11)**, pp. 48-50, (1994).
- [41]. J. Nyvlt and S. Zacek, "Effect of the rate of stirring on crystal size in precipitating or salting-out systems" *Collection of Czechoslovak Chem. Commun.*, **51**, pp. 1609-1617, (1985).
- [42]. J. Nyvlt, "Batch salting-out crystallisation" *Chemical Engineering and Processing*, **31**, pp. 3-42, (1992).
- [43]. P.A. Barata and M.L. Serrano, "Salting-out precipitation of potassium dihydrogen phosphate (KDP): II. Influence of agitation intensity" *Journal of Crystal Growth*, **163**, pp. 426-433, (1996).

- [44]. U. Zacher and A. Mersmann, "The influence of internal crystal perfection on growth rate dispersion in a continuous suspension crystallizer" *Journal of Crystal Growth*, **147**, pp. 172-180, (1995).
- [45]. M. Liiri, T. Koiranen and J. Aittamaa, "Secondary nucleation due to crystal-impeller and crystal-vessel collisions by population balances in CFD-modelling" *Journal of Crystal Growth*, **237-239**, pp. 2188-2193, (2002).
- [46]. G.A. Moldoveanu and G.P. Demopoulos, "Producing high-grade nickel sulphate with solvent displacement crystallisation" *JOM*, **54(1)**, pp. 49-53, (2002).
- [47]. I Anjort and B. Gregoire, "Electrochemical evaluation of the effect of additives on copper electrorefining", (Research Project Report), Hydrometallurgy Laboratory, McGill University, Montreal (2001).

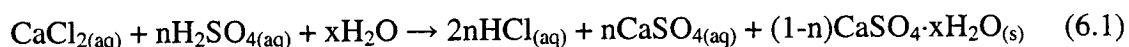
Chapter 6. Crystallisation of Gypsum from CaCl₂-HCl Media

6.1 Introduction

Chloride hydrometallurgy has been for many years applied to the refining of PGM, nickel, the pickling of steel and it has great potential to gain wider use in the future in the area of complex sulphide treatment (recovery of Zn and Pb) and processing of copper concentrates. One critical issue in the implementation of chloride hydrometallurgy is the regeneration of HCl (the lixiviant). This is done commercially by neutralisation of the pregnant leach solution with MgO (for example) and pyrohydrolysis of the metal chloride solution, a technology that is highly intensive in terms of capital and energy consumption.

Notwithstanding the high cost of pyrohydrolysis, this procedure cannot be used when CaO (lime) or CaCO₃ (limestone) are employed as neutralising agents.

One potential alternative to pyrohydrolysis is low cost HCl regeneration via atmospheric reaction of spent CaCl₂ solutions (generated by neutralisation with lime of metal chloride leach solutions) with H₂SO₄ in the temperature range 20-100°C with concomitant production of saleable-quality calcium sulphate products [1, 2]:



where $x=0$ for anhydrite, 0.5 for hemihydrate and 2 for gypsum.

As may be deduced from reaction (6.1) and determined by Li and Demopoulos [3], some of the calcium sulphate product may remain in solution (due to its solubility in HCl) and thus becoming a source of scaling upon recycling to the leaching circuit. In addition to this, during high temperature (95-100°C) chloride leaching of metal sulphides, up to 5% of the oxidized sulphide ion reports to solution as sulphate, bringing the total sulphate content even higher [4]. The accumulation of sulphate in a chloride leaching circuit cannot be allowed to continue indefinitely, and some form of sulphate control must thus be provided. Dutrizac [4] thus investigated and described various options of sulphate control in chloride leaching solutions containing ~0.3 M HCl and ≥ 22 g/L SO₄:

(a) Calcium Sulphate Precipitation by CaCl_2 Addition:

Relatively high (> 0.6 M) calcium concentrations are required to minimize the amount of soluble sulphate, reflecting a Ca/SO_4 molar ratio > 5 . The concentration of sulphate remaining in solution is reduced to the acceptable level of 1-3 g/L and calcium sulphate anhydrite (CaSO_4) as opposed to gypsum is formed (due to concentrated HCl medium and high temperatures).

(b) Precipitation of Jarosite-Type Compounds by Alkali Chlorides Addition:

Sodium and ammonium jarosite did not precipitate appreciably under the conditions examined, even for high alkali chlorides concentration (1 M), and the final solution contained elevated levels of sulphate (11-19 g/L). Potassium jarosite precipitation proved effective at high SO_4 levels (25-60 g/L) and in the absence of free HCl; however, residual SO_4 in the final solution was high (13-16 g/L).

(c) Barium Sulphate Precipitation by BaCl_2 Addition:

The addition of ~ 0.2 M BaCl_2 to the leaching solution results in the nearly quantitative precipitation of SO_4 and a slight excess achieves < 0.1 g/L SO_4 . The disadvantage is that part of the excess BaCl_2 converts by cooling to $\text{BaCl}_2 \cdot 2\text{H}_2\text{O}$ that crystallises during filtration of the leach slurry and forms voluminous precipitates that impede the separation process.

Previous research work by this author [5] revealed the ready production of gypsum (i.e. $\text{CaSO}_4 \cdot 2\text{H}_2\text{O}$) by adding 2-propanol to electrolyte solutions containing calcium ions in H_2SO_4 medium. Additionally, research work and literature data presented in Chapter 4 (Sections 4.3 and 4.4) indicate selectivity of alcohols in crystallising sulphates but not chlorides from aqueous solutions.

Based on these observations, Solvent Displacement Crystallisation (SDC) appears to have the potential of providing an alternative (to BaCl_2 addition) residual sulphate removal technique from $\text{CaCl}_2\text{-HCl}$ media by salting out calcium sulphate. This option is investigated in this Chapter. The main objective of this investigation is to examine closely the changes in solution composition and solids properties under the influence of various experimental conditions such as 2-propanol fraction, temperature, supersaturation magnitude and crystallisation regime (homogeneous vs. heterogeneous).

6.2 Experimental

6.2.1 Research Strategy

The experiments conducted for the present research work consisted of two parts: (i) in order to gain a basic understanding of the crystallisation of gypsum from HCl media with 2-propanol and establish a “reference” behaviour, solubility measurements have been conducted as a function of various factors; (ii) based on these results, critical supersaturation determinations and crystallisation tests have been developed to further investigate the evolution of the system. In all experiments, both changes in solution composition (CaSO_4 concentration) on one hand and product quality on the other were monitored (Table 6.1).

Table 6.1 Parameters considered in crystallisation of gypsum with 2-propanol

Parameter	Evaluated Aspect
Organic Fraction (expressed as O/A)	<ul style="list-style-type: none"> Equilibrium sulphate concentration in aqueous as a function of organic (O/A=0, 0.25, 0.43, 0.66, 1, 1.5, 2.33), 3 M HCl.
Chloride Content	<ul style="list-style-type: none"> Equilibrium sulphate concentration in aqueous as a function of organic in the presence of 1.5 M MgCl_2 (3 M HCl).
Temperature	<ul style="list-style-type: none"> Equilibrium sulphate concentration in aqueous as a function of temperature (21, 40 and 60°C). Influence on SDC process and crystal quality.
Supersaturation (S)	<ul style="list-style-type: none"> Critical supersaturation lines at 21 and 40°C. No S control vs. controlled S during SDC: Influence on sulphate content in solution and crystal quality.
Crystallisation Regime	<ul style="list-style-type: none"> Homogeneous vs. Heterogeneous: Influence on sulphate content in solution and crystal quality.

All solubility and critical supersaturation tests were performed in 250 mL conical flasks, using magnetic stirring, as described in Chapter 3 (Section 3.3.1., Figure 3.1).

Crystallisation tests were conducted using the 1 L batch reactor, mechanical stirring and set-up presented in Section 3.3.1., Figure 3.2.

6.2.2 Experimental Procedure

De-ionised water, reagent-grade gypsum ($\text{CaSO}_4 \cdot 2\text{H}_2\text{O}$, 98.5% purity) and concentrated HCl (37.5% concentration) were used to prepare the aqueous solutions; 2-propanol Optima-grade (99.9% purity) was employed.

- ***Solubility Measurements***

100 mL of aqueous-organic mixtures were prepared starting from solutions containing 3 M HCl and 2-propanol, with the following organic-to-aqueous ratio (O/A): 0, 0.25, 0.43, 0.66, 1.00, 1.50 and 2.33. Small amounts of $\text{CaSO}_4 \cdot 2\text{H}_2\text{O}$ crystals were added under stirring at 21°C, allowing an equilibration period of 15 minutes. When crystals in equilibrium with solution were detected (i.e. no more dissolution), salt's addition stopped and the system was allowed to equilibrate for 24 hours. Subsequently, the crystals were separated by filtration, washed, air-dried in the fume-hood at 50°C and further analysed. The mother liquor was diluted with 5% HCl and analysed for calcium via ICP. Same procedure was repeated for 40 and 60°C.

In order to study the influence of chloride content on gypsum solubility, similar tests were conducted at 40°C in the presence of 1.5 M MgCl_2 .

- ***Determination of Critical Supersaturation***

100 mL solutions containing different amounts of calcium sulphate (i.e. 5, 10, 15 and 20 g/L) and 3 M HCl were agitated with a magnetic stirrer in Erlenmeyer flasks at 21 and 40°C. Small volumes of organic were slowly added to the aqueous solutions by the means of a manual burette; after each addition, a 15-minutes equilibration period was allowed. At the moment a "cloud" was seen (initiation of the homogeneous crystallisation process), the volume of organic solvent was recorded and the solutions were stirred for 24 hr at 20°C to reach complete equilibrium (6 hr final equilibration at 40°C due to improved kinetics). Subsequently, the crystals were separated by filtration, washed, dried at ambient temperature for ~50 hr and further analysed. The mother liquor was diluted with 5% HCl and analysed for metal ion content.

- **Solvent Displacement Crystallisation Tests**

In a typical SDC test, 100 mL aqueous solution containing 3 M HCl, 15 g/L CaSO_4 at 21°C and 40 g/L CaSO_4 at 40°C, respectively, were agitated (400 rpm) in 1 L glass reactor maintained in a water bath while the organic was added from a 100 mL manual burette at various organic-to-aqueous (O/A) ratios. Subsequently, the crystals were separated by filtration, washed, dried in the oven at 50°C and further analysed; the mother liquor was diluted with 5% HCl and analysed for calcium sulphate.

Homogeneous Crystallisation, High Supersaturation: To homogeneously precipitate the inorganic salt, the organic solvent was added at once to the aqueous phase with a total O/A ratio of 1 (21°C) and 2 (40°C). The mixture was agitated for 120 minutes and samples were taken every 2, 5, 10, 15 minutes, then every 15 minutes for two hours, in order to monitor cation content and hence the kinetics of the process. Solution samples were diluted 10 times with 5% HCl solution and analysed for CaSO_4 via ICP.

Homogeneous Crystallisation, Low Supersaturation: Low S was maintained via a slow alcohol delivery, following the critical supersaturation line; the first organic addition was as to slightly exceed critical value in order to induce nucleation. After a 30-minutes equilibration period (20 min at 40°C) 2-propanol addition was resumed in a controlled, step-wise manner, as to maintain $S < S_{\text{cr,homo}}$ throughout the entire experiment (total O/A=1.15 at 21°C and 1.91 at 40°C). After each addition/stirring period solution samples were taken, diluted and analysed for calcium.

Heterogeneous Crystallisation (Seeding & Product Recycling): Low supersaturation was maintained via a slow organic delivery, at 21 and 40°C; for a certain volume of solvent corresponding to a supersaturation below the critical value, organic addition was stopped and crystalline $\text{CaSO}_4 \cdot 2\text{H}_2\text{O}$ seed (ACRÖS Organics, ~ 15 g/L) was added to the system, in order to favour the secondary nucleation process and hence crystal growth. After a 30-minutes equilibration period, organic addition was resumed in a controlled, step-wise manner, small volumes at a time, followed by 30-minutes equilibration periods (20 minutes at 40°C), as to maintain $S < S_{\text{cr,homo}}$ throughout the whole experiment. After each addition/stirring period the agitation was stopped and 2-mL samples were taken, diluted and analysed for calcium. Product recycling tests (15 g/L seed, 8 recycle runs) were conducted at 40°C only.

6.3 Systematic Solubility Studies

6.3.1 General Considerations

For optimum design of the crystallisation process, the solubility of the salt ($\text{CaSO}_4 \cdot 2\text{H}_2\text{O}$) as a function of temperature, hydrochloric acid content and organic fraction needs to be determined, according to the procedure described in Section 6.2.2.

Extensive research work conducted at McGill [3] and literature data [6, 7] offer comprehensive information about gypsum solubility in the presence of HCl at different temperatures. Therefore, this subject-matter was no further investigated, but typical solubility values are presented in Figure 6.1, in order to understand gypsum behaviour and select an optimum fixed HCl concentration for subsequent SDC experiments.

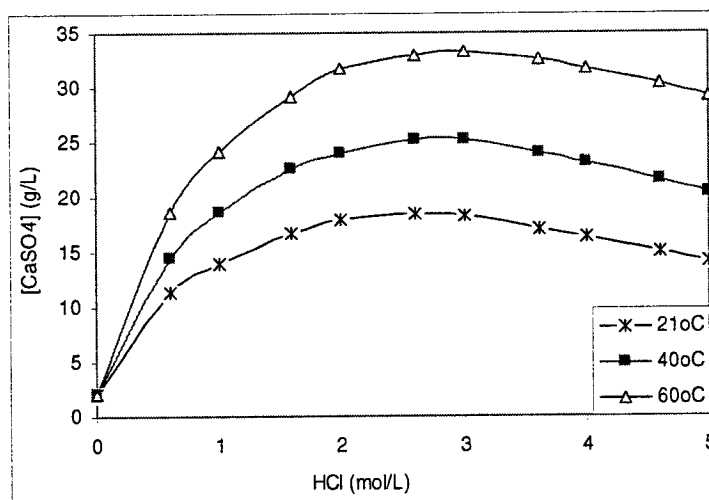
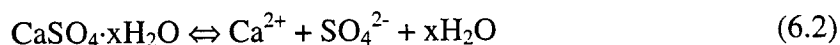


Figure 6.1 Gypsum solubility in hydrochloric acid solutions (adapted from [3])

Gypsum solubility is highly dependent on the solution composition. While in pure water gypsum it is inversely soluble with temperature [8], in concentrated acid solutions it is increasingly soluble with temperature. Solubility values determined by Li and Demopoulos [3] were found to increase with temperature and HCl concentration up to about 2.8-3 M HCl, followed by a slight decrease. Gupta [7] reported similar findings and tried to explain this behaviour on the basis of Debye-Huckel theory for strong electrolytes.

Based on these previous findings, a fixed HCl concentration of 3 M was selected for subsequent studies.

Gypsum dissolution is represented by the following equation and solubility product constant:



$$K_{sp} = a_{\text{Ca}^{2+}} \cdot a_{\text{SO}_4^{2-}} \cdot a_{\text{H}_2\text{O}}^x = m_{\text{Ca}^{2+}} \cdot m_{\text{SO}_4^{2-}} \cdot (\gamma_{\pm, \text{CaSO}_4})^2 (a_{\text{H}_2\text{O}})^x \quad (6.3)$$

where a = activity, m = molality and γ_{\pm} = mean activity coefficient.

Since the ions are soluble in “free water” only, any change in solution composition that results in decreasing the water activity will influence the solubility of the solute. Generally, water activity decreases with increasing hydrochloric acid concentration and ionic strength of solution [9, 10] and in the presence of organic miscible solvents [11-14].

6.3.2 Influence of Temperature, Organic Fraction and Chloride Content

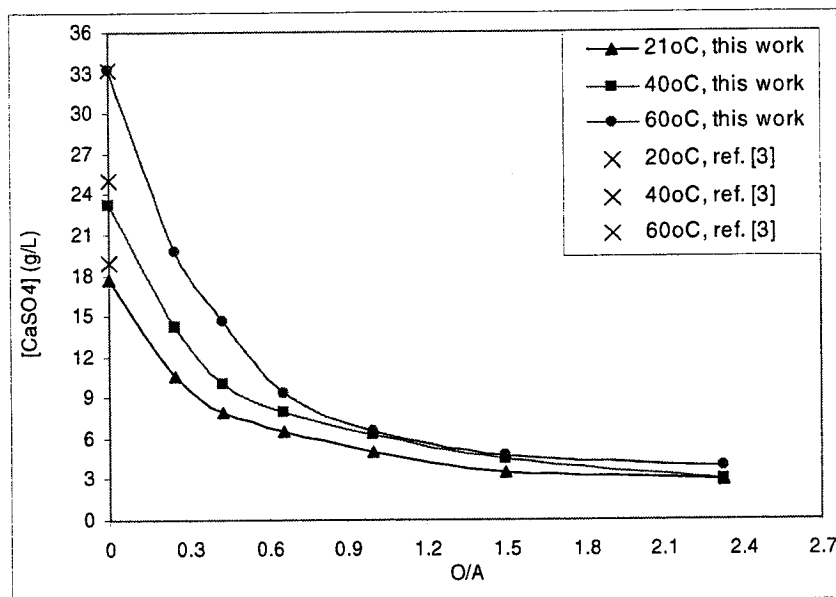
The solubility of gypsum in the system H₂O-HCl (3 M) as a function of 2-propanol (never studied before) was determined for temperatures ranging from 21 to 60°C (Table 6.2 and Figure 6.2). Values determined by Li and Demopoulos [3] at similar temperatures in the absence of organic are also indicated for comparison.

As expected, the solubility (measured as g/L CaSO₄ in the aqueous phase – not in the mixed aqueous-organic solutions) decreases with increasing organic fraction and decreasing temperature. At low O/A ratios, decreased temperature brings an additional effect in suppressing calcium sulphate solubility, but as organic fraction increases (O/A>1), the solubility tends to be influenced solely by the organic content (due most likely to removal of water molecules from the ions’ hydration spheres on one hand and on the other because of the drastic decrease of water’s dielectric constant upon organic addition, which favours ion pairing, as explained in Section 2.3.3).

Table 6.2 Gypsum solubility as a function of 2-propanol and temperature

O/A (3 M HCl)	[CaSO ₄]aq (g/L)		
	21°C	40°C	60°C
0	17.60 (18.2)*	23.20 (25)*	33.25 (33.3)*
0.25	10.60	14.23	19.72
0.43	7.91	10.00	14.57
0.66	6.60	7.95	9.30
1.00	5.07	6.25	6.53
1.50	3.42	4.43	4.72
2.33	2.87	2.96	3.85

* values from Li and Demopoulos [3]

**Figure 6.2** Gypsum solubility in the system 2-propanol-HCl (3 M)-H₂O

When the ionic strength of the solution was increased by the presence of 1.5 M MgCl_2 (test at 40°C only), gypsum solubility decreased by about 50% (compared to values in the absence of additional salt), apparently because of a decrease in water activity associated with salt's addition (Figure 6.3).

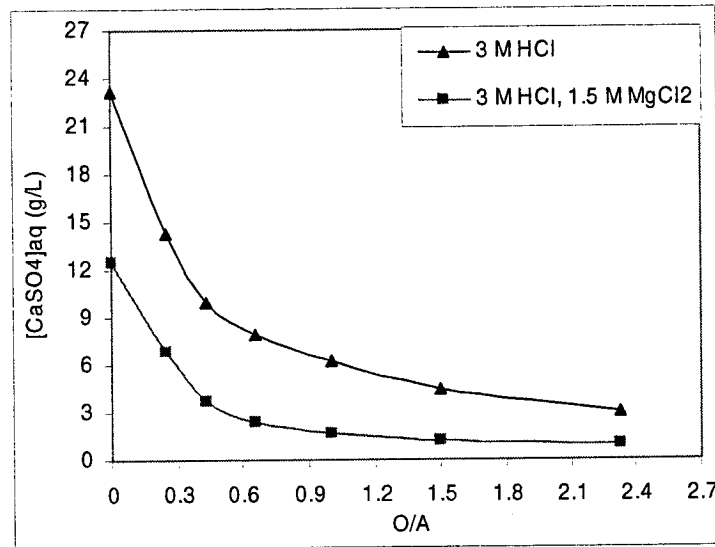


Figure 6.3 Influence of MgCl_2 presence on gypsum solubility in the system 2-propanol-HCl (3 M)- H_2O (40°C)

6.4 Critical Supersaturation at 21 and 40°C

One of the objectives of the present research work is to optimise the crystallisation conditions by conducting the process inside the metastable zone that favours large particle growth hence enhanced settling properties and filterability. In order to achieve this goal, the critical supersaturation lines for the system $\text{CaSO}_4\text{-H}_2\text{O-HCl}$ (3 M)-2-propanol were determined at 21 and 40°C (according to set-up and procedures extensively described in Sections 3.3.1, 3.3.2 and 5.2.2) and compared to the equilibrium solubility curves.

As indicated by Figure 6.4, for $S > S_{\text{cr,homo}}$, homogeneous crystallisation occurs. For any supersaturation values in the range $1 < S < S_{\text{cr,homo}}$, crystallisation is thermodynamically possible but does not start (metastable equilibrium) because of unfavourable kinetics. In order to control supersaturation below $S_{\text{cr,homo}}$ the alcohol should be added in a step-wise manner, as Demopoulos has discussed [15]. Hence, crystalline products can be obtained by controlling the supersaturation below the critical value ($S_{\text{cr,homo}}$), in the metastable (growth-dominated) zone, via a staged addition of the precipitating agent.

Moreover, if seed is introduced to the aqueous solution in the previously-mentioned supersaturation interval, heterogeneous crystallisation is initiated, ensuring thus favourable conditions for growth.

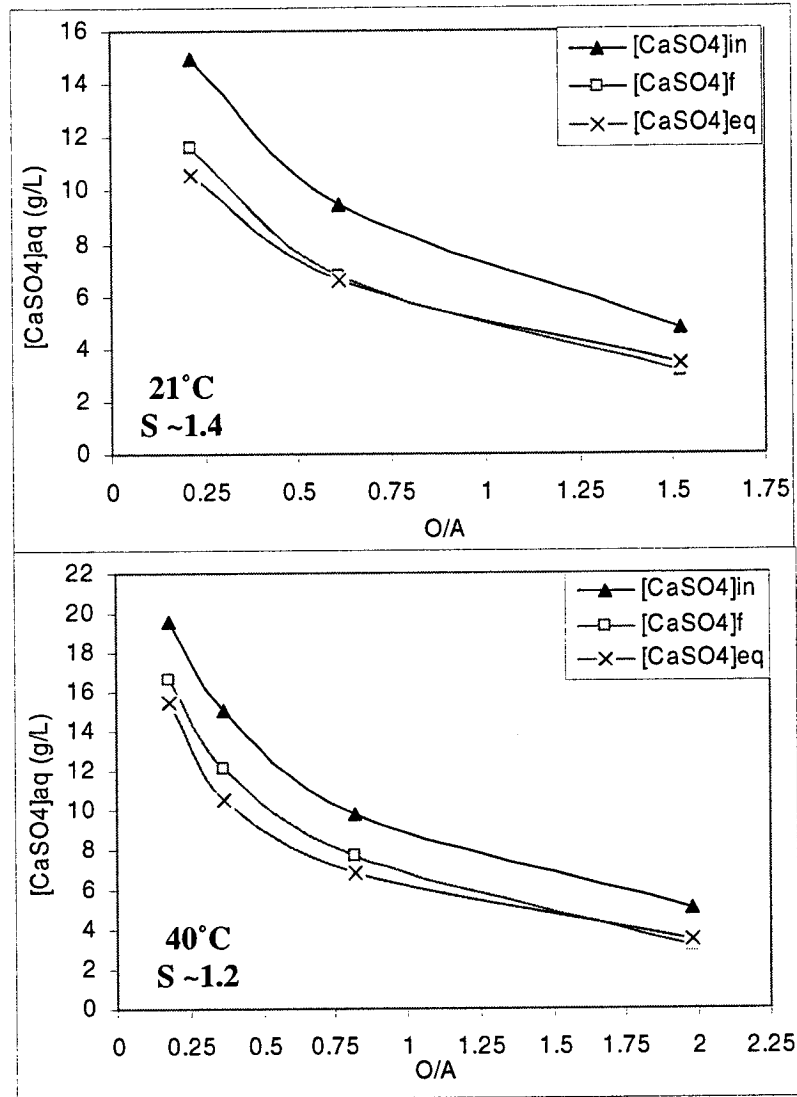


Figure 6.4 Critical supersaturation lines and metastable zone width in the system $\text{CaSO}_4\text{-H}_2\text{O-HCl}$ (3 M)-2-propanol at 21 and 40°C

Nyvtl *et al* explained [16] that the width of the metastable zone depends firstly on the probability of ion-pairing and viable nuclei formation in solution; the degree of probability depends on the inter-molecular distances and therefore on the solution concentration. Accordingly, nucleation in concentrated solutions should occur at

relatively low supersaturation levels, which is indeed the case for the system under study: the average supersaturation level is ~ 1.4 at 21°C and ~ 1.2 at 40°C , respectively. The experimental results show that the metastable zone width slightly decreases with increasing temperature. The results are similar to observations reported by Tai and Chien [17] and Franke and Mersmann [18].

6.5 Solvent Displacement Crystallisation Tests

Based on the critical supersaturation lines determined in Section 6.4, there are different possible crystallisation paths to follow to reach the targeted final concentration in solution:

- (I) High supersaturation case: The required quantity of precipitating agent (2-propanol) can be added all at once to the aqueous solution. Homogeneous (spontaneous) crystallisation leads in general to poor quality colloidal particles.
- (II) Controlled low supersaturation case: The required quantity of alcohol is added in small increments, first slightly over the critical supersaturation line in order to initiate homogeneous nucleation, then always inside the metastable zone width to promote growth. Moreover, if same-nature seed is to be added prior to $S_{\text{cr,homo}}$, heterogeneous crystallisation conditions would be met (growth on seed) and large particles are obtained.

The main objective of this section is to assess the influence of supersaturation value and crystallisation strategy on crystal product quality and residual sulphate in solution by performing comparative SDC tests at 21 and 40°C in the system $\text{H}_2\text{O-CaSO}_4\text{-HCl}$ (3 M).

6.5.1 Homogeneous Crystallisation

- ***High Supersaturation Homogeneous Crystallisation***

The aim of this study was to determine the crystallisation kinetics in the system $\text{H}_2\text{O-CaSO}_4\text{-HCl}$ (3 M) at 21 and 40°C (Figure 6.5). High supersaturation was ensured by the instantaneous addition of 2-propanol to the aqueous phase, under moderate stirring (400 rpm) and the kinetics of homogeneous crystallisation were assessed by monitoring the

aqueous calcium concentration at 21°C ($O/A=1$) and 40°C ($O/A=2$), following the experimental procedure described in Section 6.2.2. Sampling was performed at 2, 5, 10, then every 15 minutes, for 120 minutes, to analyse for calcium sulphate.

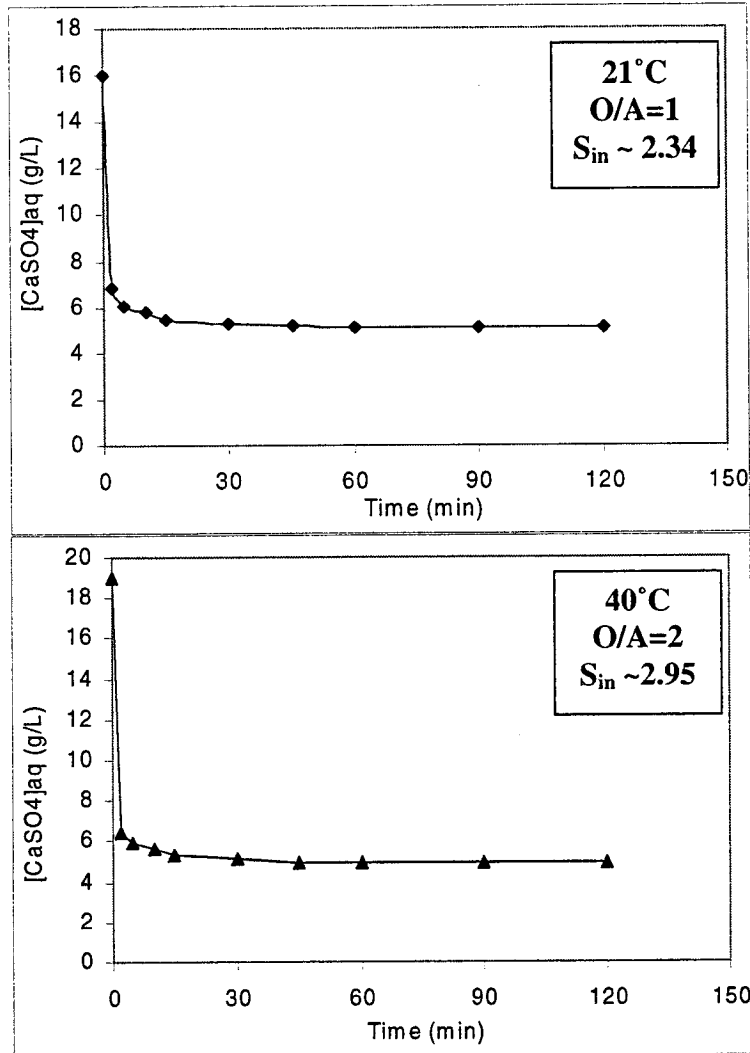


Figure 6.5 Homogeneous crystallisation kinetics of gypsum at 21 and 40°C (3 M HCl)

As per Crystallisation Theory (Sections 2.2 and 5.5), the induction period (i.e. the time lapsed before crystals become visible) is considered to be inversely proportional to the supersaturation and temperature. Generally, at low supersaturation the induction period is more lengthy and nucleation rate is slow; consequently, the crystallisation kinetics are expected to be slower. Due to the positive effect of high supersaturation on induction

time and nucleation, crystallisation kinetics of $\text{CaSO}_4 \cdot 2\text{H}_2\text{O}$ are generally fast at medium and high supersaturation values (i.e. when $S \gg S_{\text{cr,homo}}$).

Approximately 15 minutes are required by the system to attain a concentration of 5.43 g/L CaSO_4 at 21°C (corresponding to a initial supersaturation, S_{in} , of 2.34) and 5.32 g/L at 40°C (S_{in} of 2.95), respectively; the subsequent decrease to the final values of 5.15 g/L at 20°C and 4.96 g/L at 40°C, respectively, shows a plateau over the remaining time interval. These values, compared to equilibrium calcium sulphate concentrations (Section 6.3), suggest that an interval of less than 30 minutes should suffice to perform efficient homogeneous SDC tests at 21 °C.

- ***Low Supersaturation Homogeneous Crystallisation***

SDC tests at low supersaturation have been performed at 21 and 40°C in order to study and compare the influence of supersaturation magnitude on calcium sulphate concentration in solution and crystal quality (Figure 6.6). A typical test (approximate duration ~ 120 min) was conducted by adding the organic in small doses as to maintain $S < S_{\text{cr,homo}}$, according to the step-wise crystallisation path applied within the metastable zone previously determined for each temperature in Section 6.4. The initial solution composition was 3 M HCl, 15 g/L CaSO_4 at 21°C ($O/A_{\text{total}} = 1.15$) and 3 M HCl, 20 g/L CaSO_4 at 40°C ($O/A_{\text{total}} = 1.91$).

As 2-propanol was gradually added to the solution, no precipitation occurred while $S < S_{\text{cr,homo}}$. Above a certain O/A value, homogeneous crystallisation started, resulting in a sharp decrease in calcium sulphate concentration, trend that continued (although more moderately) as additional alcohol entered the system in a controlled manner, as to maintain a low supersaturation.

Final calcium sulphate in solution was ~ 4.15 g/L CaSO_4 at 21°C and ~ 3.77 g/L at 40°C, comparable to required residual sulphate values in chloride leaching (respectively 2.92 and 2.66 g/L SO_4), as indicated by Dutrizac [4]. These numbers can be further lowered if a higher O/A ratio is employed (refer to solubility data, Section 6.3).

At low S , following a short duration homogeneous nucleation event that gave birth to a relatively small number of nuclei crystals, most crystallisation takes place within the growth zone (“secondary nucleation”), avoiding the formation of colloidal

particles. In conditions of high supersaturation, Franke and Mersmann [18] demonstrated that nucleation already starts during the feeding period and an initial amorphous or poorly crystalline precursor is built first. This results in slightly higher concentration values since amorphous or poorly crystalline products have usually higher solubility compared to the crystalline phases.

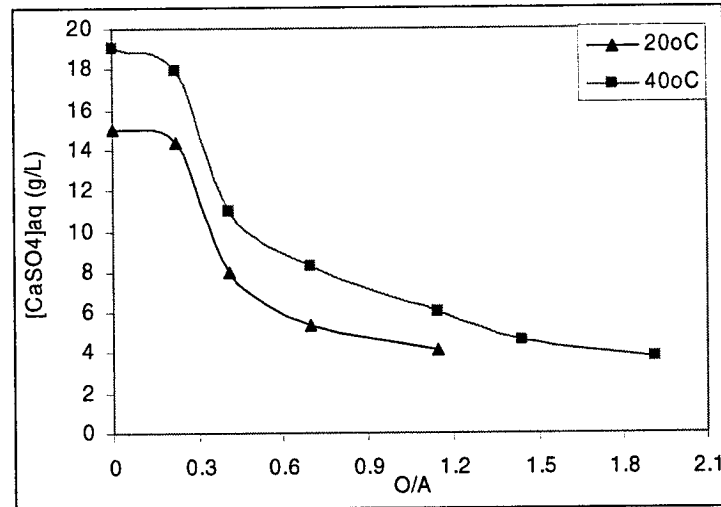


Figure 6.6 Homogeneous crystallisation of gypsum at 21 and 40°C (low S, 3 M HCl)

The effect of supersaturation magnitude and temperature on crystal quality and final metal concentration in solution is addressed in Section 6.5.3.

6.5.2 Heterogeneous Crystallisation

If same-nature crystalline seed is provided during the first stages of a precipitation process at low supersaturation ($S < S_{cr, homo}$), growth will be favoured via heterogeneous secondary nucleation on the seed's surface. Many authors [16, 17, 18] present strong evidence that in the presence of solid phase (i.e. seed) the metastable zone becomes narrower, due to higher interfacial supersaturation near the surface of seeds as compared to the bulk of solution. With increasing crystal surface available, the decrease of the supersaturation is more pronounced; if enough equilibration time is allowed, the supersaturation should approach the solubility asymptotically.

If this strategy were to be repeated for a certain number of cycles, each test using as seed the product from the previous one, visible increase in particle size is to be

expected. The advantages of producing well-grown crystals are obvious: better filterability, faster settling rate, less amount of water/mother liquor retained, smaller uptake of impurities. Deliberate seeding is often employed in industrial crystallisation to maintain a control over the product size and size distribution.

The objective of this section is to perform comparative heterogeneous crystallisation tests at 20 and 40°C to produce large-sized gypsum crystals and then to monitor the growth process by assessing some product properties.

- **Comparative SDC Tests**

A typical test was conducted by adding the organic in small doses as to maintain $S < S_{\text{cr,homo}}$, according to the step-wise crystallisation path within the metastable zone previously determined for each temperature in Section 6.4 (procedure described in Section 6.2.2). The seed (15 g/L reagent-grade $\text{CaSO}_4 \cdot 2\text{H}_2\text{O}$) was added just prior to reaching $S_{\text{cr,homo}}$ (i.e. $O/A \sim 0.16$ at 21°C and $O/A \sim 0.19$ at 40°C). Since the O/A ratio at which seed is added was in the range $1 < S < S_{\text{cr,homo}}$, there was no risk of inducing homogeneous crystallisation nor of causing dissolution of the seed crystals; instead, secondary nucleation occurred, resulting in a sharp decrease in calcium sulphate in solution (Fig. 6.7).

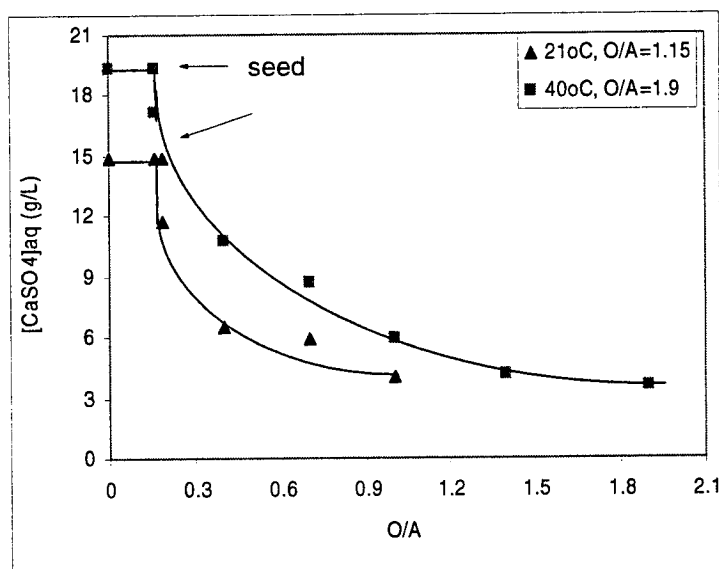


Figure 6.7 Heterogeneous crystallisation of gypsum at 21 and 40°C (15 g/L seed, low S , 3 M HCl)

A 30-min equilibration period was allowed after the seed addition step. The remaining 2-propanol was added in such a manner as to maintain a low supersaturation.

Final concentrations achieved in the aqueous phase were 4.02 g/L CaSO_4 at 21°C and 3.56 g/L at 40°C, comparable to those obtained in an un-seeded test under low supersaturation. This information suggests that the selected O/A interval for seed addition was correct. Lower O/A values would provoke seed dissolution whereas higher ratios would induce spontaneous precipitation.

- **Recycling Tests**

In a new series of tests the effect of product recycling on crystal growth under low supersaturation was studied. Following the initial seeding test, part of the product was used as seed for the following (corresponding to ~15 g/L seed); the number of product-recycling tests was arbitrarily chosen to be 8. All heterogeneous recycling tests were performed at 40°C, for $\text{O/A}_{\text{total}}=1.9$, following the procedure described in Section 6.2.2.

Table 6.3 indicates calcium sulphate concentration in solution at 40°C as a function of O/A and recycling run.

Table 6.3 Calcium sulphate concentration as a function of O/A and recycling run (40°C, low S, 15 g/L seed, 3 M HCl)

O/A	$[\text{CaSO}_4]_{\text{aq}}$ (g/L)			
	0.5	1.0	1.5	1.9
Recycling Run				
1	10.72	5.96	4.14	3.56
2	10.63	5.92	4.05	3.48
3	10.58	5.87	3.98	3.41
4	10.22	5.79	3.91	3.33
5	10.11	5.72	3.88	3.27
6	9.94	5.68	3.83	3.23
7	9.89	5.57	3.78	3.18
8	9.88	5.54	3.75	3.15

As observed, under identical conditions (in terms of temperature and O/A) similar concentration values are obtained for all 8 recycling runs; therefore, the effect of product recycling was monitored by those properties whose values are influenced by the growth process: crystal size and morphology, percent solids density, and settling velocity.

6.5.3 Data Analysis and Product Quality

- **Solution Composition**

- I. Crystallisation Strategy:

As depicted in Figure 6.8, for both temperature values under study, SDC tests performed in conditions of controlled, low supersaturation ($S < S_{cr,homo}$) resulted in lower calcium sulphate concentrations in solution than the similar tests at high supersaturation. The results were further improved when heterogeneous crystallisation tests were conducted, as the presence of seed surface can induce nucleation at degrees of supersaturation lower than those required for spontaneous nucleation.

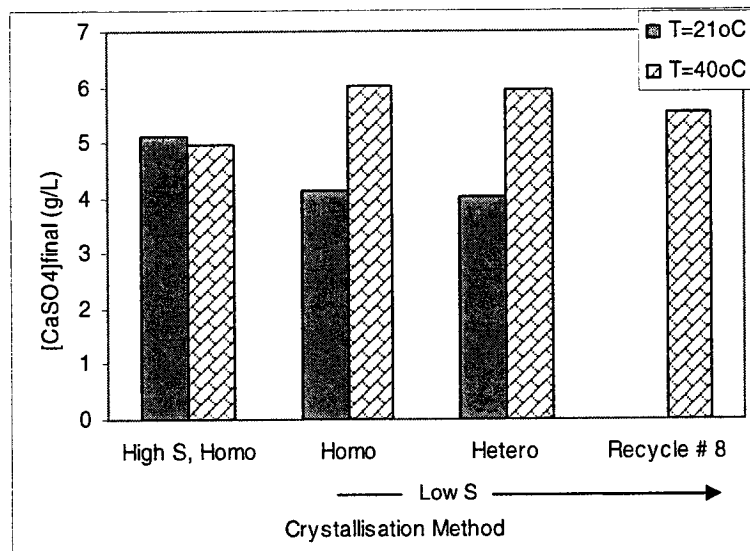


Figure 6.8 Influence of crystallisation method on residual sulphate (O/A = 1.15 in all cases except at High S and 40°C, when O/A = 1.91)

In conditions of high supersaturation, it was demonstrated [18] that nucleation already starts during the feeding period and an initial amorphous or poorly crystalline

precursor is built first. This explains slightly higher concentration values since amorphous or poorly crystalline products have usually higher solubility compared to the crystalline phases. At low S (homo/hetero), following a short duration homogeneous nucleation event that creates a relatively small number of embryos, most crystallisation takes place within the growth zone (“secondary nucleation”), avoiding the formation of colloidal particles.

In conditions of heterogeneous crystallisation, residual sulphate values reached ~ 4 g/L CaSO_4 at 21°C and ~ 6 g/L at 40°C for $\text{O/A} = 1.15$, comparable to required residual values in chloride leaching, as indicated by Dutrizac [4]. These numbers can be lowered even more if a higher O/A ratio is employed (see solubility data in Section 6.3).

II. Influence of Temperature:

As indicated by solubility data determined in Section 6.3, final calcium sulphate concentration in solution increases with temperature at constant organic and HCl content (Figures 6.2 and 6.8). Also, according to critical supersaturation values (Figure 6.4), SDC tests performed at more elevated temperatures require higher O/A ratios to initiate crystallisation; consequently, more 2-propanol is to be employed in order to reach similar final sulphate concentrations in solution at 40°C as compared to 21°C .

Elevated temperatures have a beneficial effect on crystallisation kinetics, as previously demonstrated (Section 5.6.2), translating in better incorporation of growth building blocks in the crystal lattice and hence lower final ion concentration in solution. Whereas at 40°C precipitation under high supersaturation conditions still leads to higher final calcium sulphate concentrations in solution, a controlled crystallisation under low S leads to a solid product with higher degree of crystallinity and consequently lower final metal values, closer to the equilibrium concentration.

• ***Solid Product Properties***

I. Effect of Supersaturation Magnitude and Temperature

The XRD spectra obtained for calcium sulphate products were matched to different standard spectra ($\text{CaSO}_4 \cdot x\text{H}_2\text{O}$, $x = 0, 0.5, 2$) contained in the computer's database to verify crystallinity and identify hydrate form.

Figure 6.9 gives the XRD pattern for the product obtained at 21 and 40°C (all samples produced via homogeneous crystallisation, low supersaturation). The sharp peaks indicated crystalline state; moreover, it was found that $\text{CaSO}_4\cdot 2\text{H}_2\text{O}$ (i.e. gypsum) offered the best match to the crystals produced. [23].

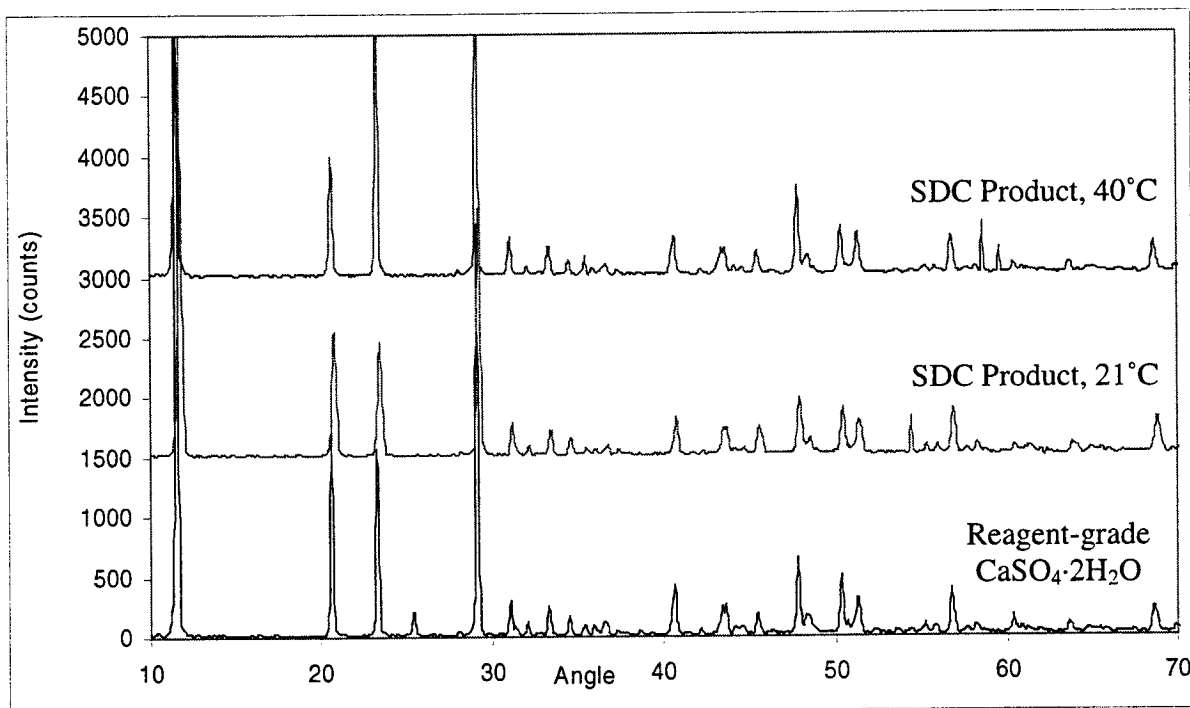


Figure 6.9 XRD spectra of $\text{CaSO}_4\cdot 2\text{H}_2\text{O}$ produced via homogeneous SDC under low supersaturation conditions at 21 and 40°C, compared to reagent-grade crystals

This is in perfect agreement with theoretical predictions [6, 19, 20, 21] that indicate gypsum to be the stable form at low and moderate temperatures (below $\sim 40^\circ\text{C}$, depending obviously on other parameters such as ionic strength hence water activity). Actually, even above 40°C gypsum is metastable and tends to form first (according to Stranski's rule, [22]), then converting to the stable anhydrite.

In order to evaluate the effect of supersaturation magnitude on the quality of the solid product, the general morphology and approximate size of the particles were established by performing Scanning Electron Microscopy (Figure 6.10).

SEM micrographs show distinct crystal morphology and size dependence on supersaturation magnitude.

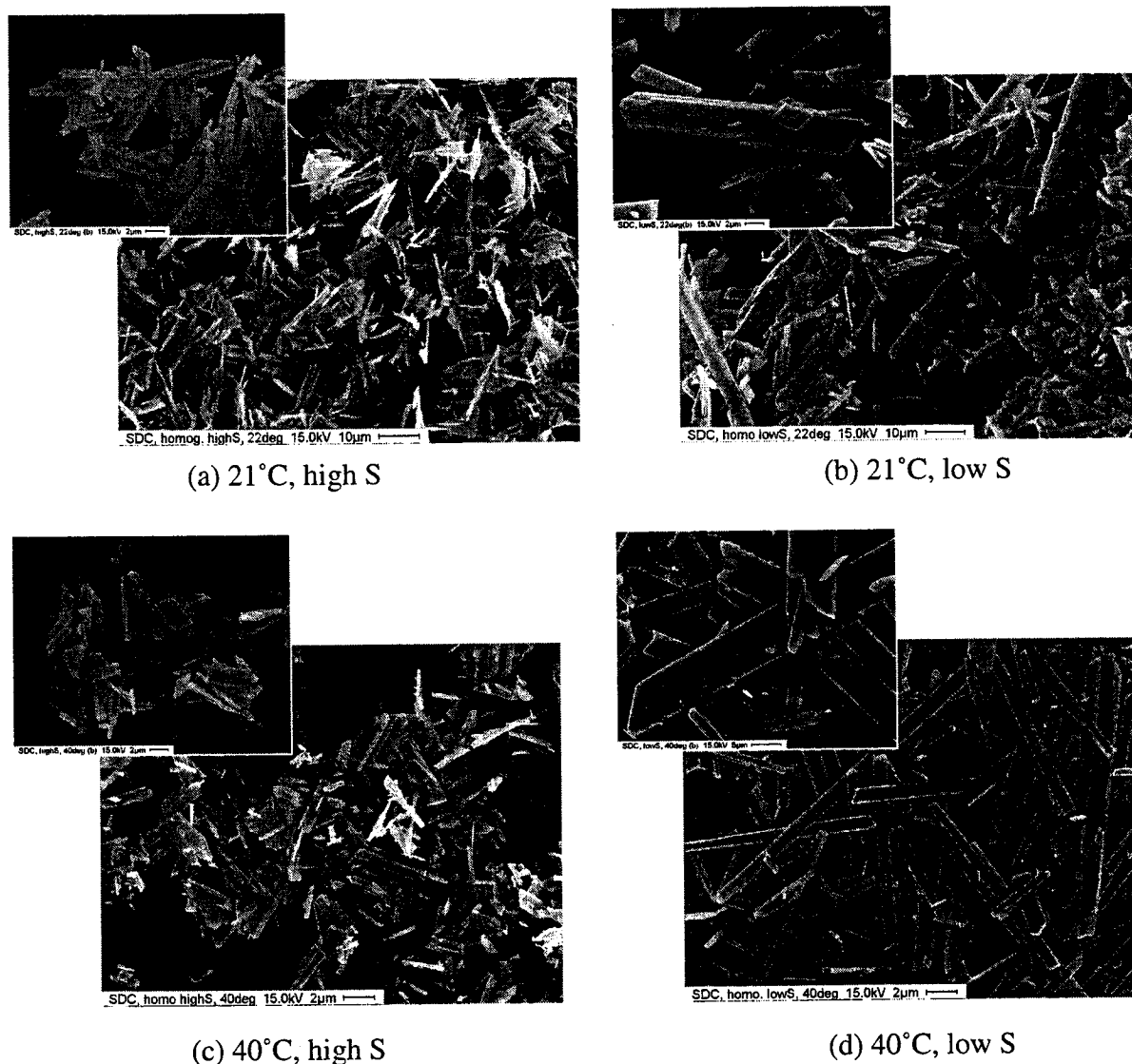


Figure 6.10 Influence of supersaturation magnitude and temperature on the quality of gypsum crystals produced via homogeneous SDC (3 M HCl)

Tests conducted at high supersaturation yielded fine, irregular crystals of $\sim 5\mu\text{m}$ average size for both temperatures, with tendency towards agglomeration (Figure 6.10 a, c). Tests conducted at low supersaturation, where the initial homogeneous generation of a smaller number of nuclei is followed by a heterogeneous growth process, show a certain increase in average particle size $> 20\mu\text{m}$ (Figure 5.21 b, d). Nielsen and Söhnel [24] indicated that at low supersaturation the nucleation is heterogeneous while at higher supersaturation it becomes homogeneous. At high supersaturation, when the number of available growth sites is not sufficient to accommodate the calcium sulphate to be deposited, additional

spontaneous nucleation occurs, fact demonstrated by the surface roughening and the presence of small crystallites, clearly stemmed from bulk nucleation. At low supersaturation, following initial nucleation, no new bulk growth sites are formed and crystallisation occurs mainly on the surface of the existing crystals.

SEM images presented in Figure 6.10 indicate a net beneficial effect of temperature on crystal morphology, especially at low supersaturation. Slightly agglomerated particles obtained at 20°C tend to grow and become better defined individually at 40°C , since the combined effect of low supersaturation and more elevated temperatures greatly favours both the growth process and the morphology.

The influence of temperature on crystal properties can be explained by understanding the beneficial effect that the elevation of temperature has on a variety of processes: (i) dehydration of ions is favoured; (ii) surface diffusion-mobility of the adsorbed solute is enhanced; (iii) the incorporation of the solute into crystal (i.e. crystallisation rate) is accelerated.

Huitema and van der Eerden [25] observed that during crystal growth, the interface is the most defect-rich region since defects form at the surface first. They studied the competition between the generation of defects at the growing surface and partial "healing" in a wider interface region and assumed that the driving force for healing is the reduction of the excess free energy of the defect and the essential kinetic parameter was the defect mobility, both factors favoured by elevated temperatures. Hence, crystals produced at higher temperatures tend to have a smoother surface and a more regular morphology.

With increasing temperature, the crystals exhibit a smoother appearance, as the shape tends to become closer to the specific acicular morphology of $\text{CaSO}_4\cdot 2\text{H}_2\text{O}$, defined by Cole and Lancucki [26] as monoclinic prismatic. Rinaudo *et al.* [27] observe that the crystals precipitated from solutions are needles elongated along the [111] face and, due to high growth rate along this direction, are terminated by vicinal faces, which do not agree with the theoretical gypsum habit.

Theoretical models for gypsum predict large [011] faces and small [111] faces, whereas the observed growth habit shows exactly the opposite [28]. This was qualitatively explained by van der Voort and Hartman [29] in terms of water absorption

on growing faces and it is argued that hydrated surfaces behave differently in the growth process. Two kinds of water molecules can be present on the faces. One kind is part of the lattice structure (as crystallisation water) and does not have to be removed before the growth can continue; this is the case for [011] face, which consequently grows faster. The other kind is hydration water, which does not belong to the crystal structure and has to be removed, lowering thus the growth rate, which is the case for [111].

II. Heterogeneous Crystallisation

The previous section demonstrated that homogeneous crystallisation under controlled (low) supersaturation conditions has beneficial effects on crystal quality and residual sulphate in solution. By providing 15 g/L gypsum seed at 21 and 40°C during the first stages of precipitation process (for $S < S_{cr, \text{homo}}$), additional growth is expected to be favoured via heterogeneous secondary nucleation on the seed's surface (Figure 6.11).

Heterogeneous crystallisation favoured growth at both temperatures; this effect is visible by comparing the appearance of the reagent-grade gypsum seed (Figure 6.11 a, irregular particles, most probably due to initial manufacturing procedures which involve grinding) to the final products of the heterogeneous SDC tests (Figure 6.11 b and c), which tend towards the predicted elongated gypsum morphology in aqueous solutions via a partial dissolution-crystallisation-growth process [30].



(a) $\text{CaSO}_4 \cdot 2\text{H}_2\text{O}$ seed

(b) SDC @ 21°C on seed

(c) SDC @ 40°C on seed

Figure 6.11 Gypsum crystals produced via heterogeneous SDC (15 g/L seed, 3 M HCl)

III. Product Recycling

Following the initial seeding experiment, part of the product was used as seed for subsequent tests (corresponding to ~ 15 g/L seed); the number of product-recycling runs was arbitrarily chosen to be 8. All recycling tests were performed at 40°C , for $O/A_{\text{total}}=1.9$, according to the procedure described in Section 6.2.2 (Figure 6.12).



(a) $\text{CaSO}_4 \cdot 2\text{H}_2\text{O}$ seed



(b) SDC product on seed



(c) 2nd recycle



(d) 4th recycle



(e) 6th recycle



(f) 8th recycle

Figure 6.12 Effect of product recycling on gypsum crystal quality (3 M HCl, 40°C , 15 g/L seed, low S, $O/A_{\text{total}}=1.9$)

As expected, increased extent of recycling leads indeed to significant growth, producing elongated particles, with smooth, defect-free surfaces. From a relative irregular morphology and average size of $\sim 50\ \mu\text{m}$ after the first seeding test (Figure 6.12 b), gypsum crystals become elongated needles of $\sim 200\ \mu\text{m}$ after the 4th recycle and $> 500\ \mu\text{m}$ after the 8th (Figure 6.12 d and f).

Since the growth process is predicted to proceed unhindered along the [111] face [27], the amount of recycling should be reduced to 4 or 5 runs (this would avoid unnecessary reagent consumption as well), due to the fact that extremely elongated crystals do not exhibit good filterability and packing properties.

It is remarkable that significant crystal erosion and fragmentation did not occur, despite increased size and slurry density that would lead to breakage by crystal-crystal, crystal-reactor or crystal-impeller collisions. This fact, completely opposite to the trend observed for $\text{NiSO}_4\cdot 6\text{H}_2\text{O}$ crystals (Sections 5.6.3 and 5.6.4), indicates that gypsum crystals are stronger, withstanding collisions at higher agitation rates (400 rpm vs. 200 rpm for nickel sulphate).

IV. Settling Velocity

As the settling velocity is a function of solids content and not a definitive indication of increased particle size, the results were not used to evaluate the precipitation for each run. However, for equivalent solids loading, the settling velocities are considered as a semi-quantitative means to evaluate crystal growth (i.e. high settling velocity = large particles).

As expected, low supersaturation and use of seed (heterogeneous crystallisation) were found to favour growth at both temperatures under study, fact assessed by the marked increase in settling velocities for the heterogeneous SDC tests (Figure 6.13). It can be noticed that elevated temperatures have a beneficial effect on particle growth, resulting in systematic higher settling velocities, in accordance with Figure 6.10.

When the effect of recycling is assessed (Figure 6.14), it is observed that heterogeneous crystallisation generates crystals that have superior settling velocity. The same results show that product recycling does not result in lower values of these properties, indicating that no fragmentation of crystals is noticed, again consistent with the SEM micrographs of Figure 6.12.

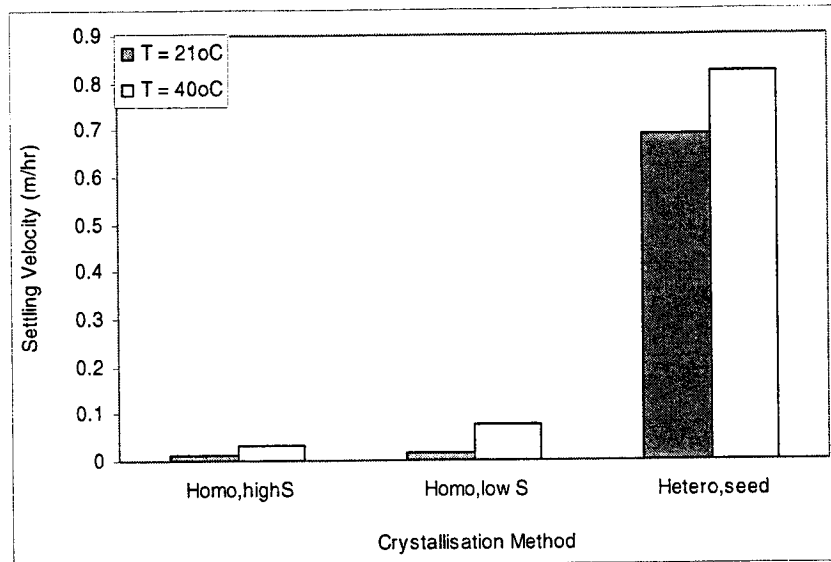


Figure 6.13 Influence of crystallisation strategy on gypsum settling velocity

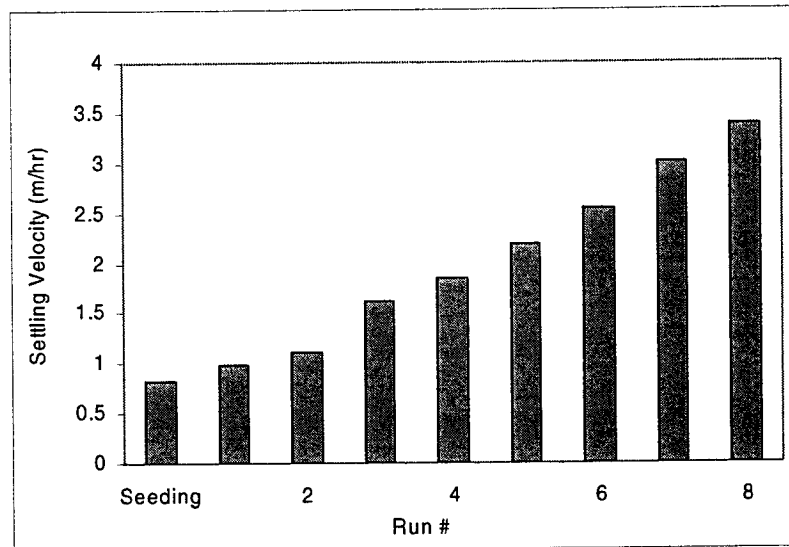


Figure 6.14 Influence of recycling on gypsum settling velocity (40°C)

V. Solids Density

The solids density (S.D.) represents another semi-quantitative measure of the growth process. Large crystals have a smaller specific surface area hence retain less water from solution. Therefore, higher solids density indicates larger particles.

The increasing trend in S.D. values proves the growth process, enhanced by the use of seed under low supersaturation conditions (Figure 6.15). Again, it can be noticed

that elevated temperatures have a beneficial effect on particle growth, resulting in systematic higher S.D., in accordance with crystal size indicated in Figure 6.10.

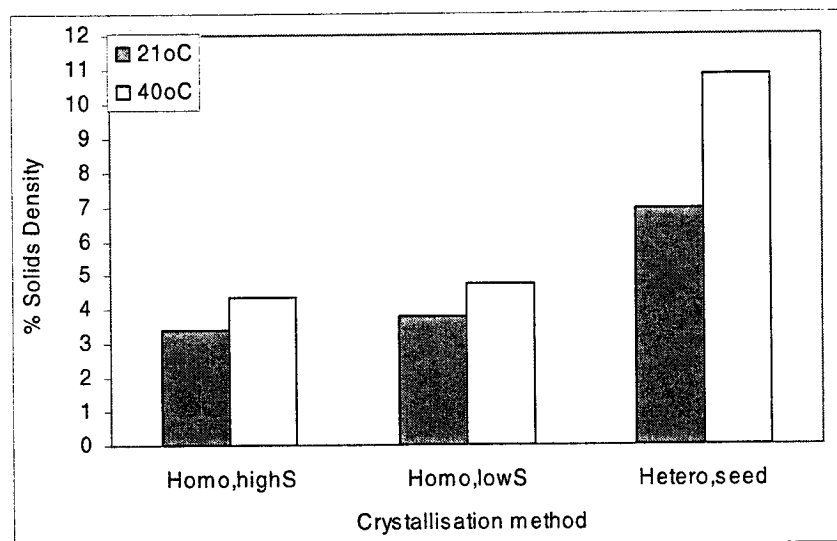


Figure 6.15 Influence of crystallisation strategy on gypsum solids density

When the effect of recycling is assessed (Figure 6.16), the information offered by the chart below is again consistent to the information given by the SEM images: heterogeneous crystallisation and product recycling strategies generate crystals that have superior solids content (i.e. larger size). The same results show that extensive product recycling does not result in lower S.D. values, indicating thus no apparent fragmentation of crystals, as noticed with the SEM images.

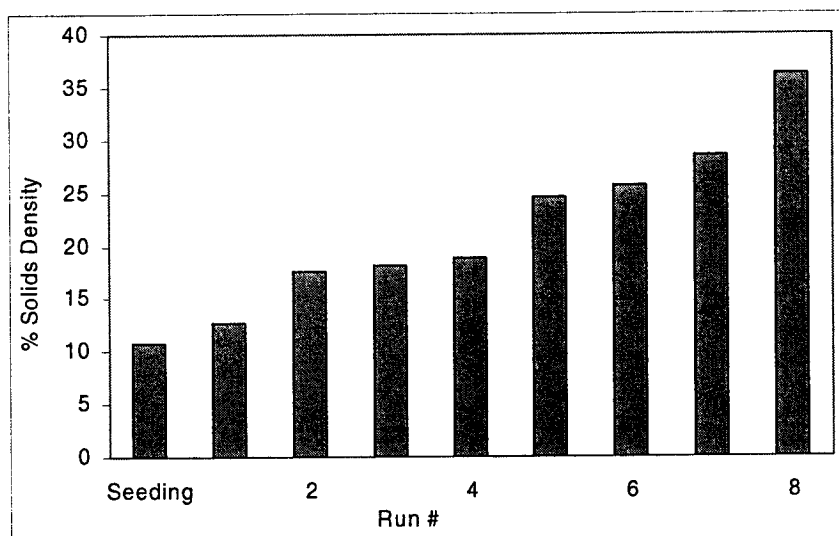


Figure 6.16 Influence of recycling on gypsum solids density (40°C)

VI. Nature of Solid Phase

Calcium sulphate, one of the most abundant sulphate minerals found in natural environment and a frequent by-product of numerous hydrometallurgical processes, exists in three main crystal phases: dihydrate, also known as gypsum ($\text{CaSO}_4 \cdot 2\text{H}_2\text{O}$, DH), hemihydrate ($\text{CaSO}_4 \cdot 1/2\text{H}_2\text{O}$, HH) and anhydrate (CaSO_4 , AH). The thermodynamic stability of these phases is a function of temperature and water activity. Therefore, metastable and stable phases can occur separately, successively or simultaneously, depending on conditions and the kinetics of the crystallisation process (Figure 6.17, [23]). It is known that the equilibrium transition temperatures are lowered by the addition of components that may decrease water activity by activating and deactivating water molecules during the phase changes, such as HCl , H_2SO_4 , Na_2SO_4 and alkaline ions (Ba^{2+}) [31].

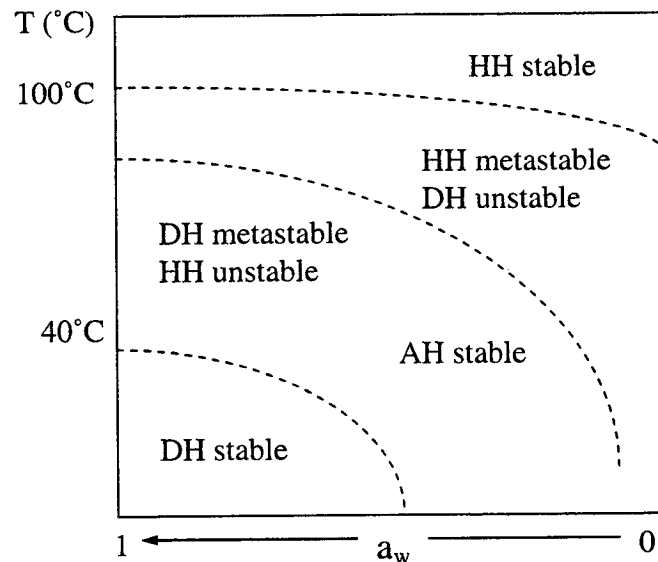


Figure 6.17 The $\text{CaSO}_4\text{-H}_2\text{O-HCl}$ phase diagram [adapted after 23]

As previously described in Sections 2.3.3 and 4.2.3, water activity in a crystallisation medium can be modified, besides other means, by changing the composition of solution via addition of organic solvents (most often low-molecular alcohols), which influence both the mole fraction and partial pressure of water [12, 13, 14]. More related to the present research work, it was demonstrated that 2-propanol addition to aqueous solutions cause the water activity to decrease from 1 in the absence of 2-propanol to 0.2 for an organic mole fraction of 0.9 [12].

Based on these findings, it was interesting to investigate whether the presence of a high 2-propanol-to-aqueous ratio of 2 at 40°C , together with a high concentration of HCl (3 M) would cause a sufficient decrease in water activity as to lower the transition line and modify the nature of the solid phase separated during SDC.

The solid product obtained via homogeneous SDC at 40°C and the product of the 8th recycling test (40°C) were analysed by XRD and the results compared to different standard spectra ($\text{CaSO}_4 \cdot x\text{H}_2\text{O}$ $x=0, 0.5, 2$) contained in the computer's database to identify hydrate form (Figure 6.18).

It was determined that $\text{CaSO}_4 \cdot 2\text{H}_2\text{O}$ (i.e. gypsum) offered the best match to the crystals produced. No other phases were detected when working at 40°C , even for high O/A ratios. It must be mentioned, nevertheless, that the overall reaction time for SDC was 120 minutes, with no additional crystal equilibration period at the end. It may be possible that, preserving the same medium composition, prolonged equilibration at 40 or 60°C to cause partial or total phase transformation, from DH to HH to AH.

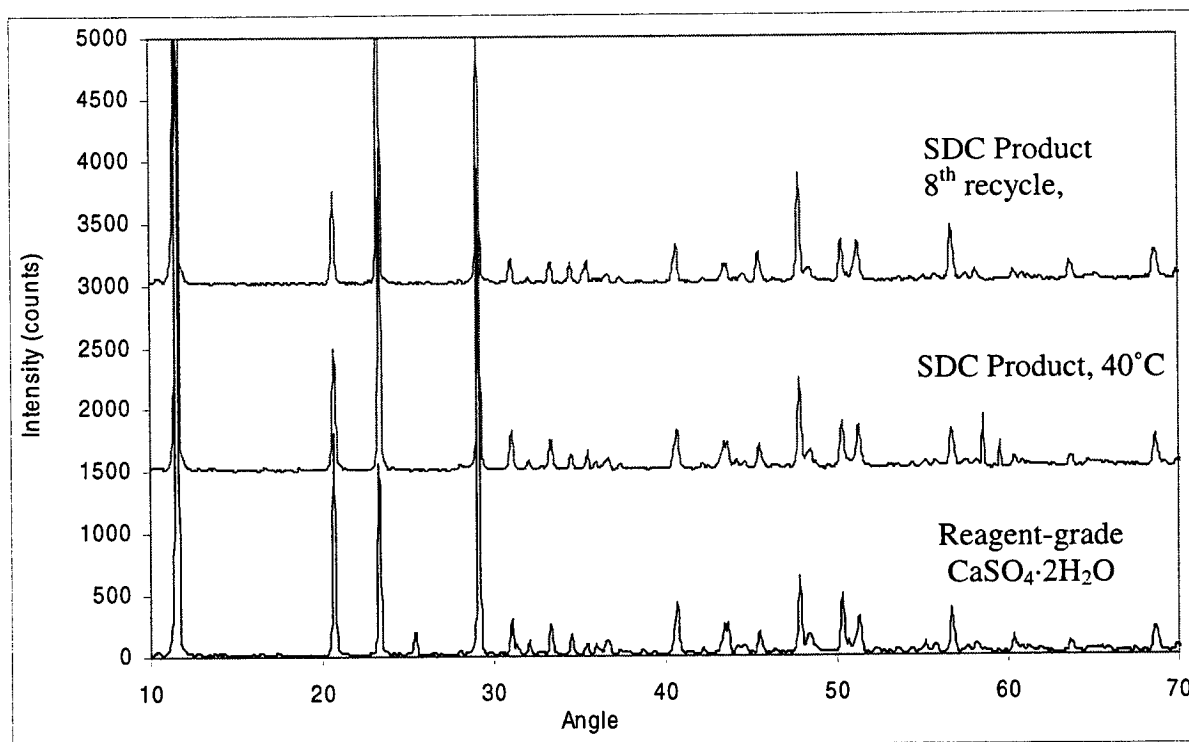


Figure 6.18 XRD spectra of $\text{CaSO}_4 \cdot x\text{H}_2\text{O}$ produced via SDC ($\text{O/A}_{\text{total}} \sim 2$, 40°C , 3 M HCl)

6.5.4 Integration of Gypsum Production via SDC with HCl Regeneration Process

As previously described, a parallel research project conducted at the Hydrometallurgy Laboratory (McGill) is seeking the development of an alternative low cost HCl regeneration process to be applied to chloride hydrometallurgy. The concept is to treat spent CaCl_2 leach liquors (generated by neutralisation with lime of metal chloride leach solutions) with concentrated H_2SO_4 in the temperature range 20-100°C to produce HCl and precipitate saleable-quality calcium sulphate products; but some residual soluble CaSO_4 fraction always remains in the reacted solution.

Solvent Displacement Crystallisation has the potential of providing an effective residual sulphate removal technique from such media, by removing calcium sulphate as gypsum. The integration of SDC technique into the actual HCl regeneration flowsheet would comprise (Figure 6.19):

- (1) Controlled addition of 2-propanol to the $\text{CaSO}_{4(\text{aq})}$ -HCl solution after HCl regeneration and gypsum precipitation via H_2SO_4 treatment;
- (2) Separation of gypsum by filtration and recycling of the HCl rich mother liquor;
- (3) Recovery of organic by low-temperature or vacuum distillation and recycling/reuse.

The use of 2-propanol in this system may be prohibited if its distillation is not selective against HCl (i.e. if there is the risk of HCl loss by vapour entrainment). However, vapour pressure data for HCl and 2-propanol in aqueous solutions [32, 33] indicate there is not such an impediment: at 80°C (distillation temperature for 2-propanol-water azeotrope), the organic partial pressure is 692 mmHg as compared to 0.73 mmHg for 3 M HCl, i.e. no hydrochloric acid is expected to be carried-over.

Depending on the working temperature and initial calcium sulphate concentration in solution, an appropriate organic-to-aqueous ratio can be selected (based on solubility data determined in Section 6.3) as to efficiently decrease sulphate concentration to acceptable levels. Moreover, if proper control of supersaturation and use of seed are employed, good quality gypsum crystals are produced.

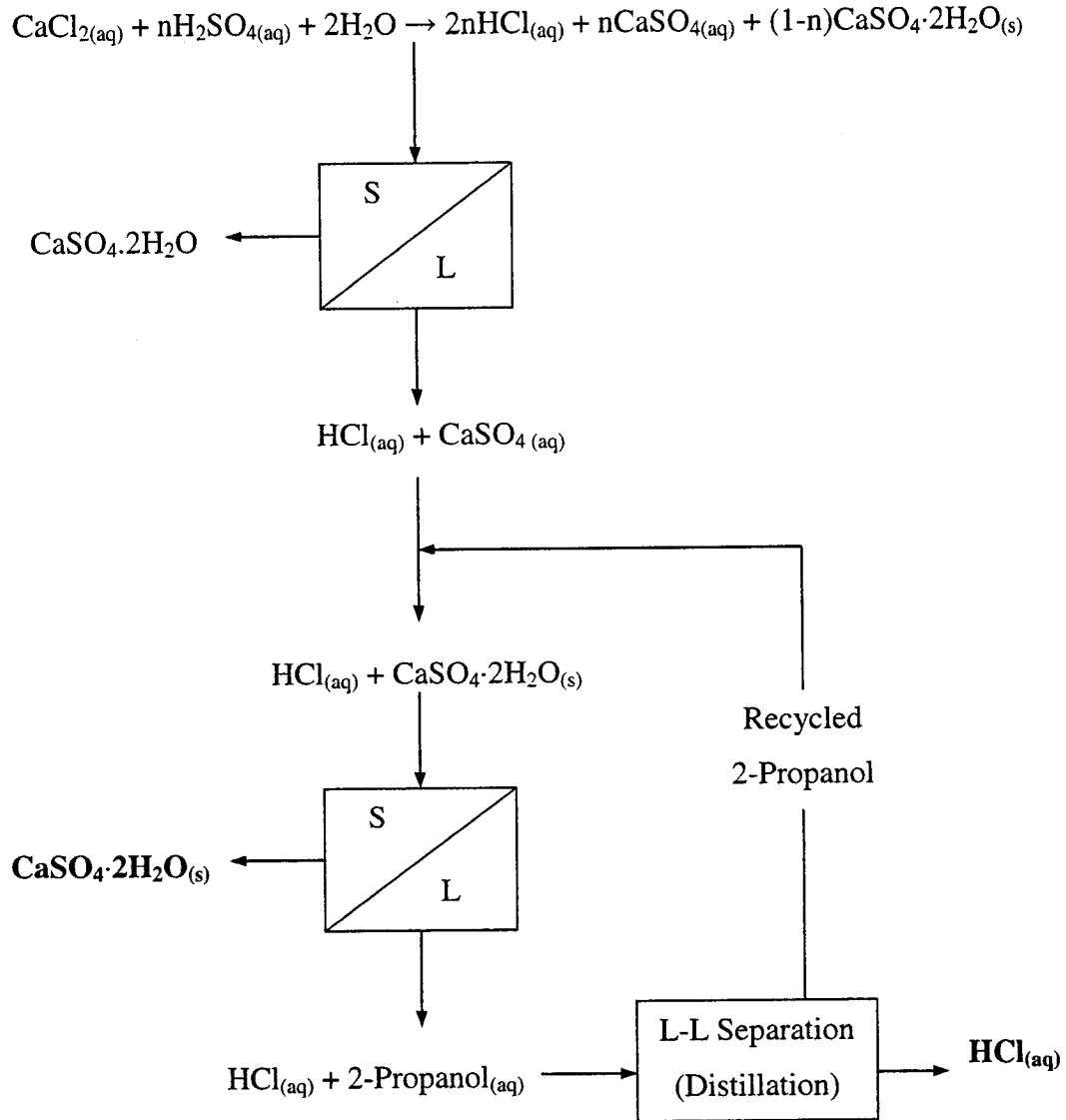


Figure 6.19 Integration of gypsum production via SDC with HCl regeneration

6.6 Summary and Conclusions

1. The present work confirmed that saleable calcium sulphate can be removed as gypsum ($\text{CaSO}_4 \cdot 2\text{H}_2\text{O}$) from HCl media by using 2-propanol. Consequently, SDC has the potential of providing an alternative residual sulphate removal technique.
2. The solubility of $\text{CaSO}_4 \cdot 2\text{H}_2\text{O}$ in 3 M HCl aqueous solutions as a function of 2-propanol content and temperature was established. The final sulphate content decreased with increasing organic fraction and with decreasing temperature.

3. The metastable zone width, an important parameter in designing controlled-crystallisation tests, has been determined at 21 and 40°C. It was found that the metastable zone width decreases with increasing alcohol concentration and temperature.
4. The crystal size, settling velocity and percent solids density of the solid product were found to depend on the method of crystallisation. High supersaturation (homogeneous crystallisation) leads to fine crystal product while low supersaturation and seeding/product recycling were found to promote growth, producing particles with improved physical properties. Additionally, temperature greatly favoured both the growth process and the crystal morphology, which tends more towards the specific elongated acicular shape.
5. Product recycling favours crystal growth with no signs of fragmentation seen.
6. DH was the only phase produced when performing SDC at 21 and 40°C in the presence of 2-propanol (3 M HCl solutions, ~120 min total reaction time).
7. A flowsheet for the integration of SDC technique into the actual HCl regeneration process was proposed. The use of 2-propanol in this system may be prohibited if its distillation is not selective against HCl (i.e. if there is the risk of HCl loss by vapour entrainment). However, vapour pressure data for HCl and 2-propanol indicate there is not such an impediment.

References

- [1]. S. Girgin and G.P. Demopoulos, "Production of the High Value Material, Alpha- CaSO_4 Hemihydrate Out of Spent CaCl_2 Solutions by Reaction with H_2SO_4 ", in *EPD Congress 2004*, (edited by M.E. Schlesinger), TMS, Warrendale, Pa., pp.627-640, (2004).
- [2]. A. Al-Othman, T. Cheng and G.P. Demopoulos, "Regeneration of HCl and Production of Saleable Gypsum by Reaction of Spent CaCl_2 Leach Solutions and H_2SO_4 " in *Wastes Processing and Recycling in Mineral and Metallurgical*

- Industries V*", (edited by S.R. Rao *et al.*), CIM, Montreal, Canada, pp. 453-468, (2004).
- [3]. Z. Li and G.P. Demopoulos, "Calcium Sulphate Solubilities in Concentrated Aqueous Chloride Solutions" in *Chloride Metallurgy 2002*, vol. II, (edited by E. Peek and G. Van Weert), CIM, Montreal, Canada, pp. 561-574, (2002).
- [4]. J.E. Dutrizac, "Sulphate control in chloride leaching processes" *Hydrometallurgy*, **23**, pp. 1-22, (1989).
- [5]. G.A. Moldoveanu, *Precipitation of Nickel Sulphate from Decopperised Acid Solution by Solvent Displacement Crystallisation*, M.Eng. Thesis, McGill University, Montreal, PQ, Canada, (1999).
- [6]. W.F. Linke and A. Seidell (editors), *Solubilities of Inorganic and Metal-Organic Compounds (a compilation)* 4th edition, Van Nostrand, Princeton, N.J., (1958).
- [7]. R.K. Gupta, "Solubility of calcium sulphate dehydrate in hydrochloric acid solutions" *J. Applied Chem.*, **18**, pp. 49-51, (1968).
- [8]. J.F. Adams and V.G. Papangelakis, "Understanding gypsum crystallisation fouling in sulphuric acid neutralisation reactions" in 7th *International Science and Technology Conference on Gypsum and Fly Ash*, pp. 4.2-4.12, Toronto, Canada, (June 2002).
- [9]. H. Majima and Y. Awakura, "Water and solute activities in the solution systems $\text{H}_2\text{SO}_4\text{-CuSO}_4\text{-H}_2\text{O}$ and $\text{HCl-CuCl}_2\text{-H}_2\text{O}$ " *Metallurgical Transactions B*, **19B**, pp. 347-354, (1998).
- [10]. J.M. Prausnitz, R.N. Lichtenthaler and E.G. Azevedo, *Molecular Thermodynamics of Fluid-Phase Equilibria*, 2nd Edition, Prentice-Hall, Englewood Cliffs, N.Y., (1986).
- [11]. H.S. Na, S. Arnold and A.B. Myerson, "Water activity in supersaturated aqueous solutions of organic solutes" *Journal of Crystal Growth* **149**, pp. 229-235, (1995).

- [12]. V.V. Udovenko and T.F. Mazanko, "Liquid-vapour equilibrium in the propan-2-ol-water and propan-2-ol-benzene system" *Russian Journal of Physical Chemistry*, **41(7)**, pp. 863-866, (1967).
- [13]. H. Zhu, C. Yuen and D.J.W. Grant, "Influence of water activity in organic solvent + water mixtures on the nature of the crystallizing drug phase. I. Theophylline." *International Journal of Pharmaceutics*, **135**, pp. 151-160, (1996).
- [14]. H. Degn and N.-U. Frigaard, "Membrane inlet manometry for the measurement of water activity in aqueous and organic solutions" *Analytica Chimica Acta*, **274**, pp. 355-359, (1993).
- [15]. G.P. Demopoulos, "Aqueous Crystallisation and Precipitation – Production of Particulate Solids with Designed Properties" *Hydrometallurgy*, (2004), in press.
- [16]. J. Nyvlt, R. Rychly, J. Gottfried and J. Wurzelova, "Metastable Zone Width of Some Aqueous Solutions" *Journal of Crystal Growth*, **6**, pp. 151-162, (1970).
- [17]. C.Y. Tai and W-C. Chien, "Effects of operating variables on the induction period of $\text{CaCl}_2\text{-Na}_2\text{CO}_3$ system" *Journal of Crystal Growth*, **237-239**, pp. 2142-2147, (2002).
- [18]. J. Franke and A. Mersmann, "The influence of the operational conditions on the precipitation process" *Chemical Engineering Science*, **50(11)**, pp. 1737-1753, (1995).
- [19]. I.S. Sirota, S.V. Dorozhkin, M.V. Kruchinina and I.V. Melikhov, "Phase transformation and dehydration of calcium sulphate dehydrate in solution studied by SEM", *Scanning*, **14**, pp. 269-275, (1992).
- [20]. C. Solberg and S. Hansen, "Dissolution of $\text{CaSO}_4 \cdot 1/2\text{H}_2\text{O}$ and precipitation of $\text{CaSO}_4 \cdot 2\text{H}_2\text{O}$. A kinetic study by synchrotron X-ray powder diffraction" *Cement and Concrete Research*, **31**, pp. 641-646, (2001).

- [21]. J. Kontrek, D. Kralj and L. Brečević, "Transformation of anhydrous calcium sulphate into calcium sulphate dehydrate in aqueous solutions" *Journal of Crystal Growth*, **240**, pp. 203-211, (2002).
- [22]. M.E. Blesa and E. Matijević, "Phase transformation in aqueous media" *Adv. Coll. Interf. Sci.*, **29**, pp. 173-231, (1989).
- [23]. M. El Moussaouiti, R. Boistelle, A. Bouhaouss and J.P. Klein, "Crystallisation of calcium sulphate hemihydrate in concentrated phosphoric acid solutions" *Chemical Engineering Journal*, **68**, pp.123-130, (1997).
- [24]. A.E. Nielsen and O. Söhnel, "Interfacial tensions electrolyte-aqueous solution, from nucleation data" *Journal of Crystal Growth*, **11**, pp. 233-242, (1971).
- [25]. E. Huitema and J.P. van der Eerden, "Defect formation during crystal growth" *Journal of Crystal Growth*, **166**, pp. 141-145, (1996).
- [26]. W.F. Cole and C.J. Lancucki, "A refinement of the crystal structure of gypsum" *Acta Crystall.*, **B30**, pp. 921-929, (1974).
- [27]. C. Rinaudo, M.C. Robert and F. Lefauchaux, "Growth and characterisation of gypsum crystals" *Journal of Crystal Growth*, **71**, pp. 803-806, (1985).
- [28]. W.M. Heijnen and P. Hartman, "Structural morphology of gypsum ($\text{CaSO}_4 \cdot 2\text{H}_2\text{O}$), brushite ($\text{CaHPO}_4 \cdot 2\text{H}_2\text{O}$) and pharmacolite ($\text{CaHAsO}_4 \cdot 2\text{H}_2\text{O}$)" *Journal of Crystal Growth*, **108**, pp. 290-300, (1991).
- [29]. E. van der Voort and P. Hartman, "The habit of gypsum and solvent interaction" *Journal of Crystal Growth*, **112**, pp. 445-450, (1991).
- [30]. G.H. Nancollas, M.M. Reddy and F. Tsai, "Calcium sulphate dihydrate crystal growth in aqueous solution at elevated temperatures" *Journal of Crystal Growth*, **20**, pp. 125-134, (1973).

- [31]. P.S.R. Prasad, N. Ravikumar, A.S.R. Krishnamurthy and L.P. Sarma, "Role of impurities in gypsum-bassanite phase transition: a comparative Raman study" *Current Science*, **75(12)**, pp. 1410-1414, (1998).
- [32]. D.L. Lide (editor), *Handbook of Chemistry and Physics*, 72nd edition, CRC Press, pp. 2.76, (1992).
- [33]. E.W. Flick (Editor), *Industrial Solvents Handbook*, 3rd edition, Publications Noyes, Parkridge, N.J, p. 223, 1985.

Chapter 7. Precipitation of Zinc Oxide from NaOH Media

7.1 Introduction

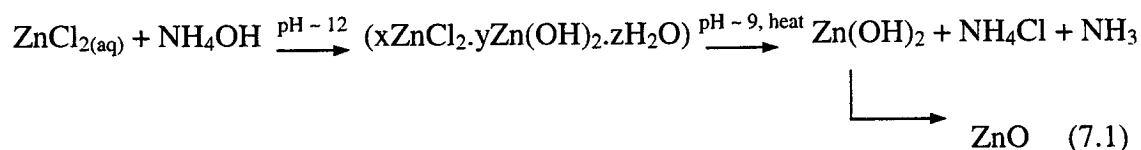
Zinc oxide (ZnO, zincite) is an important compound with various applications in metallurgical, electronic, chemical, pharmaceutical and ceramics industries [1, 2]; pyrometallurgical and hydrometallurgical processes are employed for producing zincite.

Pyrometallurgical techniques for ZnO production include roasting, plasma and flame reactor processes, which have high throughput rates but are extremely energy-intensive. Thus, Lin *et al.* [2] prepared ZnO powders by controlled O₂ and N₂ plasma pyrolysis of a Zn₅(CO₃)₂(OH)₆ precursor. Xia and Pickles [3] obtained ZnO by roasting EAF dust in the presence of NaOH at 350-450°C for 60-90 min; Li *et al.* [4] synthesised ZnO via oxidation-vapour deposition, by heating zinc dust and water at 900°C in a quartz tube for 60 min, under Ar flow. Similarly, Chen *et al.* [5] deposited nanocrystalline ZnO thin films on Si substrates by resistive thermal evaporation of metallic Zn under O₂ flow at 300°C for 2 hrs, followed by two-step annealing at 600-900°C.

Hydrometallurgical methods are more environmentally suitable and economically attractive to be employed in ZnO production, especially on small scale. They can be divided in two main classes:

(i) Acid Leach Processes:

Soluble zinc salts generated by acid leaching (mostly HCl-based) may be forced to hydrolyse upon temperature elevation or equilibration with base hence leading to zinc oxide production. The principle is to form a Zn-based hydroxy salt precursor that is unstable in hot aqueous solution (namely > 100°C) and upon equilibration/ageing decomposes to form Zn(OH)₂ which converts to ZnO. This is done by mixing an inorganic zinc salt (i.e. sulphate, nitrate, carbonate or chloride) with acetates, urea, sodium/potassium hydroxide or ammonia [6, 7], e.g.:



Thus, Nishizawa *et al.* [8] formed ZnO by decomposing a Zn-EDTA aqueous complex at 330°C for ~60 min. They assumed that, during decomposition, metallic zinc is formed by the rupture of bonds between carboxyl groups of EDTA and Zn, followed by rapid oxidation in the presence of water to form ZnO. Chittofrati and Matjevic [9] obtained ZnO dispersions by aging at 90-200°C for 2 hrs solutions of zinc nitrate in the presence of MOH (M=Na, K and NH₄OH) and related the different particle morphologies to the working conditions (i.e. temperature and type of base). Similarly, Sigoli *et al.* [10] produced ZnO by aging ZnCl₂ in urea (pH 5) at 90°C for various periods of time. Lu and Yeh [11] prepared ZnO starting from zinc nitrate and adopting NaOH and ammonia as the base source, at temperatures 100-200°C for 0.5 -2 hrs. More recently, Allen *et al.* [12], following work published by Van Weert and van Sandwijk [13] described a process that achieves precipitation of a zinc hydroxy-chloride salt which upon equilibration in slaked lime converts to zinc oxide of high purity. In other development, also by Noranda researchers [14], zinc oxide was produced by neutralisation of zinc sulphate solution with lime at ~90°C followed by a screening or flotation separation of the fine zinc oxide powder from the needle-shaped gypsum by-product.

(ii) Caustic Soda Leach Processes:

Another hydrometallurgical method widely employed is the use of a suitable lixiviant to dissolve the desired species; the leach solution thus obtained is purified using precipitation, ion exchange or solvent extraction while the salt of interest is produced from the purified solution by electrolysis or crystallisation. For zinc leaching, the lixiviant of choice is hot (95°C) caustic soda (6-12 M NaOH), due to its high selectivity towards Zn [15]. Upon caustic soda leaching (reaction 7.2), a soluble sodium zincate forms at pH > 12; the leach solution is then electrolysed to produce metal, regenerating NaOH, according to the reaction 7.3 [16]:



Caustic leaching of zinc leading to production of sodium zincate solutions is of particular interest to the recovery of zinc from EAF dusts. As alternative to electrowinning (reaction 7.3) the SDC production of zinc oxide from caustic sodium zincate solutions is investigated in this Chapter. In particular, the main objective of this

research is to evaluate if SDC (never tried before) is applicable to the system ZnO–NaOH–H₂O for the purpose of producing ZnO with simultaneous regeneration of the lixiviant (NaOH), this application relating to the caustic leaching of EAF dust [17].

7.2 Experimental

7.2.1 Research Strategy

The experiments conducted for the present research work consisted of two parts: (i) in order to gain a basic understanding of the crystallisation of zinc oxide from NaOH media with alcohols and establish a “reference” behaviour, solubility measurements have been conducted as a function of various factors; (ii) based on these results, critical supersaturation determinations and crystallisation tests have been developed to further investigate the evolution of the system. In all these experiments, both changes in solution composition (Zn(II) and NaOH concentrations) and product quality were monitored. The key parameters studied and a description of research goals are enumerated in Table 7.1.

Table 7.1 Parameters considered in crystallisation of zinc oxide with methanol

Parameter	Evaluated Aspect
Sodium Hydroxide	<ul style="list-style-type: none"> Equilibrium metal concentration in aqueous as a function of NaOH (0, 1, 2, 4, 6, 7 and 8 M NaOH). NaOH regeneration following SDC.
Organic Fraction (expressed as O/A) and Temperature	<ul style="list-style-type: none"> Equilibrium metal concentration in 6 M NaOH as a function of organic (O/A=0, 0.25, 0.43, 0.66, 1, 1.5, 2.33) and temperature (21 and 60°C).
Supersaturation (S)	<ul style="list-style-type: none"> Critical supersaturation line at 21°C.
Crystallisation Regime	<ul style="list-style-type: none"> Homogeneous vs. Heterogeneous: Influence on metal content in solution and crystal quality.

All solubility and critical supersaturation tests were performed in 250 mL conical flasks, using magnetic stirring, as described in Chapter 3 (Section 3.3.1., Figure 3.1).

Crystallisation tests were conducted using the 1 L batch reactor, mechanical stirring and set-up presented in Section 3.3.1., Figure 3.2.

7.2.2 Experimental Procedure

De-ionised water, reagent-grade zinc oxide (ZnO, 99.3% purity) and sodium hydroxide (NaOH, 98% purity) were used to prepare the aqueous solutions; methanol Optima-grade (99.9% purity) was employed.

The measurement of NaOH concentration was done by direct simple acid-base titration using standard 1 N HCl solution. To ensure reproducibility and improve the error margin, each titration experiment was repeated thrice and the average was considered (error < 1.6%). The titration procedure employed 10 mL aliquot diluted with 50 mL de-ionised water. A concentration of 6-7 M NaOH was selected to be employed throughout the experiments, as a representative value for caustic digestion in EAF dust treatment processes [17].

- ***Solubility Measurements***

- *Influence of sodium hydroxide:*

- 100 mL aqueous solution containing 0, 1, 2, 4, 6, 7 and 8 M NaOH were agitated at 21°C in 250 mL Erlenmeyer flasks and small amounts of ZnO were added. When crystals in equilibrium with solution were detected (i.e. no more dissolution), oxide's addition stopped and the system was allowed to equilibrate for 54 hours (to study dissolution kinetics). Subsequently, the crystals were separated by filtration and the mother liquor was diluted with 10 times with 1 M NaOH first, then 1 N HCl (if further dilution necessary) and analysed for zinc content.

- *Influence of organic content:*

- 100 mL of aqueous-organic mixtures were prepared starting from 6 M NaOH solutions and methanol, with the following organic-to-aqueous ratio (O/A): 0, 0.25, 0.43, 0.66, 1.00, 1.50 and 2.33. Small amounts of ZnO crystals were added under stirring at 21°C; when crystals in equilibrium with solution were detected (i.e. no more dissolution), oxide's addition stopped and the system was allowed to equilibrate for 48 hours (to study

dissolution kinetics). Subsequently, the crystals were separated by filtration and the mother liquor was diluted as previously described and analysed for zinc. Same procedure was repeated for 60°C.

- ***Determination of Critical Supersaturation***

100 mL solutions containing different amounts of Zn and 6 M NaOH were agitated at 21°C with a magnetic stirrer in Erlenmeyer flasks. Small volumes of organic were slowly added to the aqueous solutions by the means of a manual burette; after each addition, a 15-minutes equilibration period was allowed. At the moment a “cloud” was seen (initiation of the homogeneous crystallisation process), the volume of organic solvent that induced crystallisation was recorded and the solutions were stirred for 24 hours, to reach equilibrium. Subsequently, the crystals were separated by filtration and the mother liquor was diluted with NaOH and HCl and analysed for zinc.

- ***Solvent Displacement Crystallisation Tests***

General SDC Test: In a general SDC test (approximate duration 240 min), 100 mL aqueous solution containing ~ 1 M Zn and 7.5 M NaOH were agitated (400 rpm) at 21°C in 1 L glass reactor while the organic was added from a 100 mL manual burette in increments of 0.2 O/A ($O/A_{\text{total}} = 4$), followed by 20-minutes equilibration period. After each addition/stirring period solution samples were taken every 0.4 O/A, diluted and analysed for zinc. Subsequently, the crystals were separated by filtration, the solid phase was washed with distilled water to displace NaOH and then with MeOH to accelerate the drying process, dried at ambient temperature in the fume-hood and further analysed. The mother liquor was diluted with 1 M NaOH and 1 N HCl and analysed for zinc via ICP.

Homogeneous Crystallisation, High Supersaturation: To homogeneously precipitate the inorganic salt, the organic solvent was added at once to the aqueous phase (40 g/L Zn, 6 M NaOH) with a total O/A ratio of 1.5 ($S > S_{\text{cr,homo}} \sim 8$). The mixture was agitated for 240 minutes and samples were taken every 2, 5, 10, 15, 30 minutes, then every 30 minutes, in order to monitor cation content and hence the kinetics of the process. Solution samples were diluted and analysed for zinc. Subsequently, the crystals were

separated by filtration, washed, dried at ambient temperature in the fume-hood and further analysed.

Heterogeneous Crystallisation: Same test was repeated by adding ~47 g/L ZnO, corresponding to 20 g/L Zn seed material (Fisher Scientific, 99.3 % purity) to the initial solution containing a certain volume of solvent corresponding to a supersaturation below the critical value, $S_{cr,homo} \sim 8$ ($O/A = 1.3$).

7.3 Selection of Organic Solvent

Since ZnO-NaOH-H₂O is a different system from the sulphate salts in acidic media studied before, the first step in investigation was to find a suitable water-miscible organic solvent capable to precipitate ZnO.

The suitability of different organic solvents to perform SDC was tested as follows: 10 mL aqueous solution containing ~ 62 g/L Zn and ~ 300 g/L NaOH were agitated at 21°C in conical 125 mL flasks with rubber stoppers while the organic solvent was added in ratios of 10 mL at a time (i.e. $O/A = 1$, for a total $O/A = 6$); after each addition, a 15 – minutes equilibration period was allowed and the observations recorded. To ensure the attainment of equilibrium, solutions were agitated for ~ 48 hours.

Based on the knowledge accumulated in the present research (i.e. good properties and successful application to several sulphate salt systems, see Chapters 4, 5 and 6), 2-propanol was the first choice of solvent to be employed in separating ZnO from NaOH solutions. Despite the fact that 2-propanol is supposed to be total miscible with water in any proportion, phase splitting occurred upon the addition of alcohol (aqueous at the bottom), similar to solvent extraction. All 2-propanol accumulated exclusively in the upper layer with no water extraction. Even after ~ 48 hrs of vigorous agitation, still no salt precipitation or phase homogenisation was observed.

Acetone and methyl-ethyl-ketone (MEK) exhibited similar behaviour; moreover, these solvents would not be acceptable for large-scale use due to their high volatility.

Literature data describes similar phase separation behaviour of some water-miscible organic solvents in aqueous solutions of alkaline or earth salts. Zhigang *et al.* [18] reported that addition of NaCl, KCl, Na₂CO₃ and K₂CO₃ induced phase splitting in

2-propanol-water mixtures, and the two-phase region increased with increasing salt concentration, pH and decreasing temperature. They tried to empirically explain this in terms of different interactions between different inorganic salt molecules and the water molecules in solution. Stronger interactions between salt molecules and water resulted in more destruction of the 2-propanol-water structure that forms via hydrogen bonds in the absence of salt. Wu *et al.* [19] suggested that phase separation in a ternary mixture (i.e. salt-water-miscible organic) is favoured by large differences in affinities of salt ions to water and the organic component and strong self-aggregation tendency of the organic component, which becomes thus more hydrophobic, exhibiting weaker interactions with water. The larger the organic molecule, the higher the self-aggregation tendency and separation (i.e. the hydrophobic character), as note Lu *et al.* [20] for the tert-butanol-H₂O-K₂CO₃ system.

Based on this information, a water-miscible organic solvent with smaller molecule was investigated and tested in preliminary tests, as previously described. Following successful precipitation (white solid separated for O/A = 2), **methanol** (b.p. 64.6°C, complete miscibility with water, no azeotrope formation, 17.5 mm Hg vapour pressure at 20°C [21]) was selected as the most appropriate solvent to be employed in SDC of ZnO from a concentrated NaOH solution.

7.4 Systematic Solubility Studies

7.4.1 Influence of Sodium Hydroxide Content

The solubility of zinc oxide in solutions of various sodium hydroxide concentrations (0, 1, 2, 4, 6, 7, and 8 M) was determined at 21°C; two experiments were conducted to verify reproducibility (Figure 7.1). The solubility curve indicates that the solubility of zinc oxide increased with sodium hydroxide concentration, ~ 3 g/L Zn dissolved in 1 M NaOH solution to ~ 72 g/L in 8 M NaOH, with a reproducibility of ~8%. These data are consistent to the concentration values reported by Linke and Seidell for similar conditions [22]. Also, Jarupisitthorn *et al.* [15] found that zinc oxide solubility in sodium hydroxide solutions increase with NaOH concentration and temperature.

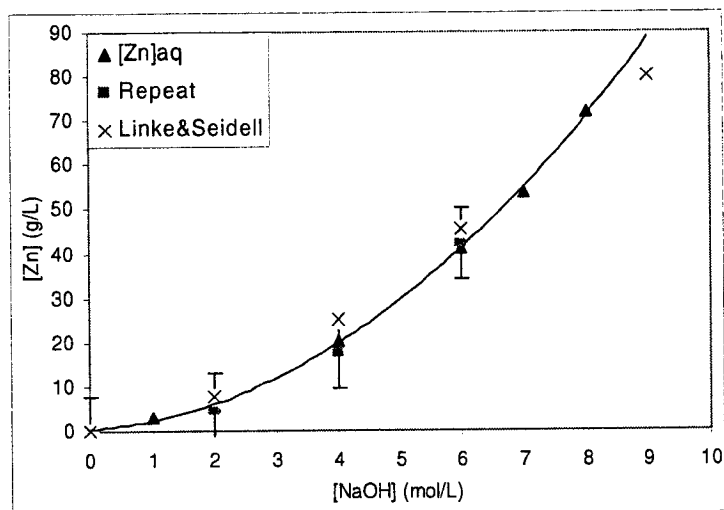


Figure 7.1 Zinc oxide solubility in sodium hydroxide at 21°C

7.4.2 Influence of Temperature and Organic Fraction

The solubility of ZnO in the system H₂O-NaOH (6 M) as a function of methanol (never studied before) was determined for 21 and 60°C (Figure 7.2); two experiments were conducted at 20°C, with a reproducibility of ~7%.

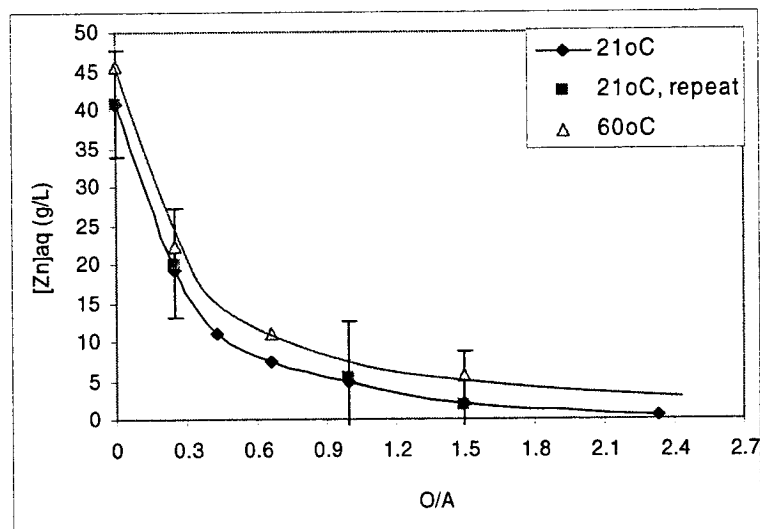


Figure 7.2 Effect of methanol and temperature on zinc oxide solubility (6 M NaOH)

As expected, the solubility (measured as g/L Zn in the aqueous phase – not in the mixed aqueous - organic solution) decreases with decreasing temperature and increasing organic

fraction, from ~ 41 g/L Zn in the absence of methanol (6 M NaOH solution) to 4.78 g/L for a $O/A = 1$ and ~ 0.7 g/L for $O/A = 2.3$, at 21°C .

But, unlike for salts like nickel sulphate (Section 5.3.2) and gypsum (Section 6.3.2), increased temperature does not bring a marked effect in favouring solubility; it seems that ZnO solubility tends to be influenced more by the organic content since there are no drastic differences in values at 21 and 60°C . For a solution containing 6 M NaOH, it can be seen (Figure 7.2) that in the absence of methanol, zinc concentration in the aqueous phase is ~ 41 g/L at 21°C and ~ 45 g/L at 60°C , whereas a volumetric ratio of alcohol to aqueous (expressed as O/A) of 1.5 is required to lower the solubility of zinc down to ~ 2 g/L at 21°C and ~ 5.5 g/L at 60°C .

7.4.3 Dissolution Kinetics

The solubility data presented above (Figures 7.1 and 7.2) were obtained by equilibrating zinc oxide salts with aqueous or mixed aqueous-organic solutions for 34 and 48 hours, respectively. To verify that equilibrium was indeed attained within the time applied, dissolution tests were conducted; the results are shown in Figure 2.3. The left-hand y-axis shows the zinc concentration in the absence of methanol, while the data for $O/A = 1$ is read off the right-hand axis (both for 6 M NaOH solutions).

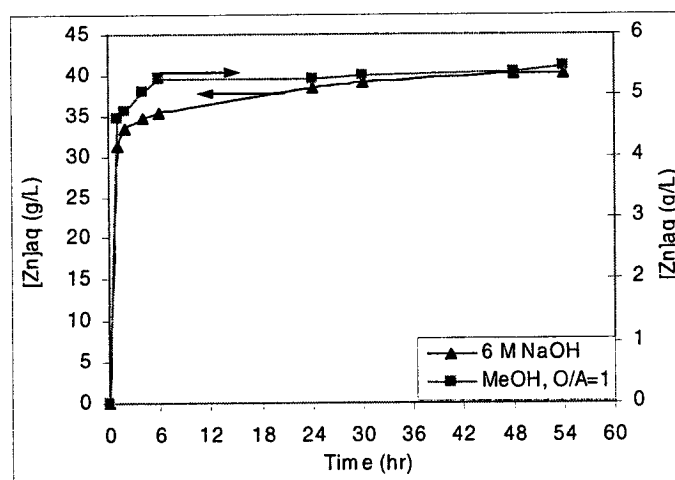


Figure 7.3 Dissolution kinetics of ZnO in 6 M NaOH at 21°C (no methanol and $O/A = 1$)

As observed, dissolution kinetics of zinc oxide (a sparingly soluble salt) is rather slow: ~ 24 hours are needed to reach equilibrium values in 6 M NaOH in the absence of methanol, whereas ~ 6 hrs are considered enough when the organic is present. Nevertheless, in both cases equilibrium had been reached since the respective equilibrium times used were 34 and 48 hrs.

7.5 Critical Supersaturation at 21°C

For optimum crystallisation conditions, the process should be conducted inside the metastable zone to promote large particle growth hence good settling properties and filterability. In order to achieve this goal, the critical supersaturation line for the system ZnO-H₂O-NaOH (6 M)-Methanol was determined at 21°C and compared to the equilibrium solubility curve (figure 7.4).

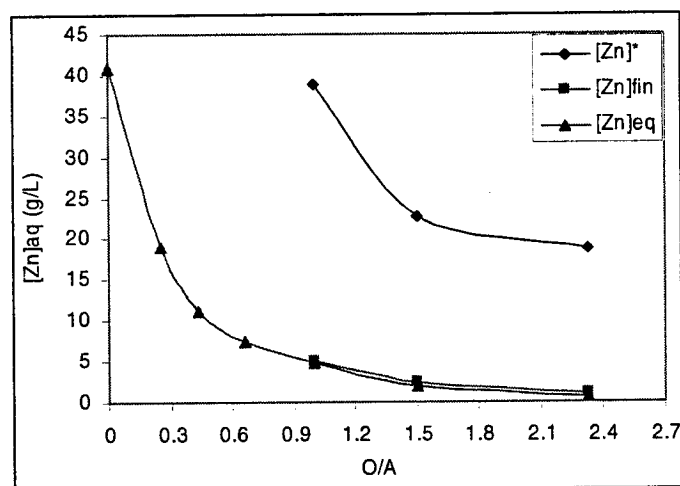


Figure 7.4 Critical supersaturation line and metastable zone width in the system ZnO-H₂O-NaOH (6 M)-Methanol at 21°C ($S_{cr, homo} \sim 8$)

Nyvlt *et al.* explained [23] that the width of the metastable zone depends firstly on the probability of ion-pairing and viable nuclei formation in solution; the degree of probability depends on the inter-molecular distances and therefore on the solution concentration. Accordingly, nucleation in solutions of sparingly soluble salts (such as ZnO) should occur at relatively high supersaturation levels as compared to highly soluble solids and the metastability window will be larger, which is indeed the case for the

system under study: at 21°C the critical supersaturation level for ZnO is ~ 8, much higher than values found for a highly soluble salt as nickel sulphate (i.e. $S \sim 1.4$, Section 5.5.2).

7.6 Solvent Displacement Crystallisation

The main objective of this section is to assess the influence of supersaturation value and crystallisation strategy on residual zinc in solution and crystal quality by performing comparative SDC tests with MeOH in the system H₂O-ZnO-NaOH (6 M) at 21°C. Finally, the mechanism of zincate decomposition process during SDC is investigated.

7.6.1 Crystallisation at 21°C

- *Preliminary SDC Test*

Once the solubility and supersaturation lines established, the next step was to conduct a preliminary SDC test in order to validate the effectiveness of methanol as salting-out agent for ZnO and to study changes in zinc concentration in solution and crystal quality.

In a general SDC test, 100 mL aqueous solution containing ~ 63 g/L Zn and 7.5 M NaOH were agitated (400 rpm) at 21°C in 1 L glass reactor while the organic was added from a 100 mL manual burette in small doses as to maintain $S < S_{cr,homo}$ (i.e. increments of 0.2 O/A, $O/A_{total} = 4$), followed by 20-minutes equilibration period. After each addition/stirring period solution samples were taken every 0.4 O/A, diluted and analysed for zinc, following the experimental procedure described in Section 7.2.2. Subsequently, the crystals were separated by filtration, washed, dried at ambient temperature in the fume-hood and further analysed. Same procedure was repeated to verify reproducibility.

Figure 7.5 presents the progression of a SDC experiment, indicating the influence of the organic fraction on the concentration of zinc in the aqueous phase; the total duration of the experiment was 240 min.

As observed, the decrease in zinc concentration occurred after ~ 60 minutes, corresponding to an O/A of ~1. Nevertheless, this process did not occur instantaneously: as the organic corresponding to O/A = 1 fraction was added under mild stirring, a certain

“induction period” elapsed (approx. 10 minutes) before signs of crystallisation were observed. The turbidity increased as the clear solution became cloudy (denoting the initiation of the nucleation process) then fine white particles started to separate. The crystallisation process continued through the rest of the experiment as more O/A fractions were added, causing a dense white suspension of extremely fine crystals to form and zinc concentration in solution to drop accordingly.

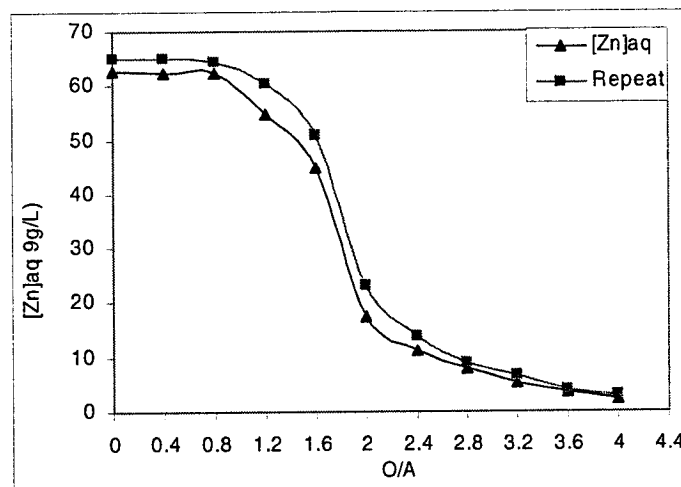


Figure 7.5 Progression of a typical homogeneous SDC test (21°C, 7.5 M NaOH)

From $O/A = 2.4$ onward, the slurry seemed to settle faster, denoting heterogeneous crystal growth. When supersaturation is maintained at low values, following a short duration homogeneous nucleation event that gives birth to a relatively small number of nuclei crystals, most crystallisation takes place within the growth zone (“secondary nucleation”), avoiding the formation of colloidal particles.

It can be observed that methanol fraction in the range $1 < O/A < 2$ has a strong effect on the crystallisation rate (sharp drop in $[Zn]_{aq}$) whereas any $2 < O/A < 4$ induces only moderate decrease. The final $[Zn]_{aq}$ corresponding to $(O/A)_{total} = 4$ was ~ 1.5 g/L, meaning that $\sim 97\%$ of zinc was precipitated.

Since $[Zn]_{aq,final}$ depends on O/A and addition-equilibration period (the temperature was not addressed in this study), a compromise must be found between the desired final metal concentration, selected amount of methanol to be employed and a reasonable experiment duration. A high O/A ratio could be added at once; the duration of

the experiment would be shortened but at the expense of the quality of the crystals (i.e. high supersaturation = small particles).

These encouraging preliminary results indicate that methanol constitutes an efficient precipitating agent capable of producing zinc oxide from alkaline aqueous solutions.

- **Precipitation Kinetics**

The aim of this study was to determine the crystallisation kinetics in the system H₂O-ZnO-NaOH (6 M) at 21°C in the absence and presence of ZnO seed (Figure 7.6).

High supersaturation was ensured by the instantaneous addition of methanol to the aqueous phase ($O/A_{\text{total}}=1.5$), under moderate stirring (400 rpm) and the kinetics of homogeneous crystallisation were assessed by monitoring the aqueous zinc concentration via periodic sampling for 4 hrs, following the experimental procedure described in Section 7.2.2. Same test was repeated by adding seed material (~47 g/L ZnO, i.e. 20 g/L Zn) to the initial solution containing a certain volume of solvent corresponding to a supersaturation below the critical value ($O/A_{\text{total}} = 1.3$).

As previously explained, the induction period is considered to be inversely proportional to the supersaturation and temperature. Generally, at low supersaturation (i.e. critical value) the induction period is more lengthy and nucleation rate is slow; consequently, the crystallisation kinetics is expected to be slower; inversely, due to the positive effect of high supersaturation on induction time and nucleation, crystallisation kinetics are faster at medium and high supersaturation values (i.e. $S > S_{\text{cr,homo}}$).

However, in the absence of seed, it can be observed that crystallisation kinetics of ZnO from a solution containing ~39 g/L Zn and 6 M NaOH is slow, with no significant drop in zinc concentration after 60 minutes (~31 g/L Zn) and no plateau values reached after 4 hours of equilibration (~17.5 g/L Zn); this is also consistent to data found for ZnO dissolution kinetics (Section 7.3.3). On the other hand, when seed is used crystallisation kinetics is much faster: After just 10 minutes, zinc concentration dropped to 28.6 g/L and ~60 minutes are required by the system to attain a concentration of ~17 g/L Zn; the subsequent decrease to the final values of ~15 g/L Zn (as compared to ~17.5 g/L Zn in the absence of seed) shows a plateau over the remaining time interval.

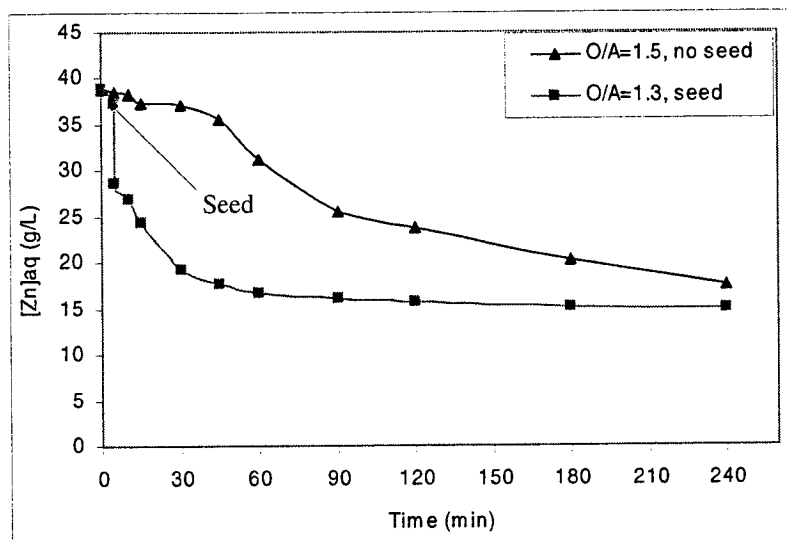


Figure 7.6 Precipitation kinetics of ZnO at 21°C in the absence and presence of seed (47 g/L ZnO seed, 6 M NaOH, 40 g/L Zn initial concentration)

In conditions of homogeneous crystallisation at high S , it was demonstrated [24] that nucleation already starts during the feeding period and an initial amorphous or poorly crystalline precursor is built first. This explains slightly higher concentration values since amorphous or poorly crystalline products have usually higher solubility compared to the crystalline phases. Under heterogeneous conditions, most crystallisation takes place within the growth zone (“secondary nucleation”), avoiding the formation of colloidal particles and leading thus to slightly lower zinc concentration values and particles with improved properties (morphology and size).

7.6.2 Solid Product Properties

Figure 7.7 gives the XRD pattern for the product obtained at 21°C, via homogeneous crystallisation, (low and high supersaturation, respectively), compared to spectrum of a reagent-grade ZnO sample. The sharp peaks indicated crystalline state (even if their intensity was somewhat smaller than standard’s peaks) and their relative position suggested the SDC product is indeed ZnO.

ICP chemical analysis performed on solid samples prepared homogeneously at low S via SDC confirmed also that the product is indeed ZnO, indicating 85% Zn

(compared to the theoretical value of 80% Zn in ZnO). Moreover, XRF analysis indicated that there is no Na contamination of the crystalline matrix (the washing process successfully removed superficial NaOH layer from the particles); the only impurity detected was SiO₂ (~between 0.04 and 0.15 wt. %).

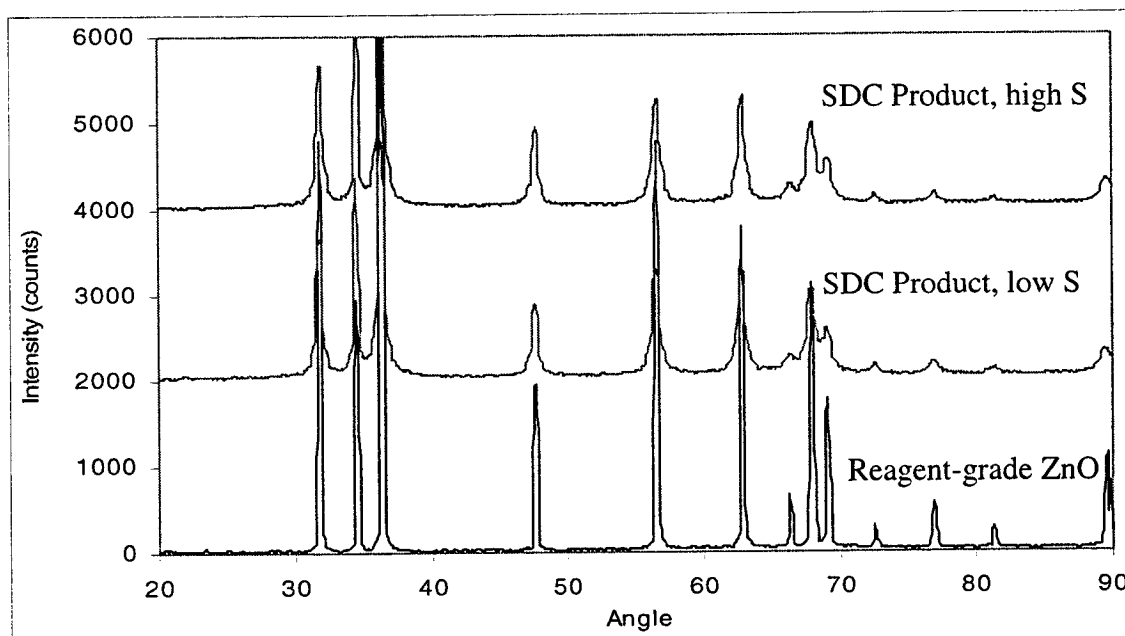


Figure 7.7 XRD spectra of ZnO produced via homogeneous SDC at 21°C, compared to reagent-grade crystals

ZnO belongs to the hexagonal wurtzite system [4, 5, 6, 25], where the Zn²⁺ cations are tetrahedrally coordinated with O²⁻ anions and vice versa (Figure 7.8). The atomic planes consist of equal numbers of zinc and oxygen ions, forming rows of Zn-O dimers; to the surface dimers are bonded dimers in the second layer. [26].

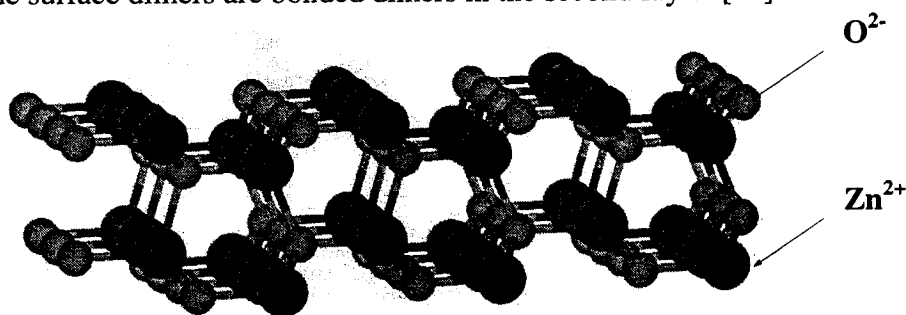


Figure 7.8 Structure of ZnO [26]

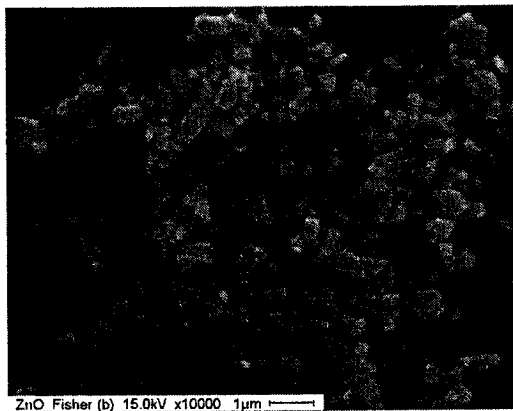
In order to evaluate the effect of supersaturation magnitude and crystallisation strategy on the quality of the solid product, the general morphology and approximate size of the particles were established by performing Scanning Electron Microscopy (Figure 7.9).

As observed from Figure 7.9, particles produced via SDC do not exhibit the hexagonal structure characteristic for ZnO. This irregular shape is due to crystallisation conditions and insufficient equilibration time to allow for crystal maturation (ripening). SEM micrographs show distinct crystal morphology and size dependence on supersaturation magnitude and crystallisation strategy.

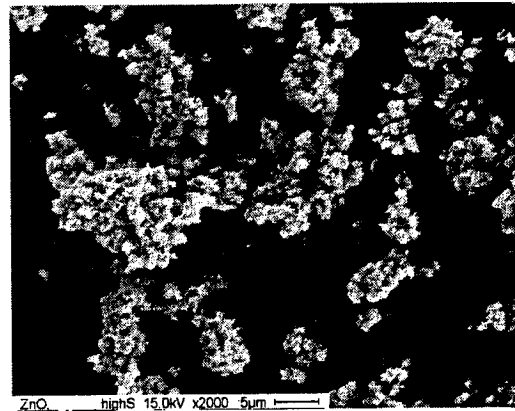
Homogeneous tests conducted at high supersaturation yielded extremely fine, irregular crystals of $< 1\mu\text{m}$ average size, with high tendency towards agglomeration (Figure 7.9 b). At high supersaturation (i.e. high O/A ratio) a high nucleation rate competes favourably with a lower growth rate of the already formed particles, allowing thus the formation of a large number of nuclei before the growth process is allowed. Therefore, when the number of available growth sites is not sufficient to accommodate the zinc oxide to be deposited, additional spontaneous nucleation occurred, fact demonstrated by the presence of small crystals, clearly stemmed from bulk nucleation.

Tests conducted at low supersaturation, where the initial homogeneous generation of a smaller number of nuclei is followed by a heterogeneous growth process, show a certain improvement in average particle size and morphology (Figure 7.9 c, d). Larger, well-dispersed porous aggregates are formed, consisting of smaller spherulitic units cemented together during crystallisation. Nielsen and Söhnel [27] indicated that at low supersaturation the nucleation is mainly heterogeneous while at higher supersaturation it becomes predominantly homogeneous.

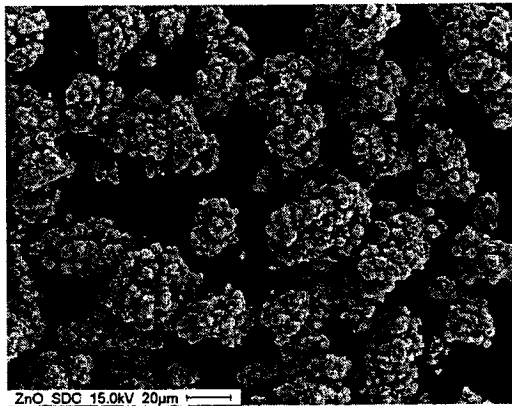
At low supersaturation, following initial nucleation, no new bulk growth sites are formed and crystallisation occurs mainly on the surface of the existing crystals. This process can be observed on the magnified detailed Figure 7.9 d, where extremely fine acicular single crystallites grow on the larger spherulitic aggregates. Similar observations have been reported by Sigoli *et al.* [10], Chittofrati and Matijevic [9] and Wang *et al.* [6] who also related the morphology to the experimental conditions (temperature, pH, presence of impurities).



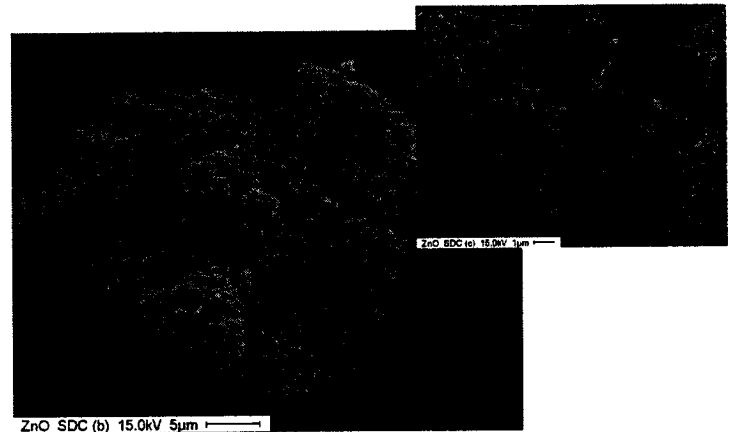
(a) reagent-grade ZnO seed



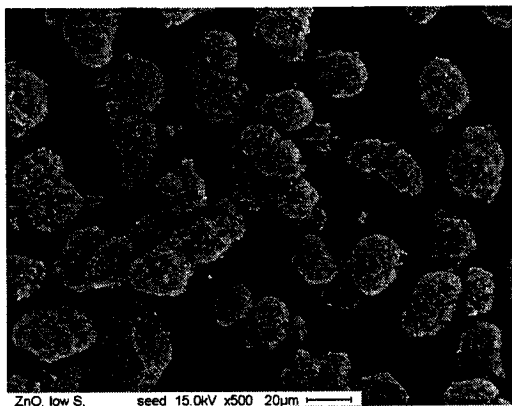
(b) homogeneous, high S



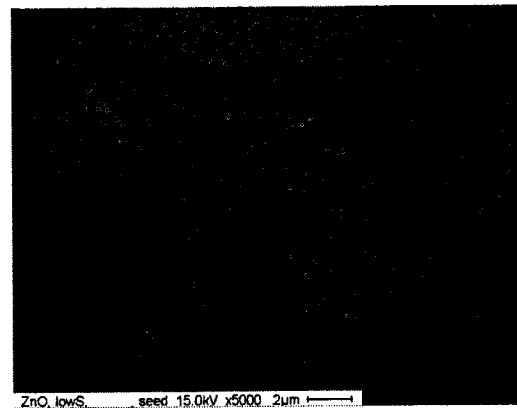
(c) homogeneous, low S



(d) homogeneous, low S, detail



(d) heterogeneous, low S



(e) heterogeneous, low S, detail

Figure 7.9 SEM micrographs of ZnO particles produced via SDC at 21°C (6 M NaOH)

Heterogeneous crystallisation favoured growth and produced larger aggregates that exhibit a more compact nature with smooth surfaces and a rather uniform particle size

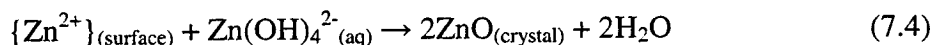
distribution, indicating a uniform growth process (Figure 7.9 d, e); this leads to a more compact filter cake, meaning less solution retention and impurity uptake.

The fine acicular crystallites are still present on the surface, and this must be considered a characteristic of ZnO particles precipitated from solution (as opposed to the hexagonal rod-like regular shape obtained via the pyrometallurgical process).

To conclude, crystallisation under low supersaturation heterogeneous conditions ensures that amorphous precursors and extensive aggregation are avoided, the external mass transport process is decelerated and the solid/liquid interface becomes less crowded, thus allowing the surface integration step to proceed uninhibited. Consequently, the particles produced under these conditions have improved physical (size) and chemical (purity) properties.

W-J. Li *et al.* [25] assume that the homogeneous nucleation and growth mechanism of ZnO consists on the formation of a cluster of growth units by a dehydration process of $\text{Zn}(\text{OH})_4^{2-}$ complexes (zincate) and the incorporation into the crystal lattice at the interface (Eqn. (7.4)); the process is diffusion-controlled, explaining thus the rather equiaxed morphology of the obtained particles.

Demianets and Kostomarov [28] explain the heterogeneous growth process of ZnO onto seed by taking into account the mechanism of the interaction between zincate anions in solution (the growth units) and crystal surfaces with different chemical compositions and charge (i.e. Zn^{2+} and O^{2-}) of the lattice (see Figure 7.9) during incorporation, via the following reactions:



7.6.3 Suggested Mechanism for Zincate - Zincite Transformation

Although insoluble in aqueous solutions at neutral pH values, when zinc oxide is immersed in water, the surface of the oxide is hydrolysed to form a thin layer of hydroxide ($\equiv\text{Zn}-\text{OH}$). Both zinc oxide and the hydroxide are amphoteric, dissolving in acids to form the hydrated Zn^{2+} cation and in alkalis to form various hydrated zincate

species, depending on the OH^- concentration (Figure 7.10); as the pH increases beyond 13, $\text{Zn}(\text{OH})_4^{2-}$ becomes the predominant species [29].

Considering this, it can be assumed that $\text{Na}_2\text{Zn}(\text{OH})_4$ is the precursor present in a 6 M NaOH aqueous solution at ambient or mild temperatures, dissociated as Na^+ and $\text{Zn}(\text{OH})_4^{2-}$ (this formula is considered to describe more accurately the hydrated zincate complex at $\text{pH} > 12$ than ZnO_2^{2-}).

So far, there has been no known research work related to precipitation of zinc oxide from alkaline solutions by using organic solvents, although Haile *et al.* [7] and Costa and Baptista [30] mention adding methanol, ethanol and amines (up to 50% by volume) to an aqueous solution already containing ZnO (obtained by treating ZnCl_2 with NaOH, and heating) to improve particle dispersion.

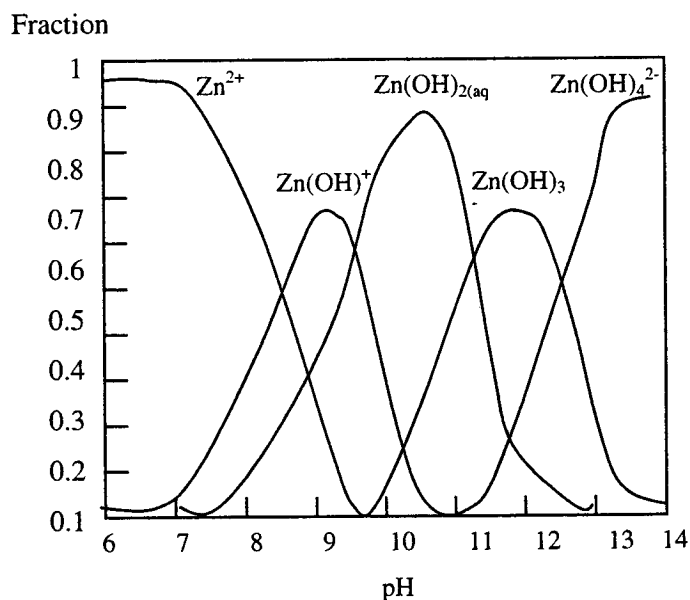


Figure 7.10 Fraction of ionic species in solution as a function of pH at 25°C (adapted from [29])

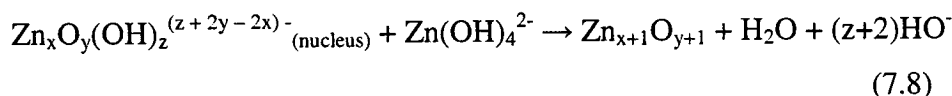
Unlike for previous SDC tests, where the alcohol would simply remove the solvent (i.e. water) from hydration sheaths of dissociated sulphate salts, causing thus salt precipitation, in this case the process seems to be more complex, possibly involving a chemical reaction catalyzed by the alcohol.

During hydrothermal ZnO precipitation, the principle is to form a Zn-based hydroxy salt precursor that is unstable in hot solution ($>100^\circ\text{C}$) and, upon

equilibration/ageing, decomposes to form Zn(OH)_2 which converts to ZnO . W-J. Li *et al.* [25] tried to explain this process in terms of temperature-induced dehydration of the hydroxy precursor upon incorporation into the ZnO lattice:



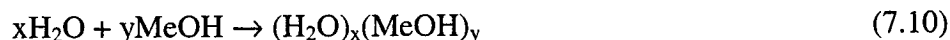
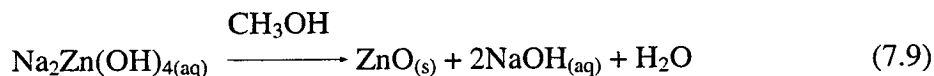
To refine this mechanism, they suggested that, at high supersaturation, growth units of Zn(OH)_4^{2-} are bonded together through a dehydration reaction, forming a cluster; when the critical size of the cluster reaches the value required for the formation of ZnO , the oxide is precipitated.



where x , y and z represent the numbers of Zn^{2+} , O^{2-} and OH^- in the lattice, respectively.

A similar phenomenon must occur during SDC, where methanol probably induces/catalyzes this decomposition process of the zincate existing in solution. Zinc oxide formation cannot be explained in terms of simple pH decrease through dilution (i.e. the phase diagram shifted to the pH regions where ZnO is insoluble), because even an elevated organic-to-aqueous ratio of 4 is not sufficient to decrease the solution alkalinity below pH 12. This was verified experimentally by diluting the caustic zinc solution to a ratio 4:1 without observing any signs of precipitation.

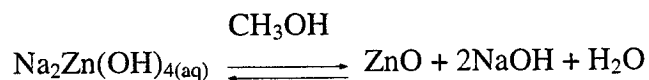
Due to its ability to form stable hydrogen bonds with water molecules (see Sections 2.3.2 and 2.3.3), it appears that the alcohol has the ability of dehydrating the zincate complex and inducing decomposition upon integration into crystal lattice, in the same manner that elevated temperatures would do. The general reaction would be:



Methanol captures water molecules but does not participate in the reaction and it can be recovered for reuse via the liquid-liquid separation technique of choice.

7.7 Regeneration of NaOH

The proposed mechanism of zincate-zincite transformation during SDC (Eqn. (7.9)) predicts that sodium hydroxide will be regenerated in the process and NaOH concentration following the crystallisation process and methanol removal should be close, if not similar, to the initial concentration of NaOH solution used to dissolve ZnO and form sodium zincate.



In order to investigate NaOH regeneration during SDC, the measurement of NaOH concentration was done by direct simple acid-base titration of initial sodium hydroxide solution, the zincate solution and the final aqueous-organic mixture (following ZnO filtration), using standard 1 N HCl, according to procedure described in Section 7.2.2. An initial solution containing 40 g/L Zn and 6 M NaOH was employed for SDC with methanol ($O/A_{\text{total}} = 4$). NaOH concentration values determined experimentally by titration were compared to theoretical values predicted by stoichiometry (Table 7.2).

Table 7.2 NaOH concentration values

Solution	NaOH _{theoretical} (stoichiometry)	NaOH _{experimental} (titration)
[NaOH] ₁ : Initial 6 M NaOH	6 mol/L (240 g/L)	6.125 mol/L (245 g/L)
[NaOH] ₂ : Free NaOH in Na ₂ ZnO ₂ solution (after part of NaOH consumed to prepare sodium zincate)	4.77 mol/L (191 g/L) (the balance of 1.225 mol/L or 91 g/L consumed to prepare sodium zincate)	4.87 mol/L (194.8 g/L)
[NaOH] ₃ : Final NaOH in aqueous-organic mixture (O/A = 4)	1.2 mol/L (48 g/L)	1.244 mol/L (49.76 g/L)
[NaOH] ₄ : Final NaOH after dilution correction (i.e. [NaOH] ₄ = [NaOH] ₃ *5)	6 mol/L (240 g/L)	6.223 mol/L (248.8 g/L)

From Table 7.2 it can be observed that NaOH is indeed regenerated following ZnO precipitation via SDC with methanol. The final NaOH concentration value of 6.223 M is within 3.7 % error margin compared to the theoretically predicted value of 6 M and within 1.6 % error compared to the initial concentration of 6.125 M experimentally determined.

7.8 Summary and Conclusions

1. The present work determined methanol to be an effective salting out agent to cause precipitation of ZnO from alkaline (NaOH) aqueous solutions. The solubility of ZnO as a function of NaOH concentration, methanol content and temperature was established. The final zinc content increased with sodium hydroxide content and temperature and decreased with increasing organic fraction.
2. The metastable zone boundary, an important parameter in designing controlled-crystallisation tests, has been determined at 20°C. As predicted by theory [23], nucleation in solutions of sparingly soluble salts such as ZnO occurred at relatively high supersaturation levels (at 20°C the critical supersaturation for ZnO is ~ 8) and the metastability window was larger.
3. Precipitation kinetics of ZnO were determined at 21°C, in the absence and presence of seed material. In the absence of seed, precipitation kinetics of ZnO were slow, with no significant drop in zinc concentration after 60 minutes and no plateau values reached after 4 hours of equilibration. As expected, when seed was used kinetics were much faster; ~60 minutes were required by the system to show a significant drop in Zn concentration.
4. The crystal quality was found to depend on the method of crystallisation. High supersaturation (homogeneous crystallisation) led to fine, highly agglomerated solid product while low supersaturation and seeding were found to promote growth, producing better grown particles.
5. The zincate-zincite transformation (i.e. ZnO precipitation) during SDC is believed to occur due to the methanol-catalyzed decomposition of a hydroxyl salt precursor

existing in solution. It appears that the alcohol has the ability of dehydrating the zincate complex and inducing decomposition upon integration into crystal lattice, in the same manner that elevated temperatures would do during the hydrothermal process. Methanol captures water molecules but does not participate in the reaction and it can be recovered for reuse via the liquid-liquid separation technique of choice.

6. It was experimentally demonstrated that sodium hydroxide is indeed regenerated in the process, as predicted by above-postulated mechanism; NaOH concentration following ZnO crystallisation was similar to the initial concentration of NaOH solution used to dissolve ZnO and form sodium zincate.

References

- [1]. J. Toyir, M. Saito, I. Yamauchi, S. Luo, J. Wu, I. Takahara and M. Takeuchi, "Development of high performance Raney Cu-based catalysis for methanol synthesis from CO₂ and H₂" *Catalysis Today*, **45**, pp. 245-250, (1998).
- [2]. Y. Lin, Z. Tang and Z. Zhang, "Preparation of nanometre zinc oxide powders by plasma pyrolysis technology and their applications" *Communications of the American Ceramics Society*, **83(11)**, pp. 2869-2871, (2000).
- [3]. D.K. Xia and C.A. Pickles, "Caustic roasting and leaching of EAF dust" *Canadian Metallurgical Quarterly*, **38(3)**, pp. 175-186 (1999).
- [4]. J.Y. Li, X.L. Chen, H.Li, M.He and Z.Y. Qiao, "Fabrication of zinc oxide nanorods" *Journal of Crystal Growth*, **233**, pp. 5-7, (2001).
- [5]. S.J. Chen, Y.C. Liu, J.G. Ma, D.X. Zhao, Z.Z. Zhi, Y.M. Lu, J.Y. Zhang, D.Z. Shen and X.W. Fan, "High-quality ZnO thin films prepared by two-step thermal oxidation of the metallic Zn" *Journal of Crystal Growth*, **240**, pp. 467-472, (2002).

- [6]. J.M. Wang, C. Zhang, L. Zhang, J.Q. Zhang and C.N. Cao, "Preparation, structure and performance of zinc oxide with high electrochemical discharge capacity" *Materials Chemistry and Physics*, **70**, pp. 254-258, (2001).
- [7]. S.M. Haile, D.W. Johnson, G.H. Wiseman and H.K. Bowen, "Aqueous precipitation of spherical zinc oxide powders for varistor applications" *Journal of American Ceramics Society*, **72(10)**, pp. 2004-2008, (1989).
- [8]. H. Nishizawa, T. Tani and K. Matsuoka, "Crystal growth of ZnO by hydrothermal decomposition of Zn-EDTA" *Communications of the American Ceramics Society*, **7**, pp. C98-C100, (1984).
- [9]. A. Chittofrati and E. Matjevic, "Uniform particles of zinc oxide of different morphologies" *Colloids and Surfaces*, **40**, pp. 65-78, (1990).
- [10]. F.A. Sigoli, M.R. Davolos and M. Jafelicci, Jr., "Morphological evolution of zinc oxide originating from zinc hydroxide carbonate" *Journal of Alloys and Compounds*, **262-263**, pp. 292-295, (1997).
- [11]. C-H. Lu and C-H. Yeh, "Influence of hydrothermal conditions on the morphology and particle size of zinc oxide powder" *International Ceramics*, **26**, pp. 351-357, (2000).
- [12]. C. Allen, P., Kondos, S. Payant, G. Van Weert, and A. Van Sandwijk, "Production of zinc oxide from complex sulfide concentrates using chloride processing", US Patent 6,395,242, May 28, 2002.
- [13]. G. Van Weert, and A. van Sandwijk, "Routes to residue-free zinc refining", *JOM*, **51(12)**, pp. 26-28, (2002).
- [14]. Y. Choi, S. Payant, J. Kim, A-M. Giove, R. Rao, and J.A. Finch, "Production of zinc oxide from acid soluble ore using precipitation method", PCT World Patent WO 02/06541, January 24, 2002.

- [15]. C. Jarupisitthorn, T. Pimtong and G. Lothongkum, "Investigation of kinetics of zinc leaching from EAF dust by sodium hydroxide" *Materials Chemistry and Physics*, **77**, pp. 531-535, (2002).
- [16]. M.K. Jha, V. Kumar and R.J. Singh, "Review of hydrometallurgical recovery of zinc from industrial wastes" *Resources, Conservation and Recycling*, **33**, pp. 1-22, (2001).
- [17]. G. Houlachi, Noranda Technology Centre, Pointe-Claire, QC, private communication, December 1999.
- [18]. T. Zhigang, Z. Rongqi and D. Zhanting, "Separation of isopropanol from aqueous solution by salting-out extraction" *Journal of Chemical Technology and Biotechnology*, **76**, pp. 757-763, (2001).
- [19]. Y.G. Wu, M. Tabata, T. Takamuku, A. Yamaguchi, T. Kawaguchi and N.G. Chung, "An extended Johnson-Furter equation to salting-out phase separation of aqueous solution of water-miscible organic solvents" *Fluid Phase Equilibria*, **192**, pp. 1-12, (2001).
- [20]. X. Lu, P. Han, Y. Zhang, Y. Wang and J. Shi, "Salting-out separation and liquid-liquid equilibrium of tertiary butanol aqueous solution" *Chemical Engineering Journal*, **78**, pp. 165-171, (2000).
- [21]. E.W. Flick (Editor), *Industrial Solvents Handbook*, 3rd edition, Publications Noyes, Parkridge, N.J, p. 223, 1985.
- [22]. W.F. Linke and A. Seidell (editors), *Solubilities of Inorganic and Metal-Organic Compounds (a compilation)* 4th edition, Van Nostrand, Princeton, N.J., (1958).
- [23]. J. Nyvlt, R. Rychly, J. Gottfried and J. Wurzelova, "Metastable Zone Width of Some Aqueous Solutions" *Journal of Crystal Growth*, **6**, pp. 151-162, (1970).

- [24]. J. Franke and A. Mersmann, "The influence of the operational conditions on the precipitation process" *Chemical Engineering Science*, **50(11)**, pp. 1737-1753, (1995).
- [25]. W-J. Li, E-W. Shi, W-Z. Zhong and Z-W. Yin, "Growth mechanism and growth habit of oxide crystals" *Journal of Crystal Growth*, **203**, pp. 186-196, (1999).
- [26]. A. Wander and N.M. Harrison, "An *ab initio* study of ZnO(1010)" *Surface Science*, **457**, L342-L346, (2000).
- [27]. A.E. Nielsen and O. Söhnel, "Interfacial tensions in electrolyte-aqueous solution, from nucleation data" *Journal of Crystal Growth*, **11**, pp. 233-242, (1971).
- [28]. L. Demianets and D.V. Kostomarov, "Mechanism of zinc oxide single crystal growth under hydrothermal conditions" *Ann. Chem. Sci. Mat.*, **26**, pp. 193-198, (2001).
- [29]. A. Degen and M. Kosek, "Effect of pH and impurities on the surface charge of zinc oxide in aqueous solution" *Journal of the European Ceramics Society*, **20**, pp. 667-673, (2000).
- [30]. M.E.V. Costa and J.L. Baptista, "Characteristics of zinc oxide powders precipitated in the presence of alcohols and amines" *Journal of the European Ceramic Society*, **11**, pp. 275-281, (1993).

Chapter 8. Dehydration of Metal Sulphate Crystals

8.1 Introduction

The term “dehydration” means removal of water (present either as free moisture or as bound moisture, i.e. water of crystallisation) from a given system. In this study, the process of dehydration addresses the removal of crystallisation water only.

The advantages of water removal from the hydrated compounds are manifold [1]:

- (1) to facilitate handling in further processing (e.g. pure Mg metal is obtained by electrolysis of anhydrous MgCl_2);
- (2) to permit satisfactory utilisation of the final product (e.g. anhydrous CaCl_2 or Al_2O_3 are used as drying agents);
- (3) to reduce shipping costs;
- (4) to increase the capacity of other equipment in the process;
- (5) to enhance the value of by-product or waste.

For the above purposes, most of the hydrated salts may be dehydrated to lower hydrates or completely anhydrous form. The most important industrial techniques for the dehydration (partial or total) of salts are summarised below.

- ***Thermal Dehydration***

Hydrated salts can be partially or completely dehydrated by the action of heat (hot air or carrier gas), at a temperature elevated enough to remove crystallisation water but inferior to salt's decomposition temperature. Partial dehydration is relatively easy to achieve at moderate temperatures, whereas the complete removal of crystallisation water requires more intensive conditions (in terms of temperature and duration). In some cases, due to use of elevated temperatures ($> 100^\circ\text{C}$ for complete water removal), the final product may present anisotropy (lattice distortion/reorientation) with respect to the initial crystal. In the process of drying, both heat and mass transfer are involved. For efficient transfer, fluidized bed driers, kilns and rotary driers are used industrially. For example, $\text{CaSO}_4 \cdot 0.5\text{H}_2\text{O}$ (plaster of Paris) is obtained by dehydration of $\text{CaSO}_4 \cdot 2\text{H}_2\text{O}$ (gypsum) at

120-150°C, whereas at higher temperatures the anhydrate is formed. Partial or total dehydration of barium and magnesium salts can also be achieved [2, 3, 4].

- ***Dehydration using Organic Solvents***

Due to high temperatures involved, thermal dehydration is an energy-intensive technique and can lead to product anisotropy or decomposition of the salt. To minimise such risks, it is desirable to achieve partial or total water removal at moderate temperatures, by using organic solvents, either miscible or immiscible with water. Usually, dehydration of higher hydrates via this procedure proceeds in stages.

The choice of solvent depends on many factors, e.g. if the dehydration is to be carried out by azeotropic distillation (i.e. water removal via distillation whereas the organic is recirculated), then it would be preferable to use hydrophobic solvents, whereas by using equilibrium techniques (i.e. extraction) the choice falls on hydrophilic organic solvents with affinity to leach or extract water from the hydrated compound.

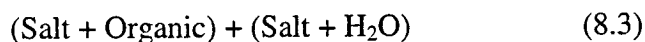
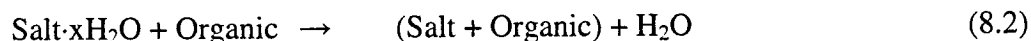
- (a) Dehydration by Azeotropic Distillation

In this method of dehydration, the hydrated salt is suspended in a suitable hydrophobic solvent with high boiling point and the suspension is heated to the boiling point of the dispersion medium, under mechanical stirring. The vapours are condensed and separated into two immiscible layers: water is removed and the organic solvent is fed back to the distillation column.

Thus, Bergmann [5] patented in 1947 the production of anhydrous compounds by boiling hydrated MSO_4 ($\text{M}=\text{Na}, \text{K}, \text{Mg}, \text{Fe(II)}, \text{Cu}$) and MCl ($\text{M}=\text{Li}, \text{Ba}, \text{Ca}, \text{Cu}$) in water-immiscible organic solvents with high boiling point, such as acetals, ketals and derivatives of ethylene glycol. Nencetti and Pennacchi [6, 7] obtained 100% dehydration of $\text{Na}_2\text{SO}_4 \cdot 10\text{H}_2\text{O}$ by azeotropic distillation with benzene and 50% dehydration of $\text{MSO}_4 \cdot 7\text{H}_2\text{O}$ ($\text{M}=\text{Fe(II)}$ and Mg) with xylene. Finally, Vyas and Gavini [8] achieved step-wise total dehydration of $\text{BaCl}_2 \cdot 2\text{H}_2\text{O}$ with carbon tetrachloride, of $\text{SrCl}_2 \cdot 6\text{H}_2\text{O}$ with benzene and kerosene and partial dehydration of $\text{MgCl}_2 \cdot 6\text{H}_2\text{O}$ with toluene (to tetrahydrate), xylene (to dihydrate) and kerosene (to monohydrate). They reported that the water removal rate was found to be first order and the dehydration extent was independent of distillation rate.

(b) Dehydration by Leaching-Extraction

In this method, one of the components of hydrated salts, either crystallisation water molecules or anhydrous salt are partially or completely leached (or extracted) by use of organic solvents with affinity for water (miscible or partly miscible):



Thus, Vyas and Gavini [9] obtained monohydrate compounds by equilibrating $\text{BaCl}_2 \cdot 2\text{H}_2\text{O}$ and $\text{SrCl}_2 \cdot 6\text{H}_2\text{O}$ in low boiling point water miscible organic solvents (such as methanol, ethanol, propanol, formic acid and acetic acid) at 50 and 70°C. They reported that dehydration kinetics and extent of water removal increased with temperature, equilibration time and length of organic chain (i.e. $\text{PrOH} > \text{EtOH} > \text{MeOH}$). More recently, Gartner and Witkamp [10] produced anhydrous sodium carbonate (soda ash, Na_2CO_3) by equilibrating sodium sesquicarbonate (trona, $\text{Na}_2\text{CO}_3 \cdot \text{NaHCO}_3 \cdot 2\text{H}_2\text{O}$) in ethylene glycol at 55°C. The role of organic solvent was to reduce water activity, which in turn decreased the stability of trona; thus, the transition temperature between the hydrated form and the anhydrous one was reduced. The method was patented [11] by extending the use of organic solvent (5-20% by wt.) to low-molecular weight alcohols, ethers, carbonyl compounds, polyols, polyamines and condensed products of thereof, all with boiling points below 90°C.

- ***Dehydration by Formation of Intermediate Compounds***

In this method, a compound which can react easily with hydrated salt is added to it; at the required conditions, the compound displaces crystallisation water molecules, thereby forming an intermediate. Subsequently, this intermediate compound will be easily decomposed to produce the anhydrous salt. The most common application of this technique is the complete dehydration of $\text{MgCl}_2 \cdot 6\text{H}_2\text{O}$, when ammonium chloride or ammonia are added to the magnesium salt, to convert it to either $\text{NH}_4\text{Cl} \cdot \text{MgCl}_2 \cdot 6\text{H}_2\text{O}$ or $\text{MgCl}_2 \cdot 6\text{NH}_3$, which at 350-450°C are decomposed to anhydrous MgCl_2 , H_2O and NH_4Cl or NH_3 , respectively [12].

The main objective of the present study is to investigate if 2-propanol is capable of achieving partial or total crystallisation water removal from gypsum ($\text{CaSO}_4 \cdot 2\text{H}_2\text{O}$) and copper sulphate pentahydrate ($\text{CuSO}_4 \cdot 5\text{H}_2\text{O}$) under mild, less energy-intensive conditions.

8.2 Experimental

For the preparation of all solutions or suspensions used in this study, de-ionized water, reagent-grade gypsum ($\text{CaSO}_4 \cdot 2\text{H}_2\text{O}$, 98.5% purity), copper sulphate ($\text{CuSO}_4 \cdot 5\text{H}_2\text{O}$, 100% purity) and 2-propanol Optima-grade (99.9% purity) were employed. Additionally, in the experiments involving gypsum, aqueous solutions containing 3 M HCl and 1.5 M MgCl_2 were prepared starting from reagent-grade hydrochloric acid (37.5% concentration) and magnesium chloride (99-102% purity).

- **General Experimental Procedure**

Measured amounts of metal sulphate and 2-propanol were added to 500 mL Erlenmeyer flasks plugged with rubber stoppers, at 21°C. The flasks were equipped with Teflon-coated stirring bars and placed on a stirring magnetic plate to ensure vigorous agitation hence complete slurry suspension. For the tests conducted at higher temperatures (40 and 60°C), the flasks were immersed in a clear vinyl water bath fitted with a Cole-Parmer heating circulator; the water was mixed, heated and maintained at the desired temperature with an accuracy of $\pm 1^\circ\text{C}$ (Figure 3.1, Section 3.3.1).

- I. Dehydration of Calcium Sulphate Dihydrate

100 mL of aqueous-organic mixtures were prepared starting from solutions containing 3 M HCl and 2-propanol (O/A = 1.00 and 2.00, respectively). 10% (wt/vol) $\text{CaSO}_4 \cdot 2\text{H}_2\text{O}$ crystals were added under stirring (i.e. 10 g gypsum/100 ml solution) at 60°C, allowing an equilibration period of 15 minutes. Following equilibration periods of 6 and 24 hr, respectively, the crystals were separated by filtration, washed with hot water and 2-propanol, air-dried in the fume-hood at 50°C and further analysed. In order to study the influence of chloride content on gypsum dehydration, similar tests were conducted in the presence of 1.5 M MgCl_2 at 60°C.

II. Dehydration of Copper Sulphate Pentahydrate

300 mL pure 2-propanol were maintained at different temperatures (21, 40 and 60°C, respectively), while 10% (wt/vol) $\text{CuSO}_4 \cdot 5\text{H}_2\text{O}$ crystals were added under stirring (i.e. 30 g salt). In order to maintain low pH and avoid possible copper hydrolysis upon water release, concentrated H_2SO_4 was added to the mixture (corresponding to 25 g/L). Following equilibration periods of 3, 6 24 and 30 hrs, respectively, the crystals were separated by filtration, washed with 2-propanol, air-dried in the fume-hood at 50°C and further analysed. A similar test was performed at 60°C using azeotrope (contains 88% wt. 2-propanol) instead of pure alcohol.

The effect of recycling on crystallisation water removal, i.e. repulping of partly dehydrated $\text{CuSO}_4 \cdot x\text{H}_2\text{O}$ crystals ($x=3$ and 1) with fresh pure 2-propanol (10% solid content), was tested at 60°C for 6 hrs.

• **Characterisation of Solid Product**

The confirmation of crystalline phases and the determination of the number of crystallisation water molecules were achieved by X-ray Powder Diffraction analysis (XRD), using a Phillips PW1710 machine. The spectrum obtained for a certain sample was matched to different standard spectra contained in the computer's database.

The general morphology and approximate size of the particles were established by performing Scanning Electron Microscopy (SEM) using a JEOL 840A scanning microscope at 15kV on gold-coated samples.

The solids composition in terms of metal species was determined by digesting a known amount of solid in 5% HCl solution and performing ICP analysis.

The number of crystallisation water molecules was estimated by the Thermo-Gravimetric Analysis method (TGA) as the percent weight loss upon gradual heating, using a Perkin-Elmer TGA7 Thermogravimetric Analyzer.

8.3 Results and Discussion

8.3.1 Calcium Sulphate Dihydrate

Calcium sulphate, one of the most abundant sulphate minerals found in natural environment and a frequent by-product of numerous hydrometallurgical processes, exists in three main crystal phases: dihydrate, also known as gypsum ($\text{CaSO}_4 \cdot 2\text{H}_2\text{O}$, DH), hemihydrate ($\text{CaSO}_4 \cdot 1/2\text{H}_2\text{O}$, HH) and anhydrate (CaSO_4 , AH). The thermodynamic stability of these phases is a function of temperature and water activity. Therefore, metastable and stable phases can occur separately, successively or simultaneously, depending on conditions and the kinetics of the crystallisation process. It is known that the equilibrium transition temperatures are lowered by the addition of components that may decrease water activity by activating and deactivating water molecules during the phase changes, such as HCl, H_2SO_4 , Na_2SO_4 and alkaline ions (Ba) [13]. This behaviour is graphically explained in the phase diagram depicted in Figure 6.17 (Chapter 6).

As previously described in Sections 2.3.3 and 4.2.3, water activity in a crystallisation medium can be modified, besides other means, by changing the composition of solution via addition of organic solvents (most often low-molecular alcohols), which influence both the mole fraction and partial pressure of water [14, 15, 16]. More closely to the present research work, it has been reported that 2-propanol addition to aqueous solutions cause the water activity to decrease from 1 in the absence of 2-propanol to 0.2 for an organic mole fraction of 0.9 [14].

It was previously determined (Section 6.5.3-VI) that by equilibrating gypsum crystals at 40°C for 2 hrs, $O/A = 2$ (following homogeneous SDC tests and also 8 recycling runs, all in the presence of 3 M HCl), the only final phase detected was gypsum (Figure 6.18). Furthermore, as determined by Girgin and Demopoulos [17], dehydrate converts to HH/AH upon equilibration in HCl/ CaCl_2 media at 80°C .

Based on these findings, it was interesting to investigate whether the presence of a high 2-propanol-to-aqueous ratio ($O/A = 1$ and 2 , respectively) at an intermediate temperature (i.e. 60°C), together with a high concentration of HCl (3 M) and MgCl_2 (1.5 M) would cause a sufficient decrease in water activity as to lower the transition line and modify the nature of the solid phase, from DH to HH.

The solid product obtained by equilibrating gypsum crystals in aqueous-organic mixtures at 60°C for 6 and 24 hrs, respectively, in the absence and presence of MgCl₂ (Figures 8.1 and 8.2) were analysed by XRD and the results compared to different standard spectra (CaSO₄·xH₂O x=0, 0.5, 2) contained in the computer's database to identify hydrate form.

If dehydration occurs, the released crystallisation water perturbs the crystal structure and induces a rearrangement of calcium and sulphate ions, forming pseudomorphs, change that should translate in modifications of the XRD spectrum of initial compound [13, 18].

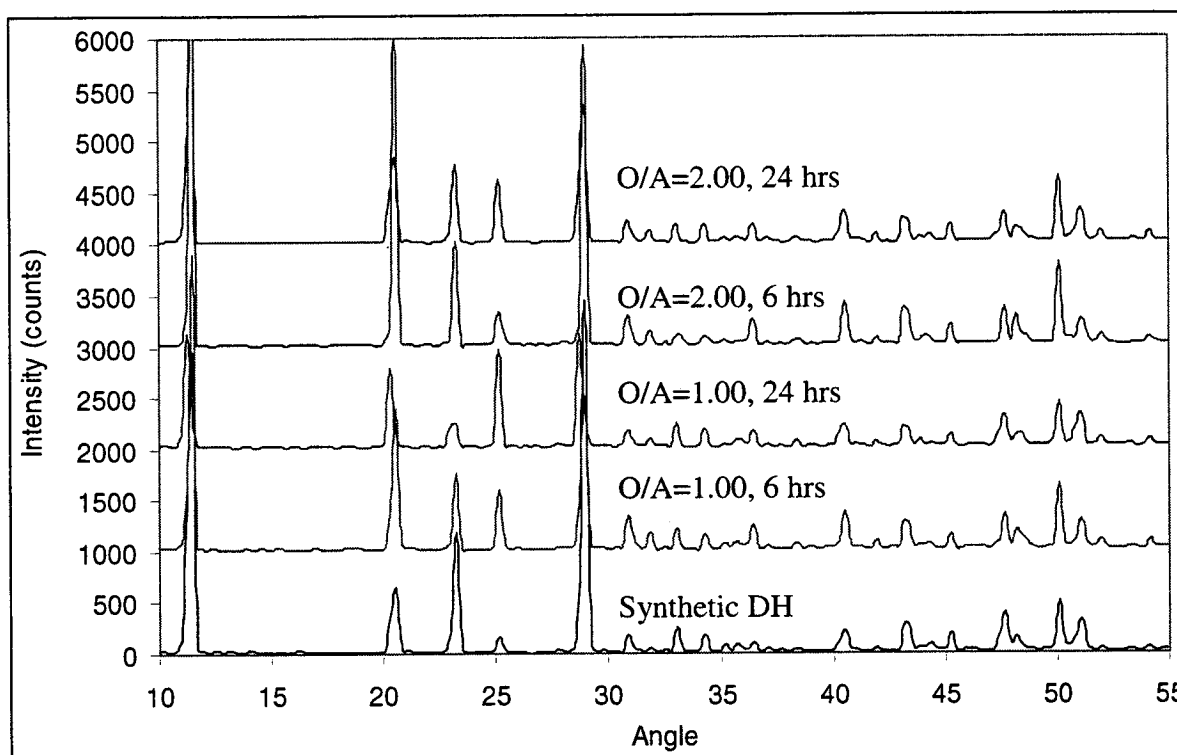


Figure 8.1 XRD monitoring of gypsum dehydration with 2-propanol at 60°C (3 M HCl)

From Figure 8.1, it was determined that CaSO₄·2H₂O (DH, characteristic peak of 100% relative intensity at 2θ angle ~11.6) offered the most probable match to the crystals equilibrated in 3 M HCl solution at 60°C in the presence of 2-propanol.

No HH/AH phases were detected (characteristic peak of ~70% relative intensity at 2θ angle of ~14.75), but the peaks appearing at 2θ angle of ~25 could indicate the possible presence of small amounts of AH.

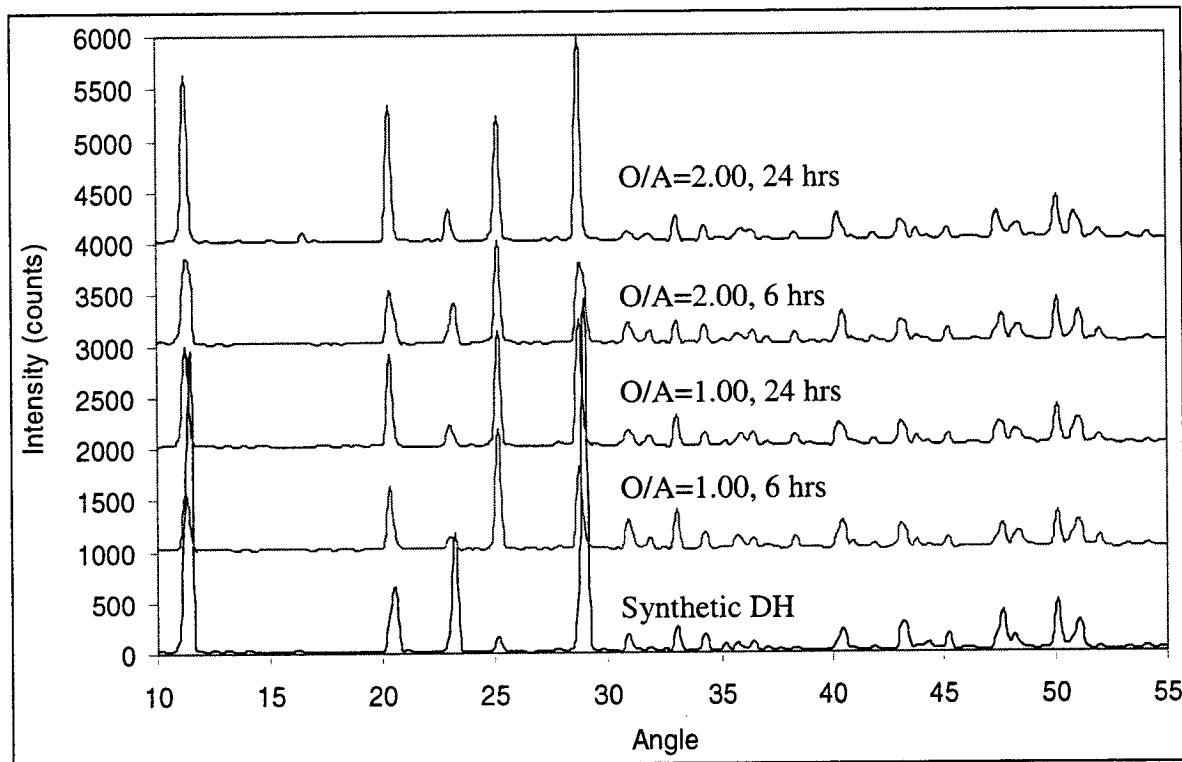
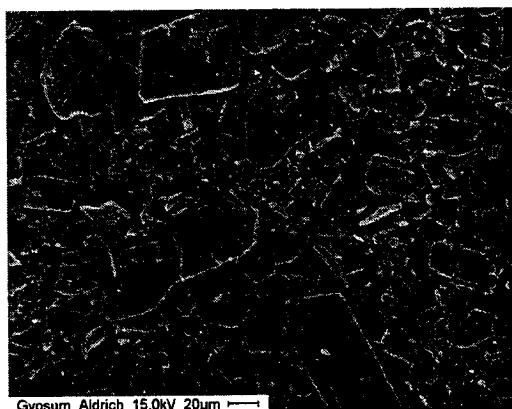


Figure 8.2 XRD monitoring of gypsum dehydration with 2-propanol at 60°C (3 M HCl, 1.5 M MgCl₂)

Tests conducted at 60°C in the presence of 3 M HCl and 1.5 M MgCl₂ led to similar results (Figure 8.2). The relative increase in peaks intensity for equilibrated crystals may be due to partial amorphous phase dissolution and therefore increase in degree of crystallinity. The sample equilibrated with O/A=2 for 24 hrs shows a small peak at 2θ angle of ~ 16.5, which nevertheless does not offer sufficient proof to indicate HH (characteristic peak at 2θ ~ 14.75).

Moreover, SEM micrographs of calcium sulphate crystals before (i.e. gypsum, Figure 8.3 a) and after equilibration tests for 24 hrs at 60°C in mixtures of O/A=2 in the absence and presence of MgCl₂ (Figure 8.3 b and c, respectively) preserve the same appearance, indicating that no major phase transformation occurred.

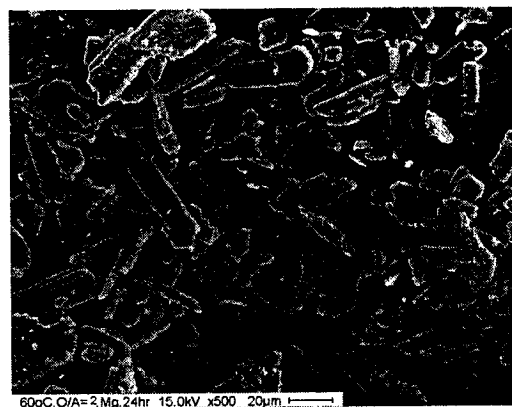
The phase transformation mechanism would involve a secondary nucleation mechanism, collision breeding of nuclei, followed by concomitant DH dissolution and growth of new phase [19]. The characteristic morphology for HH and AH is fine acicular crystals, whereas all samples studied presented the classical plate-like structure of DH [19, 20].



(a) reagent-grade CaSO₄·2H₂O



(b) O/A=2, 3 M HCl, no MgCl₂



(c) O/A=2, 3 M HCl, 1.5 M MgCl₂

Figure 8.3 Calcium sulphate crystals before and after equilibration for 24 hrs at 60°C in aqueous-2-propanol mixtures (O/A=2, 3 M HCl)

As mentioned earlier, in a parallel study aiming to produce alpha-hemihydrate in chloride media it has been found that DH converts to HH/AH at 80°C and ≥ 3 M HCl after 5 hours of equilibration [17]. It was inferred that the addition of 2-propanol would further lower the water activity hence making possible conversion to proceed at lower temperature, i.e.

60°C. No doubt the solution chemistry of mixed organic-aqueous chloride solutions is such that does not allow for simple application of the rule. Refer in this respect to Chapter 4 where it was found the addition of 2-propanol to chloride solutions to increase rather than lower the solubility of metal chloride salts. No doubt this issue requires a separate in-depth study, which is beyond of the scope of this work.

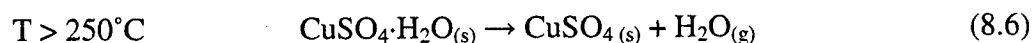
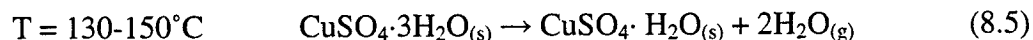
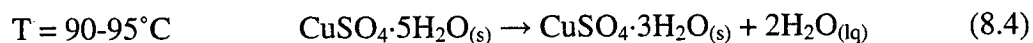
Finally, to rule out the possibility of inadvertently having HH converted to DH during the handling of the product (it has been reported that metastable HH will rapidly transform in DH in the temperature interval of 25-40°C, if the relative humidity of the medium is > 75%, phase transition time varying between 3 and 14 hrs [21]) special measures were taken that involved the following handling procedure: Equilibrated calcium sulphate crystals were washed with hot water and 2-propanol and dried in the oven at 50°C, under low relative humidity conditions. This procedure has been extensively verified and confirmed by other researchers of the McGill Hydrometallurgy Research Group to prevent conversion of DD to HH and vice-versa [17, 22]. Hence, it can be concluded that equilibration of gypsum crystals for up to 24 hours at 60°C in an aqueous-organic mixture containing 3 M HCl, 1.5 M MgCl₂ and 2-propanol (O/A = 1.00 and 2.00, respectively) did not induce the designed phase changes dehydration.

8.3.2 Copper Sulphate Pentahydrate

Copper sulphate pentahydrate (CuSO₄·5H₂O) is produced by crystallisation (usually vacuum cooling) for use in agriculture, as a mineral additive to animal food, in flotation of Zn/Pb concentrates (it acts as activator), in copper electrowinning and as an intermediate in the electronics industry [23].

Copper sulphate exists in three main crystal phases: pentahydrate (CSP, CuSO₄·5H₂O), trihydrate (CST, CuSO₄·3H₂O) and monohydrate (CSM, CuSO₄·H₂O). In contact with water, CSP is the stable phase under standard conditions, transforming into CST at 96°C, which in turn becomes unstable at ~ 130°C, transforming into CSM [24]. The formation of anhydrous copper sulphate as a stable form occurs only at elevated temperatures (> 250°C) in perfect dry conditions, and upon cooling it can convert back to

monohydrate if the relative humidity is high; above 600°C, decomposition of anhydrous copper sulphate occurs [25]. Dehydration proceeds according to the reactions [26]:



The thermodynamic stability of these phases is a function of temperature and water activity. Therefore, metastable and stable phases can occur separately, successively or simultaneously, depending on conditions and the kinetics of the crystallisation process. The equilibrium transition temperatures are lowered by the addition of components that may decrease water activity by activating and deactivating water molecules during the phase changes, such as sulphuric acid [27], other salts or organic solvents [14].

For reasons stated at the beginning of Section 8.1, it is sometimes preferable to reduce the number of crystallisation water molecules prior to further processing or shipping.*

For copper sulphate, this process has been accomplished so far either by applying heat (which is energy-intensive) or by resorting to tedious procedures involving chemical reactions and heating. Thus, Kovacs *et al.* [28] produced CSM by neutralising the free sulphuric acid content of melted CSP with an alkaline agent such as sodium, potassium or ammonium hydroxide, carbonate or hydrocarbonate, and removing four crystallisation water by drying the product at 80-150°C for 1 hr.

Based on previous knowledge related to properties of certain hydrophilic organic solvents (i.e. possibility to bind water molecules and thus initiate crystal dehydration), we investigated if 2-propanol is capable of achieving partial or total crystallisation water removal from CSP under milder, less energy-intensive conditions.

* For example, the present work was initiated following discussions with engineers from Canadian Copper Refineries in East Montreal, QC, who were interested to lower the shipping costs of copper sulphate pentahydrate used as flotation agent in their New Brunswick Zn/Pb mill concentrator.

Thus, $\text{CuSO}_4 \cdot 5\text{H}_2\text{O}$ crystals (10% wt/vol solids content) were equilibrated with pure 2-propanol at 21, 40 and 60°C for 3, 6, 24 and 30 hrs, as described in Section 8.2, to study the influence of temperature and residence time on dehydration extent. A single test was performed at 60°C using azeotrope (contains 88% wt. 2-propanol), to assess the influence of existing water on the system. The effect of solvent renewal on crystallisation water removal, i.e. repulping of partly dehydrated $\text{CuSO}_4 \cdot x\text{H}_2\text{O}$ crystals ($x=3$ and 1) with fresh pure 2-propanol (10% wt/vol solids content), was tested at 60°C for 6 hrs.

Table 8.1 offers a summary of the crystal dehydration tests, a brief description of experimental conditions and the final results (number of crystallisation water molecules determined via XRD and TGA analyses, Appendix E).

Table 8.1 Synopsis of copper sulphate dehydration with 2-propanol (10% wt/vol solids)
IN: 30 g $\text{CuSO}_4 \cdot 5\text{H}_2\text{O}$ (i.e. 10.82 g H_2O), 300 mL organic solvent

T (°C)	Time (hrs)	$\text{CuSO}_4 \cdot 5\text{H}_2\text{O}$		$\text{CuSO}_4 \cdot 3\text{H}_2\text{O}$		$\text{CuSO}_4 \cdot \text{H}_2\text{O}$	H_2O Released (ml)	[Cu] _{sol} (ppm)	Aqueous- Organic Sol'n OUT (mL)
		OUT		OUT		OUT			
		(g)	(%)	(g)	(%)	g (%)			
21	3	27.75	98.50	0.51	1.80	-	0.69		295
	6	26.21	92.00	2.29	8.00	-	0.81 3.09		
	24	11.77	46.00	13.82	54.00	-		0.25	
40	3	27.18	94.00	1.72	6.00	-	0.59		290
	6	23.81	79.36	6.2	20.64	-	0.70 4.32	0.35	
	24	0.43	1.60	25.42	98.30	-	5.36	0.37	
	30	-	0	21.85	(mixt.)	tri/mono		0.40	
60	3	-	0	20.95	100	-	5.59	0.30	280
	6	-	0	22.61	100	-	5.17 4.50	0.36	
	24	-	0	25.31	100	-	8.66	0.38	
	30	-	0	-	0	21.58 (100%)		0.42	
60 (Aze.)	6	26.60	100	-	0	-	1.25		285
	24	28.92	~100	traces	0	-	0.41	41.60	

Crystal repulping tests: 60°C, 6 hrs, pure 2-propanol, 10% solids content	
Crystals IN	Crystals OUT
30 g CuSO ₄ ·5H ₂ O	22.61 g CuSO ₄ ·3H ₂ O
20 g CuSO ₄ ·3H ₂ O	17.3 g CuSO ₄ ·H ₂ O
15 g CuSO ₄ ·H ₂ O	14.3 g CuSO ₄ ·H ₂ O

- **Experimental Results and Nature of Solid Phase**

During equilibration of copper sulphate pentahydrate in 2-propanol, it was observed that, depending on conditions, the solution becomes cloudy due to a population of extremely fine bluish-white particles in suspension while heavier deep-blue crystals accumulated at the bottom. At the end of the experiment, the solution was decanted, the coarser crystals retrieved and the fine particles separated by filtration from the mother liquor. Upon drying, both solid products were weighed, analysed by XRD and the results compared to different standard spectra (CuSO₄·xH₂O x=1, 3 and 5) contained in the computer's database to identify hydrate form. If dehydration occurs, the released crystallisation water perturbs the crystal structure and induces a rearrangement of copper and sulphate ions, change that should translate in modifications of the XRD spectrum of initial compound. The number of crystallisation water molecules was also estimated by the TGA method, as the percent weight loss upon gradual heating. Percentage of hydrate formed/detected was approximately evaluated comparing the mass of final product fractions to the initial mass of pentahydrate introduced.

From Table 8.1, it can be observed that the extent of dehydration (i.e. volume of released water) strongly depends on both the temperature and equilibration time.

At 21°C, the main phase is the pentahydrate for short residence time (98-92% for 3-6 hrs), whereas after 24 hrs approx. 50% of the crystals converted to trihydrate. The continuation of the experiment for 30 hrs was not envisaged since only slightly more CST was expected to form.

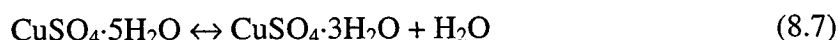
At 40°C, the percentage of trihydrate increases with residence time, from 6% after 3 hrs to 98% after 24 hrs (the balance being pentahydrate). Further equilibration for 30 hrs leads to a mixture of trihydrate and monohydrate, with no pentahydrate detected.

A temperature of 60°C completes the 100% pentahydrate-to-trihydrate conversion in 3 hrs only, whereas exclusively monohydrate was found after 30 hrs.

The losses in final aqueous-organic solution are attributed to evaporation (since it increased with temperature) and retention in the filter cake (during decantation and filtration).

The copper content detected in solution following equilibration is the result of copper sulphate dissolution in traces of water removed from the crystals; although slightly increasing with elevated temperatures and prolonged equilibration periods, the low concentration (< 0.5 ppm Cu) is explained both in terms of the small quantity of water displaced and extremely low solubility of copper sulphate pentahydrate in 2-propanol [24]. When using azeotrope at 60°C for 24 hours, copper concentration in solution reaches ~42 ppm due to higher water content of azeotrope (10 % vol/vol).

The experiments involving azeotrope at 60°C did not result in definite crystal dehydration, the pentahydrate with small amounts of trihydrate being the only phase detected after 24 hrs. According to Le Châtelier's principle, the presence of water in the system (the azeotrope contains 12% H₂O by wt.) does not allow the dehydration equilibrium to proceed towards water loss (eqn. (8.7)); moreover, the azeotrope is already "saturated" with water molecules and does not show the same affinity to form hydrogen bonds with new molecules as a pure organic:



Repulping experiments at 60°C demonstrated that the trihydrate can be further converted to the monohydrate by equilibration in fresh organic for 6 hrs (i.e. in total for 12 hours), whereas the same was achieved in 30 hours without repulping. On the other hand, further repulping of the monohydrate with fresh 2-propanol failed to produce the anhydrous salt. This is not surprising, since the conversion temperature from monohydrate to anhydrous form is extremely elevated (> 250°C) and the decrease in water activity under the present experimental conditions was not apparently strong enough to sufficiently lower this transition temperature.

To summarise, the most efficient and rapid procedure to obtain copper sulphate monohydrate from the pentahydrate is to equilibrate the latter for 3-6 hrs at 60°C to

produce the trihydrate, which will be further equilibrated at 60°C in fresh organic for 6 hrs to form the monohydrate.

In addition to beneficial influence of temperature and equilibration time, Wendlandt [26] showed that the dehydration process is also a function of particle size, vapour pressure-temperature curve of the hydrate system, reactor geometry, stirring rate, etc. Considering these, it can be inferred that, at constant temperature, the use of a larger-sized reactor with mechanical impeller (as opposed to flasks with magnetic stirring bars) and finer copper sulphate particles (i.e. grind) would shorten the dehydration time and increase the percentage of lower hydrate formed. Also, if a more elevated temperature is sought for more efficient and rapid dehydration, another water-miscible organic solvent with higher boiling point may be selected.

- ***Crystal Dehydration Mechanism***

Most phase transformation mechanisms involve a dissolution-recrystallisation process, in which the initial crystal gradually dissolves in its own dislodged (unbound) crystallisation water, then the new phase nucleates (mainly homogeneously) in the volume of solution [20].

Cabrera and Vermilyea [29] indicated that the dissolution of a single close-packed face of a crystal should be the reciprocal of its growth, i.e. the growth unit will integrate/disintegrate at a site of the lowest binding energy for its orientation, step, kink or vacancy (Figure 8.4). This statement holds true at very low undersaturations only, but at higher undersaturations there are important differences in the sources of available steps. Balykov *et al.* [30] signal strong asymmetry of growth and dissolution processes even for small deviations from equilibrium. They demonstrated that kink density monotonically increases with supersaturation and decreases with undersaturation and generally growth rates are always higher than the corresponding dissolution rates. If the corners and edges of the crystal are exposed, they will also act as source of steps. A dissolving crystal will not be bounded by low index faces but by curved or rough surfaces from which the atoms can be removed at any point. The dissolution rate will depend on whether the crystals are isotropic or anisotropic and the nature of the rate-controlling step (i.e. transport, surface or mixed), which in turn is influenced by agitation, temperature and dissolution medium.

If dissolution is transport-controlled, then the rate is independent of crystal habit, whereas the opposite is true for surface/mixed control [31].

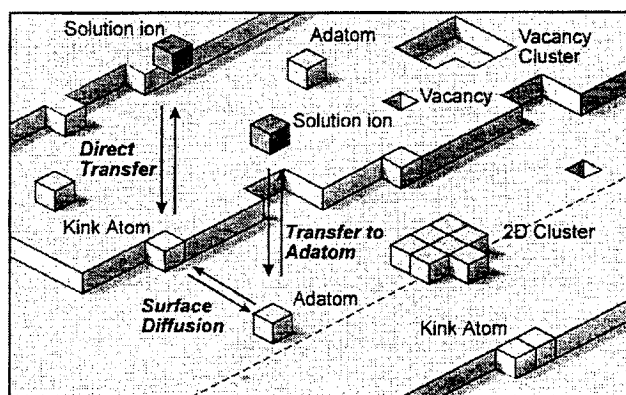


Figure 8.4 The continuous surface growth (or dissolution) model [30]

During copper sulphate equilibration with 2-propanol, the surface defects of the crystal (dislocations, grain boundaries, etc.) act as sorption sites for organic molecules which adhere at the surface to form a superficial layer. This process is similar to polymer swelling in solvents prior to dissolution. From these sites, organic molecules diffuse deeper into the bulk of the solid along the defects and are capable of forming hydrogen bonds with crystallisation water molecules from the lattice and eventually removing them from the solid in a liquid form. The existence of liquid water near the surface or in the bulk of crystal favours additional dissolution of copper and sulphate ions, by loosening them from the lattice and removing them via solvation [32].

When the organic-aqueous solution becomes supersaturated with respect to copper sulphate, the new phase starts precipitating as a lower hydrate form (since part of the water is bound by the organic and unavailable to report to the hydrate). The point where a clear copper sulphate solution forms is never reached; the mixture always contains crystals (both hydrate forms) in equilibrium with an organic-aqueous mixture. This process is gradual and continuous until equilibrium between water in solution and water in solid form is reached (i.e. the organic becomes saturated with water and cannot bond/remove additional molecules) or until the crystals are in their entirety converted to the most stable hydrate form.

Tereshkova [33] suggests a new concept of the mechanism of crystal dehydration, involving a spiral character (decaying spiral) of water removal, including multiple evolution/adsorption cycles, which explains why it is so difficult to obtain certain anhydrous compounds under moderate conditions. During these stages of separation, partial return to the system, reaction with the hydrolysis products and repeated evolution, only part of the water is removed in each cycle, but overall the fraction of water retained by the substance decreases. The mechanism of reversible consecutive dehydration is characterised by the increase of enthalpy (per mole of removed water) from cycle to cycle and this causes difficulties in separating the residual crystallisation water, necessitating an increase in temperature (rather than in the duration of heating at a definite temperature). The stable retention of residual water in some compounds is associated with the crystal structure of various forming hydrates, i.e. the strength of hydrogen bonds between crystallisation water molecules and the presence of these bonds between water molecules and existing oxyanions (such as SO_4^{2-} in the case of copper sulphate) in the lattice. To facilitate water removal and crystal dehydration, this kind of bonds must be either absent or present in a limited amount.

Following the validation via XRD and TGA of type of crystal hydrate produced, the respective particles were also investigated by SEM to study any change in morphology upon phase transformation (Figure 8.5).

Copper sulphate pentahydrate belongs to the triclinic-pinacoidal system with cell parameters $a = 6.12\text{\AA}$, $b = 10.7\text{\AA}$, $c = 5.97\text{\AA}$, $\alpha = 82^\circ$, $\beta = 107^\circ$, $\gamma = 102^\circ$, forming thick prismatic crystals; the trihydrate crystallises in the monoclinic system with cell parameters $a = 5.59\text{\AA}$, $b = 13.03\text{\AA}$, $c = 7.34\text{\AA}$, $\beta = 97.1^\circ$ while the monohydrate is orthorhombic-dipyramidal with cell parameters $a = 6.69\text{\AA}$, $b = 8.39\text{\AA}$, $c = 4.82\text{\AA}$ [33].

From Figure 8.5, it can be observed that the pentahydrate crystals retain their characteristic prismatic shape, indicating that no dissolution/phase transformation occurred. Trihydrate and monohydrate particles have small size and irregular morphology (not crystallising in the “perfect” predicted system), which suggests homogeneous nucleation and precipitation from solution following dissolution of original phase.

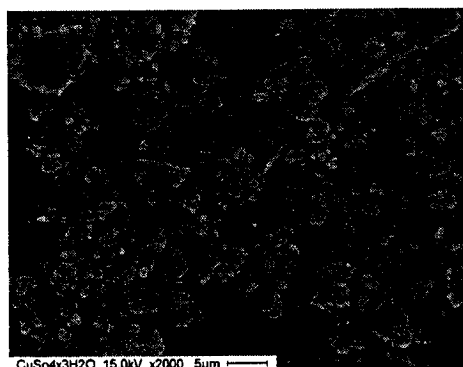
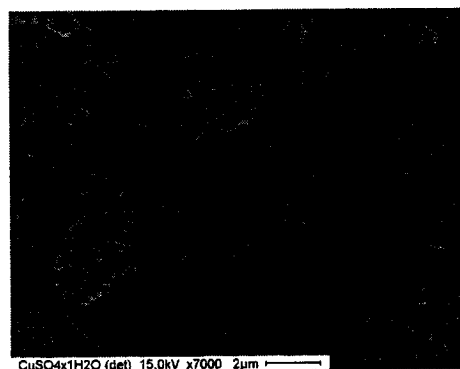
(a) $\text{CuSO}_4 \cdot 5\text{H}_2\text{O}$ (21°C, 6 hrs)(b) $\text{CuSO}_4 \cdot 3\text{H}_2\text{O}$ (60°C, 6 hrs)(c) $\text{CuSO}_4 \cdot \text{H}_2\text{O}$ (60°C, 30 hrs).

Figure 8.5 SEM micrographs of various copper sulphate hydrates

8.4 Summary and Conclusions

1. This study confirmed 2-propanol to be an effective agent to cause dehydration of copper sulphate pentahydrate ($\text{CuSO}_4 \cdot 5\text{H}_2\text{O}$) to trihydrate ($\text{CuSO}_4 \cdot 3\text{H}_2\text{O}$) and monohydrate ($\text{CuSO}_4 \cdot \text{H}_2\text{O}$), respectively.
2. For copper sulphate, the extent of dehydration strongly depends on temperature, equilibration time and renewal of solvent: at constant temperature, the extent of dehydration increases with equilibration time whereas an increase in temperature drastically shortens the phase transformation time; finally, repulping in fresh solvent of partially dehydrated crystals further enhances the extent of dehydration.
3. At 21°C, the main phase is the pentahydrate for short residence time, whereas after 24 hrs approx. 50% of the crystals converted to trihydrate. At 40°C, the percentage of trihydrate increases with residence time, to 98% after 24 hrs (the

balance being pentahydrate), and a mixture of trihydrate and monohydrate is detected after 30 hrs. At 60°C, complete pentahydrate-trihydrate conversion occurs in 3 hrs only, whereas exclusively monohydrate is found after 30 hrs.

4. The experiments involving azeotrope at 60°C did not result in definite crystal dehydration, the pentahydrate with small amounts of trihydrate being the only phase detected after 24 hrs.
5. The phase transformation mechanism involves apparently a dissolution-recrystallisation process, in which the initial crystal gradually dissolves in its own dislodged (unbound) crystallisation water, and then the new phase nucleates (mainly homogeneously) in the volume of solution.
6. In contrast to copper sulphate pentahydrate, 2-propanol failed to induce dehydration of gypsum when equilibrated for 6 and 24 hours at 60°C in an aqueous-organic mixture containing 3 M HCl, 1.5 M MgCl₂ and 2-propanol (O/A = 1.00 and 2.00, respectively). Apparently there exists a complex (not understood) interaction between alcohol and chloride-based aqueous solutions that rendered 2-propanol ineffective.

References

- [1]. G. Surendranath and S.N. Vyas, "Dehydration of salts" *Chemical Industry Developments, Incorporating CP&E*, **11**, pp. 23-26, (1977).
- [2]. R.K. Osterheld and P.R. Bloom, "Dehydration kinetics for barium chloride dehydrate crystals" *The Journal of Physical Chemistry*, **82(14)**, pp. 1591-1596, (1978).
- [3]. G.J. Kipouros and D.R. Sandoway, "A thermo-chemical analysis of the production of anhydrous MgCl₂" *Journal of Light Metals*, **1**, pp. 111-117, (2000).
- [4]. S.S. Berdonosov, V.Y. Lebedev, I.V. Melikhov and E.V. Kozorezova, "Dehydration of Crystal Hydrates in Microwave Fields" *Russian Journal of Physical Chemistry*, **69(4)**, pp. 666-668, (1995).

- [5]. E. Bergmann, "Process for the dehydration of inorganic salts", GB Patent No. GB 595128, issued November 27, 1944.
- [6]. G. Nencetti and A. Pennacchi, "Drying and dehydration of hydrated salts by azeotropic distillation" *Chim. Ind.* **46(5)**, pp. 518-525, (1964).
- [7]. M. Baccaredda, G. Nencetti and R. Tartarelli, "Dehydration of hydrated inorganic salts by azeotropic distillation" Italian Patent No. IT 713334, issued September 21, 1966.
- [8]. S.N. Vyas and S.N. Gavini, "Dehydration of salts using water-immiscible organic solvents" *Indian Journal of Technology*, **24**, pp. 322-324, (1986).
- [9]. S.N. Vyas and S.N. Gavini, "Dehydration of salts using organic solvents" *Indian Journal of Technology*, **20**, pp. 211-214, (1982).
- [10]. R.S. Gärtner and G.J. Witkamp, "Wet calcining of trona (sodium sesquicarbonate) and bicarbonate in a mixed solvent" *Journal of Crystal Growth*, **237-239**, pp. 2199-2204, (2002).
- [11]. R.M. Geertman, G.J. Witkamp, J.A.M. Meijer, H. Oosterhof and G.M. van Rosmalen, "Production of water-free soda" US Patent No. US 6334989, issued January 1, 2002.
- [12]. M.M. Hourn, F.S. Wong, D.H. Jenkins, G.J. Sheehan and M. Kodama "Anhydrous magnesium chloride" US Patent No. US 6143270, issued September 7, 2000.
- [13]. P.S.R. Prasad, N. Ravikumar, A.S.R. Krishnamurty and L.P. Sarma, "Role of impurities in gypsum-bassanite phase transition: a comparative Raman study" *Current Science*, **75(12)**, pp. 1410-1414, (1998).
- [14]. V.V. Udovenko and T.F. Mazanko, "Liquid-vapour equilibrium in the propan-2-ol-water and propan-2-ol-benzene system" *Russian Journal of Physical Chemistry*, **41(7)**, pp. 863-866, (1967).

- [15]. H. Zhu, C. Yuen and D.J.W. Grant, "Influence of water activity in organic solvent + water mixtures on the nature of the crystallizing drug phase. I. Theophylline." *International Journal of Pharmaceutics*, **135**, pp. 151-160, (1996).
- [16]. H. Degn and N.-U. Frigaard, "Membrane inlet manometry for the measurement of water activity in aqueous and organic solutions" *Analytica Chimica Acta*, **274**, pp. 355-359, (1993).
- [17]. S. Girgin and G.P. Demopoulos, "Production of the High Value Material, Alpha-CaSO₄ Hemihydrate Out of Spent CaCl₂ Solutions by Reaction with H₂SO₄", in *EPD Congress 2004*, (edited by M.E. Schlesinger), TMS, Warrendale, Pa., pp.627-640, (2004).
- [18]. E.M. Sipple, P. Bracconi, P. Dufour and J.C. Mutin, "Electronic microdiffraction study of structural modifications resulting from the dehydration of gypsum. Prediction of the microstructure of resulting pseudomorphs" *Solid State Ionics*, **141-142**, pp. 455-461, (2001).
- [19]. G.H. Nancollas, M.M. Reddy and F. Tsai, "Calcium sulphate dihydrate crystal growth in aqueous solution at elevated temperatures" *Journal of Crystal Growth*, **20**, pp. 125-134, (1973).
- [20]. I.S. Sirota, S.V. Dorozhkin, M.V. Kruchinina and I.V. Melikhov, "Phase transformation and dehydration of calcium sulphate dihydrate in solution studied by SEM", *Scanning*, **14**, pp. 269-275, (1992).
- [21]. T.K. Chan and B.W. Darvell, "Effect of storage conditions on calcium sulphate hemihydrate-containing products" *Dental Materials*, **17**, pp. 134-141, (2001).
- [22]. Y. Ling, "*Direct Production of Alpha-Calcium Sulphate Hemihydrate from Sulphate Media*", PhD Thesis, McGill University, Montreal, PQ, 2004.
- [23]. M. Giuliatti, M.M. Seckler, S. Derenzo and J.V. Valarelli, "Changes in copper sulphate crystal habit during cooling crystallisation" *Journal of Crystal Growth*, **166**, pp. 1089-1093, (1996).

- [24]. W.F. Linke and A. Seidell (editors), *Solubilities of Inorganic and Metal-Organic Compounds (a compilation)* 4th edition, Van Nostrand, Princeton, N.J., (1958).
- [25]. R.V. Siriwardane, J.A. Poston, Jr., E.P. Fisher, M.S. Shen, A.L. Miltz, "Decomposition of the sulphates of copper, iron (II), iron (III), nickel and zinc: XPS, SEM, DRIFTS, XRD and TGA study" *Applied Surface Science*, **152**, pp. 219-236, (1999).
- [26]. W.W. Wendlandt, "A new look at the thermal properties of copper sulphate pentahydrate" *Thermochimica Acta*, **1**, pp. 419-427, (1970).
- [27]. H. Majima and Y. Awakura, "Water and solute activities in the solution systems $H_2SO_4-CuSO_4-H_2O$ and $HCl-CuCl_2-H_2O$ " *Metallurgical Transactions B*, **19B**, pp. 347-354, (1998).
- [28]. F. Kovacs, A. Ándor and T. Palagyi, "Process for the preparation of stable copper (II) sulphate monohydrate applicable as trace element additive in animal fodders" US Patent No. US 4315915, issued February 16, 1982.
- [29]. N. Cabrera and D.A. Vermilyea, "The growth of crystals from solution" in *Growth and Perfection of Crystals*, (edited by R.H. Doremus, B.W. Roberts and D. Turnbull), pp. 393-408, Wiley, New York, N.Y., (1958).
- [30]. L.N. Balykov, M. Kitamura, I.L. Maksimov and K. Nishioka, "Growth and dissolution kinetics in step structure" *Journal of Crystal Growth*, **198/199**, pp. 32-37, (1999).
- [31]. H. Burt and A.G. Mitchell, "Effect of habit modification on dissolution rate" *International Journal of Pharmaceutics*, **5**, pp. 239-251, (1980).
- [32]. G.E. Yakubov and V.I. Boiko, "The thermodynamic equation for the dissolution of solids in liquids" *Journal of Molecular Liquids*, **91**, pp. 33-46, (2000).

- [33]. S.G. Tereshkova, "Mechanism of reversible consecutive dehydration of phosphate crystal hydrates" *Russian Journal of Physical Chemistry*, **68(4)**, pp. 666-670, (1994).
- [34]. M Giuliatti, M.M Seckler, S Derenzo, L.H. Schiavon, J. Nyvlt and J.V. Valarelli, "Effect of selected parameters on crystallisation of copper sulphate pentahydrate" *Cryst. Res. Technol.*, **34(8)**, pp. 959-967, (1999).

Chapter 9. Synopsis

9.1 Introduction

Key findings from each component of this work have already been summarised at the end of each of the previous Chapters. In this Chapter, global conclusions are given by considering the whole of the work rather than the individual parts. Subsequently, what is considered as an original contribution to knowledge is outlined, and finally ideas for continuation of this work are provided.

9.2 Global Conclusions

The method of Solvent Displacement Crystallisation (SDC) was studied in the present research work and proposed as a cleaner, less energy-intensive alternative to some conventional crystallisation methods. The technique involves the addition of low-boiling point, water-miscible organic solvents (MOS) to aqueous solutions to cause the crystallisation of inorganic salts, based on the concept of "salting out effect". This enables the separation of electrolytes from their aqueous solutions via precipitation and filtration. The solvent is subsequently recovered for reuse by employing relatively inexpensive low-temperature or vacuum distillation.

On the basis of the findings of the systematic study undertaken in this work, the following global conclusions can be drawn:

1. After subjecting the laboratory results to a theoretical analysis, it was concluded that SDC occurs because of the competition between the polar organic molecules and inorganic ions for the water molecules. When water-miscible organic solvents are added to the electrolyte solution, they modify the structure, properties and behaviour of water, leading to changes in the mobility and solvation of inorganic ions. Since the organic solvent exhibits a higher affinity for water due to its ability to form stable hydrogen bonds with water molecules, this leads to progressive capture of hydration water, causing thus salt precipitation. The addition of organic solvent affects thus the

water activity, which decreases upon organic addition; since the ions are soluble in “free water” only, any change in solution composition that results in decreasing the water activity will influence the solubility of the dissolved solute.

2. Criteria for the selection of organic solvents with suitable physical and chemical properties were established and various organic compounds were screened to determine their amenability to SDC. It was established that the main properties to be considered were: miscibility with water (polar character), low dielectric constant, boiling point under 90°C, not reactive with aqueous phase elements, non-toxic, inexpensive. Based on these general criteria, the following organic solvents believed to provide the best salting-out performances were selected for further practical testing: methanol, ethanol, 2-propanol, tert-butanol, acetone, methyl-ethyl-ketone (MEK), ethyl-acetate and isopropyl-acetate. Finally, **2-propanol** was considered to meet most of the selection criteria outlined in Section 4.2.1 for the organic solvent of choice in SDC and opted for use in further systematic in-depth studies.
3. The applicability of this crystallisation technique to various salt systems of practical interest in hydrometallurgy (i.e. sulphate and chloride compounds) was studied, by developing a screening procedure at 21°C. Regarding the crystallisation of sulphate salts from the system $\text{MSO}_4\text{-H}_2\text{SO}_4\text{-H}_2\text{O}$, 2-propanol acted as an efficient salting-out agent for the metal sulphates tested (with the exception of Fe^{3+} compound, which was not precipitated). An organic-to aqueous (O/A) ratio of 4 removed more than 90% of metal from solution (with the exception of magnesium) in the form of crystalline sulphates with various number of crystallisation water molecules. The differences in crystallisation behaviour were attributed to differences in hydration energy (ΔH), defined as the energy required for a hydrated ion to be separated from its bound water; this is the measure of the hydration of the ion relative to the bulk solvent. As a general rule when comparing the hydration energy for different ions, the smaller the ΔH the easier it is for the water molecules to be removed from the hydration sphere.
4. None of the tested metal chlorides (MgCl_2 , ZnCl_2 , FeCl_2 , AlCl_3) could be successfully separated from $\text{HCl-H}_2\text{O}$ system with 2-propanol. As the alcohol was

added to the aqueous solution, it formed a homogeneous mixture without separating the salt, even for high organic contents. This was explained in terms of enhanced metal chlorides solubilities in non-aqueous solvents relative to water by formation of chloro-complexes of larger stability constants. The preferential formation of chloro-complexes in mixed aqueous or organic solvents is the result of the almost linear drastic increase in the activity of Cl^- with mole fraction of organic.

5. Because of the promise in applying SDC to nickel sulphate recovery in copper electrorefining, the system 2-propanol- NiSO_4 - H_2O - H_2SO_4 was selected for in-depth study. It was determined that SDC at low supersaturation in the presence of seed/recycled crystals (within the metastable zone) promotes growth of tetragonal α - $\text{NiSO}_4 \cdot 6\text{H}_2\text{O}$ with excellent settling/dewatering properties and chemical purity superior to the crystals produced by conventional evaporative crystallisation..
6. The present work determined that calcium sulphate can be removed as gypsum ($\text{CaSO}_4 \cdot 2\text{H}_2\text{O}$) from HCl media (mixed sulphate-chloride) by using 2-propanol. Consequently, SDC has the potential of providing an alternative residual sulphate removal technique from CaSO_4 - CaCl_2 -HCl media.
7. It was established that SDC is applicable to the system Na_2ZnO_2 - NaOH - H_2O (of interest to zinc recovery by caustic leaching of EAF dust) to produce ZnO and regenerate NaOH. 2-propanol addition to the highly alkaline media induced liquid-liquid separation (i.e. the organic was salted out from the aqueous layer); this separation in a ternary mixture (i.e. salt-water-miscible organic) is favoured by large differences in affinities of salt ions to water and the organic component and strong self-aggregation tendency of the organic component, which becomes thus more hydrophobic, exhibiting weaker interactions with water. The larger the organic molecule, the higher the self-aggregation tendency and separation (i.e. the hydrophobic character); consequently, **methanol**, a water-miscible organic solvent with a smaller molecule was subsequently employed.

8. The zincate-zincite transformation (i.e. ZnO precipitation) during SDC is believed to occur due to the methanol-catalyzed decomposition of a hydroxyl salt precursor existing in solution. Zinc oxide formation cannot be explained in terms of simple pH decrease through dilution (i.e. the phase diagram shifted to the pH regions where ZnO is insoluble); more probably, due to its ability to form stable hydrogen bonds with water molecules, it appears that the alcohol has the ability of dehydrating the zincate complex and inducing decomposition upon integration into crystal lattice, in the same manner that elevated temperatures would do during the hydrothermal process.
9. This study confirmed 2-propanol to be an effective agent to cause dehydration of copper sulphate pentahydrate crystals ($\text{CuSO}_4 \cdot 5\text{H}_2\text{O}$) to trihydrate ($\text{CuSO}_4 \cdot 3\text{H}_2\text{O}$) and monohydrate ($\text{CuSO}_4 \cdot \text{H}_2\text{O}$), respectively. For copper sulphate, the extent of dehydration strongly depends on both the temperature and equilibration time: at constant temperature, the extent of dehydration increases with equilibration time whereas an increase in temperature drastically shortens the phase transformation time. The phase transformation mechanism involves a dissolution-recrystallisation process, in which the initial crystal gradually dissolves in its own dislodged (unbound) crystallisation water, and then the new phase nucleates (mainly homogeneously) in the volume of solution.

9.3 Claims to Originality

1. It is the first time that a systematic study of Solvent Displacement Crystallisation, as it applies to the removal of metal salts from aqueous solutions was undertaken, both from a fundamental perspective and from the standpoint of application to hydrometallurgical processes.
2. The underlying principles of chemistry, structural aspects and solvation phenomena that govern the salting-out process in aqueous-organic mixtures were identified and described and a physical model was developed, contributing towards the scientific understanding of the SDC process.

3. Selection criteria for suitable organic solvents were established, relating for the first time the physical and chemical properties of the organics to fundamentals of the process and the experimental conditions. Classes of suitable solvents were identified and screening tests were performed to better assess the organics' behaviour.
4. It was the first time that supersaturation control and seed addition/product recycling were applied in conjunction to the SDC method.
5. For the first time, it was demonstrated that superior crystallisation results are obtained when SDC is controlled within the metastable zone established via solubility and critical supersaturation measurements. In this respect the comprehensive study of nickel sulphate hexahydrate crystallisation constitutes an original contribution to knowledge.
6. Equally novel is the effective use of SDC in lowering the residual sulphate content of HCl-MeCl_x media in the form of gypsum.
7. For the first time it has been demonstrated that apart from salt crystallisation, methanol, when applied to alkaline zinc media (namely Na₂ZnO₂-NaOH-H₂O), induces precipitation of ZnO with simultaneous regeneration of NaOH. The methanol-assisted mechanism of ZnO precipitation was proposed to be equivalent to that of hydrothermal precipitation, with methanol playing the dehydrating role played by the temperature in the latter system.
8. For the first time, low boiling point organic solvents were employed to induce phase transformation and crystal dehydration for copper sulphate, at temperatures below the thermodynamically-predicted transition temperatures. The extent and kinetics of the dehydration process were evaluated as a function of several factors.

9.4 Recommendations for Future Work

Future work of both fundamental and practical nature is proposed below, that may advance further the knowledge and technology of Solvent Displacement Crystallisation and its potential applications.

1. Chemical thermodynamic data should be reviewed, to develop models estimating the activities (both water and salt) and solubilities in aqueous-organic mixtures.
2. Screening and selection of organic solvents with suitable chemical and physical properties that can induce crystallisation in chloride systems should be investigated, and subsequent in-depth SDC tests on systems of practical interest (i.e. MgCl_2 , ZnCl_2) should be conducted.
3. It is proposed to study the selectivity issue during SDC in multiple salt systems, by assessing: (a) the extent to which an additional component influences the behaviour of the salt to be recovered; (b) the selectivity windows in certain salt groups (e.g. CoSO_4 - NiSO_4 and CuSO_4 - NiSO_4) that allow the possibility of fractional precipitation; (c) co-precipitation of mixed salts during SDC; (d) SDC in mixed sulphate-chloride solutions.
4. The aqueous-organic solvent separation following SDC should be investigated, in order to design an efficient separation technique that prevents organic losses and aqueous phase contamination by organic carry-over. In this context the separation of 2-propanol in highly caustic solvents should be further investigated.

Appendix A. Modified Free Acid Titration Methodology

Free acid concentration in strong $\text{H}_2\text{SO}_4\text{-MSO}_4$ ($\text{M}=\text{Fe}$, Zn , Ni , etc.) solutions is impossible to be accurately determined using direct pH measurements; analysis by simple neutralisation with an alkaline titrant alone is very problematic also. For example, titrating with NaOH proves ineffective as neutralisation raises the analyte's pH, causing result-distorting metal hydrolysis to occur. Consequently, a method utilising a complexing agent was considered.

Rolia and Dutrizac [1] developed an analytical method that employed EDTA as a complexing agent; Mg_2EDTA solution is added to the diluted aliquot sample prior to neutralisation to exchange Mg^{2+} for the hydrolysable metals present in the analyte. This prevents any acid-producing metal hydrolysis to occur. However, since problems were encountered in applying this procedure to the experimental samples of interest, regardless of metal-acid medium, modifications to this methodology were necessary.

Principe [2] modified and adapted the previously described technique in order to develop an accurate acid-measurement means in $\text{H}_2\text{SO}_4\text{-MSO}_4$ ($\text{M}=\text{Fe}$ and Zn) solutions based on the endpoint pH value without the risk of errors (5-20%) induced by the unmodified method. The present research project adopts Principe's method and applies it to the system $\text{H}_2\text{SO}_4\text{-NiSO}_4$.

- ***Preparation of Standards***

Daily standardisation not only determines the endpoint pH, but also corrects for pH calibration error and $\text{Mg}_2\text{EDTA}^{2-}$ variations among batches. The procedure involved the preparation and use of one standard (solution A) of composition comparable to the experimental samples of interest. A second standard (solution B), also of comparable composition to experimental samples, was prepared and used to validate the standardisation with solution A. Acid levels of solutions A and B were different, respecting upper and lower limits of a range in which the experimental samples fall (Table A.1). A detailed description of this analytical method follows.

Table A.1 Preparation of H₂SO₄-NiSO₄ standard solutions

Standard Type	1N NaOH (mL)	Endpoint pH (*)	[H ₂ SO ₄] _{estimated} (g/L)	[H ₂ SO ₄] _{calculated} (g/L)	Ni (g/L)
A	4.05	6.344	200	198.76	17.96
B	6.08	6.339	300	297.95	18.63

(*) value slightly differs upon daily standardisation

- ***Titration Methodology***

I. Titration Procedure

- (1) The glass pH electrode (Fisher Accu-pHast) is calibrated by using three buffer solutions of pH 1, 4 and 7.
- (2) pour 50 mL of Mg₂EDTA solution into 150 mL beaker equipped with a magnetic stirring bar, mounted in auto-titration set-up (Radiometer Copenhagen Titrab™90), equipped with a high precision ABU 900 Autoburette System and glass pH electrode;
- (3) pipet 1.00 mL of sample into same beaker, under mild agitation;
- (4) dilute with de-ionised water to 120 mL mark on beaker (by eye);
- (5) perform “standardisation” or “sample measurement”.

II. Standardisation

- (1) use the two standard solutions (A and B) previously described (sulphuric acid and nickel content may differ but should respect the concentration range of the experimental samples);
- (2) use solution A as the standardisation analyte and prepare the titration solution as in the “Titration Procedure” above;
- (3) set titrator to allow for a manual shutdown;
- (4) calculate the amount of NaOH 1N needed to neutralise analyte solutions A and B;
- (5) press RUN to start auto-titrator feeding 1N NaOH to solution A;
- (6) record the exact solution pH value at which the calculated titrant volume has been added (endpoint pH);
- (7) press STOP to end standardisation titration (manual shutdown);

- (8) program the titrator by setting the pH endpoint to the recorded value ($\text{pH}_{\text{endpoint}}$) and enable automatic predose to a set pH value ($\text{pH}_{\text{predosed}} < \text{pH}_{\text{endpoint}}$), to reduce overall titration time;
- (9) follow the “Titration Procedure” above using solution B as the analyte, to verify that standardisation just performed as valid;
- (10) follow “Sample Measurement” as detailed below;
- (11) the determined acid concentration should equal the known acid concentration:
 - (a) if not equal, redo standardisation with solutions A and B
 - (b) if equal, standardisation was properly performed; experimental samples may now be analysed (“Titration Procedure” then “Sample Measurement”).

III. Sample Measurement

- (1) set to pertinent stored ENDPOINT methodology;
- (2) press RUN to add 1N NaOH titrant automatically;
- (3) following automatic shutoff, the total volume added to reach end-point is printed;
- (4) calculate the acid concentration:

$$m_a = N_a * E_g * V_{\text{sol}}$$

where:

- E_g = the gram-equivalent (g/equiv)
- V_{sol} = the total volume of solution (mL)
- $N_a = V_b * N_b / V_a$: acid's normal concentration (equiv/L)
- V_a = volume of analyte used in titration (mL)
- V_b = volume of NaOH used in titration (mL)
- N_b = NaOH normal concentration (equiv/L)

References

- [1]. E. Rolia, J.E. Dutrizac, “The Determination of Free Acid in Zinc Processing Solutions”, *Canadian Metallurgical Quarterly*, **23(2)**, pp. 159-167, (1984).
- [2]. F.T Principe, “Separation of Iron (III) from Zinc Sulfate-Sulfuric Acid using Organophosphoric Acid Extractants”, M.Eng. Thesis, McGill University, Montreal, PQ, (1999).

Appendix B. Liquid-Liquid Separation Techniques

B.1 Fractional Distillation

When the boiling-point differences of two components are not large ($< 30^{\circ}\text{C}$), fractional distillation, as opposed to simple distillation, must be used to achieve a good separation. Pavia *et al.* [1] give detailed information on distillation techniques and related theoretical background in their comprehensive book.

- *Principles of Fractional Distillation*

When an ideal solution of two liquids (L1 and L2) is separated by simple distillation, the first vapour produced will be enriched in the lower-boiling point component (say L1), as indicated by the 2-propanol-water phase diagram (Figure B.1).

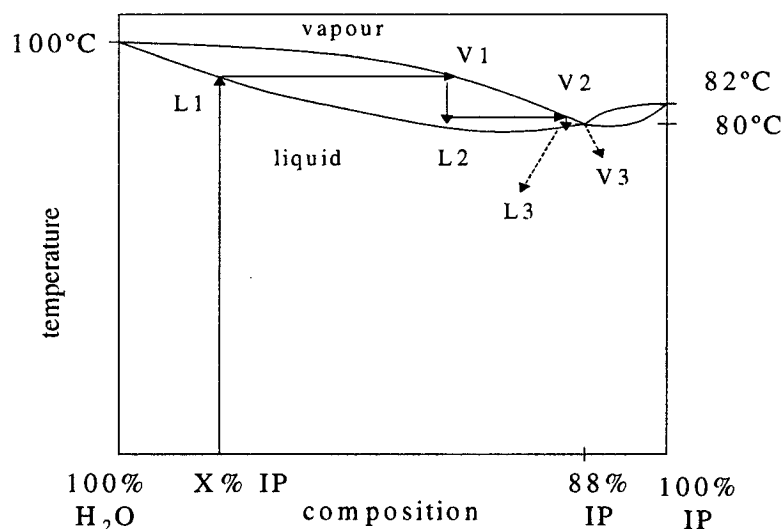


Figure B.1 2-propanol-water phase diagram (adapted from [1])

Analysis of the condensed phase will determine that the distillate does not contain pure L1, since the boiling-point difference between L1 and L2 is below 30°C . Likewise, the liquid remaining in the distilling flask will contain a larger amount of the higher-boiling point component but will not be pure L2. However, if redistilled, each of these fractions would become enriched in the lower-boiling point component (L1). After a certain

number of redistillations, one should obtain distillate that would be essentially pure L1 and a residue that would be pure L2.

Fractional distillation, by using a column inserted between the distilling flask and the distilling head, accomplishes all the redistillation cycles required in a single step. The column is insulated and filled with a suitable packing material (glass beads, glass helices, stainless steel sponge, etc.) that allows a mixture of L1 and L2 to be subjected to many vaporisation-condensation cycles continuously as it moves up the column (Figure B.2).

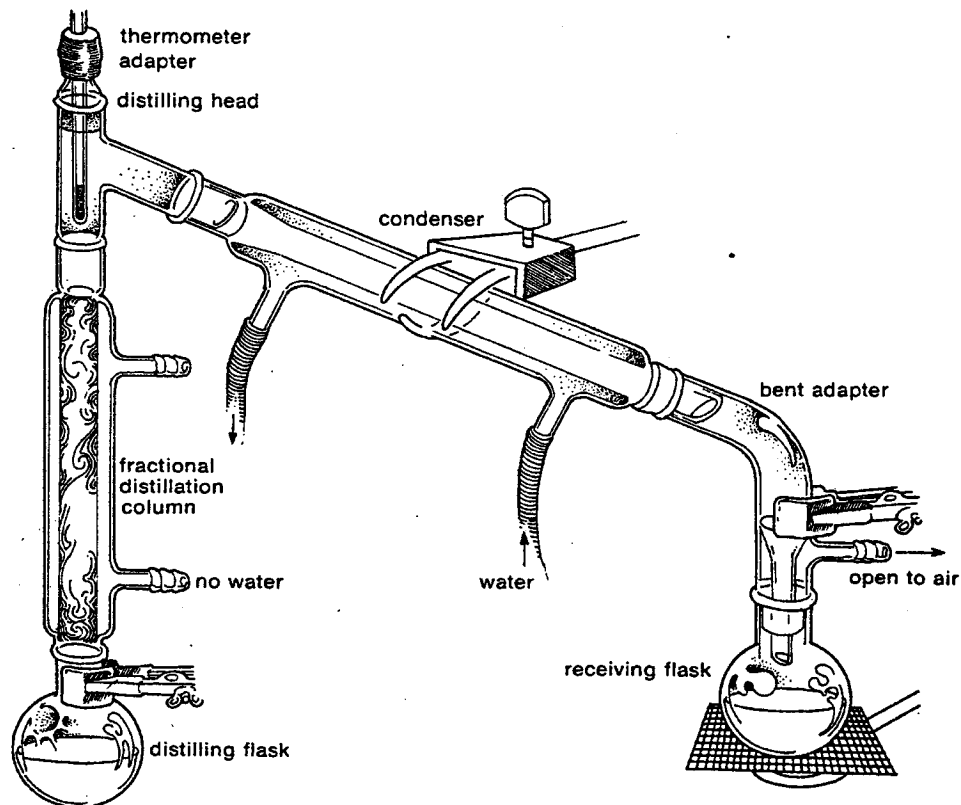


Figure B.2 Fractional distillation set-up [1]

With each cycle, the composition of the vapour is progressively enriched in the lower-boiling point component, thus nearly pure L1 emerges from the top of the column, condenses and passes into the receiving flask as the first fraction. The distillation must be carried out slowly to ensure numerous vaporisation-condensation cycles and to avoid column flooding (otherwise, the efficiency of separation decreases), but fast enough to maintain a constant rate at which material collects in the receiver.

The temperature at the thermometer bulb should remain constant as a pure component is removed; when most of the component is distilled, the distillation rate decreases and the temperature raises again.

- **Column Efficiency**

The number of theoretical plates gives a good measure of column efficiency. Each theoretical plate corresponds to a simple distillation, or one vaporisation-condensation cycle. For example, if a liquid mixture requires five vaporisation-condensation equilibria within the column to be efficiently separated, a packed column with five theoretical distillation plates should be used (the first theoretical plate always corresponds to the initial vaporisation from the distilling flask).

The relation between the number of theoretical plates needed to separate a two-component mixture and the difference between the boiling points of the components are given in table B.1. However, since columns are seldom operated at equilibrium, more theoretical plates than listed may be necessary for a complete separation.

Table B.1 Theoretical plates required to separate liquid mixtures by distillation [1]

Boiling-point difference (°C)	# Theoretical plates
108	1
72	2
54	3
43	4
36	5
20	10
10	20
7	30
4	50
2	100

As observed, the number of theoretical plates (efficiency) of the column must increase as the boiling-point differences between the components decrease for the separation to be adequate.

- ***Fractional Distillation of 2-Propanol-Water Azeotrope***

Many mixtures of compounds, because of intermolecular attractions or repulsions, do not show ideal behaviour and thus Raoult's law is not followed. The law states that the partial vapour pressure of component A in the solution (P_A) equals the vapour pressure of pure A (P_A^0) times its mole fraction (N_A) in the solution; same expression can be written for B.

The type of vapour-liquid diagram that results from such a non-ideal behaviour in the case of 2-propanol-H₂O system is a minimum-boiling-point diagram; the minimum point in such a diagram correspond to a constant-boiling point mixture called an azeotrope. The azeotrope has a fixed composition (88% 2-propanol, 12% H₂O wt/wt) which cannot be altered by fractional distillation and a fixed boiling point (80.4°C); hence, an azeotrope acts as if it were a pure compound.

A minimum-boiling-point azeotrope results from a slight incompatibility of the substances, which leads to higher-than-expected combined vapour pressures from the solution; the higher combined vapour pressures bring about a lower boiling point for the mixture. The behaviour on fractional distillation of a 2-propanol-water mixture of composition X can be described according to the phase diagram in Figure B.1.

The phase diagram relates the composition of the boiling liquid (lower curve) and its vapour (upper curve) as a function of temperature. The horizontal lines represent the vaporisation step of a given vaporisation-condensation cycle and indicates the composition of the vapour in equilibrium with liquid at a given temperature. Each of the vertical lines represents the condensation step; the composition does not change as the temperature drops on condensation.

The mixture is heated (XL1) until is observed to boil (L1). The vapour (V1) will be richer in the lower-boiling point component (the azeotrope) than the original mixture. The condensate (L2) is vaporised again within the column to give V2. The process continues, following the lines to the right, until the azeotrope is obtained (V3). The distillate is not pure 2-propanol, but contains 88% alcohol and 12% water. The contents of the distilling flask become progressively richer in the higher-boiling point component as the distillation proceeds. When all the alcohol is removed as azeotrope, pure water remains, distilling at 100°C.

If complete separation is required, an azeotropic distillation should be employed to obtain pure anhydrous 2-propanol. However, this procedure is more complicated since it involves the addition of an inert solvent as a third phase and comprises two separate distillation sessions.

As the azeotrope contains 88% 2-propanol (wt/wt), it is considered efficient enough to be employed as such as salting out agent for nickel sulphate in SDC tests. Therefore, the present research project considered only the fractional distillation as a simple means of separation.

- ***Experimental Procedure***

The fractional distillation test was performed employing the set-up presented in figure B.1. The water-organic mixture was brought to boiling point (80-81°C) in a 1000-mL Pyrex round-bottom flask heated by a Glas-Col hemispherical heating mantle; the temperature was controlled by a Dayton variable auto-transformer. The vapour phase was enriched in the lower-boiling point component through an insulated Kimax brand distillation column (300mm in length) packed with Pyrex glass beads ($\phi = 4$ mm) while the temperature was read using a thermometer inserted into the distilling head.

The organic phase was condensed in a water-cooled, Kimax brand, Liebig-type condenser (400 mm in length) and collected in a 1000-mL Pyrex round-bottom receiving flask.

- ***Material balances***

Based on the data derived from the typical crystallisation test presented in Section 5.4 and distillation trial, Table B.2 gives general material balances for nickel, 2-propanol and water.

The losses of organic and Ni/water/solution can most likely be assigned to a combination of causes such as: moisture retained in the cake, sampling and column hold up during distillation.

Table B.2 Materials mass balances

NICKEL		
IN	100 mL NiSO ₄ .6H ₂ O solution at 25 g/L Ni = 2.5 g Ni	Total in: 2.5 g Ni
OUT	98 mL aqueous @ 6.55 g/L Ni = 0.64 g Ni 5.41 g NiSO ₄ .6H ₂ O = 1.20 g Ni Samples taken during SDC = 0.35 g Ni	Total out: 2.19 g Ni Nickel closure: 87.6%
2-PROPANOL		
IN	150 mL for SDC = 117 g 2-propanol 25 mL for cake wash = 19.5 g 2-propanol	Total in: 175 mL = 136.5 g 2-PROPANOL
OUT	160 mL azeotrope (88%wt 2-propanol) = 114.04 g 12.27 mL samples taken during SDC = 9.57 g	Total out: 123.61 g 2-propanol 2-propanol closure: 90.55%
WATER		
IN	100 mL = 100 g H ₂ O	Total in: 100 g
OUT	2.22 g H ₂ O as crystallisation water 60 mL = 60 g H ₂ O after distillation 15.55 g in azeotrope 18.73 g in aqueous samples	Total out: 96.5 g H ₂ O Water closure: 96.5%

B2. Pervaporation (Membrane Separation)

Pervaporation starts to gain laboratory and industrial recognition as a cost-effective and energy-saving membrane technique for separating azeotropic, close-boiling or aqueous-organic mixtures (such as low molecular weight alcohols and ketones) based on selective adsorption in the membrane's pores and diffusivity differences.

Separation by pervaporation depends on size, adsorption strength and mobility of molecules being separated.

In pervaporation, a liquid feed contacts the feed side of a membrane and the permeate side is typically under vacuum to provide a driving force for vapour permeate.

Hydrophobic (or organophilic) membranes are used to remove organics from water via selective organic adsorption and subsequent diffusivity (when the water fraction is higher), whereas hydrophilic membranes are employed for dewatering organics, i.e. permselective separation of water (when the organic fraction is higher).

- **Organic Membranes**

Hydrophilic organic membranes are generally composite membranes consisting of a highly permeable support layer (substrate) coated with a thin and highly selective separation layer (alternating coats of oppositely-charged polyelectrolytes). Most common polymers for substrate are polypropylene, polysulphone, polyacrylonitrile, polydimethylsiloxane and polyamides, on which polyanions (e.g. polyacrylic acid, alginic acid, polystyrene-sulphonic acid) and polycations (e.g. chitosan, polyallylamine hydrochloride and polyethylenimine) are deposited by alternating adsorption. The selectivities and permeabilities of the composite membranes depend strongly on the chemical structure and increase with increasing charge density of the polyelectrolytes.

For example, Meier-Haack *et al.* [3] reported high separation factors in the dewatering of 2-propanol and ethanol containing less than 30% by wt. water (the permeate contained > 99% H₂O) with composite membranes consisting of polyamide-6 substrate and six double (alternating) layers of polyethylenimine and polyacrylic or alginic acid, which displayed good long-term stability (i.e. no swelling or decrease in permeate flux).

Although some hydrophobic polymer membranes offer high separation factors, they usually have thermal and chemical limitations. Based on this impediment, Tuan *et al.* [4] tried to develop zeolite (silicalite)-based inorganic membranes.

- **Inorganic Membranes**

Zeolite membranes have high thermal, mechanical and chemical stability, offering the additional advantage of a great versatility. Silicate-based membranes are hydrophobic, but the hydrophobic/hydrophilic nature can be modified by isomorphous substitution of trivalent metals (i.e. Al, Ge, Fe and B) into the zeolite framework and changing the Si/metal ratio. The pore size can also be adjusted by choosing the appropriate zeolite and

by exchanging cations of different diameters, whereas the acidic/basic nature can be modified by exchanging extra-framework metal cations with H^+ .

Tuan *et al.* [4] reported that simple hydrophobic silicate membranes exhibited moderate alcohol/water separation factors (10-60) for aqueous streams containing 5% (wt.) low molecular weight alcohols, and the separation factor increased with the number of carbon atoms in the alcohol chain, from methanol to 1-propanol.

When hydrophilic (metal-doped) zeolitic membranes were used, the separation factors were generally three times higher than with simple silicate-based membrane, with best results in the order B>Al>Ge>Fe-substituted zeolite. The diffusivities of alcohols through pores decreased with increasing carbon number. Increasing temperatures have a beneficial effect on separation factors due to increased organic molecule mobility and diffusion rate.

References

- [1]. D.L. Pavia, G.M. Lampman and G.S. Kriz, jr., *Introduction to Organic Laboratory Techniques (a contemporary approach)*, Saunders College Publishing, Philadelphia, Pa., pp. 514-635, (1982).
- [2]. C. Penning, "Solvent Recovery by Distillation", in *Solvent Problems in Industry*, edited by G. Kakabadse, Elsevier, New York, N.Y., pp. 151-162, (1984).
- [3]. J. Meier-Haack, W. Lenk, D. Lehmann and K. Lunkwitz, "Pervaporation separation of water/alcohol mixtures using composite membranes based on polyelectrolyte multilayer assemblies" *Journal of Membrane Science*, **184**, pp. 233-243, (2001).
- [4]. V.A. Tuan, S. Li, J.L. Falconer and R.D. Noble, "Separating organics from water by pervaporation with isomorphously-substituted MFI zeolite membranes" *Journal of Membrane Science*, **196**, pp. 111-123, (2002).

Appendix C. Physical and Electrochemical Properties of 2-Propanol

2-propanol, $\text{CH}_3\text{CHOHCH}_3$, is the simplest secondary alcohol, also designated under the following conventional and non-conventional terms: isopropyl alcohol, secondary propyl alcohol, isopropanol, dimethylcarbinol, per-spirit, petrohol, avantine [1].

C.1 Physical Properties

2-propanol is a colourless, flammable liquid with a pleasant, characteristic odour, but has a bitter taste. It is stable under normal conditions and soluble in water (miscible) in all proportions. Its solvent properties are excellent with respect to natural fats and oils, essential oils, waxes, hydrocarbons, alkaloids, resins and organic compounds. It does not solvate most of inorganic compounds, for which acts as an effective salting-out agent.

Physical constants of isopropanol are given in table C.1.

Table C.1 Physical properties of 2-propanol [2]

Property	Value	Property	Value
Acidity (as acetic acid)	0.002% (wt)	Max. Acceptable Conc.	200ppm in air
Boiling point (760mm)	82.3°C	Molecular weight	60.09
Dielectric constant (20°C)	18.62	Non-volatile matter	0.002g/100mL
Dipole moment	1.68 Debye	Purity	99.5%
Fire hazard	dangerous	Refractive index (20°C)	1.3772
Flash pt. (open cup)	15°C	Specific conductivity	$3.5 \cdot 10^{-6}$ mhos/cm
Freezing pt.	-87.7°C	Specific gravity (20°C)	0.786
Heat of combustion	7970 cal/g	Specific heat (20°C)	0.596 cal/g°C
Heat of fusion	21.08 cal/g	Surface tension (20°C)	21.7 dynes/cm
Heat of vaporization (b.p)	165 cal/g	Vapour pressure (20°C)	33 mmHg
Limit of flammability	2.65% (vol)	Viscosity (20°C)	2.4 cps

- **Toxicity**

Only slight to moderate toxic effects of 2-propanol on humans have been reported [1]. Ingestion may have a small effect on respiration, but the pulse slows and the appetite is lost. However, prolonged ingestion of large doses causes coma at lower blood concentrations than ethanol.

Although it has a narcotic effect on the central nervous system, the danger from inhalation is slight due to its low volatility and relatively high boiling point. The maximum allowable concentration of 2-propanol vapours for an 8-hr exposure has been estimated at 200 ppm, but no harmful intermediates are formed by the animal metabolism. If ingested, it diffuses into all the tissues and is partially changed to acetone before elimination by lungs (detected in breath after 15 min) and kidneys (detected in urine after 1hr).

C.2 Electrochemical Behaviour of 2-Propanol

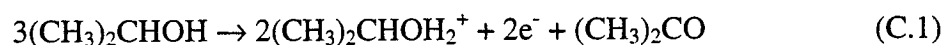
Since the present research project proposes the use of 2-propanol as a salting-out agent to be employed in conjunction with the copper electrorefining (Cu ER) process (refer to Section 5.7), it is important to determine its electrochemical behaviour during electrolysis.

Rehioui and Johansson [3] and Rao and Roy [4] studied the reactions that limit the potential range of 2-propanol at a platinised platinum electrode in both acidic and alkaline media (Pt/Pt electrodes exhibit a high overpotential for O₂ evolution and are passive in almost any media). They found that polarisation was very high in acid medium compared to that in alkaline medium, and decreased with increasing temperature.

I. Oxidation Limit

Direct anodic oxidation of aliphatic saturated alcohols to the corresponding carbonyl compounds is usually ineffective, because the extremely high oxidation potentials of these alcohols make the direct removal of an electron from the lone-pair electrons on the oxygen atom difficult. Saturated aliphatic alcohols generally have ionisation potentials greater than 10 eV, because oxygen is fairly electronegative and the unshared pair of

electrons is tightly held to the molecule. Consequently, alcohols are difficult to oxidise at the anode [5, 6]. Anodic oxidation of 2-propanol solutions containing 0.05M sodium perchlorate occurs at 1.32 V (vs. SHE), resulting in an acidification of the medium and formation of acetone:



The reaction is found to be first order with respect to 2-propanol but approaches zero order as the alcohol concentration is above 0.2 M [4].

II. Reduction Limit

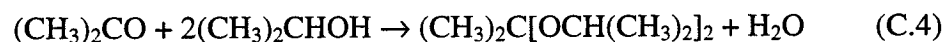
During electrolysis of 2-propanol- NaClO_4 solutions, H_2 evolved at the Pt electrode at -0.98 V (vs. SHE):



When reactions (C.1) and (C.2) take place in the electrolysis cell, the net result is decomposition of 2-propanol according to the reaction:



Formation of water arises from a chemical side-reaction (acid-catalysed) between acetone and 2-propanol, assumed to be:



In conclusion, 2-propanol has a larger accessible potential range than water (from 1.32 to -0.98 V vs. SHE, for platinum electrodes and even more for less-noble metallic electrodes) and it should be electrochemically stable during Cu ER process.

References

- [1]. J.A. Monick, *Alcohols: Their Chemistry, Properties and Manufacture*, Reinhold Book Corporation, New York, N.Y., pp. 119-125, (1968).
- [2]. E.W. Flick, *Industrial Solvents Handbook*, 3rd edition, Publications Noyes, Parkridge, N.J, p. 223, (1985).
- [3]. A. Rehioui and G. Johansson, "Electrochemical Behaviour of Isopropanol at Platinum Electrodes" *Talanta*, **18**, pp. 329-337, (1971).
- [4]. K.V. Rao and C.B. Roy, "Anodic Oxidation of Isopropanol on Platinised Platinum Electrode" *Indian Journal of Chemistry*, **19A**, pp. 840-845, (1980).
- [5]. S. Ross, M. Filkenstein and E. Rudd, *Anodic Oxidation*, Academic Press, New York, N.Y., pp. 262-293, (1975).
- [6]. T. Shono, *Electroorganic Chemistry as a New Tool In Organic Synthesis*, Springer-Verlag, New York, N.Y., pp. 29-37, (1984).

Appendix D. Nickel Concentration Profiles during SDC Tests

- *Homogeneous Crystallisation Experiments (Controlled, Low Supersaturation)*

Table D.1 Progression of low S homogeneous SDC tests at 10, 21 and 40°C, based on the respective critical supersaturation lines determined in Section 5.5.2 ($O/A_{total}=1.5$)

Step #	Time (min)	O/A _{per step} 10°C	[Ni] _{aq} (g/L)	O/A _{per step} 21°C	[Ni] _{aq} (g/L)	Step #	Time (min)	O/A _{per step} 40°C	[Ni] _{aq} (g/L)
1	0	0	19.2	0	19.35	1	0	0	45
2	30	0.54	14.78	1.05	13.44	2	15	0.53	39
3	60	1.02	7.37	1.25	10.78	3	30	0.66	34.86
4	90	1.6	4.4	1.6	6.83	4	45	0.77	29.5
						5	60	0.88	25.7
						6	75	1	22
						7	90	1.1	19.5
						8	105	1.2	17
						9	120	1.34	15
						10	135	1.5	12.5

Controlled supersaturation tests at 40°C required more steps of 2-propanol addition, due to the narrower metastable zone (see Figure 5.13)

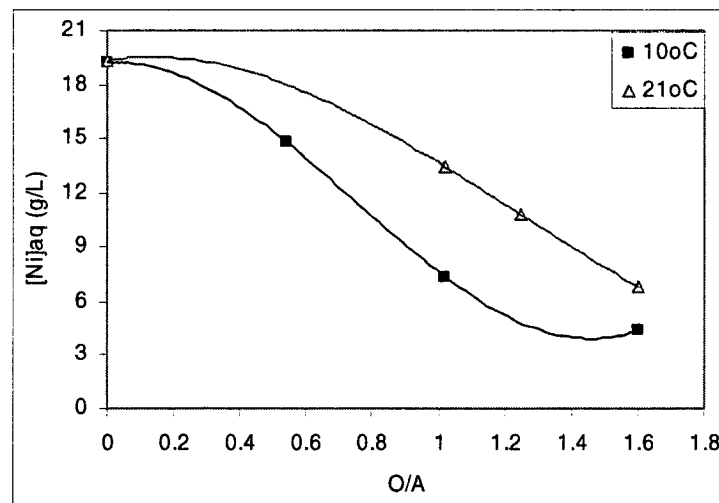


Figure D.1 Homogeneous crystallisation tests at 10 and 21°C (low supersaturation, step-wise addition of alcohol, 250 g/L H₂SO₄)

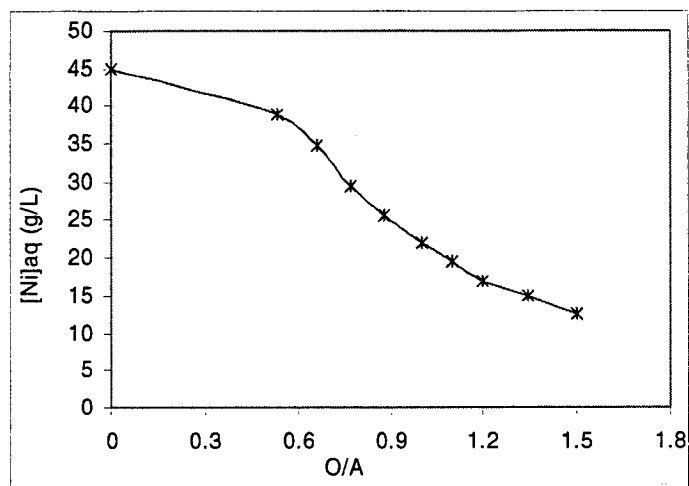


Figure D.2 Homogeneous crystallisation tests at 40°C (low supersaturation, step-wise addition of alcohol, 550 g/L H₂SO₄)

- *Heterogeneous Crystallisation Experiments (Controlled Supersaturation, Seeding)*

Recycling tests were conducted under constant, similar conditions, following the same procedure, leading thus to similar nickel concentration profiles.

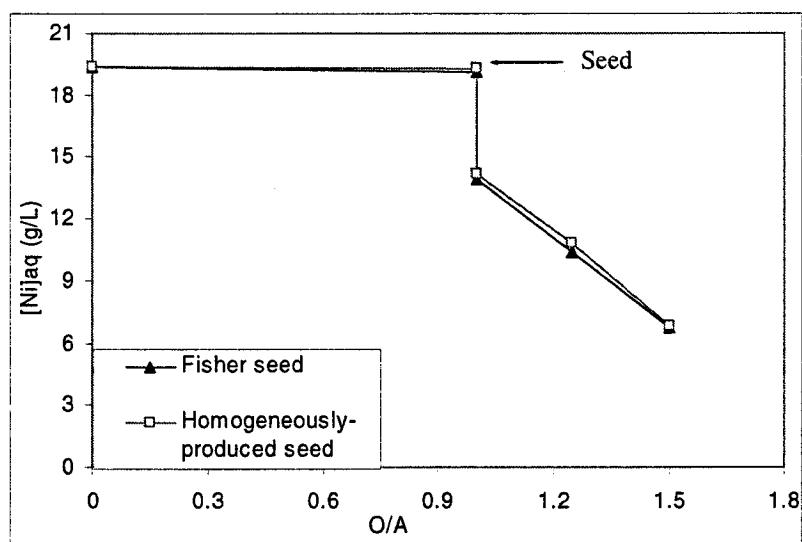


Figure D.3 Comparative heterogeneous crystallisation tests at 21°C (80 g/L seed, low supersaturation, step-wise addition of alcohol, 250 g/L H₂SO₄)

Table D.2 Progression of heterogeneous SDC tests at 21°C (80 g/L NiSO₄·6H₂O seed, O/A_{total}=1.5, 250 g/L H₂SO₄)

Time(min)	O/A	[Ni] _{aq} (g/L) (Fisher seed)	[Ni] _{aq} (g/L) (SDC-made seed)
0	0	19.35	19.35
5 (+ seed)	1	19.12	19.3
30	1	13.88	14.16
60	1.25	10.34	10.78
90	1.5	6.77	6.81

- **Ageing (Crystal Equilibration) Tests**

Table D.3 Progression of the heterogeneous SDC ageing test (21°C, 50 g/L NiSO₄·6H₂O seed, O/A_{total}=1, 250 g/L H₂SO₄)

Time (min)	[Ni] _{aq} (g/L)	O/A
0	47.5	0
5	46.95	0.28
60	38.42	0.28
120	32.8	0.4
180	19.38	0.63
240	10.42	1

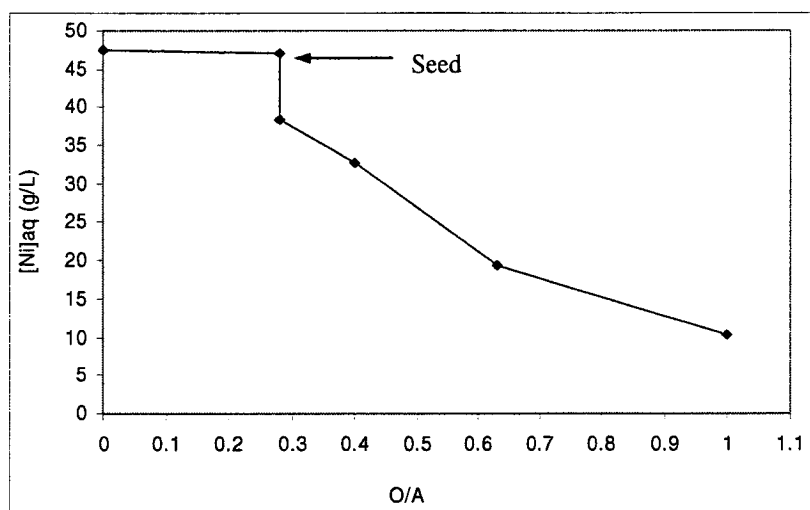
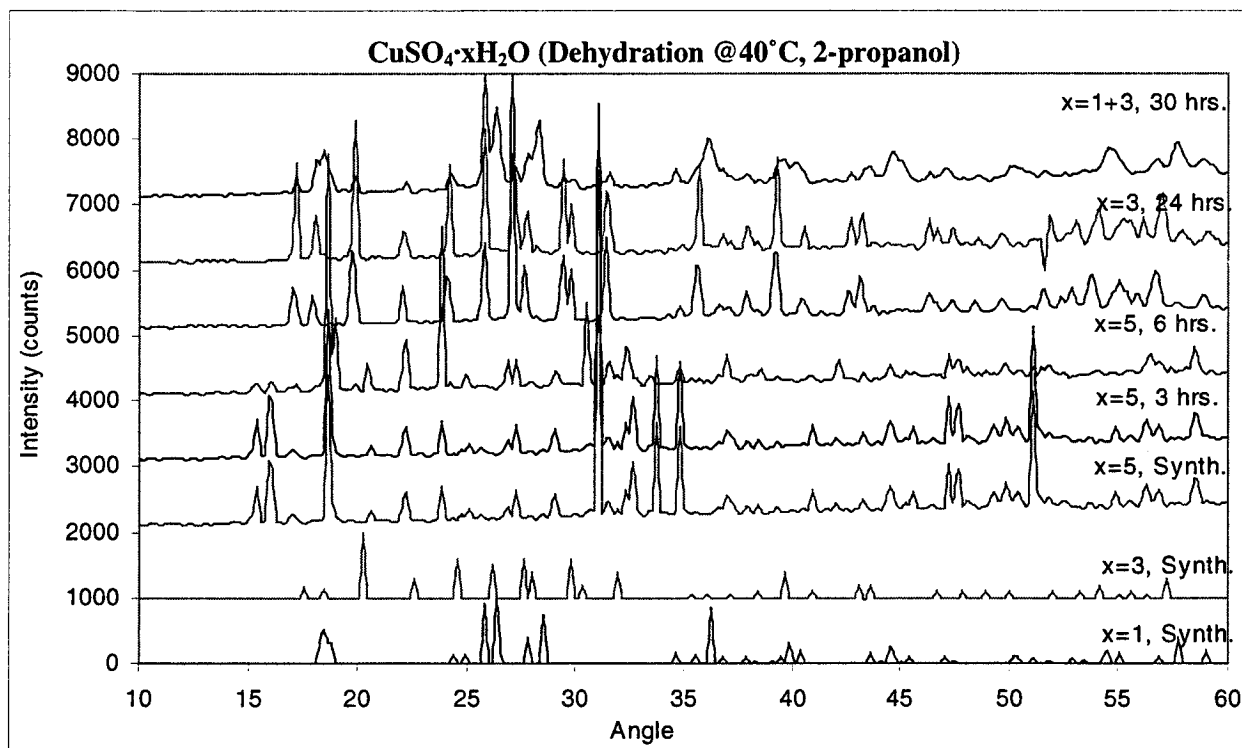
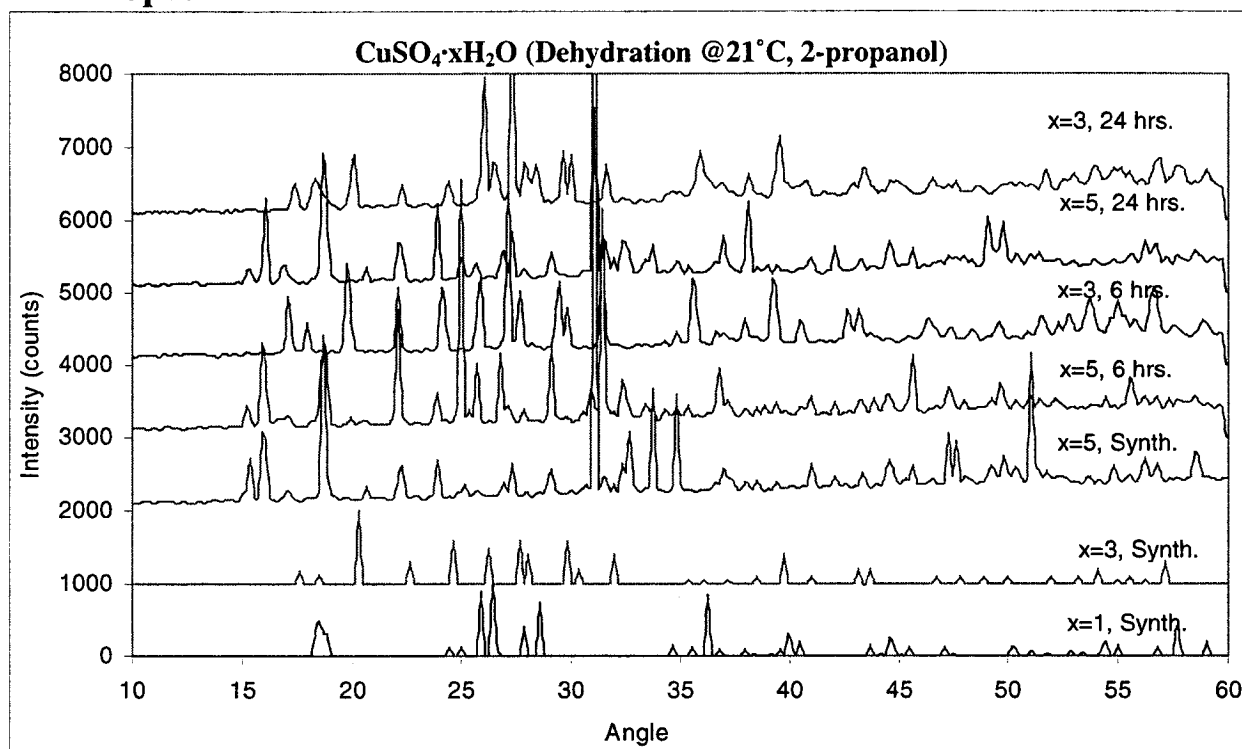
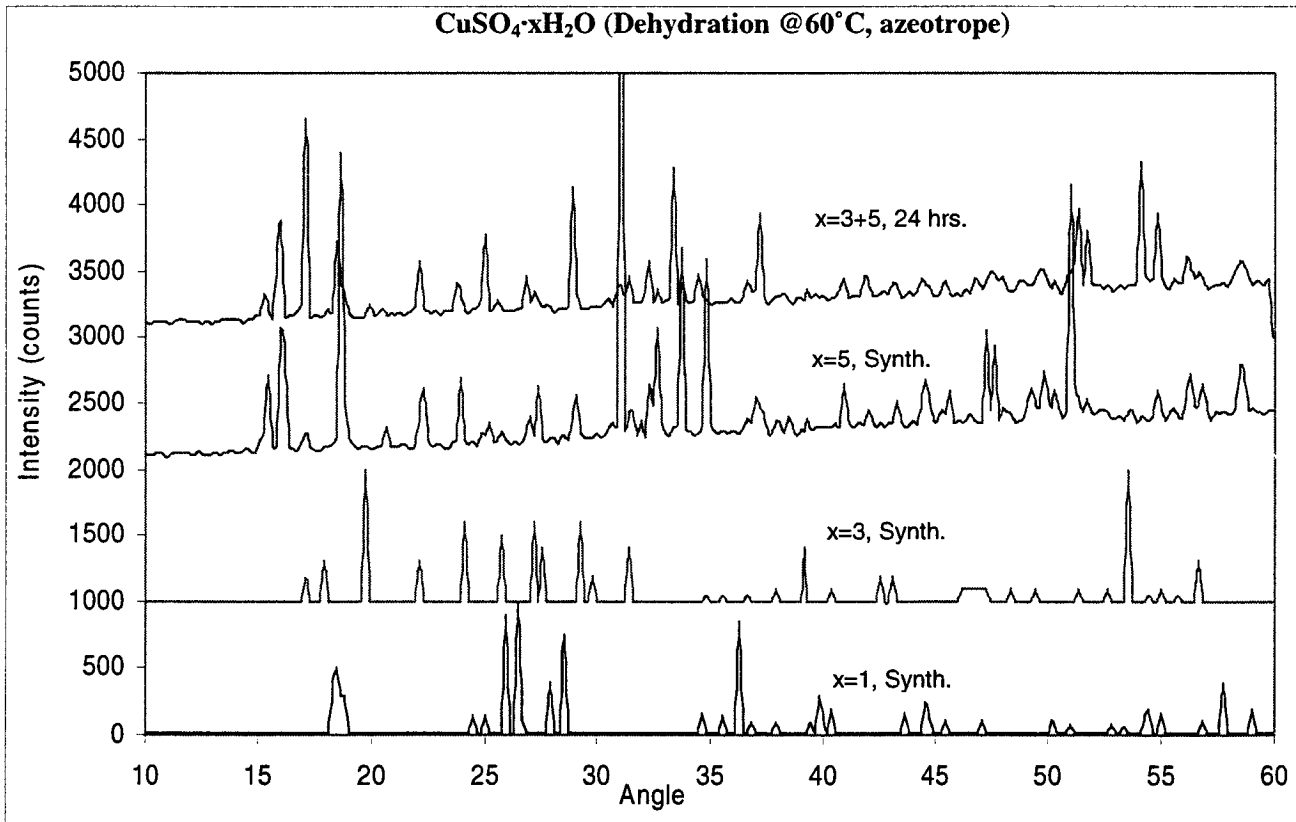
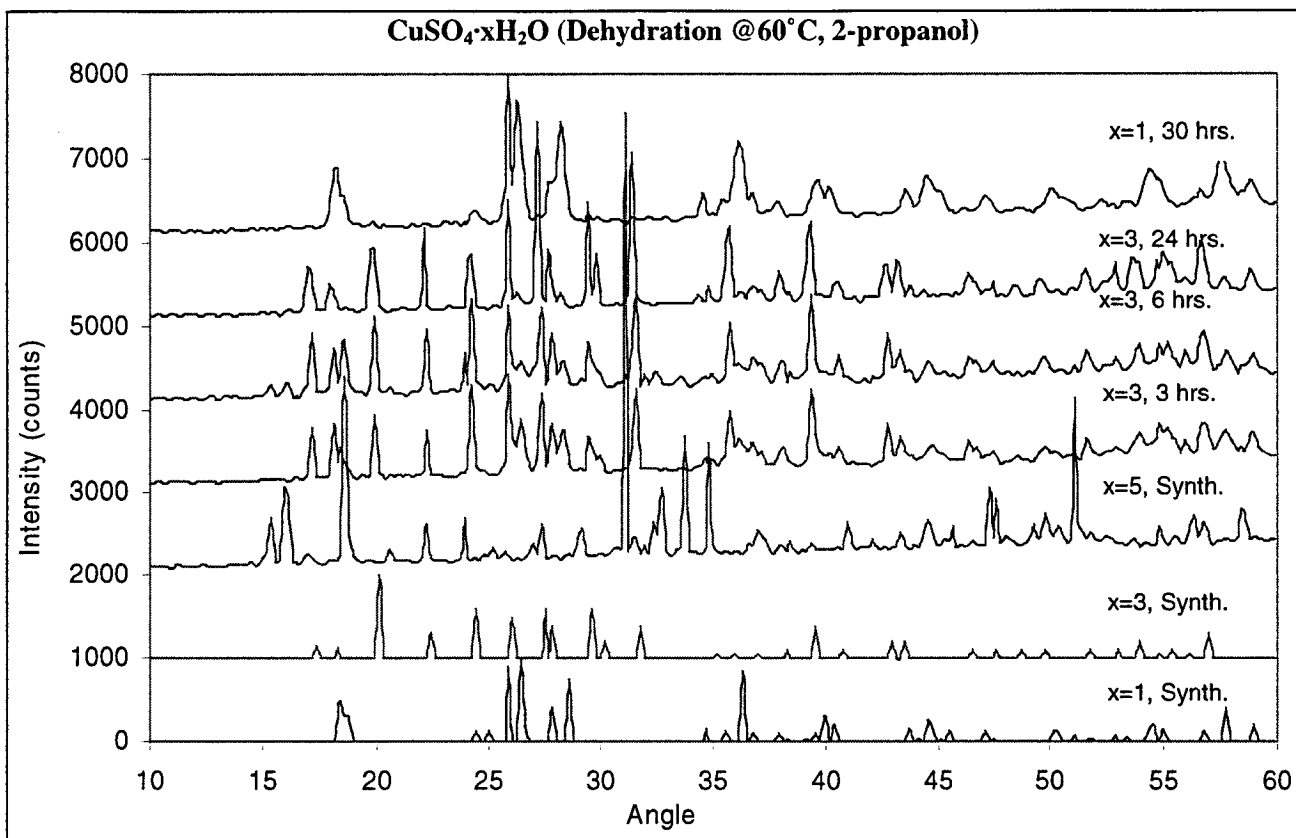


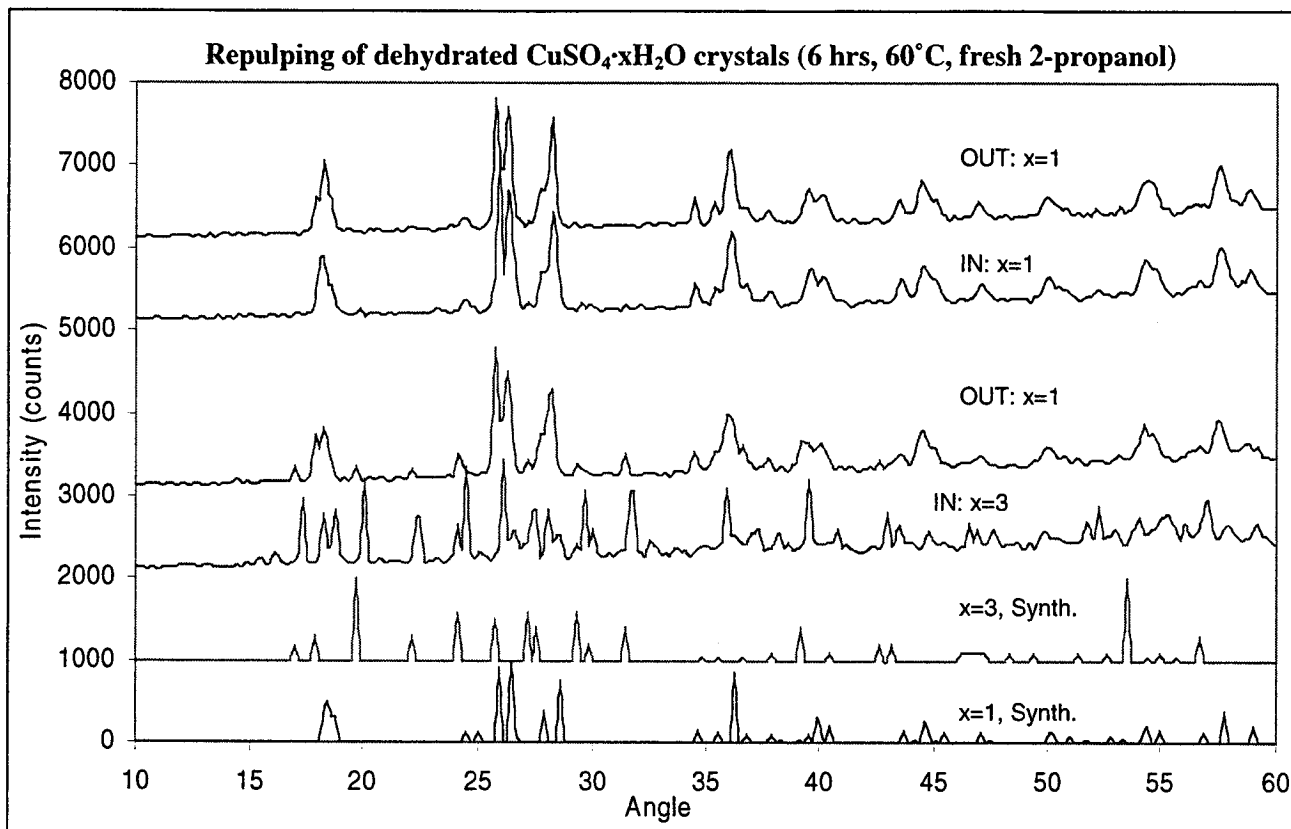
Figure D.4 Heterogeneous crystallisation ageing test at 21°C (50 g/L seed, low supersaturation, step-wise addition of alcohol, 250 g/L H₂SO₄)

Appendix E. Confirmation of Crystallisation Water Molecules for Copper Sulphate Following Dehydration Tests

I. XRD Spectra

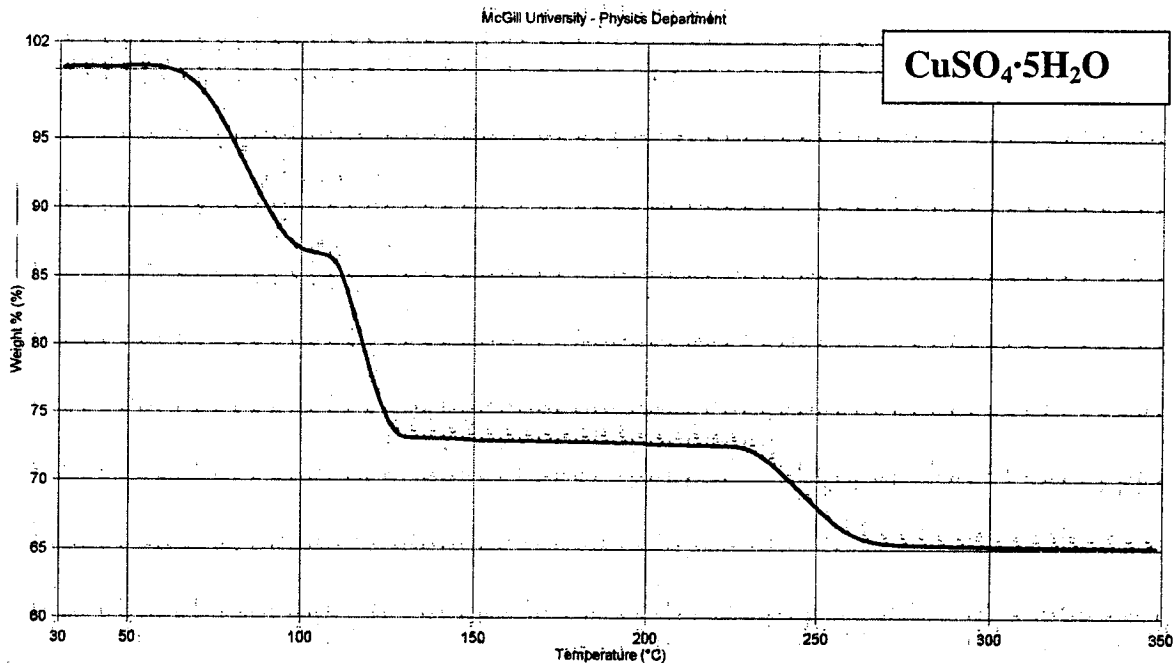






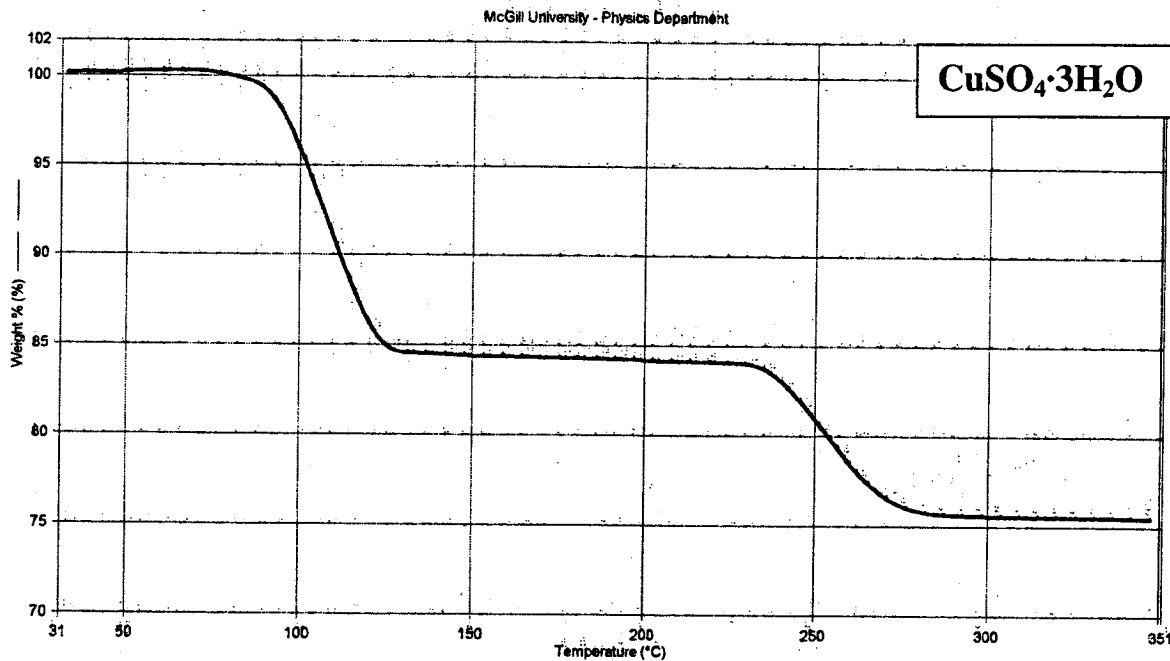
II. TGA Spectra

Filename:	D:\PEV\pyns\data\hydrom...CuSO4-5.tgd	IP, 20deg, 24 hr: CuSO4-5.tgd
Date Collected:	6/25/2003 3:24:09 PM	Unsubtracted Weight % (%): Steps: 1-8
Baseline Filename:		
Operator ID:	Georgiana	
Sample ID:	IP, 20deg, 24 hr	
Sample Weight:	6.433 mg	
Comment:		



1) Hold for 1.0 min at 50.00°C	5) Hold for 1.0 min at 200.00°C
2) Heat from 50.00°C to 150.00°C at 10.00°C/min	6) Heat from 200.00°C to 300.00°C at 10.00°C/min

Filename:	D:\PEV\pyns\data\CuSO4-3.tgd	IP, 40deg, 24 hr: CuSO4-3.tgd
Date Collected:	6/25/2003 2:28:16 PM	Unsubtracted Weight % (%): Steps: 1-8
Baseline Filename:		
Operator ID:	Georgiana	
Sample ID:	IP, 40deg, 24 hr	
Sample Weight:	9.396 mg	
Comment:		

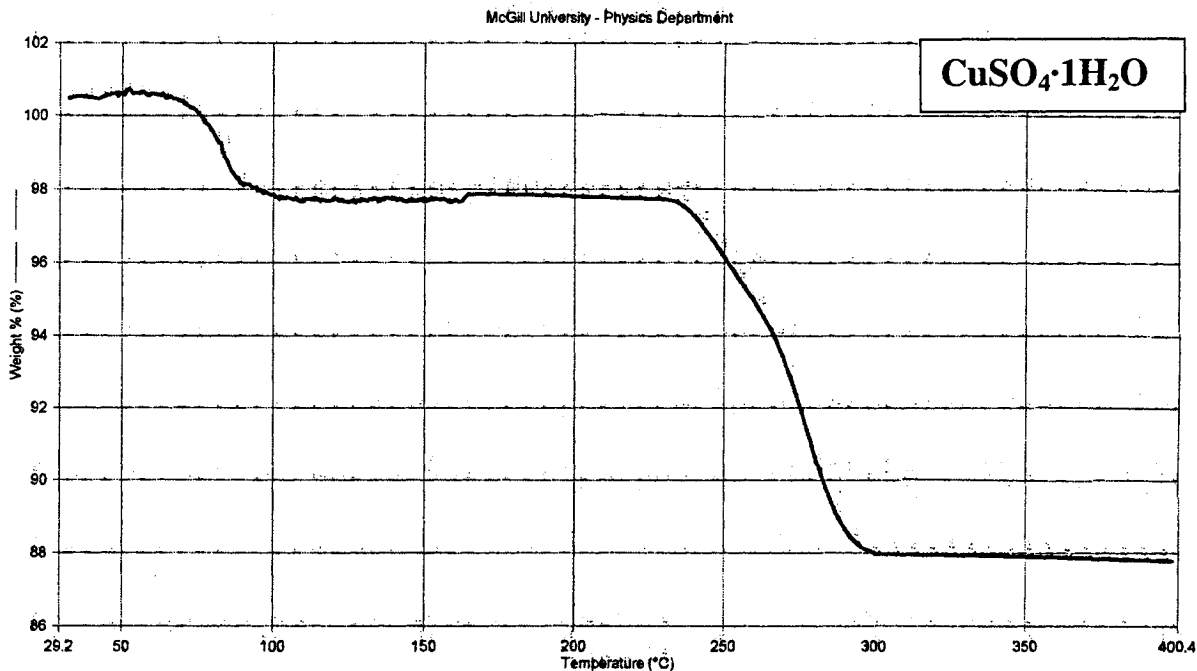


1) Hold for 1.0 min at 50.00°C	5) Hold for 1.0 min at 200.00°C
2) Heat from 50.00°C to 150.00°C at 10.00°C/min	6) Heat from 200.00°C to 300.00°C at 10.00°C/min
3) Hold for 1.0 min at 150.00°C	7) Hold for 1.0 min at 300.00°C
4) Heat from 150.00°C to 200.00°C at 20.00°C/min	8) Heat from 300.00°C to 350.00°C at 20.00°C/min

6/25/2003 2:30:09 PM

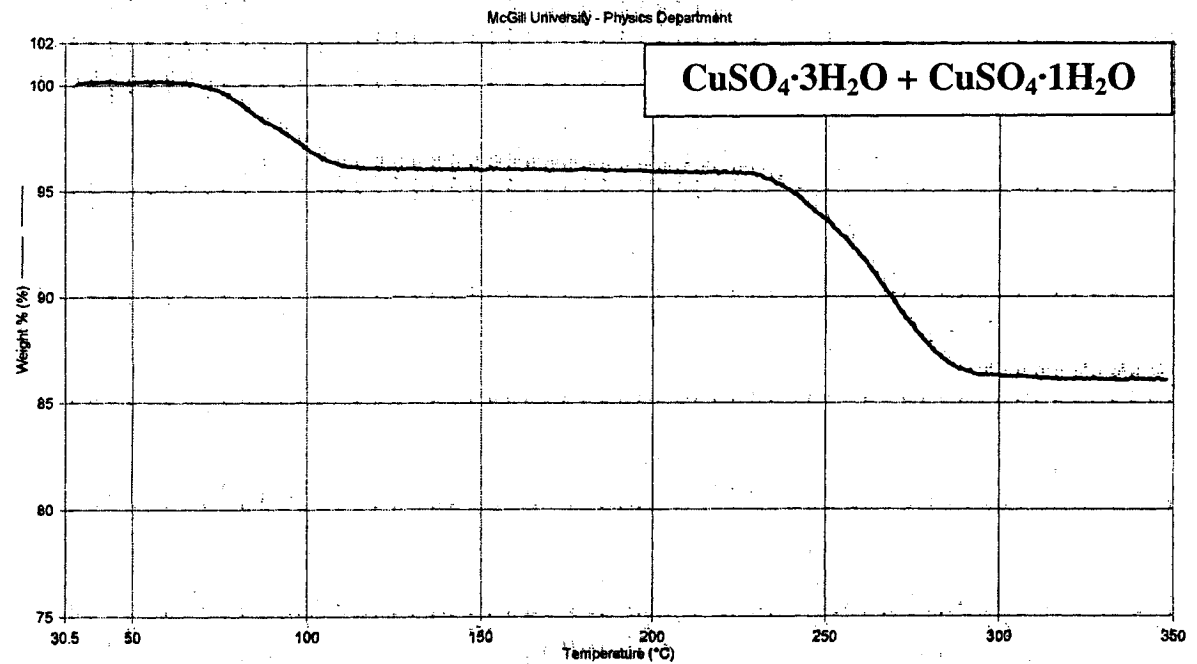
Appendix E. Confirmation of Crystallisation Water Molecules for Copper Sulphate 264

Filename: d:\pel\pys\data\hydrom...l\cuso4-1.tgd IP, 60deg, 30 hr: CuSO4-1.tgd
 Data Collected: 6/25/2003 1:35:08 PM Unsubtracted Weight % (%): Steps: 1-8
 Baseline Filename:
 Operator ID: Georgiana
 Sample ID: IP, 60deg, 30 hr
 Sample Weight: 6.888 mg
 Comment:



1) Hold for 1.0 min at 50.00°C
 2) Heat from 50.00°C to 150.00°C at 10.00°C/min
 3) Hold for 1.0 min at 150.00°C
 4) Heat from 150.00°C to 200.00°C at 20.00°C/min
 5) Hold for 1.0 min at 200.00°C
 6) Heat from 200.00°C to 300.00°C at 10.00°C/min
 7) Hold for 1.0 min at 300.00°C
 8) Heat from 300.00°C to 400.00°C at 20.00°C/min
 6/25/2003 1:45:35 PM

Filename: d:\pel\pys\data\hydrom...l\cuso4-x.tgd IP, 40deg, 30 hr: CuSO4-x.tgd
 Data Collected: 6/25/2003 4:14:58 PM Unsubtracted Weight % (%): Steps: 1-8
 Baseline Filename:
 Operator ID: Georgiana
 Sample ID: IP, 40deg, 30 hr
 Sample Weight: 6.695 mg
 Comment:



1) Hold for 1.0 min at 50.00°C
 2) Heat from 50.00°C to 150.00°C at 10.00°C/min
 3) Hold for 1.0 min at 150.00°C
 4) Heat from 150.00°C to 200.00°C at 20.00°C/min
 5) Hold for 1.0 min at 200.00°C
 6) Heat from 200.00°C to 300.00°C at 10.00°C/min
 7) Hold for 1.0 min at 300.00°C
 8) Heat from 300.00°C to 350.00°C at 20.00°C/min
 6/25/2003 4:18:27 PM